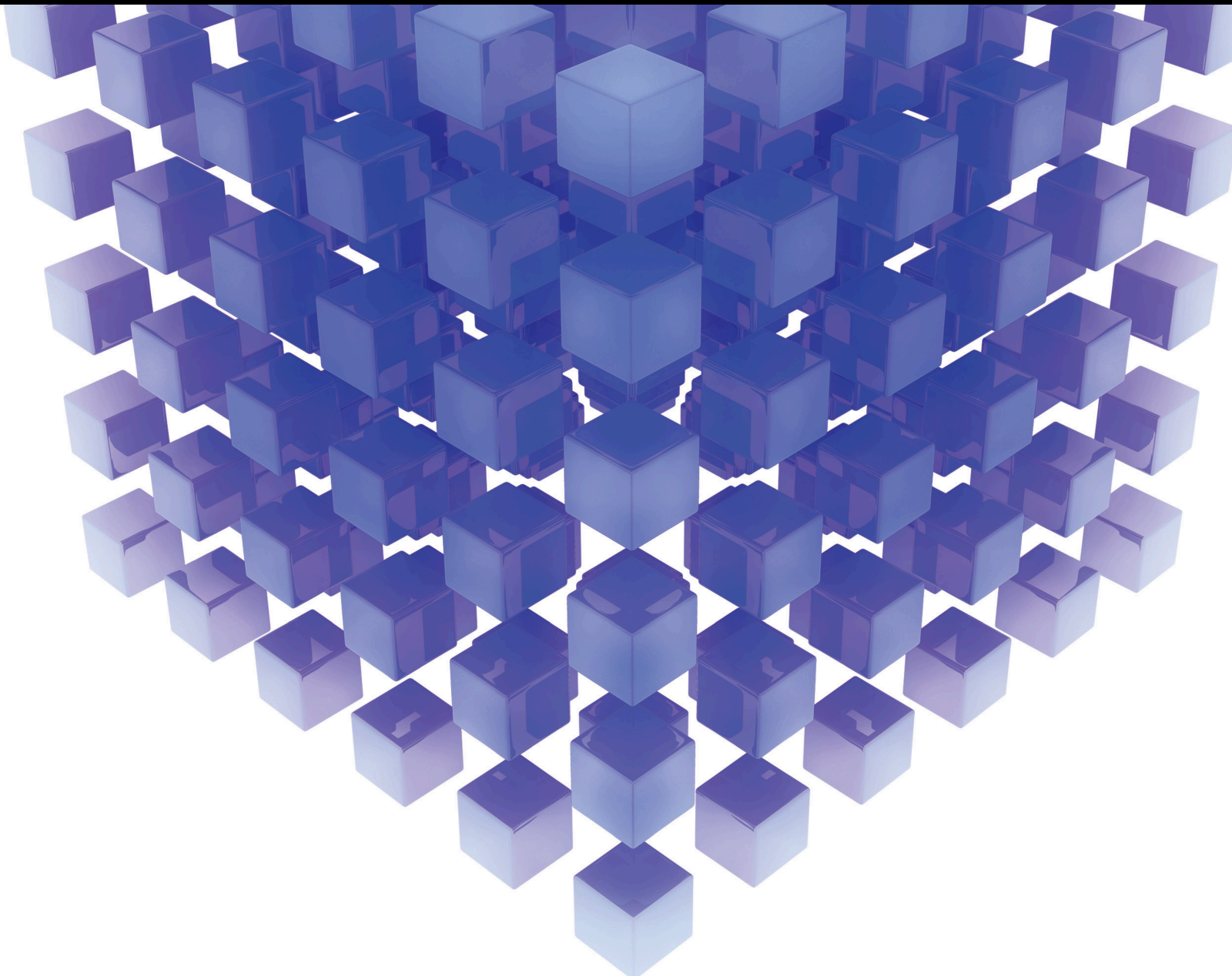


Mathematical Problems in Engineering

Environmental Systems Modelling and Analysis Under Changing Conditions

Lead Guest Editor: Xander Wang

Guest Editors: Aili Yang, Adam Fenech, and Huiyan Cheng





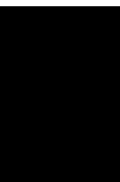
Environmental Systems Modelling and Analysis Under Changing Conditions

Mathematical Problems in Engineering

Environmental Systems Modelling and Analysis Under Changing Conditions

Lead Guest Editor: Xander Wang

Guest Editors: Aili Yang, Adam Fenech, and Huiyan
Cheng



Copyright © 2021 Hindawi Limited. All rights reserved.

This is a special issue published in “Mathematical Problems in Engineering.” All articles are open access articles distributed under the Creative Commons Attribution License, which permits unrestricted use, distribution, and reproduction in any medium, provided the original work is properly cited.

Chief Editor

Guangming Xie, China

Editorial Board

Mohamed Abd El Aziz, Egypt
Ahmed A. Abd El-Latif, Egypt
Mahmoud Abdel-Aty, Egypt
Mohammad Yaghoub Abdollahzadeh
Jamalabadi, Republic of Korea
Rahib Abiyev, Turkey
Leonardo Acho, Spain
José Ángel Acosta, Spain
Daniela Addressi, Italy
Paolo Addresso, Italy
Claudia Adduce, Italy
Ramesh Agarwal, USA
Francesco Aggogeri, Italy
Ricardo Aguilar-Lopez, Mexico
Ali Ahmadian, Malaysia
Tarek Ahmed-Ali, France
Elias Aifantis, USA
Akif Akgul, Turkey
Guido Ala, Italy
Andrea Alaimo, Italy
Reza Alam, USA
Nicholas Alexander, United Kingdom
Salvatore Alfonzetti, Italy
Nouman Ali, Pakistan
Mohammad D. Aliyu, Canada
Juan A. Almendral, Spain
Watheq Al-Mudhafar, Iraq
Mohammad Alomari, Jordan
Ali Saleh Alshomrani, Saudi Arabia
José Domingo Álvarez, Spain
Cláudio Alves, Portugal
Juan P. Amezquita-Sanchez, Mexico
Lionel Amodeo, France
Sebastian Anita, Romania
Renata Archetti, Italy
Muhammad Arif, Pakistan
Sabri Arik, Turkey
Francesco Aristodemo, Italy
Fausto Arpino, Italy
Alessandro Arsie, USA
Edoardo Artioli, Italy
Rashad Asharabi, Saudi Arabia
Fumihiko Ashida, Japan
Farhad Aslani, Australia

Mohsen Asle Zaeem, USA
Andrea Avanzini, Italy
Richard I. Avery, USA
Viktor Avrutin, Germany
Mohammed A. Awadallah, Malaysia
Muhammad Uzair Awan, Pakistan
Francesco Aymerich, Italy
Sajad Azizi, Belgium
Michele Bacciocchi, Italy
Seungik Baek, USA
Khaled Bahlali, France
Pedro Balaguer, Spain
Stefan Balint, Romania
Ines Tejado Balsera, Spain
Alfonso Banos, Spain
Jerzy Baranowski, Poland
Tudor Barbu, Romania
Andrzej Bartoszewicz, Poland
Sergio Baselga, Spain
S. Caglar Baslamisli, Turkey
David Bassir, France
Chiara Bedon, Italy
Azeddine Beghdadi, France
Andriette Bekker, South Africa
Abdellatif Ben Makhlof, Saudi Arabia
Denis Benasciutti, Italy
Ivano Benedetti, Italy
Rosa M. Benito, Spain
Elena Benvenuti, Italy
Giovanni Berselli, Italy
Giorgio Besagni, Italy
Michele Betti, Italy
Pietro Bia, Italy
Carlo Bianca, France
Vittorio Bianco, Italy
Vincenzo Bianco, Italy
Simone Bianco, Italy
David Bigaud, France
Sardar Muhammad Bilal, Pakistan
Antonio Bilotta, Italy
Sylvio R. Bistafa, Brazil
Bartłomiej Błachowski, Poland
Chiara Boccaletti, Italy
Guido Bolognesi, United Kingdom

Rodolfo Bontempo, Italy
Alberto Borboni, Italy
Marco Bortolini, Italy
Paolo Boscariol, Italy
Daniela Boso, Italy
Guillermo Botella-Juan, Spain
Boulaïd Boulkroune, Belgium
Abdesselem Boulkroune, Algeria
Fabio Bovenga, Italy
Francesco Braghin, Italy
Ricardo Branco, Portugal
Maurizio Brocchini, Italy
Julien Bruchon, France
Matteo Bruggi, Italy
Michele Brun, Italy
Maria Elena Bruni, Italy
Vasilis Burganos, Greece
Maria Angela Butturi, Italy
Raquel Caballero-Águila, Spain
Guillermo Cabrera-Guerrero, Chile
Filippo Cacace, Italy
Pierfrancesco Cacciola, United Kingdom
Salvatore Caddemi, Italy
zuowei cai, China
Roberto Caldelli, Italy
Alberto Campagnolo, Italy
Eric Campos, Mexico
Salvatore Cannella, Italy
Francesco Cannizzaro, Italy
Maosen Cao, China
Javier Cara, Spain
Raffaele Carli, Italy
Ana Carpio, Spain
Rodrigo Carvajal, Chile
Caterina Casavola, Italy
Sara Casciati, Italy
Federica Caselli, Italy
Carmen Castillo, Spain
Inmaculada T. Castro, Spain
Miguel Castro, Portugal
Giuseppe Catalanotti, United Kingdom
Nicola Caterino, Italy
Alberto Cavallo, Italy
Gabriele Cazzulani, Italy
Luis Cea, Spain
Fatih Vehbi Celebi, Turkey
Song Cen, China

Miguel Cerrolaza, Venezuela
M. Chadli, France
Gregory Chagnon, France
Ludovic Chamoin, France
Xiaoheng Chang, China
Ching-Ter Chang, Taiwan
Kuei-Lun Chang, Taiwan
Qing Chang, USA
Dr. Prasenjit Chatterjee, India
Kacem Chehdi, France
Peter N. Cheimets, USA
Chih-Chiang Chen, Taiwan
Xiao Chen, China
He Chen, China
Zhiwen Chen, China
Chien-Ming Chen, China
Xinkai Chen, Japan
Shyi-Ming Chen, Taiwan
Kebing Chen, China
Xue-Bo Chen, China
Xizhong Chen, Ireland
Zeyang Cheng, China
Qiang Cheng, USA
Luca Chiapponi, Italy
Ryoichi Chiba, Japan
Francisco Chicano, Spain
Nicholas Chileshe, Australia
Tirivanhu Chinyoka, South Africa
Adrian Chmielewski, Poland
Seongim Choi, USA
Ioannis T. Christou, Greece
Hung-Yuan Chung, Taiwan
Simone Cinquemani, Italy
Roberto G. Citarella, Italy
Joaquim Ciurana, Spain
John D. Clayton, USA
Francesco Clementi, Italy
Piero Colajanni, Italy
Giuseppina Colicchio, Italy
Vassilios Constantoudis, Greece
Francesco Conte, Italy
Enrico Conte, Italy
Alessandro Contento, USA
Mario Cools, Belgium
Gino Cortellessa, Italy
Juan Carlos Cortés, Spain
Carlo Cosentino, Italy

Paolo Crippa, Italy
Erik Cuevas, Mexico
Guozeng Cui, China
Maria C. Cunha, Portugal
Mehmet Cunkas, Turkey
Peter Dabnichki, Australia
Luca D'Acerno, Italy
Zhifeng Dai, China
Weizhong Dai, USA
Pei Dai, China
Purushothaman Damodaran, USA
Bhabani S. Dandapat, India
Giuseppe D'Aniello, Italy
Sergey Dashkovskiy, Germany
Adiel T. de Almeida-Filho, Brazil
Fabio De Angelis, Italy
Samuele De Bartolo, Italy
Abílio De Jesus, Portugal
Pietro De Lellis, Italy
Alessandro De Luca, Italy
Stefano de Miranda, Italy
Filippo de Monte, Italy
José António Fonseca de Oliveira Correia, Portugal
Jose Renato de Sousa, Brazil
Michael Defoort, France
Alessandro Della Corte, Italy
Laurent Dewasme, Belgium
Sanku Dey, India
Gianpaolo Di Bona, Italy
Angelo Di Egidio, Italy
Roberta Di Pace, Italy
Francesca Di Puccio, Italy
Ramón I. Diego, Spain
Yannis Dimakopoulos, Greece
Rossana Dimitri, Italy
Alexandre B. Dolgui, France
José M. Domínguez, Spain
Georgios Dounias, Greece
Bo Du, China
Z. Du, China
George S. Dulikravich, USA
Emil Dumic, Croatia
Bogdan Dumitrescu, Romania
Saeed Eftekhar Azam, USA
Antonio Elipe, Spain
Anders Eriksson, Sweden

R. Emre Erkmen, Canada
Francisco Periago Esparza, Spain
Gilberto Espinosa-Paredes, Mexico
Leandro F. F. Miguel, Brazil
Andrea L. Facci, Italy
Giovanni Falsone, Italy
Hua Fan, China
Nicholas Fantuzzi, Italy
Muhammad Shahid Farid, Pakistan
Hamed Faroqi, Iran
Mohammad Fattahi, Iran
Yann Favennec, France
Fiorenzo A. Fazzolari, United Kingdom
Giuseppe Fedele, Italy
Roberto Fedele, Italy
Zhongyang Fei, China
Mohammad Ferdows, Bangladesh
Arturo J. Fernández, Spain
Jesus M. Fernandez Oro, Spain
Massimiliano Ferraioli, Italy
Massimiliano Ferrara, Italy
Francesco Ferrise, Italy
Constantin Fetecau, Romania
Eric Feulvarch, France
Iztok Fister Jr., Slovenia
Thierry Floquet, France
Eric Florentin, France
Gerardo Flores, Mexico
Alessandro Formisano, Italy
FRANCESCO FOTI, Italy
Francesco Franco, Italy
Elisa Francomano, Italy
Juan Frausto-Solis, Mexico
Shujun Fu, China
Juan C. G. Prada, Spain
Matteo Gaeta, Italy
Mauro Gaggero, Italy
Zoran Gajic, USA
Jaime Gallardo-Alvarado, Mexico
Mosè Gallo, Italy
Akemi Gálvez, Spain
Rita Gamberini, Italy
Maria L. Gandarias, Spain
Xingbao Gao, China
Yan Gao, China
Hao Gao, Hong Kong
Shangce Gao, Japan

Zhong-Ke Gao, China
Zhiwei Gao, United Kingdom
Giovanni Garcea, Italy
José García, Chile
Luis Rodolfo Garcia Carrillo, USA
Jose M. Garcia-Aznar, Spain
Akhil Garg, China
Harish Garg, India
Alessandro Gasparetto, Italy
Gianluca Gatti, Italy
Oleg V. Gendelman, Israel
Stylianos Georgantzinis, Greece
Fotios Georgiades, India
Parviz Ghadimi, Iran
Georgios I. Giannopoulos, Greece
Agathoklis Giaralis, United Kingdom
Pablo Gil, Spain
Anna M. Gil-Lafuente, Spain
Ivan Giorgio, Italy
Gaetano Giunta, Luxembourg
Alessio Gizzi, Italy
Jefferson L.M.A. Gomes, United Kingdom
HECTOR GOMEZ, Chile
José Francisco Gómez Aguilar, Mexico
Emilio Gómez-Déniz, Spain
Antonio M. Gonçalves de Lima, Brazil
David González, Spain
Chris Goodrich, USA
Rama S. R. Gorla, USA
Veena Goswami, India
Xunjie Gou, Spain
Jakub Grabski, Poland
Antoine Grall, France
George A. Gravvanis, Greece
Fabrizio Greco, Italy
David Greiner, Spain
Jason Gu, Canada
Federico Guarracino, Italy
Michele Guida, Italy
Muhammet Gul, Turkey
Hu Guo, China
Jian-Ping Guo, China
Zhaoxia Guo, China
Dong-Sheng Guo, China
Quang Phuc Ha, Australia
Li Haitao, China
Petr Hájek, Czech Republic

Muhammad Hamid, United Kingdom
Shigeyuki Hamori, Japan
Xingsi Han, China
Zhen-Lai Han, China
Weimin Han, USA
Renke Han, United Kingdom
Thomas Hanne, Switzerland
Xinan Hao, China
Mohammad A. Hariri-Ardebili, USA
Khalid Hattaf, Morocco
Xiao-Qiao He, China
Yu-Ling He, China
Defeng He, China
Fu-Qiang He, China
salim HEDDAM, Algeria
Ramdane Hedjar, Saudi Arabia
Jude Hemanth, India
Reza Hemmati, Iran
Nicolae Herisanu, Romania
Alfredo G. Hernández-Diaz, Spain
M.I. Herreros, Spain
Eckhard Hitzer, Japan
Paul Honeine, France
Jaromir Horacek, Czech Republic
S. Hassan Hosseinnia, The Netherlands
Yingkun Hou, China
Xiaorong Hou, China
Lei Hou, China
Yunfeng Hu, China
Gordon Huang, Canada
Can Huang, China
Sajid Hussain, Canada
Asier Ibeas, Spain
Wubshet Ibrahim, Ethiopia
Orest V. Iftime, The Netherlands
Przemyslaw Ignaciuk, Poland
Muhammad Imran, Pakistan
Giacomo Innocenti, Italy
Emilio Insfran Pelozo, Spain
Alessio Ishizaka, France
Nazrul Islam, USA
Benoit Iung, France
Benjamin Ivorra, Spain
Breno Jacob, Brazil
Tushar Jain, India
Amin Jajarmi, Iran
Payman Jalali, Finland

Mahdi Jalili, Australia
Prashant Kumar Jamwal, Kazakhstan
Łukasz Jankowski, Poland
Fahd Jarad, Turkey
Samuel N. Jator, USA
Juan C. Jauregui-Correa, Mexico
Kandasamy Jayakrishna, India
Reza Jazar, Australia
Khalide Jbilou, France
Isabel S. Jesus, Portugal
Chao Ji, China
Linni Jian, China
Qing-Chao Jiang, China., China
Bin Jiang, China
Peng-fei Jiao, China
Ricardo Fabricio Escobar Jiménez, Mexico
Emilio Jiménez Macías, Spain
Xiaoliang Jin, Canada
Maolin Jin, Republic of Korea
Zhuo Jin, Australia
Dylan F. Jones, United Kingdom
Viacheslav Kalashnikov, Mexico
Mathiyalagan Kalidass, India
Tamas Kalmar-Nagy, Hungary
Zhao Kang, China
Tomasz Kapitaniak, Poland
Julius Kaplunov, United Kingdom
Konstantinos Karamanos, Belgium
Michal Kawulok, Poland
Irfan Kaymaz, Turkey
Vahid Kayvanfar, Iran
Krzysztof Kecik, Poland
Chaudry M. Khaliq, South Africa
Mukhtaj Khan, Pakistan
Abdul Qadeer Khan, Pakistan
Mostafa M. A. Khater, Egypt
MOHAMMAD REZA KHEDMATI, Iran
Kwangki Kim, Republic of Korea
Nam-Il Kim, Republic of Korea
Philipp V. Kiryukhantsev-Korneev, Russia
P.V.V Kishore, India
Jan Koci, Czech Republic
Ioannis Kostavelis, Greece
Sotiris B. Kotsiantis, Greece
Frederic Kratz, France
Vamsi Krishna, India
Kamalanand Krishnamurthy, India

Petr Krysl, USA
Edyta Kucharska, Poland
Krzysztof S. Kulpa, Poland
Kamal Kumar, India
Michal Kunicki, Poland
Cedrick A. K. Kwuimy, USA
Kyandoghere Kyamakya, Austria
Ivan Kyrchei, Ukraine
Davide La Torre, Italy
Márcio J. Lacerda, Brazil
Risto Lahdelma, Finland
Giovanni Lancioni, Italy
Jaroslaw Latalski, Poland
Antonino Laudani, Italy
Hervé Laurent, France
Agostino Lauria, Italy
Aimé Lay-Ekuakille, Italy
Nicolas J. Leconte, France
Kun-Chou Lee, Taiwan
Dimitri Lefebvre, France
Eric Lefevre, France
Marek Lefik, Poland
Gang Lei, Saudi Arabia
Yaguo Lei, China
Kauko Leiviskä, Finland
Thibault Lemaire, France
Ervin Lenzi, Brazil
Roman Lewandowski, Poland
Zhen Li, China
ChenFeng Li, China
Jun Li, China
Yang Li, China
Yueyang Li, China
Jian Li, USA
Jian Lin, China
Mingwei Lin, China
En-Qiang Lin, USA
Zhiyun Lin, China
Yao-Jin Lin, China
Bo Liu, China
Sixin Liu, China
Wanquan Liu, China
Yu Liu, China
Heng Liu, China
Yuanchang Liu, United Kingdom
Lei Liu, China
Jianxu Liu, Thailand

Bin Liu, China
Bonifacio Llamazares, Spain
Alessandro Lo Schiavo, Italy
Jean Jacques Loiseau, France
Francesco Lolli, Italy
Paolo Lonetti, Italy
Sandro Longo, Italy
António M. Lopes, Portugal
Sebastian López, Spain
Pablo Lopez-Crespo, Spain
Cesar S. Lopez-Monsalvo, Mexico
Luis M. López-Ochoa, Spain
Ezequiel López-Rubio, Spain
Vassilios C. Loukopoulos, Greece
Jose A. Lozano-Galant, Spain
Gabriele Maria Lozito, Italy
Songtao Lu, USA
Rongxing Lu, Canada
Zhiguo Luo, China
Gabriel Luque, Spain
Valentin Lychagin, Norway
Junhai Ma, China
Dazhong Ma, China
Antonio Madeo, Italy
Alessandro Magnani, Belgium
Toqeer Mahmood, Pakistan
Fazal M. Mahomed, South Africa
Arunava Majumder, India
Paolo Manfredi, Italy
Adnan Maqsood, Pakistan
Giuseppe Carlo Marano, Italy
Damijan Markovic, France
Filipe J. Marques, Portugal
Luca Martinelli, Italy
Rodrigo Martinez-Bejar, Spain
Guiomar Martín-Herrán, Spain
Denizar Cruz Martins, Brazil
Francisco J. Martos, Spain
Elio Masciari, Italy
Franck Massa, France
Paolo Massioni, France
Alessandro Mauro, Italy
Jonathan Mayo-Maldonado, Mexico
Fabio Mazza, Italy
Pier Luigi Mazzeo, Italy
Laura Mazzola, Italy
Driss Mehdi, France

Dr. Zahid Mehmood, Pakistan
YUE MEI, China
Roderick Melnik, Canada
Xiangyu Meng, USA
Debiao Meng, China
Jose Merodio, Spain
Alessio Merola, Italy
Mahmoud Mesbah, Iran
Luciano Mescia, Italy
Laurent Mevel, France
Constantine Michailides, Cyprus
Mariusz Michta, Poland
Prankul Middha, Norway
Aki Mikkola, Finland
Giovanni Minafò, Italy
Hiroyuki Mino, Japan
Dimitrios Mitsotakis, New Zealand
saleh mobayen, Taiwan, R.O.C., Iran
Nikunja Mohan Modak, India
Sara Montagna, Italy
Roberto Montanini, Italy
Francisco J. Montáns, Spain
Gisele Mophou, France
Rafael Morales, Spain
Marco Morandini, Italy
Javier Moreno-Valenzuela, Mexico
Simone Morganti, Italy
Caroline Mota, Brazil
Aziz Moukrim, France
Shen Mouquan, China
Dimitris Mourtzis, Greece
Emiliano Mucchi, Italy
Taseer Muhammad, Saudi Arabia
Josefa Mula, Spain
Jose J. Muñoz, Spain
Giuseppe Muscolino, Italy
Dino Musmarra, Italy
Marco Mussetta, Italy
Ghulam Mustafa, Pakistan
Hariharan Muthusamy, India
Hakim Naceur, France
Alessandro Naddeo, Italy
Benedek Nagy, Turkey
Omar Naifar, Tunisia
Mariko Nakano-Miyatake, Mexico
Keivan Navaie, United Kingdom
Adrian Neagu, USA

Erivelton Geraldo Nepomuceno, Brazil
Luís C. Neves, United Kingdom
AMA Neves, Portugal
Dong Ngoduy, New Zealand
Nhon Nguyen-Thanh, Singapore
Papakostas Nikolaos, Ireland
Jelena Nikolic, Serbia
Tatsushi Nishi, Japan
Shanzhou Niu, China
Xesús Nogueira, Spain
Ben T. Nohara, Japan
Mohammed Nouari, France
Mustapha Nourelfath, Canada
Kazem Nouri, Iran
Ciro Núñez-Gutiérrez, Mexico
Włodzimierz Ogryczak, Poland
Roger Ohayon, France
Krzysztof Okarma, Poland
Mitsuhiro Okayasu, Japan
Diego Oliva, Mexico
Alberto Olivares, Spain
Enrique Onieva, Spain
Calogero Orlando, Italy
Sergio Ortobelli, Italy
Naohisa Otsuka, Japan
Taoreed Owolabi, Nigeria
Cenap Özel, Turkey
Pawel Packo, Poland
Arturo Pagano, Italy
Roberto Palma, Spain
Alessandro Palmeri, United Kingdom
Pasquale Palumbo, Italy
Li Pan, China
Weifeng Pan, China
K. M. Pandey, India
Chandan Pandey, India
Jürgen Pannek, Germany
Elena Panteley, France
Achille Paolone, Italy
George A. Papakostas, Greece
Xosé M. Pardo, Spain
You-Jin Park, Taiwan
Manuel Pastor, Spain
Petr Páta, Czech Republic
Pubudu N. Pathirana, Australia
Surajit Kumar Paul, India
Sitek Paweł, Poland

Luis Payá, Spain
Alexander Paz, Australia
Igor Pažanin, Croatia
Libor Pekař, Czech Republic
Francesco Pellicano, Italy
Marcello Pellicciari, Italy
Bo Peng, China
Zhi-ke Peng, China
Xindong Peng, China
Zhengbiao Peng, Australia
Haipeng Peng, China
Jian Peng, China
Yuxing Peng, China
Mingshu Peng, China
Marzio Pennisi, Italy
Maria Patrizia Pera, Italy
Matjaz Perc, Slovenia
A. M. Bastos Pereira, Portugal
Ricardo Perera, Spain
F. Javier Pérez-Pinal, Mexico
Michele Perrella, Italy
Francesco Pesavento, Italy
Ivo Petras, Slovakia
Francesco Petrini, Italy
Hoang Vu Phan, Republic of Korea
Lukasz Pieczonka, Poland
Dario Piga, Switzerland
Antonina Pirrotta, Italy
Marco Pizzarelli, Italy
Javier Plaza, Spain
Goutam Pohit, India
Kemal Polat, Turkey
Dragan Poljak, Croatia
Jorge Pomares, Spain
Hiram Ponce, Mexico
Sébastien Poncet, Canada
Volodymyr Ponomaryov, Mexico
Jean-Christophe Ponsart, France
Mauro Pontani, Italy
Cornelio Posadas-Castillo, Mexico
Francesc Pozo, Spain
Aditya Rio Prabowo, Indonesia
Anchasa Pramuanjaroenkij, Thailand
Christopher Pretty, New Zealand
Leonardo Primavera, Italy
Luca Pugi, Italy
Krzysztof Puszynski, Poland

Goran D. Putnik, Portugal
Chuan Qin, China
Jianlong Qiu, China
Giuseppe Quaranta, Italy
Vitomir Racic, Italy
Ahmed G. Radwan, Egypt
Hamid Rahman, Pakistan
Carlo Rainieri, Italy
Kumbakonam Ramamani Rajagopal, USA
Venkatesan Rajinikanth, India
Ali Ramazani, USA
Angel Manuel Ramos, Spain
Higinio Ramos, Spain
Muhammad Afzal Rana, Pakistan
Amer Rasheed, Pakistan
Muhammad Rashid, Saudi Arabia
Manoj Rastogi, India
Alessandro Rasulo, Italy
S.S. Ravindran, USA
Abdolrahman Razani, Iran
Alessandro Reali, Italy
Jose A. Reinoso, Spain
Oscar Reinoso, Spain
Haijun Ren, China
X. W. Ren, China
Carlo Renno, Italy
Fabrizio Renno, Italy
Shahram Rezapour, Iran
Ricardo Riaza, Spain
Francesco Riganti-Fulginei, Italy
Gerasimos Rigatos, Greece
Francesco Ripamonti, Italy
Marcelo Raúl Risk, Argentina
Jorge Rivera, Mexico
Eugenio Roanes-Lozano, Spain
Bruno G. M. Robert, France
Ana Maria A. C. Rocha, Portugal
Luigi Rodino, Italy
Francisco Rodríguez, Spain
Rosana Rodríguez López, Spain
Alessandra Romolo, Italy
Abdolreza Roshani, Italy
Francisco Rossomando, Argentina
Jose de Jesus Rubio, Mexico
Weiguo Rui, China
Rubén Ruiz, Spain
Ivan D. Rukhlenko, Australia

Chaman Lal Sabharwal, USA
Kishin Sadarangani, Spain
Andrés Sáez, Spain
Bekir Sahin, Turkey
John S. Sakellariou, Greece
Michael Sakellariou, Greece
Salvatore Salamone, USA
Jose Vicente Salcedo, Spain
Alejandro Salcido, Mexico
Alejandro Salcido, Mexico
Salman saleem, Pakistan
Ahmed Salem, Saudi Arabia
Nunzio Salerno, Italy
Rohit Salgotra, India
Miguel A. Salido, Spain
Zabidin Salleh, Malaysia
Roque J. Saltarén, Spain
Alessandro Salvini, Italy
Abdus Samad, India
Nikolaos Samaras, Greece
Sylwester Samborski, Poland
Ramon Sancibrian, Spain
Giuseppe Sanfilippo, Italy
Omar-Jacobo Santos, Mexico
J Santos-Reyes, Mexico
José A. Sanz-Herrera, Spain
Evangelos J. Sapountzakis, Greece
Musavarah Sarwar, Pakistan
Marcelo A. Savi, Brazil
Andrey V. Savkin, Australia
Tadeusz Sawik, Poland
Roberta Sburlati, Italy
Gustavo Scaglia, Argentina
Thomas Schuster, Germany
Lotfi Senhadji, France
Junwon Seo, USA
Michele Serpilli, Italy
Joan Serra-Sagrasta, Spain
Silvestar Šesnić, Croatia
Erhan Set, Turkey
Gerardo Severino, Italy
Ruben Sevilla, United Kingdom
Stefano Sfarra, Italy
Mohamed Shaat, United Arab Emirates
Mostafa S. Shadloo, France
Dr. Zahir Shah, Pakistan
Kamal Shah, Pakistan

Leonid Shaikhet, Israel
Xingling Shao, China
Hao Shen, China
Xin Pu Shen, China
hang shen, China
Bo Shen, Germany
Dimitri O. Shepelsky, Ukraine
Weichao SHI, United Kingdom
Jian Shi, China
Suzanne M. Shontz, USA
Babak Shotorban, USA
Zhan Shu, Canada
Angelo Sifaleras, Greece
Nuno Simões, Portugal
Harendra Singh, India
Thanin Sitthiwiratham, Thailand
Seralthan Sivamani, India
S. Sivasankaran, Malaysia
Christos H. Skiadas, Greece
Konstantina Skouri, Greece
Neale R. Smith, Mexico
Bogdan Smolka, Poland
Delfim Soares Jr., Brazil
Alba Sofi, Italy
Francesco Soldovieri, Italy
Raffaele Solimene, Italy
Bosheng Song, China
Yang Song, Norway
Jussi Sopanen, Finland
Marco Spadini, Italy
Paolo Spagnolo, Italy
Bernardo Spagnolo, Italy
Ruben Specogna, Italy
Vasilios Spitas, Greece
Sri Sridharan, USA
Ivanka Stamova, USA
Rafał Stanisławski, Poland
Miladin Stefanović, Serbia
Florin Stoican, Romania
Salvatore Strano, Italy
Yakov Strelniker, Israel
Xiaodong Sun, China
Qiuye Sun, China
Qiuqin Sun, China
Zong-Yao Sun, China
Shuaishuai Sun, Australia
Suroso Suroso, Indonesia
Sergey A. Suslov, Australia
Nasser Hassen Sweilam, Egypt
Andrzej Swierniak, Poland
M Syed Ali, India
Andras Szekrenyes, Hungary
Kumar K. Tamma, USA
Yong (Aaron) Tan, United Kingdom
Marco Antonio Taneco-Hernández, Mexico
Hafez Tari, USA
Alessandro Tasora, Italy
Sergio Teggi, Italy
Ana C. Teodoro, Portugal
Efstathios E. Theotokoglou, Greece
Jing-Feng Tian, China
Alexander Timokha, Norway
Stefania Tomasiello, Italy
Gisella Tomasini, Italy
Isabella Torcicollo, Italy
Francesco Tornabene, Italy
Javier Martinez Torres, Spain
Mariano Torrisi, Italy
Thang nguyen Trung, Vietnam
Sang-Bing Tsai, China
George Tsiatas, Greece
Antonios Tsourdos, United Kingdom
Le Anh Tuan, Vietnam
Federica Tubino, Italy
Nerio Tullini, Italy
Emilio Turco, Italy
Ilhan Tuzcu, USA
Efstratios Tzirtzilakis, Greece
Filippo Ubertini, Italy
Marjan Uddin, Pakistan
Mohammad Uddin, Australia
Serdar Ulubeyli, Turkey
FRANCISCO UREÑA, Spain
Panayiotis Vafeas, Greece
Giuseppe Vairo, Italy
Jesus Valdez-Resendiz, Mexico
Eusebio Valero, Spain
Stefano Valvano, Italy
Marcello Vasta, Italy
Carlos-Renato Vázquez, Mexico
Miguel E. Vázquez-Méndez, Spain
Martin Velasco Villa, Mexico
Kalyana C. Veluvolu, Republic of Korea
Franck J. Vernerey, USA

Georgios Veronis, USA
Vincenzo Vespri, Italy
Renato Vidoni, Italy
Venkatesh Vijayaraghavan, Australia
Anna Vila, Spain
Francisco R. Villatoro, Spain
Francesca Vipiana, Italy
Stanislav Vitek, Czech Republic
Jan Vorel, Czech Republic
Michael Vynnycky, Sweden
Hao Wang, USA
Qingling Wang, China
Zenghui Wang, South Africa
C. H. Wang, Taiwan
Yong Wang, China
Guoqiang Wang, China
J.G. Wang, China
Zhenbo Wang, USA
Ji Wang, China
Shuo Wang, China
Yung-Chung Wang, Taiwan
Hui Wang, China
Zhibo Wang, China
Kang-Jia Wang, China
Yongqi Wang, Germany
Xinyu Wang, China
Weiwei Wang, China
Fu-Kwun Wang, Taiwan
Dagang Wang, China
Bingchang Wang, China
Roman Wan-Wendner, Austria
Fangqing Wen, China
P.H. Wen, United Kingdom
Waldemar T. Wójcik, Poland
Wai Lok Woo, United Kingdom
Zhizheng Wu, China
Zhibin Wu, China
QiuHong Wu, China
Changzhi Wu, China
Yuqiang Wu, China
Xianyi Wu, China
Michalis Xenos, Greece
hao xiao, China
Xue-Jun Xie, China
Xiao Ping Xie, China
Lei Xu, China
Qingzheng Xu, China

Lingwei Xu, China
Hang Xu, China
Zeshui Xu, China
Qilong Xue, China
Joseph J. Yame, France
Chuanliang Yan, China
Zhiguo Yan, China
Xinggong Yan, United Kingdom
Ray-Yeng Yang, Taiwan
Weilin Yang, China
Jixiang Yang, China
Mijia Yang, USA
Zhihong Yao, China
Min Ye, China
Jun Ye, China
Luis J. Yebra, Spain
Peng-Yeng Yin, Taiwan
Muhammad Haroon Yousaf, Pakistan
Yuan Yuan, United Kingdom
Qin Yuming, China
Abdullahi Yusuf, Nigeria
Akbar Zada, Pakistan
Elena Zaitseva, Slovakia
Arkadiusz Zak, Poland
Daniel Zaldivar, Mexico
Ernesto Zambrano-Serrano, Mexico
Francesco Zammori, Italy
Vittorio Zampoli, Italy
Rafal Zdunek, Poland
Ahmad Zeeshan, Pakistan
Ibrahim Zeid, USA
Nianyin Zeng, China
Bo Zeng, China
Junyong Zhai, China
Tongqian Zhang, China
Wenyu Zhang, China
Xuping Zhang, Denmark
Haopeng Zhang, USA
Jian Zhang, China
Kai Zhang, China
Xiaofei Zhang, China
Qian Zhang, China
Yinyan Zhang, China
Xianming Zhang, Australia
Hao Zhang, China
Yong Zhang, China
Tianwei Zhang, China



Lingfan Zhang, China
Yifan Zhao, United Kingdom
Yongmin Zhong, Australia
Zebo Zhou, China
Debao Zhou, USA
Jian G. Zhou, United Kingdom
Zhe Zhou, China
Quanxin Zhu, China
Wu-Le Zhu, China
Gaetano Zizzo, Italy
Zhixiang Zou, China


Contents

Environmental Systems Modelling and Analysis under Changing Conditions

Xander Wang , Aili Yang , Adam Fenech, and Huiyan Cheng




Editorial (2 pages), Article ID 9780860, Volume 2021 (2021)

Dynamic Evolution of Public's Positive Emotions and Risk Perception for the COVID-19 Pandemic: A Case Study of Hubei Province of China

Yongbao Zhang, Jingqi Gao, Xiaowei Luo, Xiang Wu , and Haoqi Bao

Research Article (14 pages), Article ID 6680303, Volume 2021 (2021)

Ecosystem-Based Adaptation for the Impact of Climate Change and Variation in the Water Management Sector of Sri Lanka

Bhabishya Khaniya , Miyuru B. Gunathilake , and Upaka Rathnayake 


Review Article (10 pages), Article ID 8821329, Volume 2021 (2021)

A Study on Evaluating Water Resources System Vulnerability by Reinforced Ordered Weighted Averaging Operator

Meiqin Suo , Jing Zhang, Lixin He , Qian Zhou, and Tengteng Kong

Research Article (9 pages), Article ID 5726523, Volume 2020 (2020)

A Birandom Chance-Constrained Linear Programming Model for CCHP System Operation Management: A Case Study of Hotel in Shanghai, China

Zhe Bao, Ye Xu , Wei Li, Xu Wang, Meng R. Li, Ji H. Li, and Han S. Yang


Research Article (16 pages), Article ID 1589415, Volume 2020 (2020)

Pricing Decisions in Closed-Loop Supply Chains with Competitive Fairness-Concerned Collectors

Yadong Shu , Ying Dai , and Zujun Ma 

Research Article (15 pages), Article ID 4370697, Volume 2020 (2020)

An Inexact Inventory Theory-Based Water Resources Distribution Model for Yuecheng Reservoir, China

Meiqin Suo , Fuhui Du, Yongping Li, Tengteng Kong, and Jing Zhang

Research Article (13 pages), Article ID 6273513, Volume 2020 (2020)

Editorial

Environmental Systems Modelling and Analysis under Changing Conditions

Xander Wang ^{1,2}, **Aili Yang** ³, **Adam Fenech**,^{1,2} and **Huiyan Cheng**³

¹Canadian Centre for Climate Change and Adaptation, University of Prince Edward Island, St Peters, Charlottetown, Canada

²School of Climate Change and Adaptation, University of Prince Edward Island, Charlottetown, Canada

³School of Environmental Science and Engineering, Xiamen University of Technology, Xiamen, China

Correspondence should be addressed to Xander Wang; xxwang@upeu.ca

Received 30 November 2021; Accepted 30 November 2021; Published 9 December 2021

Copyright © 2021 Xander Wang et al. This is an open access article distributed under the Creative Commons Attribution License, which permits unrestricted use, distribution, and reproduction in any medium, provided the original work is properly cited.

Environmental systems models are essential for understanding the dynamics and mechanisms of various environmental issues (e.g., air pollution, water pollution, floods, droughts, and climate change). Most importantly, they are widely used to predict future outcomes of environmental systems in support of effective decision making and policy development. However, most of the models are based on a stationary condition which by default assumes that no significant changes will occur in the future. It has been reported frequently in recent years that such a stationary assumption no longer holds in the context of global climate change and intensive human activities. Many boundary conditions and internal parameters in these models have been changed over time, which leads to considerable uncertainty in future prediction. Therefore, addressing the changing conditions in the process of environmental system modelling and analysis is becoming one of the most challenging issues in the field.

This special issue aims to collect recent advances in methodologies, models, tools, and applications for environmental systems modelling and analysis under changing and/or uncertain conditions, such as increasing temperature, changing precipitation patterns, sea-level rise, land cover/use change, urbanization, and policy changes. In this special issue, we have published 6 papers which involve a variety of modelling approaches to address the changing and uncertain conditions in environmental systems. A brief introduction for each paper is provided as follows.

The paper entitled “Dynamic Evolution of Public’s Positive Emotions and Risk Perception for the COVID-19

Pandemic: A Case Study of Hubei Province of China” by Zhang et al. investigates how the COVID-19 dynamic situation affects the public’s risk perception and emotions. The social risk amplification framework is first used as the theoretical basis to collect and analyze the COVID-19 data in Hubei Province, China from January 20, 2020, to April 8, 2020. The autoregressive integrated moving average based time-series prediction model is then adopted to analyze the dynamic evolution and fluctuation trends of public positive emotion and risk perception during the initial development of the pandemic. The methodological framework introduced in this study can be potentially used for understanding the rapid and dynamic evolution of public emotion and risk perception in similar catastrophic and uncertain situations.

The paper entitled “Ecosystem-Based Adaptation for the Impact of Climate Change and Variation in the Water Management Sector of Sri Lanka” by Khaniya et al. aims to showcase the effectiveness and benefits of utilizing the ecosystem-based adaptation approach to help protect the water sector in Sri Lanka from the changing climate. In particular, a wide range of benefits in water supply regulation, water quality regulation, and moderation of extreme events have been identified through the implementation of ecosystem-based adaptation approach in the water management sector in Sri Lanka. This case study for Sri Lanka can provide an important scientific reference for other nations around the world to develop adaptive water management measures in the context of climate change.

The paper entitled “A Study on Evaluating Water Resources System Vulnerability by Reinforced Ordered

Weighted Averaging Operator” by Suo et al. proposes a reinforced ordered weighted averaging operator by incorporating the extended ordered weighted average operator and principal component analysis into a multicriteria decision analysis framework. The proposed method is applied for assessing the vulnerability of a water resources system in Handan, China, in order to demonstrate its effectiveness in solving multicriteria decision analysis problems in environmental systems which usually involve multiple indicators and different weights.

The paper entitled “A Birandom Chance-Constrained Linear Programming Model for CCHP System Operation Management: A Case Study of Hotel in Shanghai, China” by Bao et al. proposes a birandom chance-constrained linear programming (BCCLP) model to help identify the optimal operation strategies for the combined cooling, heating, and power (CCHP) system under random uncertainties. The effectiveness of the proposed BCCLP model in handling the random uncertainties associated with the operation management of energy systems is demonstrated through a case study for a hotel-based gas-fired CCHP system in Shanghai, China.

The paper entitled “Pricing Decisions in Closed-Loop Supply Chains with Competitive Fairness-Concerned Collectors” by Shu et al. proposes a fairness concern utility system to help address the pricing issues in a closed-loop supply chain with one manufacturer, one retailer, and two competitive collectors. The influence of competitive strength and the degree of fairness-concerned collectors on the pricing decisions are studied through one centralized and four decentralized models. The methodological framework proposed in this study can be potentially used to help gain some managerial insights into the pricing decisions in environmental systems.

The paper entitled “An Inexact Inventory Theory-Based Water Resources Distribution Model for Yuecheng Reservoir, China” by Suo et al. proposes an inexact inventory theory-based water resources distribution model to help optimize the water allocation management practices. The proposed model integrates the techniques of inventory model, inexact two-stage stochastic programming, and interval-fuzzy mathematics programming into a general modelling framework to deal with multiple uncertainties and policy scenarios related to reservoir-based water allocation issues. A case study for the Yuecheng Reservoir in the Zhanghe River Basin, China, is conducted to demonstrate the effectiveness of the proposed model.

We hope that the readers will find this special issue interesting and the published papers will stimulate further research advancement in environmental systems modelling and analysis under changing and uncertain conditions.

Conflicts of Interest

We declare that there are no conflicts of interest regarding the publication of this special issue and this editorial.

Acknowledgments

We would like to thank all the authors for their contributions and all the reviewers for their valuable comments and feedback.

Xander Wang
Aili Yang
Adam Fenech
Huiyan Cheng

Research Article

Dynamic Evolution of Public's Positive Emotions and Risk Perception for the COVID-19 Pandemic: A Case Study of Hubei Province of China

Yongbao Zhang,¹ Jingqi Gao,¹ Xiaowei Luo,² Xiang Wu ,¹ and Haoqi Bao³

¹School of Engineering and Technology, China University of Geosciences, Beijing 100083, China

²College of Engineering, City University of Hong Kong, Hong Kong 999077, China

³School of Energy Engineering, Zhejiang University, Hangzhou 310058, China

Correspondence should be addressed to Xiang Wu; wuxiang@cugb.edu.cn

Received 13 October 2020; Revised 1 January 2021; Accepted 21 March 2021; Published 31 March 2021

Academic Editor: Xander Wang

Copyright © 2021 Yongbao Zhang et al. This is an open access article distributed under the Creative Commons Attribution License, which permits unrestricted use, distribution, and reproduction in any medium, provided the original work is properly cited.

The spread of COVID-19 pandemic and the participation of Internet information are continually changing the public's positive emotions and risk perception. However, relatively little is known about the underlying mechanism of how the COVID-19 dynamic situation affects the public's risk perception and emotions. This study uses the social risk amplification framework (SRAF) as the theoretical basis to collect and analyze Hubei Province data from January 20 to April 8, 2020, including the number of newly diagnosed people per day, the proportion of positive emotional posts in Weibo, and the Baidu search index (BSI). The autoregressive integrated moving average (ARIMA) based time-series prediction model is used to analyze the dynamic evolution laws and fluctuation trends of Weibo positive emotions and risk perception during the development of the pandemic. The conclusion of the study is that positive emotions are negatively correlated with risk perception, the severity of the pandemic situation is negatively correlated with positive emotions, and the severity of the pandemic situation is positively correlated with risk perception. The public has a keen response to the dynamics of the pandemic situation and the government's decision-making behavior, which is manifested by the significant changes in positive emotions and risk perception in the corresponding period. The research results can provide a reference for government departments to guide the public to establish an objective risk perception and maintain positive and stable emotions in similar catastrophes.

1. Introduction

So far, COVID-19 is still spreading around the world. Almost all countries and regions have adopted different forms and different levels of response measures, whether at the government, organization, or individual level [1]. Articles in the *Lancet*, an authoritative medical journal, prove that, in the process of responding to the COVID-19 pandemic, personal behavior is essential to control the spread of the virus [2]. The public's emotions and risk perceptions have been shown to significantly affect individual behavior [3], not only changing the normal working lifestyle of the public but also affecting the stability of social order [4].

Risk perception is an activity in which the public uses their intuition to conduct a risk assessment [5]. Human behavior and response depend on the risk they perceive [6]. The public's risk perception of COVID-19 is not only affected by external environments such as economic level, media reports, and government management [7] but also closely related to personal emotions and psychological states [8]. The greater perceived risk in a particular situation usually corresponds to more cautious behavior and more negative emotions [9]. The social risk amplification framework (SRAF) can reflect how emotional stability and prior preparation affect risk perception. It is believed that the interaction of emergencies with psychological, social, and cultural factors may weaken or amplify risk perception [10].

Perceived risk is an important driving force for the public to accept the government's epidemic prevention policies and adopt preventive behaviors. Inadequate government preparation and lack of effective supervision will lead to disastrous results [11]. Joel surveyed Twitter users in 12 countries during the epidemic and pointed out that, in crisis situations, social media plays an important role in monitoring public risk perception and guiding public communication [12]. Yan's research on Chinese people shows that, in the early stages of the pandemic, if social media promptly conveys information from the government and decision makers, it can guide people's behavior and minimize the losses caused by the pandemic [13].

In the context of the Internet era, the public's behavior choices in the event of a crisis are susceptible to the risk perception and emotional infection brought about by the large amount of information generated by social media in the short term. During the pandemic, especially in isolation and lockdown, the public's information sharing through social media has attracted more and more attention [12]. The public's understanding of the virus and the risks of the current pandemic are not clear enough, and each country is different. It even shows extreme cases of public overreaction and indifference to the crisis [14, 15]. Irrational activities during the pandemic are not conducive to effective self-protection by the public and have a great negative impact on the antipandemic activities of the entire society. To this end, it is important to keep abreast of the public opinion of the COVID-19 pandemic and accurately assess the dynamic evolution of positive emotional and risk perception in crises.

Similar to Twitter, Sina Weibo is the most widely used social networking platform in China and has become a place for gathering information [16]. It contains a large number of news hotspots and the emotional tendency of netizens and plays an important role in the spread of emergencies and other emergencies [17]. Baidu is the most popular search engine in China. Baidu search volume is not the exact search volume of a word, but the weighted sum of the query frequency of the word called Baidu search index (BSI) [18]. It is considered as a reflection of the user's attention to certain content [19]. Due to the huge influence, emergencies often attract the attention of the whole society in a short period, and there will be a sharp increase in related search volume and active comment areas in Weibo, Baidu, and other social media, forming a large number of complex and diverse data. In the past, the research on emotions mainly used questionnaires, and the results were often biased; the research on risk perception was mainly concentrated natural disasters such as typhoons and earthquakes, and the research methods were traditional; the time-series prediction research was mainly applied to the field of economics and finance, and quantitative comparisons of public's emotions were rarely conducted. For the above reasons, this study focuses on Hubei Province, China (one of the regions severely damaged by the pandemic), uses the number of newly diagnosed people every day to reflect the severity of the pandemic, uses Weibo posts to obtain public's positive emotions data, and uses BSI to reflect the degree of risk perception. Based on the analysis by SPSSAU online application software (version

20.0. <https://spssau.com>), this paper uses autoregressive integrated moving average (ARIMA) time-series prediction model to show the overall trend and abnormal changes and combined current news and Weibo comments for data analysis and interpretation.

In the context of the COVID-19 pandemic and community lockdown, it is of great significance to study the relationship and dynamic trends among the public's positive emotions, risk perception, and severity of the pandemic in Hubei Province. The data collection and data analysis methods of this study are novel and reasonable, and the results are quite convincing, which can provide references for similar disaster research. This research can scientifically and effectively analyze the positive emotions and risk perceptions of the public in Hubei Province in response to COVID-19 and provide theoretical basis and suggestions for government departments to guide the public to establish correct risk perceptions and maintain stable emotions during disasters.

2. Literature Review

2.1. Positive Emotions. Fredrickson believes that positive emotions are a person's unique response to things, and it is a temporary pleasure [20]. According to the theory of emotion cognition, emotions are given or set by human beings in the process of evolution to adapt to the environment [21]. Both positive and negative emotions have evolved gradually in response to an environment with existential threats and are closely related to certain events. Traditional emotion analysis technology is mainly based on natural language processing and machine learning. It determines the emotional orientation of the text by analyzing the relationship between emotional expression and the topic or using data to test and train the machine [22]. These methods require a lot of data and complex operations, so emotional research with the help of the Internet has gradually shown its own advantages.

With the rapid development of social media, social networks such as Twitter, Weibo, and Facebook are gradually changing people's lives. More and more people are willing to express their attitudes and emotions on social networks. Therefore, more and more researchers are applying the emotional theory of psychology to the emotional analysis of online texts. A nine-year study shows that Internet behavior can predict people's positive emotions [23]. On the basis of the Profile of Mood States (POMS) psychological scale, Pepe and Bollen constructed the POMS-1 scale suitable for Twitter research, which can measure the public's mental state from six aspects. They asked subjects to send e-mails to their future selves and analyzed subjects' attitudes towards the future from the emotions contained in the e-mails. Pepe and Bollen matched the vocabulary to the emotion words in the e-mail, and one point would be added when an emotional word appeared. A numerical value is obtained after accumulation, and the corresponding emotional index is obtained by standardization and other processing [24].

For the classification of emotions, Dong et al. used the relevant theory of emotional structure to create a basic social

emotion measurement vocabulary based in Weibo and divided basic social emotions into five categories: happiness, disgust, sadness, anger, and fear [25]. Watson and Tellegen summarized a “positive-negative emotion model,” that is, positive and negative emotions are two basic dimensions independent of each other [26]. For the measurement of emotion, Kim chose vocabulary matching technology to define the emotional tendency of the text by judging whether there was a vocabulary in the lexicon. Jiang et al. studied the expression and measurement of emotions in Weibo emoticons [27]. During the COVID-19 pandemic, the people of Hubei are under lockdown. The long-term community closure affects the public’s mental health [28]. However, there are few studies on public positive emotions in public health emergencies; thus, further research and analysis are needed. Based on the above, this study uses Internet tools to collect positive emotion data in Weibo during the COVID-19 pandemic, which can more scientifically and effectively analyze the dynamic changes of the public’s positive emotion in response to crisis events.

2.2. Risk Perception. Risk perception is a process in which the public judges the dangers of the external environment and makes relevant decisions based on their own subjective feelings about risks [5]. Research on risk perception originated from psychological research. Since then, due to frequent natural disasters and man-made accidents, risk perception and risk management research have become more closely linked. Starr found that people’s perception of risk not only is related to the evaluation of risk itself but also takes into account people’s subjective scales [29]. Fischhoff and Slovic obtained the risk preference and the trade-off standard between risk and return through questionnaire surveys and proposed a psychometric paradigm in the field of risk management [30], which greatly promoted and developed the research progress of risk perception.

Slovic et al. [31] believed that risk perception could be quantified and predicted through five levels, namely, frequency of death, subjective fatal estimation, potential for disasters, significance of death, and qualitative characteristics. Thirty years ago, Weinstein and Douglas explored the public’s risk perception of disaster events from the perspective of social-cultural theory paradigm and believed that the individual’s social background, cultural level, belief, and other factors are closely related to public risk perception [32]. Recent studies have shown that people’s perception of pandemic risk is influenced by factors such as personality traits, gender, media, economy, and government [33]. Generally speaking, people often rely on the news media as a source of information exchange to assess risks. Therefore, the media will influence their initial understanding of the disease. At the same time, values and culture are quietly affecting the pandemic prevention behaviors of different countries and regions [34]. Bronfman and Cifuentes used the individual roles, human benefits, and people’s fear of risk as measurement factors to explore the differences in risk perception among different groups [35]. Roberts explored the impact of panic on people’s risk perception by building-

related models [36]. Coyne studied the psychological effects of the combined effect of the subjective and objective emotions of the affected population under stress. It is believed that the postdisaster emergency response emotion is the main factor causing the psychological fluctuations of the affected people [37]. Recent studies have shown that the attention and emotional expression of the epidemic information in Twitter can be used to describe the public’s risk perception of COVID-19 [12]. Tang analyzed and calculated the public’s perception of social risks based on the Baidu Search Index (BSI) [38]. In order to quantitatively study the public’s risk perception of COVID-19, we applied this method to express the risk perception with the frequency of online searches.

In summary, most current research studies believe that risk perception is one of the important driving factors of behavioral decision-making, and the influence of the emotions of disaster-affected groups on risk perception and behavior has also become the research direction of some scholars. In the context of such a serious global pandemic, a comprehensive exploration of public’ risk perceptions and emotions has more theoretical and practical significance.

2.3. Social Risk Amplification Framework (SRAF). Kasperson first puts the effect of risk communication under the social background to conduct research, revealing the nature of risk and quantifying its level from the perspective of information dissemination network and public response. He proposed that, in the process of communication from the source of information to the dissemination intermediary and then to the recipient of the information, the signal would increase or decrease, and the information content would also be distorted to a certain extent. This phenomenon is defined as the social amplification effect of risk in the field of risk communication and is also called as the social risk amplification framework (SRAF). SRAF can help to explain the two stages of information. The first stage focuses on transmitting the information to the amplification station, conducting social awareness understanding and impact assessment, and then taking action. The second stage is the reaction and influence mechanism within the society [39].

In real life, the SRAF of risk perception usually leads to adverse consequences. It can enlarge or reduce the unknown risks and potential threats caused by accidents, pollution, and outbreaks. The impact of the amplification process of risk perception sometimes exceeds the direct impact of the disaster itself. The SRAF has an important impact on the dissemination of disaster warning information at the level of emergency evacuation strategies and, therefore, has become a major research focus in the current risk management field. Through the study of dangerous information flow and risk perception, Lindell and Perry built a decision-making model of individual protection behavior and identified the three-stage decision-making process of public protection behavior [40]. In addition, they also analyzed the family structure of people in multihazard areas and explored the internal relationship among it, individual risk perception, and protective behavior decision-making [41].

The SRAF can reflect how emotional stability and preparation affect risk perception. It is believed that the interaction of emergencies and psychological, social, cultural, and other factors may weaken or amplify risk perception. If the risk perception is amplified, it indicates that the individual has lower emotional stability, which is characterized by anxiety, aggression, and pessimism; on the contrary, the decrease of risk perception shows higher characteristics of emotional stability, such as optimism and calm. At the same time, emotional stability and preparation are complementary. Higher emotional stability enables individuals to prepare and respond to emergencies more fully [10] and respond positively and optimistically to disasters.

2.4. ARIMA Time-Series Analysis. ARIMA time-series analysis is a method for processing dynamic data in chronological order based on the recorded data. It relies on curve fitting and parameter estimation to analyze its trend over time, investigate its own statistical laws, and then predict the future value of the target [42]. The ARIMA time-series prediction model is also denoted as ARIMA (p, d, q). The ARIMA (p, d, q) model is a summed autoregressive moving average model, where p is the number of autoregressive terms, q is the number of moving average terms, and d is the number of differences made to make the original sequence stationary. To find the best model prediction result, it is necessary to use the principle of minimum Akaike information criterion (AIC) value, through statistical analysis, to obtain the optimal prediction of the future value of the sequence.

Time-series analysis has been widely used in finance, climate change, industrial production, and other fields. Li et al. performed time-series analysis and modeling of aerosols between the United States and China from 2003 to 2015. The results showed that ARIMA had a good prediction ability for time-series with significant seasonality [43]. Perzyk et al. took the product temperature in the factory as an example to conduct time-series prediction analysis and detect and quantitatively evaluate the overall trend, periodicity, and amplitude of parameter changes [44]. Narayanan et al. used ARIMA time-series analysis to study the trend of premonsoon precipitation in western India [45]. Singh et al. used the death toll data of five countries with severe COVID-19 outbreaks to establish a comprehensive prediction model based on ARIMA time series [46]. Coincident with this article, we all hope that the forecast results can help the government take countermeasures in advance.

3. Method

This section gives a detailed introduction to the sources of the research data and analysis methods. First, select the research period and object according to the objective reality and obtain the original data from Weibo, Baidu, official website of the National Health Commission of China, and other platforms, respectively, and then classify the emotion of Weibo to select posts with public's positive emotions.

Then, the three variables, the proportion of positive emotional posts, the BSI, and the daily increase in the number of diagnoses, were analyzed by correlation and ARIMA time-series prediction. Under the SRAF framework, the dynamic changes of the public's positive emotions and risk perception during the global pandemic are explored.

3.1. Research Subjects and Research Period. This study selects Weibo users in Hubei Province, China, as the analysis subjects, for the following reasons. First, within the territory of China, COVID-19 was first discovered in the South China Seafood Wholesale Market in Wuhan, Hubei. Second, Hubei Province is the hardest hit by the COVID-19 pandemic in China. The Hubei Weibo data collected in this study take January 20, 2020, as the starting time. From that day on, the National Health Commission of China began to publish the national (province) pandemic data, taking April 8, 2020, as the deadline, and on that day, Wuhan City, Hubei Province, announced the lifting of the city blockade.

3.2. Data Collection

3.2.1. The Proportion of Positive Emotional Posts in Weibo. This research used the advanced search function of Sina Weibo (version 10.6.2) to search for all original posts with the keyword "COVID-19" from January 20, 2020, to April 8, 2020, in Hubei area in units of days, and 20 samples were taken evenly every day using systematic sampling techniques. The total samples include 1600 Weibo posts for 80 days. Take January 20, 2020, as an example to introduce the Weibo sampling process. Firstly, we set the time period from 0:00 on January 20, 2020, to 0:00 on January 21, 2020, entered the keyword "COVID-19," the limited area is Hubei, the post type is original, and the search results in a total of 974 Weibo posts, $N=947$, and numbered from top to bottom. Secondly, in order to ensure that the daily sample is representative, 20 posts were selected at regular intervals from 947 Weibo posts, $n=20$. According to the formula $k=N/n$, the number of intervals for extracting Weibo is calculated, and the interval $k=49$ ($974/20=48.7$, take an integer). Finally, the extraction is performed at an interval of 49, and finally, 20 Weibo posts are extracted.

Refer to Dong's microblog-based basic social emotion measurement vocabulary for emotion classification, which divides 818 words into five basic social emotions: happiness, sadness, disgust, anger, and fear [25]. According to the positive-negative emotion model proposed by Watson and Tellegen, the above five basic social emotions are divided into positive and negative emotions.

Emotional classification of extracted Weibo posts: if happy emotions such as "Happy" and "Relief" are found in the post, we add 1 to the value of positive emotions (statistics in positive emotions); if we find words such as "sarcasm," "confused," and "panic," we add 1 to the value of negative emotions (statistics in negative emotions) [16]. Finally, the positive and negative Weibo values are accumulated, and the proportion of positive emotional posts in Weibo is calculated. What needs to be emphasized is that when dividing

emotions if the following two posts that are not suitable for cooperation in this research are statistically required, then select nearby posts as a substitute. The principle of substitution is to give priority to the data below the invalid Weibo and then consider the above, until the Weibo posts of a certain emotion is judged. The details are as follows:

- (1) If there are no obvious emotion words or multiple emotion words in the Weibo posts, which cannot determine the specific emotion of the Weibo posts, then select other nearby Weibo posts instead
- (2) Since this study mainly discusses the public's views on COVID-19, the Weibo posts published by newspapers, media, government, and other subjects are not the public's emotional expression, so they are not included in the statistics, and other Weibo posts in the vicinity will be selected instead

3.2.2. Baidu Search Index (BSI). Baidu News hot word search engine platform provides daily BSI. This study draws on the frequency of online search behavior proposed by Tang and Xu to express risk perception [19, 38] and uses Baidu News hot word search engine to retrieve the keyword "COVID-19."

The search time is from January 20 to April 8, 2020, and the tool is Baidu News hot word search engine "PC terminal + mobile terminal" (<http://index.baidu.com>). By using the search volume of Hubei Province netizens on Baidu website as the database and COVID-19 as the object, scientifically analyze and calculate the frequency of the COVID-19 search in Baidu web search, weighted and standardized to obtain BSI, which can be used to express the level of daily public's risk perception.

3.2.3. The Daily Increase in the Number of Diagnoses. The number of newly confirmed cases is a key factor in measuring the severity of the pandemic [47]. This study counted the newly diagnosed people every day in Hubei Province published by the official website of the National Health Commission of China (<http://www.nhc.gov.cn>) from January 20 to April 8, 2020. The number of newly diagnosed people every day is used to reflect the severity of the COVID-19 pandemic.

3.2.4. Data Summary. After 80 days of statistics and sorting, the original data of the proportion of positive emotional posts in Weibo, the Baidu Search Index (BSI), and the number of newly diagnosed people per day are formed. The original data are the basis for subsequent analysis and drawing. However, it is not difficult to find from the original data that the largest value is BSI, which is 83928, and the smallest value is the proportion of positive emotions, which is 20%. The range of data on the proportion of positive emotional posts, the BSI, and the number of newly diagnosed persons per day is very large. In order to better horizontal comparison and linear regression analysis, the data were standardized by z -score.

For example, when displaying the trend of three variables in a graph or performing linear regression analysis, the standardized data are used. The principle of the z -score standardization method is to rely on the standard deviation and the mean of the original data for standardization. It is the most common standardization method by default in SPSSAU online statistical analysis software (version 20.0, <https://spssau.com>). The conversion result retains four decimal places. After standardization, the proportion of positive emotional posts in Weibo is used to reflect the public's positive emotions, the BSI is used to reflect the risk perception level, and the number of newly diagnosed people is used to reflect the severity of the pandemic.

3.3. Data Analysis Methods

3.3.1. Correlation Analysis. In this study, SPSSAU online analysis software (<https://spssau.com>) was used to conduct a correlation analysis. The analysis factor is the raw data of the three sets of variables: the proportion of positive emotional posts, the BSI, and the number of newly diagnosed people every day.

3.3.2. Linear Regression Analysis. Linear regression analysis is a method of predicting the future value of a random variable related to it based on the change of one or a group of independent variables. Regression analysis needs to establish a regression equation describing the correlation between variables. If the regression function is a linear function, it is said that the variables are linearly related. This three-group linear analysis is one-variable linear regression analysis, including two variables, one is the independent variable and the other is the dependent variable. When performing the linear regression analysis, it is more appropriate to use standardized data.

In the F test method of linear regression analysis, the adjusted R^2 is used to indicate the degree of explanation of the independent variable to the dependent variable; the standardized coefficient indicates the coefficient of the independent variable in the regression equation, and the larger the value, the greater the impact on the independent variable 'Larger'. The F value is the result of analysis of variance, which is used to summarize the significance of the regression equation. The p value corresponding to the F value is less than 0.05, and it is considered that there is a correlation between the two variables; the closer the value is to 0, the better the correlation is.

3.3.3. ARIMA-Based Time-Series Prediction Model. ARIMA is a general time-series prediction model. As a data mining tool, time series helps researchers to better understand the nature of the development process of things and can predict the future value of variables based on historical data recorded in chronological order [48].

During the COVID-19 pandemic, public's positive emotions and risk perception will fluctuate greatly as the pandemic develops. In order to explain and predict this kind

of fluctuations, this study introduces the ARIMA time-series prediction model to visually show the changing laws and fluctuation trends of positive emotions and risk perception. In the model, the fitted value in a different period is compared with the real value, and the objective reasons that affect its change are analyzed according to the objective event.

3.3.4. Explanatory Analysis of Emotional and Risk Perception of Online News/Weibo Viewpoints of Obviously Changing Nodes. The explanatory analysis focuses on the positive emotions in Weibo and BSI during the pandemic. On the basis of ARIMA time-series prediction results, in order to further explore the reasons for the significant changes in positive emotions and risk perception, we conducted an explanatory analysis of the rear performance and fitting results of these two variables.

In view of the four objective situations of low positive emotions, high positive emotions, high degree of risk perception, and low degree of risk, we calculated and selected the time periods with the largest deviation between the true value and the fitted value. Then, we collected major news events and pandemic dynamics that may affect emotions and risk perception in this period and explored whether these news events and pandemic dynamics can significantly affect the changes in emotion and risk perception.

4. Results

This section uses the research methods provided above to organize and analyze the data. Firstly, we used SPSSAU to perform basic analysis such as standardization and normality test on the data, then performed correlation and linear regression analysis, and drew the change trend graph of the three sets of variables. In addition, the ARIMA time-series prediction model is used to fit and predict the proportion of positive emotional posts in Weibo and BSI. Finally, we combined major news events and pandemic dynamics during the pandemic to explain and analyze the actual causes of significant fluctuations in public emotions and risk perception.

4.1. Normality Test. Perform normality test analysis on the number of newly confirmed cases, the BSI, and the proportion of positive emotional posts. Because the samples of the three sets of data are larger than 50 samples, the *K-S* test method is selected. In detail, the number of newly confirmed cases, the Baidu search index, and the proportion of positive emotion microblogs all show significant ($p < 0.05$), which means the number of newly confirmed cases, the BSI, and the proportion of positive emotional posts do not have the characteristics of normality as shown in Table 1.

4.2. Correlation Analysis of the Number of Newly Confirmed Cases, the BSI, and the Proportion of Positive Emotional Posts. Through the preliminary analysis of SPSSAU, it is found that the three sets of data in this study do not have the

characteristic of normality, so the Spearman correlation coefficient is used to indicate the strength of the correlation. The results of the correlation analysis are shown in Table 2.

The correlation analysis results show that the three sets of data are significant at the 0.01 level, which proves that there is a strong correlation between the number of newly confirmed cases, the BSI, and the proportion of positive emotional posts.

4.3. Linear Regression Analysis

4.3.1. Linear Regression Analysis of Positive Emotion and Risk Perception. According to the correlation analysis results and literature data, we take the standardized proportion of positive emotions as the independent variable and the standardized BSI, namely, risk perception, as the dependent variable and perform linear regression analysis. The analysis results are shown in Table 3.

Linear regression analysis found that the R^2 value of the model is 0.651, which means that the proportion of positive emotional posts in Weibo can explain the 65.1% change in risk perception. The model passed the *F* test ($F = 145.576$ and $p \leq 0.001$), which means that the proportion of positive emotions will affect risk perception. The model formula is $BSI = 0.000 - 0.807 * \text{proportion of positive emotions}$.

The regression coefficient value of the proportion of positive emotional posts in Weibo is -0.807 ($t = -12.065$ and $p \leq 0.001$), which can be summarized as the proportion of positive emotional posts in Weibo has a significant negative correlation with risk perception.

4.3.2. Linear Regression Analysis of the Severity of the Pandemic Situation and the Proportion of Positive Emotional Posts. Using the same method as the above linear regression analysis, the number of newly diagnosed cases after standardization, that is, the severity of the pandemic was used as the independent variable, and the proportion of positive emotional posts in Weibo was the dependent variable. Linear regression analysis was performed. The R^2 value of the model is 0.228, which means that the severity of the pandemic can explain the reason for the change of 22.8% of the proportion of positive emotions. The model passed the *F* test ($F = 22.984$ and $p \leq 0.001$), which means that the severity of the pandemic will affect the proportion of positive emotional posts in Weibo. The model formula is the proportion of the positive emotional posts = $0.000 - 0.477 * \text{the number of newly diagnosed people}$.

The regression coefficient of the severity of the pandemic is -0.477 ($t = -4.794$, $p \leq 0.001$), which can be summarized as follows: the severity of the pandemic has a significant negative correlation with the proportion of the positive emotional posts in Weibo.

4.3.3. Linear Regression Analysis of the Severity of Pandemic and Risk Perception. Using the same method as the above linear regression analysis, the number of newly confirmed cases after standardization, that is, the severity of the

TABLE 1: The results of normality test.

	Sample	Mean	Std	Skew	Kurtosis	K-S		S-W	
						Statistic	<i>p</i>	Statistic	<i>p</i>
The number of newly confirmed cases	80	860.638	1877.408	5.543	39.274	0.323	0.000**	0.458	0.000**
BSI	80	26560.63	17845.89	1.206	1.03	0.184	0.000**	0.862	0.000**
The proportion of positive emotional posts	80	0.527	0.231	0.081	-1.478	0.156	0.000**	0.901	0.000**

p* < 0.05 and *p* < 0.01.

TABLE 2: The Spearman correlation analysis results.

	The number of newly confirmed cases	BSI	The proportion of positive emotional posts
The number of newly confirmed cases	1	—	—
BSI	0.870**	1	—
The proportion of positive emotional posts	-0.869**	-0.908**	1

Note. **p* < 0.05 and ***p* < 0.01..

TABLE 3: Linear regression analysis results of the perception positive emotional posts and risk perception.

Linear regression analysis results (<i>n</i> = 64)									
	Unstandardized coefficient		Standardized coefficient	<i>t</i>	<i>p</i>	VIF	<i>R</i> ²	Adjust <i>R</i> ²	<i>F</i>
	<i>B</i>	Standard deviation							
Constant	0.000	0.066	—	0.000	1.000	—			<i>F</i> (1,78) = 145.576, <i>p</i> ≤ 0.001
The proportion of positive emotional posts	-0.807	0.067	-0.807	-12.065	≤0.000**	1.000	0.651	0.647	

Note. Dependent variable: BSI; D-W value: 0.549. **p* < 0.05 and ***p* < 0.01.

pandemic was used as the independent variable, and the standardized BSI, that is, risk perception, as the dependent variable, was used for linear regression analysis. The *R*² value of the model is 0.123, which means that the severity of the pandemic can explain the 12.3% change in risk perception. The model passed the *F* test (*F* = 10.926 and *p* ≤ 0.001), which means that the severity of the pandemic will affect the risk perception. The model formula is risk perception = -0.000 + 0.351 * the severity of the pandemic.

The regression coefficient of the severity of the pandemic is 0.351 (*t* = 3.305 and *p* ≤ 0.001), which can be summarized as the severity of the pandemic has a significant positive correlation with risk perception.

4.4. *The Overall Trend of the Proportion of Positive Emotional Posts, the Number of Newly Diagnosed People, and the BSI.* Use SPSSAU to process the standardized proportion of positive emotional posts, the number of newly diagnosed people, and the BSI and draw the changing trend, as shown in Figure 1.

As can be seen in figure 1, the relationship between the three variables generally conforms to the laws derived from the above study, that is, the proportion of positive emotional posts has a significant negative correlation with risk perception, the severity of the pandemic has a significant negative correlation with the proportion of positive emotional posts, and the severity of the pandemic has a significant positive correlation with risk perception.

However, there are abnormal fluctuations in certain periods, indicating a sudden change in public's emotions and risk perception. The reasons for these mutations will be explained objectively below.

4.5. *ARIMA Time-Series Prediction Results.* In order to explore the deep-seated reasons that affect emotion and risk perception, this paper carries out ARIMA time-series analysis. The model used to predict the proportion of positive emotional posts in Weibo, also the fitting value of BSI, and calculate the deviation of the real value from the fitting value to reflect the fluctuation degree of emotion and risk perception. Figures 2 and 3 are plotted based on the data of the real and fitted values.

4.6. *Explanatory Analysis of Emotional and Risk Perception of Online News/Weibo Viewpoints of Obviously Changing Nodes.* This section focuses on the proportion of positive emotional posts in Weibo and the BSI during the pandemic. In order to perform an explanatory analysis on the real performance and the fitted results, the point when the real value and the fitted value were significantly different was found, and major news events and Weibo posts that may affect emotion and risk perception were also collected at the time.

4.6.1. *Explanatory Analysis of Positive Emotional Fluctuations. (1) Low Positive Emotions.* According to the result of prediction and analysis in figure 2 by ARIMA,

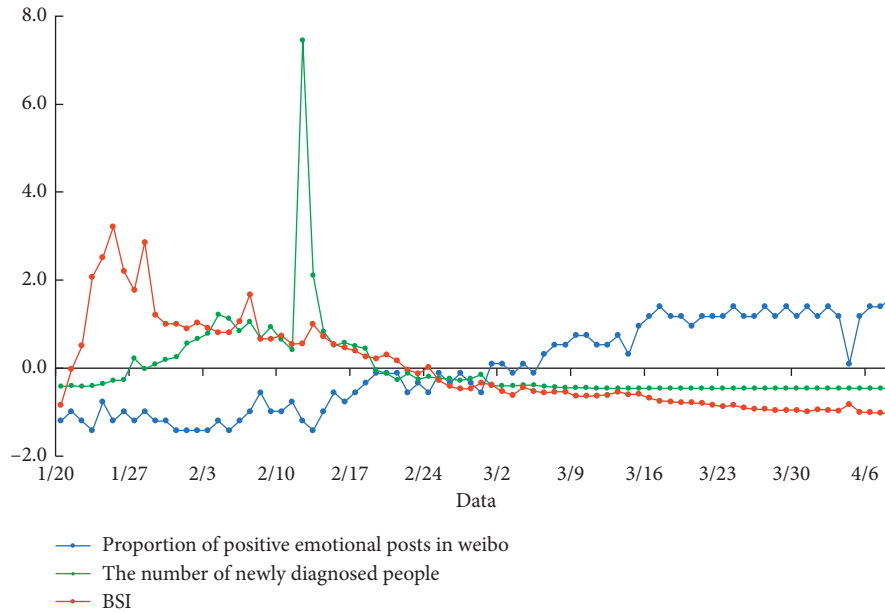


FIGURE 1: Change trend of the proportion of positive emotional posts, the number of newly diagnosed people, and the BSI.

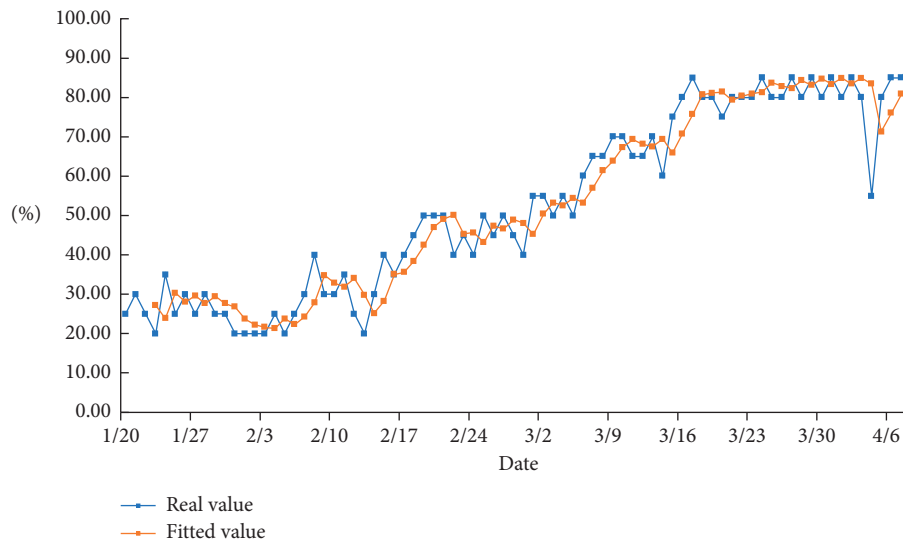


FIGURE 2: Simulated fitting trend graph of the proportion of positive emotional posts.

we selected five days in which the real value of the positive emotions in the Weibo posts was most significantly lower than the fitted value, which is collated in Table 4.

Searching and sorting out the pandemic situation and major news events at the corresponding time points, we found several events as described below. Wuhan blocked the city on January 23; the number of newly diagnosed people per day surged on February 12; many doctors such as Peng Yinhua and Liu Zhiming died on February 22 due to COVID-19; the WHO raised the pandemic risk level on February 29; National Mourning Day was observed on April 4. News events and pandemic dynamics are associated with fluctuations in positive emotions. From the news events shown in Table 4 and above, the real value of

the proportion of positive emotional posts is significantly lower than the fitted value, and the public's emotions show a more negative trend, in line with the above analysis. The surge in the number of infected people during the pandemic and the news of the spread of the pandemic will cause the public to panic, the published Weibo views become pessimistic, and the real value of the positive emotion ratio is significantly lower than the fitted value.

(2) *High Positive Emotions.* According to the result of prediction and analysis in figure 2 by ARIMA, we selected five days in which the real value of the positive emotion in Weibo posts was most significantly higher than the fitted value, which is collated in Table 5.

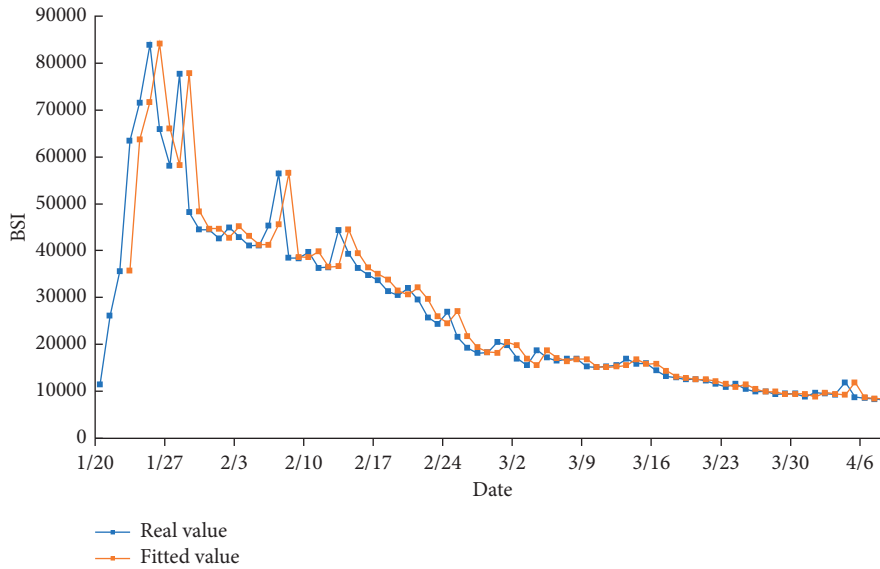


FIGURE 3: Simulated fitting trend graph of BSI.

Searching and sorting out the pandemic situation and major news events at the corresponding time points, we found the Raytheon Mountain Hospital was put into use on February 8; the potential drug “Favipiravir” was approved for listing on February 14–15; the major square cabin hospitals were closed on March 6–10; on March 16–18, there were no newly diagnosed cases in Wuhan; Wuhan lifted the city blockade on April 8. News events and pandemic dynamics are associated with fluctuations in positive emotions. Every positive action and research progress of the government and scientific research institutions, as well as the news events of the weakened pandemic, will make the public more optimistic and publish more positive opinions in Weibo. As shown in Table 5, the real value of the positive Weibo ratio is significantly higher than the fitted value, and the public’s emotions show a significantly positive state, which is consistent with the analysis of the objective facts above. It can be concluded from this that news reports will have a great influence on the fluctuation of public’s emotion, and the positive information disseminated by the government and the media will play a vital role in stabilizing public’s emotion.

4.6.2. Explanatory Analysis of BSI

(1) High BSI. According to the result of prediction and analysis in ure 3 by ARIMA, we selected three days in which the real value in BSI is most significantly lower than the fitted value, which is collated in Table 6.

Searching and sorting out the pandemic situation and major news events at the corresponding time points, we found Wuhan blocked the city on January 23; the WHO raised the pandemic risk level on February 29; and National Mourning Day was observed on April 4. The occurrence of the above incidents has caused extensive searches by netizens, and people’s perception of risk has been significantly improved. Comparing the data of the proportion of positive

TABLE 4: Period data with a low proportion of positive emotional posts.

Data	Real value (%)	Fitted value (%)	Deviation	Symbol
1/23	20.00	27.27	36.33	—
2/12	25.00	34.07	36.27	—
2/22	40.00	50.14	25.34	—
2/29	40.00	48.10	20.26	—
4/4	55.00	83.47	51.76	—

Note. (1) Deviation = |real value-fitted value|/real value [49], which is used to reflect the degree of difference between the real value and the fitted value and to find out the period when the abnormal value occurs. (2) The symbol reflects the relationship between the real value and the fitted value. If the real value is greater than the fitted value, the column of the symbol is “+;” otherwise, it is “-.” (3) The percentages here are kept to two decimal places. (4) Tables 5–7 are the same as Table 4.

TABLE 5: Period data with a high proportion of positive emotional posts.

Data	Real value (%)	Fitted value (%)	Deviation	Symbol
2/8	40.00	27.86	30.35	+
2/14	30.00	25.13	16.23	+
3/6	60.00	53.20	11.33	+
3/16	80.00	70.80	11.50	+
4/8	90.00	83.51	7.21	+

TABLE 6: Data with high BSI period.

Data	Real value	Fitted value	Deviation	Symbol
1/23	63502	35747	43.71	+
2/29	20507	18235	11.08	+
4/4	11943	9252	22.53	+

emotional posts in Weibo in the same period, the real value of the three-day data is significantly lower than the fitted value, and the emotion tends to be negative. This finding also validates the research conclusion of Bhandari and Hallowell

[50], namely, positive emotions will make the public underestimate the perceived risks, negative emotions will increase people's risk perception, and the proportion of positive emotional posts has a negative correlation with risk perception.

(2) *Low BSI*. According to the result of prediction and analysis in ure 3 by ARIMA, we selected three days in which the real value in BSI is most significantly higher than the fitted value, which is collated in Table 7.

Searching and sorting out the pandemic situation and major news events at the corresponding time points, we found Raytheon Mountain Hospital was put into use on February 8th; IgM/IgG antibody rapid test kit was put into use on February 14-15, and the potential drug "Favipiravir" was approved for listing on the same day; on March 16th to 18th, the first batch of Chinese National Aid Medical Team returned, and there were no newly diagnosed people in Wuhan. The government's positive measures and scientific research progress have reduced people's perception of risk, and the frequency of online searches has been reduced. It can be seen from Table 7 that the corresponding BSI has decreased over the past few days, which is lower than the fitted value. Besides, these days are also days when the proportion of positive emotional posts in Weibo is high, and people's emotions are very positive. From this, we can draw a conclusion similar to Choi [51] and Duan et al. [52]. Government actions and authoritative media reports will affect people's perception of risk. Accordingly, the BSI will change greatly. The government and authoritative media will play a critical role in reducing the public's perception of risk.

5. Discussion

Although the research on emotion or risk perception has been quite in-depth in many fields, we believe that, in the context of such a severe COVID-19 pandemic, it is still relatively novel and of great significance to comprehensively analyze the public's positive emotions and risk perception. Hubei, as the region with the worst pandemic in China, has basically returned to normal living order. However, the world is still in the battle for a long time with COVID-19 [53]. The pandemic information on the Internet and reality will affect the public's emotions and risk perceptions, which in turn will affect individuals and even social behavior. Therefore, based on network data, this article studies the public's positive emotions and risk perceptions during the pandemic situation and supplements and improves the viewpoints of previous studies, to provide a useful reference for the analysis of public psychology and behavior under such sudden disasters.

5.1. Discussion of Research Methods and Processes. In recent years, content platform monitoring and prediction of pandemic diseases through search engines and social networks have become a hot research area. Most of the research is based on search data from Twitter [54] and Google [55], but few are conducted through Baidu and Sina Weibo. This

TABLE 7: Data with low BSI period.

Data	Real value	Fitted value	Deviation (%)	Symbol
2/8	38461	56576	47.10	—
2/14	39332	44515	13.18	—
3/16	14468	15918	10.02	—

research integrates multidisciplinary knowledge, uses the SRAF, searches keywords through Weibo to obtain positive emotion data, and uses BSI to obtain risk perception data. Compared with the questionnaire survey, the number of survey target groups is larger, and the scope is wider. The research target can cover the entire survey area more scientifically, and the data are more convincing. Secondly, during the pandemic period, questionnaires, interviews, surveys, and psychological tests are restricted by isolation, martial law, and other situations. Sina Weibo and Baidu hot word search engines provide efficient and scientific research methods. In terms of data representation, during the data collection process of this study, the research object received an emotional statistical survey without their awareness. The information collected is more accurate and credible, and it can better reflect the true feelings of the respondents. It will not be affected by the public subjective level, so the data quality is higher. Similarly, Tao et al. used the comments and search data in social media to analyze the relationship in tourist satisfaction and air quality in the scenic area, providing a reference for scenic area management [56].

5.2. Discussion of Research Results. According to the research results, we believe that the proportion of positive emotions in Weibo is negatively correlated with the BSI, which means that when the public's emotions have a negative tendency, risk perception will be greatly increased. A study proved this conclusion from another angle. Research on employees in Shanghai, China, shows that employees who are more sensitive to the COVID-19 risks show higher negative emotions and work stress [57]; the severity of the pandemic is negatively correlated with the proportion of positive emotions, which means as the severity of the pandemic continues to increase, the people's emotions become negative, and the proportion of positive emotions will show a downward trend. This is not surprising at all. The results of a survey of more than 50,000 people proved our judgment. During the pandemic, the psychological pressure and the sense of frustration of the public were significantly higher [58]; the severity of the pandemic is positively correlated with the BSI, which shows that the increase in the pandemic will cause widespread public concern. People's perception of risk has improved significantly. Information about the deterioration or rapid spread of the pandemic on the Internet may cause the public to panic. The specific manifestation is that the public opinion in Weibo has become pessimistic, and the real value of the positive emotion ratio is much lower than the fitting value of the prediction model; apart from this, the severe pandemic situation will also cause extensive searches by netizens. The real value of the BSI will be much higher than the fitted value of the prediction model,

indicating that the public's perception of risks has increased significantly. Similar to our research results, Carmen studied the comprehensive indicators of the impact of COVID-19 on the health of community. The research shows that the frequency of online search is highly correlated with the severity of the pandemic [59]. It is interesting and gratifying to find that the strong statements and behaviors of the country or government, and the news events, where the pandemic is controlled or weakened, will cause the public to generate positive emotions, which is specifically expressed by publishing more positive and optimistic Weibo views. The real value of the proportion of positive emotional posts in Weibo is significantly higher than the fitted value of the prediction model. The positive actions of the government and major scientific research progress have reduced people's perception of risk, which is manifested by the reduction in the frequency of online search. The real value of the BSI is significantly lower than the fitted value of the prediction model.

From the statistical graphs drawn by the real values of the three, it can be seen that the changing trend generally conforms to the research conclusion, but in some periods, it does not change completely according to this law, and there are some abnormal mismatches (for example, in some periods, with the increase of the number of newly diagnosed people, the proportion of positive emotions also increases). In this study, the BSI and the proportion of positive emotional posts in Weibo were analyzed. Analyzed by ARIMA time series, the periods with obvious differences were sorted out. After analyzing the important pandemic information and prevention and control policies at home and abroad during these periods, it was found that dramatic changes in the pandemic situation and the prevention and control policies that caused the fluctuation of public's positive emotions and risk perception. This proves the influence of authoritative media on public's emotion and risk perception from the side, and it provides a theoretical reference for government departments to guide the public to correctly view and respond to the pandemic.

5.3. Lead the Public to Maintain Positive Emotions and Reasonable Risk Perception. In recent years, the influence of social networks on people's opinions and decisions has become greater and greater, and it has attracted widespread attention [60]. The description of disasters in the network can weaken or enhance the perception of risk and ultimately affect the action [61]. When a crisis or conflict occurs, scientific and effective risk communication is essential. Research results in the field of food safety show that the government uses social media for risk communication, which increases people's positive emotions about food safety and promotes rational risk response [62]. In order to understand how disaster risk is perceived and shared and its impact on public's emotions, the SRAF provides a perspective for observing risks. Different communication media and amplification stations can affect public risk perception [63]. Studies have shown that nonprofessional groups are more sensitive to public hazards than experts. Non-authoritative groups, as information amplifying stations,

may transform information and increase social risk perception [64]. At a time when global connections are getting closer, the Internet has become more open, making it possible for false and harmful information to spread through social media. So far, some people have strictly adhered to these restrictions to prevent infection, such as maintaining hand hygiene and necessary social isolation. However, others have ignored or procrastinated government regulations and still frequently appear on crowded beaches or bar [65]. This eloquently proves that the public's emotions and perception of risks associated with COVID-19 differ greatly in different places and individuals [15].

The government, relying on official media such as television, newspapers, and the Internet, plays an important role in notifying the public about health issues, shaping the public's attitude toward pandemic policies, and influencing public decision-making and behavior [66]. The government establishes a clear and coordinated communication strategy to deal with major public health disasters, which can gain the trust of citizens in a rapidly developing situation and avoid the public's blind optimism or panic about the pandemic [1]. The government's words and deeds on social media can influence the individual's anti-epidemic actions. Correspondingly, the government and policy makers are also inspired by the public's emotions and cognition in online media [7]. Enhancing accurate and adequate information communication between the government and the public can help the public maintain positive emotions and establish a good sense of risk. In the early stage of the epidemic, the Vietnamese government used video and music on the Internet to guide people to form healthy habits and achieved good results [67]. The research by Chen and Davies proves this and believes that the government maintains an open way to accurately and strategically explain the health crisis facing the public, which helps reduce public anger and panic. [16, 53]. Obviously, doing this job well is a challenge for every country and government. This research has an important reference value for leaders and decision makers to deal with similar disasters and crises. Because it provides the connection and influencing factors of the public's positive emotions and risk perceptions in crises situations, it proves that the information in social media will greatly affect the public's cognition and behavior. This knowledge once again reminds the government to pay attention to the role of social media in disaster management, enhance the communication between the government and the public, and guide the public to maintain positive emotions and reasonable risk perception.

5.4. Limitations and Future Directions. This study has several limitations. Firstly, this study focuses on the dynamic changes of the public's positive emotions and risk perception in Hubei Province during the pandemic. Therefore, the sample source is limited to Hubei, and the sample range can be expanded in subsequent studies. Secondly, online data collection and analysis did not include all the public in the research scope. Individuals such as the elderly and children who are not good at online communication cannot be

investigated. Because the network is virtual, it cannot accurately reflect the impact of gender and age differences on public's emotion and risk perception during the pandemic. Finally, the judgment of positive emotions in this study mainly relies on the text of Weibo comments, expressions, and image expressions in Weibo communication [27], which are not included in the statistics due to the limitation of emotion division standards. In the follow-up research, these limitations deserve careful analysis and discussion.

6. Conclusion

This study collects data related to COVID-19 in Hubei Province, China, from January 20 to April 8, 2020, including the proportion of positive emotional posts in Weibo, the number of newly diagnosed daily, and the BSI. Through analysis and research on the correlation, linear regression, and ARIMA time-series model of the three sets of data, the following conclusions are drawn. The proportion of positive emotional posts in Weibo is negatively correlated with the level of risk perception, the severity of the pandemic is negatively correlated with the proportion of positive emotions, and the severity of the pandemic is positively correlated with the degree of risk perception. Information about the deterioration or rapid spread of the pandemic on the Internet may cause the public to panic. Specifically, the real value of the positive emotion ratio of Weibo is significantly lower than the fitting value of the prediction model, the number and frequency of Baidu searches increase, and the public's level of risk perception is significantly improved. Contrary to this, the strong decision-making, behavior, and positive pandemic news events of the state or government will cause the public to generate positive emotions, reduce the number and frequency of Baidu searches, and reduce people's risk perception level. By observing the changing trend of variables, the proportion of positive emotional posts in Weibo, the number of newly diagnosed cases, and the BSI, it can be found that the volatility of the curve generally conforms to the relationship drawn from the research conclusions. However, at certain specific points in time, sudden pandemic events or government decisions can cause some abnormal fluctuations in the proportion of positive emotions and BSI. Based on the research results, we outline some policy suggestions.

The public is increasingly using social media to gain the risk perception of the pandemic and express their emotions. Therefore, the government must have the necessary tools to extract this valuable information in a comprehensive manner and consider this in the subsequent decision-making process.

The words and deeds of the government greatly affect the decision-making and behavior of the public. The government's communication of risk information with the public in official media such as television, newspapers, and the Internet can guide the public to maintain the positive emotions and reasonable risk perception. This is of great significance in this long-term struggle against COVID-19.

Data Availability

The original data used to support the findings of this study are available from the corresponding author upon request.

Conflicts of Interest

The authors declare that there are no conflicts of interest regarding the publication of this paper.

Acknowledgments

This work was supported by the MOE (Ministry of Education in China) Project of Humanities and Social Sciences (18YJCZH191) and Fundamental Research Funds for the Central Universities of China (2652019073).

References

- [1] Y. B. D. Bruin, A.-S. Lequarre, J. McCourt et al., "Initial impacts of global risk mitigation measures taken during the combatting of the COVID-19 pandemic," *Safety Science*, vol. 128, Article ID 104773, 2020.
- [2] R. M. Anderson, H. Heesterbeek, D. Klinkenberg, and T. D. Hollingsworth, "How will country-based mitigation measures influence the course of the COVID-19 epidemic?" *The Lancet*, vol. 395, no. 10228, pp. 931–934, 2020.
- [3] E. A. Waters, "Feeling good, feeling bad, and feeling at-risk: a review of incidental affect's influence on likelihood estimates of health hazards and life events," *Journal of Risk Research*, vol. 11, no. 5, pp. 569–595, 2008.
- [4] Y. Liu, C. Xie, S. She et al., "Emotion and aversion towards timing ambiguity in the perception of environmental risks," in *Proceedings of the 2013 International Conference on Management Science and Engineering (ICMSE)*, pp. 1433–1438, Harbin, China, July 2013.
- [5] P. Slovic, "Perception of risk," *Science*, vol. 17, pp. 43–54, 1987.
- [6] R. N. Rimal and K. Real, "Perceived risk and efficacy beliefs as motivators of change: use of the risk perception attitude (RPA) framework to understand health behaviors," *Human Communication Research*, vol. 29, no. 3, p. 370, 2003.
- [7] S. T. Heydari, L. Zarei, A. K. Sadati et al., "The effect of risk communication on preventive and protective behaviours during the COVID-19 outbreak: mediating role of risk perception," *BMC Public Health*, vol. 21, no. 1, 2021.
- [8] D. Herrero-Fernández, P. Parada-Fernández, M. Oliva-Macías, and R. Jorge, "The influence of emotional state on risk perception in pedestrians: a psychophysiological approach," *Safety Science*, vol. 130, Article ID 104857, 2020.
- [9] R. M. Hogarth, M. Portell, and A. Cuxart, "What risks do people perceive in everyday life? A perspective gained from the experience sampling method (ESM)," *Risk Analysis*, vol. 27, no. 6, pp. 1427–1439, 2007.
- [10] A. Bec and S. Becken, "Risk perceptions and emotional stability in response to Cyclone Debbie: an analysis of twitter data," *Journal of Risk Research*, Article ID 1673798, 2019.
- [11] E. Samadipour, F. Ghardashi, and N. Aghaei, "Evaluation of risk perception of COVID-19 disease: a community-based participatory study," *Disaster Medicine and Public Health Preparedness*, vol. 2, pp. 1–20, 2020.

- [12] J. Dyer and B. Kolic, "Public risk perception and emotion on Twitter during the Covid-19 pandemic," *Applied Network Science*, vol. 5, no. 1, p. 99, 2020.
- [13] Q. Yan, Y. Tang, D. Yan et al., "Impact of media reports on the early spread of COVID-19 epidemic," *Journal of Theoretical Biology*, vol. 502, Article ID 110385, 2020.
- [14] M. A. Borg, "Cultural determinants of infection control behaviour: understanding drivers and implementing effective change," *Journal of Hospital Infection*, vol. 86, no. 3, pp. 161–168, 2014.
- [15] T. L. D. Huynh, "Does culture matter social distancing under the COVID-19 pandemic?" *Safety Science*, vol. 130, Article ID 104872, 2020.
- [16] Q. Chen, C. Min, W. Zhang, G. Wang, X. Ma, and R. Evans, "Unpacking the black box: how to promote citizen engagement through government social media during the COVID-19 crisis," *Computers in Human Behavior*, vol. 110, Article ID 106380, 2020.
- [17] W. Huang, X. Yao, and Q. Wang, "Research on Weibo emotion classification based on context," *Lecture Notes in Computer Science (Including Subseries Lecture Notes in Artificial Intelligence and Lecture Notes in Bioinformatics)*, vol. 11354, pp. 222–231, 2019.
- [18] K. Liu, T. Wang, Z. Yang et al., "Using Baidu Search Index to predict dengue outbreak in China," *Scientific Reports*, vol. 6, p. 38040, 2016.
- [19] N. Xu and X. Tang, "A causality analysis of societal risk perception and stock Market volatility in China," *Journal of Systems Science and Systems Engineering*, vol. 27, no. 5, pp. 613–631, 2018.
- [20] B. L. Fredrickson, "The role of positive emotions in positive psychology: the broaden-and-build theory of positive emotions," *American Psychologist*, vol. 56, no. 3, pp. 218–226, 2001.
- [21] R. Reisenzein, "Cognition and emotion: a plea for theory," *Cognition and Emotion*, vol. 33, no. 1, pp. 109–118, 2019.
- [22] B. Pang and L. Lee, "Opinion mining and sentiment analysis," *Foundations and Trends in Information Retrieval*, vol. 2, no. 1–2, pp. 1–135, 2008.
- [23] A. Hartanto, J. C. Yong, W. X. Toh, S. T. H. Lee, G. Y. Q. Tng, and W. Tov, "Cognitive, social, emotional, and subjective health benefits of computer use in adults: a 9-year longitudinal study from the Midlife in the United States (MIDUS)," *Computers in Human Behavior*, vol. 104, Article ID 106179, 2020.
- [24] A. Pepe and J. Bollen, "Between conjecture and memento: shaping a collective emotional perception of the future," 2008, <https://arxiv.org/abs/0801.3864>.
- [25] Y. Dong, H. Chen, X. Tang et al., "Collective emotional reaction to societal risks in China," in *Proceedings of the 2015 IEEE International Conference on Systems, Man, and Cybernetics*, IEEE, Hong Kong, China, October 2015.
- [26] D. Watson and A. Tellegen, "Toward a consensual structure of mood," *Psychological Bulletin*, vol. 98, no. 2, pp. 219–235, 1985.
- [27] F. Jiang, Y.-Q. Liu, H.-B. Luan et al., "Microblog sentiment analysis with emoticon space model," *Journal of Computer Science and Technology*, vol. 30, no. 5, pp. 1120–1129, 2015.
- [28] S. Mashwani, "The coronavirus (COVID-19) pandemic's impact on mental health," *International Journal of Health Planning and Management*, vol. 35, no. 5, pp. 993–996, 2020.
- [29] C. Starr, "Social benefit versus technological risk," *Science*, vol. 165, no. 3899, pp. 1232–1238, 1969.
- [30] B. Fischhoff, P. Slovic, S. Lichtenstein, S. Read, and B. Combs, "How safe is safe enough? A psychometric study of attitudes towards technological risks and benefits," *Policy Sciences*, vol. 9, no. 2, pp. 127–152, 1978.
- [31] P. Slovic, B. Fischhoff, and S. Lichtenstein, "Why study risk perception?" *Risk Analysis*, vol. 2, no. 2, pp. 83–93, 1982.
- [32] G. Weinstein and M. Douglas, "Risk and culture: an essay on the selection of technological and environmental dangers acceptable risk," *American Political Science Review*, vol. 77, 1983.
- [33] A. L. PedrosaL. Bitencourt et al., "Emotional, behavioral, and psychological impact of the COVID-19 pandemic," *Frontiers in Psychology*, vol. 11, Article ID 566212, 2020.
- [34] S. Dryhurst, C. R. Schneider, J. Kerr et al., "Risk perceptions of COVID-19 around the world," *Journal of Risk Research*, vol. 23, no. 7–8, pp. 994–1006, 2020.
- [35] N. C. Bronfman and L. A. Cifuentes, "Risk perception in a developing country: the case of Chile," *Risk Analysis*, vol. 23, no. 6, pp. 1271–1285, 2003.
- [36] A. R. Roberts, "Assessment, crisis intervention, and trauma treatment: the integrative ACT intervention model," *Brief Treatment and Crisis Intervention*, vol. 2, no. 1, pp. 1–22, 2002.
- [37] J. C. Coyne and G. Downey, "Social factors and psychopathology: stress, social support, and coping processes," *Annual Review of Psychology*, vol. 42, no. 1, pp. 401–425, 1991.
- [38] X. Tang, "Applying search words and BBS posts to societal risk perception and harmonious society measurement," in *Proceedings of the 2013 IEEE International Conference on Systems, Man, and Cybernetics (SMC 2013)*, pp. 2191–2196, Manchester, UK., October 2013.
- [39] R. E. Kasperon, O. Renn, P. Slovic et al., "The social amplification of risk: a conceptual framework," *Risk Analysis*, vol. 8, no. 2, pp. 177–187, 1988.
- [40] M. K. Lindell and R. W. Perry, "The protective action decision model: theoretical modifications and additional evidence," *Risk Analysis*, vol. 32, no. 4, p. 616, 2012.
- [41] M. K. Lindell and S. N. Hwang, "Households' perceived personal risk and responses in a multihazard environment," *Risk Analysis*, vol. 28, no. 2, pp. 539–556, 2008.
- [42] S. M. Pandit and S.-M. Wu, *Time Series and System Analysis, with Applications*, Wiley, Hoboken, NJ, USA, 1983.
- [43] X. Li, C. Zhang, B. Zhang, and K. Liu, "A comparative time series analysis and modeling of aerosols in the contiguous United States and China," *Science of the Total Environment*, vol. 690, pp. 799–811, 2019.
- [44] M. Perzyk, K. Krawiec, and J. Kozłowski, "Application of time-series analysis in foundry production," *Archives of Foundry Engineering*, vol. 9, no. 3, pp. 109–114, 2009.
- [45] P. Narayanan, A. Basistha, S. Sarkar, and S. Kamna, "Trend analysis and ARIMA modelling of pre-monsoon rainfall data for western India," *Comptes Rendus Geoscience*, vol. 345, no. 1, pp. 22–27, 2013.
- [46] S. Singh, K. S. Parmar, J. Kumar et al., "Development of new hybrid model of discrete wavelet decomposition and autoregressive integrated moving average (ARIMA) models in application to one month forecast the casualties cases of COVID-19," *Chaos, Solitons & Fractals*, vol. 135, 2020.
- [47] L. Zhou, J.-M. Liu, and X.-P. Dong, "COVID-19 seeding time and doubling time model: an early epidemic risk assessment tool," *Infectious Diseases of Poverty*, vol. 9, no. 1, pp. 1–9, 2020.
- [48] D.-M. Xue and Z.-Q. Hua, "ARIMA based time series forecasting model," *Recent Advances in Electrical & Electronic Engineering (Formerly Recent Patents on Electrical & Electronic Engineering)*, vol. 9, no. 2, pp. 93–98, 2016.
- [49] M. N. Martinez and M. J. Bartholomew, "What does it 'mean'? A review of interpreting and calculating different

- types of means and standard deviations,” *Pharmaceutics*, vol. 9, no. 2, 2017.
- [50] S. Bhandari and M. Hallowell, *Emotional States and Their Impact on Hazard Identification Skills*, ASCE Library, Reston, VA, USA, 2016.
- [51] D.-H. Choi, W. Yoo, G.-Y. Noh, and K. Park, “The impact of social media on risk perceptions during the MERS outbreak in South Korea,” *Computers in Human Behavior*, vol. 72, pp. 422–431, 2017.
- [52] T. Duan, H. Jiang, and X. Deng, “Government intervention, risk perception, and the adoption of protective action recommendations: evidence from the COVID-19 prevention and control experience of China,” *International Journal of Environmental Research and Public Health*, vol. 17, no. 10, p. E3387, 2020.
- [53] G. Davies, “The epidemic severity index: estimating relative local severity of novel disease outbreaks,” 2020.
- [54] P. Panagiotopoulos, J. Barnett, A. Z. Bigdeli, and S. Sams, “Social media in emergency management: twitter as a tool for communicating risks to the public,” *Technological Forecasting and Social Change*, vol. 111, pp. 86–96, 2016.
- [55] J. R. Ortiz, H. Zhou, D. K. Shay et al., “Monitoring influenza activity in the United States: a comparison of traditional surveillance systems with Google Flu Trends,” *PLoS One*, vol. 6, no. 4, p. e18687, 2011.
- [56] Y. Tao, F. Zhang, C. Shi et al., “Social media data-based sentiment analysis of tourists’ air quality perceptions,” *Sustainability (Switzerland)*, vol. 1118 pages, 2019.
- [57] C. A. Warden, A. R. Warden, S. C.-T. Huang et al., “Job tension and emotional sensitivity to COVID-19 public messaging and risk perception,” *Population Health Management*, 2020.
- [58] Q. Han, B. Zheng, M. Agostini et al., “Associations of risk perception of COVID-19 with emotion and mental health during the pandemic,” *Journal of Affective Disorders*, vol. 284, no. 1, pp. 247–255, 2021.
- [59] C. Herrero and A. Villar, “A synthetic indicator on the impact of COVID-19 on the community’s health,” *PLoS One*, vol. 15, no. 9, Article ID e0238970, 2020.
- [60] W. Li and H. Xu, “Text-based emotion classification using emotion cause extraction,” *Expert Systems with Applications*, vol. 41, no. 4, pp. 1742–1749, 2014.
- [61] N. Pidgeon and K. Henwood, “Chapter 4. the social amplification of risk framework (SARF): theory, critiques, and policy implications,” *Risk Communication and Public Health*, pp. 53–69, 2010.
- [62] T. M. Ha, S. Shakur, and K. H. Pham Do, “Linkages among food safety risk perception, trust and information: evidence from Hanoi consumers,” *Food Control*, vol. 110, 2020.
- [63] D. E. Alexander, “Social media in disaster risk reduction and crisis management,” *Science and Engineering Ethics*, vol. 20, no. 3, pp. 717–733, 2014.
- [64] J. Fellenor, J. Barnett, C. Potter, J. Urquhart, J. D. Mumford, and C. P. Quine, “The social amplification of risk on twitter: the case of ash dieback disease in the United Kingdom,” *Journal of Risk Research*, vol. 21, no. 10, pp. 1163–1183, 2018.
- [65] L. Cori, F. Bianchi, E. Cadum et al., “Risk perception and COVID-19,” *International Journal of Environmental Research and Public Health*, vol. 17, no. 9, 2020.
- [66] T. A. Morton and J. M. Duck, “Communication and health beliefs,” *Communication Research*, vol. 28, no. 5, pp. 602–626, 2001.
- [67] H. T. L. Duc, “The COVID-19 containment in Vietnam: what are we doing?” *Journal of Global Health*, vol. 10, no. 1, 2020.

Review Article

Ecosystem-Based Adaptation for the Impact of Climate Change and Variation in the Water Management Sector of Sri Lanka

Bhabishya Khaniya , **Miyuru B. Gunathilake** , and **Upaka Rathnayake** 

Department of Civil Engineering, Faculty of Engineering, Sri Lanka Institute of Information Technology, Malabe, Sri Lanka

Correspondence should be addressed to Upaka Rathnayake; upakanjanjeewa@gmail.com

Received 7 September 2020; Revised 27 October 2020; Accepted 17 February 2021; Published 25 February 2021

Academic Editor: Xander Wang

Copyright © 2021 Bhabishya Khaniya et al. This is an open access article distributed under the Creative Commons Attribution License, which permits unrestricted use, distribution, and reproduction in any medium, provided the original work is properly cited.

The climate of Sri Lanka has been fluctuating at an alarming rate during the recent past. These changes are reported to have pronounced impacts on the livelihoods of the people in the country. Water is central to the sustainable functioning of ecosystems and wellbeing of mankind. It is evident that pronounced variations in the climate will negatively impact the availability and the quality of water resources. The ecosystem-based adaptation (EbA) approach has proved to be an effective strategy to address the impact of climate change on water resources in many parts of the world. The key aim of this paper is to elaborate the wide range of benefits received through implementation of EbAs in field level, watershed scale, and urban and coastal environments in the context of Sri Lanka. In addition, this paper discusses the benefits of utilizing EbA solutions over grey infrastructure-based solutions to address the issues related to water management. The wide range of benefits received through implementation of EbAs can be broadly classified into three categories: water supply regulation, water quality regulation, and moderation of extreme events. This paper recommends the utilization of EbAs over grey infrastructure-based solutions in adaptation to climate change in the water management sector for the developing region due its cost effectiveness, ecofriendliness, and multiple benefits received on long-term scales. The findings of this study will unequivocally contribute to filling existing knowledge and research gaps in the context of EbAs to future climate change in Sri Lanka. The suggestions and opinions of this study can be taken into account by decision makers and water resources planning agencies for future planning of actions related to climate change adaptation in Sri Lanka.

1. Introduction

Climate change/variability and its implementation towards water resources management are two linked concerns for today's world. Climate change/variability can be illustrated as the "change in the state of the climate which can be identified (e.g., using statistical tests) by changes in the mean and/or variability of its properties which persist for an extended period, typically decades or longer [1]. Many researchers believed that the emission of greenhouse gases (GHGs) and changes in the land use are two main reasons for the present alterations in the climate [2]. Sri Lanka, compared to the other countries, gives a lower priority to the GHGs emissions [3].

Climates are to change unpredictably due to the way humans are using environmental resources for concentrated benefits. It is likely to expect increase in the frequency and

magnitude of unpredictable precipitation events for some of the regions in the world. However, some other regions are expected to be direr in the future [4]. Developing countries like Sri Lanka are more prone to the vulnerable impacts of climate change, especially facing challenges on natural systems linked meticulously with natural resource management and regulation of biodiversity services [5]. There are many lines of evidence for the climate variations in Sri Lanka [6, 7]. Impacts of these variations to water resource management, biodiversity conservation, and human health are highly realized in Sri Lankan context as Sri Lanka is recognized as one of the most valuable countries in terms of richness in natural resources together with climatic and topographical variations within a small land territory [8]. This environment is (was and will be) damaged due to the extreme rainfall events and prolonged drought [9, 10]. It was observed that the mean atmospheric temperature in Sri Lanka

has been increased by 0.016°C per year from 1961 to 1990. Therefore, the increment is 0.5°C for the 30 years. However, globally this happened at a rate of 0.013°C (0.39°C for the 30 years). Therefore, there is no doubt that Sri Lanka was affected more than most of the other countries by rising atmospheric temperatures [1, 11, 12]. It was further observed that the Sri Lankan annual rainfall was on average decreased by 144 mm during the years 1961 to 1990 in comparison to the previous 30 years (1931 to 1960) [13, 14]. Sri Lanka has a wide spatial variation of its rainfall and it varies from 900 mm (dry zones) to 5000 mm (wet zone). Therefore, the variation in rainfall from one place to another is significantly diversified. Thus, this annual rainfall decrement is calculated based on the average annual rainfall values. Nevertheless, Sri Lanka was ranked second among countries that are mostly affected by extreme climate events in 2017 [15].

It is anticipated that the future climate of the country is also expected to change drastically. Literature gives many predictions according to various climate models on Sri Lanka. However, most of the research was carried out for Special Report on Emissions Scenarios (SRES) by Intergovernmental Panel on Climate Change (IPCC). De Silva [16] predicted that the atmospheric temperature would rise by 1.6°C in year 2050 for the A2 emission scenario and rise by 1.2°C for the B2 scenario. It was predicted that the country's north, northeastern, and northwestern regions would be highly affected by these cases. Importantly, these are in dry zone of the country bounded by the sea. Therefore, the adverse impacts due to the sea water level change are immeasurable [17].

However, the research world has now migrated to Representative Concentration Pathway (RCP) scenarios in climate prediction. These scenarios are based on the greenhouse gas concentration trajectory, which is adopted by the IPCC. However, they are not based on emissions. IPCC 5th assessment report in 2014 showcases four RCP scenarios, RCP2.6, RCP4.5, RCP6, and RCP8.5, for different conditions. These climate scenarios were widely used in the climatic projections and related studies [18], including in Sri Lanka [19–22]. These studies have shown the importance of climate change and its projection for future years.

Not only does the climate change (variation) affect the sea water levels but also it has an effect on many physical phenomena. It is cross-sectoral and, hence, impacts the natural resources, food security, agriculture, energy production, human health, ecosystem, and so forth [23]. Therefore, restoration and expansion of water infrastructure developments are directly impacted by the ongoing climate change and climate variations [4]. In addition, the rapid population growth in most of the developing countries has increased the climate change/variation impacts [24, 25]. This is critical in Sri Lanka as it is an island covered by sea. Natcom [26] projected that the sea level rise will reach 1 m by the year 2070. Therefore, it is clear that, to withstand the adverse impacts of climate variability and climate change in Sri Lanka, immediate actions that are demonstrated by sustainable practices have to be taken. It might not be possible to stop the climate change or climate variation in the world. However, minimization or mitigation is one

possible way to overcome the issues of climate change. In addition, adaptation can be considered a better option to get used to the impact of climate change and live with that. If appropriate adaptation actions do not take place at the required time, the risks and damage can be easily amplified [4].

Climate change and water resources management are two linked activities. Therefore, water plays a vital role when it comes to adaptation for climate change [27]. It is reported that 31% of labour and 12% of National Gross Domestic Product (GDP) are involved in agriculture-related activities which are highly sensitive to climate [28]. The future projected decreases in rainfalls and increases in temperature will cause detrimental impacts on agricultural sector, leaving people under increased poverty and hunger.

Climate change in Sri Lanka will threaten both surface and groundwater resources, upon which Sri Lankans highly rely for domestic purposes. The combined impacts of prolonged droughts and sea level rise will amplify the risk of sea water intrusion to coastal aquifers in Sri Lanka and alter tidal series in shoreline areas, which will thereby deplete the availability of freshwater resources [29]. On the contrary, high rainfall levels expected in the wet zones of Sri Lanka will lead to high rates of soil erosion [17]. Baba [3] estimated that the coastal erosion along the shoreline region in Sri Lanka is near 0.35 m per year. Therefore, not only mitigating the climate change impacts but also adaptation is highly important to the countries like Sri Lanka. The ecosystem-based adaptation (EbA) approach offers solutions to primary water management issues and multitude of auxiliary benefits using a more holistic approach [30]. Ecosystem-based adaptation offers nature-based solutions that are defined as “the forgotten solution,” having robust potential to mitigate climate change effects establishing profound ground on implementation of sustainable development goals [31].

Therefore, this paper elaborates the wide range of benefits received through implementation of EbAs in field level, watershed scale, and urban and coastal environments in the context of Sri Lanka. In addition, the paper discusses the benefits of utilizing EbA solutions over grey infrastructure-based solutions to address the issues related to water management in Sri Lanka, while referring to the literature.

2. Importance of Ecosystem to the Climate Change Adaptation

Climate change adaptation is increasingly being adopted as a part of ecosystem-based adaptation, where ecosystem services are conceptualized as a dominant way to reduce climate change impacts [32]. Historically, ecosystem-based adaptation measures were only comprehended as the contrivance to mitigate flooding in the floodplain areas; nevertheless, current practices are oriented towards environmental and social sustainability enhancing human wellbeing by uplifting the livelihood wellbeing of marginalized group of people [33, 34].

Economic concept of demand and supply has been supplementing the close link between ecosystem offered facilities and to management policies regarding conservation of ecosystem properties [35]. These trade-offs need to be monitored for lucrative restoration of biodiversity to maintain adequate supply of ecosystem services [36].

The exploration of the relationship between ecosystem-based approaches and climate change adaptation is scrutinized through cost-benefit analysis, while it is also a difficult impractical practice [37]. This section discusses the benefits and services offered by the ecosystems, while emphasizing the importance of ecosystems self-regulating services as the backdrop for adaptation to climate change and eventually to achieve the targeted sustainable development. Ecosystems provide numerous benefits to uplift the economy of a nation provisioning goods and services to meet the local people's day-to-day needs [8].

The services offered by ecosystems are mainly classified into 4 categories: provisioning services, regulating services, cultural services, and supporting services. Safe passage to food, fuel, timber, and other necessities is under the provisioning services category. Climate regulation, regulating water quality and quantity, erosion regulation, and hazard regulation fall under the category of regulation services. Recreational activities and inspirational activities come under the cultural services category, while soil formation and nutrient cycling processes come under the category of supporting services of the ecosystem [38]. Ecosystems were identified as the core elements for addressing the impacts of climate change by the global communities [39]. This can lead to achieving the sustainable development in the ecosystem [40]. In present times, ecosystem-based approach has carried aspirations of ecosystem services model, which is popularly reforming as a value of economic importance while providing biodiversity services [41, 42].

Ecosystem-based adaptation (EbA) is usually cost-effective as it offers consistent financial benefits on the long term relative to the other micromanagement strategies [43]. In addition, the strategies are easily managed according to the ever-changing climate change, even with indigenous level techniques and knowledge [40]. Many international frameworks, including United Nations Framework Convention on Climate Change (UNFCCC) and Sendai Framework for Disaster Risk Reduction (SFDRR), have identified the necessity of EbAs in adapting to and mitigating the climate change risks [44]. At the same time, most of the developing countries have cultivated leading thoughts regarding climate change adaptation, while pledging financial assistance form developed nations [45]. However, it is often debated whether this funding would contribute to successful implementation of ecosystem-based approaches [46]. With growing greenhouse emissions from the developed regions around the world, compensation has to be negotiated, which would help developing countries mobilize the resources to implement adaptation measures to combat detrimental effects of climate change for which they are not directly accountable [47]. It is very challenging to adapt to a particular funding mechanism as novel financial setups of adaptation to climate change require intense political dialogues [48].

Woronecki [25] highlighted how power relations play an important role in combining social factors to empower ecosystem adaptation strategies to contest climate change, especially in context of developing countries, where political dimension weighs heavy relative to developmental concerns of country citizen. Hence, diverse funding mechanisms suitable for a particular country based on country's national policy, political setup, willingness and commitment of respective governments to carry out adaptation measures, and their past contributions towards adaptation initiatives should be highly prioritized.

3. Ecosystem-Based Adaptation Measures for Water Management in Sri Lanka

Sri Lanka is one of the foremost countries to practice ecosystem-based adaptation measures (since historical times) to mitigate climate change effects imparting robust techniques for water resource management [48–50]. Contour drains (Figure 1(a)) and contour walls (Figure 1(b)) are two examples to mitigate the landslides and soil erosion in the central hills in Sri Lanka (see Figure 1). The people in Sri Lanka have been using these simple techniques since ancient times. In addition, people used to prefer home gardening over mass-scale farming (Figure 1(c)) in the hill country of Sri Lanka. These are several EbAs quite often practiced in Sri Lanka. These techniques were observed in Serupitiya and Nuwara Eliya area to mitigate the landslides and soil erosion [25].

Besides this, UNDP-led project for ecological tank restoration at Kurunegala district is another adaptation measure featuring ancient water management system of Sri Lanka [53].

In recent times, ecosystem-based adaptation measures have been highly recognized as tools to minimize water-related disasters [54, 55]. The potential EbA approaches, which can be implemented in Sri Lanka to combat the issues driven in water resources management due to the ongoing climate change, are detailed in this section. The relative advantages of EbA-based solutions over grey infrastructure solutions in local scale, watershed level, urban settings, and coastal environments are also reckoned through this section.

3.1. Ecosystem-Based Adaptation Options in Watershed Areas

3.1.1. Conservation of Forests in Sri Lanka. Conservation of forests in relation to ecosystem-based adaptation to climate change is rarely discussed in Sri Lankan context [25, 56]. Local people usually perceive forest just as natural resource to fulfill daily domestic needs which would uplift their household economy [57]. Sri Lanka has lost a significant percentage of forest cover over the last decades due to urbanization and various development activities [58]. These reductions are directly related to swing in climatic factors extreme radiations, prolonged drought, and severe heat [59].

Reforestation and afforestation are two important ways to conserve the forest cover [25]. Reforestation is growing new trees in the areas where there was a recent forest cover, while afforestation is growing new trees in new (fresh) areas.



FIGURE 1: Ecosystem-based adaptation in central hill, Sri Lanka. (a) Contour drains, Serupitiya [51]. (b) Contour walls, Serupitiya [51]. (c) Home gardening, Dayagama [52].

Forests provide an extensive support to keep the Earth in a balanced ecosystem. Trees that are considered a vital part of ecosystem help to conserve biodiversity, prevent soil erosion, enhance water quality indicators, benefit carbon sequestration, maintain sediment retention capability, offer tourism payback, and offer other diverse facilities for ecosystem regulation [55].

It is a well-known fact that the falling leaves increase the organic content in soil, which thereby increases the water-holding capacity of soils [30]. This is one of the most important natural activities in reducing the downstream floods. The increased interception due to afforestation and infiltration plays a significant role to reduce the magnitude of floods during extreme rainfall events [30].

Sri Lanka has recently implemented a number of projects to enhance its forest cover. Native trees-planting projects carried out in Uyanwatta area Raigama (on 29/11/2013), Atabage area (on 24/01/2015), Kalugala area (on 03/02/2015), Hedigalla area (on 13/06/2015), Akmeemana area (on 14/11/2015), Rakwana area (number of days in 2017–2020), Kathlana area (on 13/01/2018), and Illukpathakanda Kalawana area (in 2020) are few examples of short-term projects carried out [60]. In addition, various mass-scale projects are being carried out to increase the forest cover in the Sri Lanka with the help of governmental and nongovernmental organizations. However, for the developing

countries like Sri Lanka, integrating sustainability concepts within forest resource management while prioritizing community participation linked within community-based approach would be essential [61]. These attempts will ultimately benefit the country in securing a better world for the future generations. Amendment of existing policies, introduction of new comprehensive policies, and enforcement of coordination among all the parties would address the gaps to set up framework for forest management and should also be essential. On the long term, this jump to institutionalize the adaptation framework would help Sri Lanka not only to prevent disaster reduction but also to regulate benefits that can be reserved from ecosystem services.

3.1.2. Riparian Buffer Strips in Sri Lanka. United States Department of Agriculture's National Resources Conservation Service (USDA-NRCS) defines buffer strips as vegetated or forested areas adjacent to the streams, lakes, or rivers of herbaceous vegetation, which preserve the water quality and aquatic habitats. This vegetation could be trees, shrubs, or a combination of trees or shrubs established at the edge of the watershed along the stream. The flow from the cropland is passed through the buffer strips, while nutrients

(e.g., nitrogen and phosphorus) and sediments are retained in the buffer strips [62]. Hence, buffer strips replicate the process of conventional water treatment plants [63].

Growing trees along the banks of the rivers is not a new thing to Sri Lanka. Sri Lankans might not know the technical name for the process; however, they have protected the riverbanks by growing various types of trees. This is similar to providing riparian buffer strips. Bamboo tree (*Bambusoideae*) is one of the most common trees that anyone can see along the rivers to protect soil erosion. In addition, trees like Midella (*Barringtonia racemosa*), Kumbuk (*Terminalia arjuna*), and Rambuk (*Erianthus arundinaceus*) are frequently found along the rivers [64]. These trees not only protect the soil erosion but also protect the nearby settlements by holding flood water during the flood. However, urbanization and other human activities have threatened these trees along the riverbanks. Construction industry has consumed a lot of Bamboo trees. However, a little restoration has been taken to revert back the greenery of the ecosystem.

Nevertheless, use of riparian buffer strips in Sri Lanka is highly valued in terms of agricultural sustainability as a way to protect water resources from pollution for irrigation purposes [65]. Riparian buffer zone development was carried out at Deduru Oya (*Oya is one of the local terms for river*) basin as bioengineering practice to conserve riverbank [64]. Along with this, the NeoSynthesis Research Centre (NSRC), an organization focused on sustainable agricultural practices and natural landscape restoration, is working to rehabilitate the bank areas of various riverbanks such as Maha Oya, Hulu Ganga (*Ganga is another local term for river*), Rakwana Ganga, and Mathatilla Oya using riparian buffer strips to prevent contamination of water resources while remediating the spatial landscape heterogeneity with active participation from the community people.

However, use of riparian buffer strips in Sri Lanka is not entrenched with any government rules, neither there are any regulating bodies to promote community engagement to riparian buffer zone development. Therefore, government organizations should urge to develop an adaptable framework for implementation of riparian buffer strips encouraging public level commitment nourishing sociocultural thoughts to familiarize local people with the formulated development policy.

3.1.3. Usage of Natural Wetlands in Sri Lanka. Wetlands offer multiple benefits to the mankind and the environment by providing a wide spectrum of ecosystem supports, while acting as hydrological buffer system [66]. Wetland restoration and conservation have been identified as an improved integrated water management technique, for example, implementation of wetlands as an adaptation tool to sustainable water management at Murray-Darling Basin, Australia, under climate change scenario [35, 67]. Wetlands have common characteristics of terrestrial and aquatic systems and of both lotic and lentic systems [35]. Variety of hydrological, biological, and geochemical processes facilitates the functions of wetlands [68]. Wetlands explicitly

support millions of people through water purification (removal of nitrogen and phosphorus), mitigating the severity of floods (attenuation of flood peaks and retention of surface waters), providing aesthetic beauty and recreational areas, providing space for wildlife habitat and biodiversity conservation, providing fertile soil for agricultural production, and providing timber and fuel [69]. Carbon sequestration is another benefit received by wetland, which is an important provision in terms of climate regulation [70]. In addition, coastal wetlands reduce the severity of coastal flooding by acting as a barrier against saline water intrusion [30]. Since wetlands and marshes store excess rainfall during extreme events, additional energy costs for pumping can be minimized. Apart from this, wetlands demonstrate favorable role to handle various activities such as groundwater recharge, erosion resistor, storm protection, and shoreline stabilization [71]. In present times, wetlands ecosystems are likewise treated as key resource to disaster risk reduction due to climate change specifically in urban setting [72].

Wetlands are treated as major value for ecotourism, aesthetic beauty, and recreation in Sri Lanka. Approximately, they cover 15% of the total land area in Sri Lanka [73]. Colombo, the capital city of the country, along with the coastal regions in Sri Lanka is surrounded by spacious natural wetlands linked with each other; nevertheless, there are ample lines of evidence supporting that these wetlands have undergone several hydrological alterations and their functionality are at prudent risk in perspective of multiple stressors triggered by human attitude to utilize the ecosystem services recklessly [74]. While anticipating wetlands to eliminate climate change risks, it is equally important to preserve the existing wetlands such as freshwater wetlands, lagoons, estuaries, swamp forests, and man-made wetlands which will comfort struggle against climate change [75]. Shifts in ecological regimes due to land encroachment and excessive discharge of wastewater on wetlands causing environmental degradation have put devastating insecurity on future performances of Sri Lankan wetlands. These issues can only be resolved through close monitoring of land use changes by applying modelling techniques to study the changes. There are various initiatives being formulated by Ramsar Convention and United Nations Framework Convention on Climate Change (UNFCCC) under supervision of Government of Sri Lanka to improve resiliency on wetland conservation [23, 76]. This action programme should be in line with cultural setting of the society; theoretical background studies delivered through research and national water resource management policy.

Nevertheless, it is important to exhibit the importance of two wetland systems in the western belt of Sri Lanka. The Muthurajawela marsh and Kolonnawa marsh offer multiple benefits to the living beings in the surrounding areas [77]. The flood waters received during high rainfall seasons from upper reaches are buffered. Then, they are discharged slowly to the Negombo lagoon, hence reducing the negative impacts of flooding on the downstream areas. The lagoon also acts as a source of freshwater delta to moderate salinity and pollution levels. It is estimated that the economic value received through flood attenuation and industrial and

domestic wastewater purification due to these lagoons is around 500,000 United States Dollars (USD) per year [30]. Therefore, it is highly important to conserve the existing wetlands from the developing activities and then to use them effectively to adapt to the ongoing climate change.

3.2. Ecosystem-Based Adaptation Options in Coastal Ecosystems

3.2.1. Mangrove, Coastal Marshes, Dunes, and Barrier Reefs. Mangroves, coastal marshes, dunes, and barrier reefs are regarded as parts of coastal ecosystem. They offer varied functionality analogous to grey infrastructure measures such as dikes, levees, and sea walls in line with associated economical cost [78]. These natural breakwaters result in absorbing the energy of ocean waves, thus reducing the structural damage [79]. The mangrove forests reduce the severity of storm surges protecting upland areas from coastal vulnerability [80, 81]. The role played by mangroves to protect people and properties in recent tsunami was regarded to be magnificent contribution towards the disaster prevention [82, 83]. Nianthi and Shaw [29] reported that coral reefs, which are natural protector of sea erosion, were partially affected due to 2004 Indian Ocean tsunami depicting the role in coastal protection. Nonetheless, the reefs are evidenced to be declining due to mining works [84].

The mangrove forests provide additional income for the people in proximate areas through accelerated fish and shrimp farming as these forests provide home to majority of commercial fish species [30]. It is estimated that the current mangrove cover in Sri Lanka is around 87 km². Mangrove forests are scattered in the Jaffna peninsula and northwestern, northeastern, and eastern belts of Sri Lanka. Satyanarayana et al. [85] suggested that Jaffna peninsula along with Kaluwanchikudy-Komari is found to be in vulnerable condition due to reduction in mangroves, dunes, and reefs cover while Yala, Puttalam, and Trincomalee remain resilient. Therefore, Sri Lanka as an island and its coastlines are severely vulnerable to the impacts from climate change causing disruptions on water networks [86].

Due to human interactions and lack of conservation policies of mangroves in perspective of climate change, they are successively transforming as narrow strips today. The main causes of depletion of mangrove in Sri Lanka are accounted to land encroachment for agricultural purposes, urban development, and diminution of forest resources [87]. It is recorded that 23 species of mangroves are found in Sri Lanka, and 3 of them are listed in the National Red List of Sri Lanka [88]. *Bruguiera cylindrica* (L.) Blume (*Mal Kadol* in local language), *Sonneratia alba* Sm. (*Yak Kirala* in local language), and *Xylocarpus granatum* J. König (*Mutti Kadol* in local language) are the three types of endangered mangroves in Sri Lanka. Hence, to reinstate the mangroves as climate change shield, quality saplings should be replanted in the tidal areas with collaboration from local authorities and relevant ministries. It is recommended that these measures should be industrialized as microengineering program generating employment to the local people using

integrated modality system. These postdevelopment activities should be monitored closely by collective efforts from all the pertinent authorities. Coastal vegetation such as coconut trees, palm trees, and Casuarina plantations is given more attention by the local communities; however, less attention was given to the mangroves. The local community believes that it is the responsibility of the respective councils and the governments. Therefore, the authors suggest that a detailed study should be conducted assessing multicriteria parameters considering the socioecological thoughts, geomorphological characteristics, land-use phenomenon, and scientific understanding of vegetation patterns in conserving the coastal ecosystem.

3.3. Ecosystem-Based Adaptation Options in Urban Settings. Ecosystem-based adaptation in urban areas is extremely important due to the rapid urbanization in the world. Rapid urbanization is not controlled or planned in most of the cities. Therefore, this is a critical issue when addressing the impact of climate change. Increased rainfalls and high intensified rainfall due to climate change are two devastating issues for urbanized area as they can bring flash floods. Therefore, adaptation plans play an important role in mitigating the climate change impacts. However, little information is available on using EbAs in urban areas for mitigating the climate change impacts [89].

Sri Lanka has given much attention to introducing EbAs in its capital city, Colombo. This is due to continuous flooding in the city. Even in an event of an average rainfall in Colombo city, a small flood can be observed (at least on roads). Therefore, EbAs were introduced to reduce the surface runoff in particular. Recently renovated parks are examples for these EbAs. These parks were introduced as jogging tracks so that the parks can also be used for the recreational facilities in addition to the EbAs. Bellanwila jogging track, Nawala walking track, and Diyatha Uyana track are few of the recently developed parks. Infiltration is increased from these green parks; thus, it is expected to reduce the peak surface runoff to Colombo city. These facilities were recently implemented in nearby suburbs and excellent outcomes are witnessed.

Green buildings are another attraction to Colombo city. It is not only ecofriendly but also aesthetically attractive. Clear point residence is such high-rise buildings in Rajagiriya in the heart of Colombo. Natural air cooling due to the green cover in 42 floors made the adaptation to the increased atmospheric temperature. In addition, the green energy supply promotes less burden to the environment. Therefore, this is an excellent example for the usage of EbAs in Colombo. However, more of these types of EbAs are required in congested cities like Colombo. Nevertheless, finding enough space is a challenging activity.

4. Summary and Conclusions

The advantages in implementation of EbAs in field level, watershed level, and urban and coastal environments in Sri Lanka are discussed through this paper. This research paper discusses the main benefits of utilizing EbA solutions over grey infrastructure solutions to address issues related to water

management. It is clear that multifunctionality of EbA approach provides a series of cobenefits apart from the primary solutions, when compared to grey infrastructure-based solutions. Mainly, the benefits of EbAs can be classified into water supply regulation, moderation and extreme events, and water quality regulation. Since EbA solutions are cost-effective solutions, they can be incorporated to address issues related to water management in the developing region. Worldwide scientific community has recognized the importance of integrating nature-based solutions for long-term policy planning in the context of climate change, soil and water conservation, and so forth. Increasing awareness on EbAs and associated costs and benefits, capacity building, and knowledge sharing among agencies and financing should be conducted for EbAs. Methods should be developed to monitor and evaluate the progress of these EbA measures in Sri Lanka. Life cycle assessment and effective monitoring of these EbA approaches should be carried out. The benefits and lessons learnt should also be shared with the general public. Integration of EbA options into the policy development agenda should include assessment of knowledge support, integration of national development, and capacity building. EbA solutions should be addressed after analyzing local hydrology, resources availability, and climatic conditions. It is equally important to understand the capacity of ecosystems. Hence, sustainable utilization of EbAs relies on understanding and respecting the assimilative capacity of ecosystems.

Data Availability

The review data which authors have used for this review paper are available from the corresponding author upon request.

Conflicts of Interest

The authors declare that they have no conflicts of interest.

Acknowledgments

The authors would like to acknowledge the support and motivations provided by Engineers, Anura Panditharathne, Anura Gunathilake, and Pushpika Panditharathne, and Professor Mukand S. Babel to conduct this research. The research was conducted at Faculty of Engineering, Sri Lanka Institute of Information Technology, Sri Lanka.

References

- [1] IPCC, "Climate change 2007," in *Synthesis Report. Contribution of Working Groups I, II and III to the Fourth Assessment Report of the Intergovernmental Panel on Climate Change*, R. K. Pachauri and A. Reisinger, Eds., p. 104, IPCC, Geneva, Switzerland, 2007.
- [2] V. H. Dale, R. A. Efrogmson, and K. L. Kline, "The land use-climate change-energy nexus," *Landscape Ecology*, vol. 26, no. 6, pp. 755–773, 2011.
- [3] N. Baba, "Sinking the pearl of the Indian Ocean: climate change in Sri Lanka," *Global Majority E-Journal*, vol. 1, no. 1, pp. 4–16, 2010.
- [4] IPCC, "Climate change," in *Synthesis Report. Contribution of Working Groups I, II and III to the Fifth Assessment Report of the Intergovernmental Panel on Climate Change*, R. K. Pachauri and L. A. Meyer, Eds., p. 151, IPCC, Geneva, Switzerland, 2014.
- [5] P. Lamsal, L. Kumar, K. Atreya, and K. P. Pant, "Vulnerability and impacts of climate change on forest and freshwater wetland ecosystems in Nepal: a review," *Ambio*, vol. 46, no. 8, pp. 915–930, 2017.
- [6] W. A. J. M. De Costa, "Climate change research in Sri Lanka: are we investing enough?" *Journal of the National Science Foundation of Sri Lanka*, vol. 40, no. 4, pp. 281–282, 2012.
- [7] P. Kurukulasuriya and M. I. Ajwad, "Application of the ricardian technique to estimate the impact of climate change on smallholder farming in Sri Lanka," *Climatic Change*, vol. 81, no. 1, pp. 39–59, 2006.
- [8] J. Kottawa-Arachchi and M. Wijeratne, "Climate change impacts on biodiversity and ecosystems in Sri Lanka: a review," *Nature Conservation Research*, vol. 2, no. 3, pp. 2–22, 2017.
- [9] I. M. S. P. Jayawardena, D. W. T. T. Darshika, H. M. R. Herath, and C. Herath, "Recent trends in climate extreme indices over Sri Lanka," *American Journal of Climate Change*, vol. 07, no. 04, pp. 586–599, 2018.
- [10] L. Zubair, Z. Yahiya, P. Agalawatte, and R. Lokuhetti, "The El Niño event of 2015/16 in Sri Lanka predictions, preparedness, communication and impacts," in *Climate Change Secretariat, NEELAHARITHA-The Climate Change Magazine of Sri Lanka*, pp. 40–46, Ministry of Mahaweli Development and Environment, Battaramulla, Sri Lanka, 2016.
- [11] L. Chandrapala, "Long-term trends of rainfall and temperature in Sri Lanka," in *Climate Variability and Agriculture*, Y. P. Abrol, S. Gadgil, and G. B. Pant, Eds., pp. 153–162, Narosa Publishing House, New Delhi, India, 1996.
- [12] T. K. Fernando and L. Chandrapala, "Global warming and rainfall variability—Sri Lankan situation," in *Proceedings of the 47th Annual Session of Sri Lanka Association for the Advancement of Science (SLASS)*, p. 138, Colombo, Sri Lanka, June 1992.
- [13] L. Chandrapala, "Calculation of areal precipitation of Sri Lanka on district basis using voronoi tessellation method," in *Proceedings of National Symposium on Climate Change, Central Environmental Authority*, Colombo, Sri Lanka, March 1996.
- [14] H. M. Jayatillake, L. Chandrapala, B. R. S. B. Basnayake, and G. H. P. Dharmaratne, "Water Resources and climate change," in *Proceedings of Workshop on Sri Lanka National Water Development Report*, N. T. S. Wijesekera, K. A. U. S. Imbulana, and B. N. Paris, Eds., World Water Assessment Programme (WWAP), Marseille, France, 2005.
- [15] D. Eckstein, M. Hutfls, and M. Wings, *Global Climate Risk Index 2019*, Germanwatch, Bonn, Germany, 2018.
- [16] C. S. De Silva, "Impacts of climate change on water resources in Sri Lanka," in *Proceedings of the 32nd WEDC International Conference on Sustainable Development of water resources, water supply and environmental sanitation*, pp. 502–508, Colombo, Sri Lanka, November 2006.
- [17] Ministry of Environment, *Strengthening Capacity for Climate Change Adaptation Sector Vulnerability Profile: Agriculture and Fisheries*, Climate Change Secretariat Sri Lanka, Battaramulla, Sri Lanka, 2010.
- [18] X. Chong-Hai and X. Ying, "The projection of temperature and precipitation over China under RCP scenarios using a CMIP5 multi-model ensemble," *Atmospheric And Oceanic Science Letters*, vol. 5, no. 6, pp. 527–533, 2012.

- [19] K. Dissanayaka and R. Rajapakse, "Long-term precipitation trends and climate extremes in the Kelani River basin, Sri Lanka, and their impact on streamflow variability under climate change," *Paddy And Water Environment*, vol. 17, no. 2, pp. 281–289, 2019.
- [20] T. Gopalakrishnan and L. Kumar, "Potential impacts of sea-level rise upon the Jaffna Peninsula, Sri Lanka: how climate change can adversely affect the coastal zone," *Journal Of Coastal Research*, vol. 36, no. 5, p. 951, 2020.
- [21] S. Jayasinghe and L. Kumar, "Modeling the climate suitability of tea [*Camellia sinensis*(L.) O. Kuntze] in Sri Lanka in response to current and future climate change scenarios," *Agricultural And Forest Meteorology*, vol. 272–273, pp. 102–117, 2019.
- [22] C. Kariyawasam, L. Kumar, and S. Ratnayake, "Invasive plant species establishment and range dynamics in Sri Lanka under Climate Change," *Entropy*, vol. 21, no. 6, p. 571, 2019.
- [23] S. Woroniecki, C. Wamsler, and E. Boyd, "The promises and pitfalls of ecosystem-based adaptation to climate change as a vehicle for social empowerment," *Ecology and Society*, vol. 24, no. 2, p. 4, 2019.
- [24] N. Huq, A. Bruns, L. Ribbe, and S. Huq, "Mainstreaming ecosystem services based climate change adaptation (eba) in Bangladesh: status, challenges and opportunities," *Sustainability*, vol. 9, no. 6, p. 926, 2017.
- [25] S. Woroniecki, "Enabling environments? examining social co-benefits of ecosystem-based adaptation to climate change in Sri Lanka," *Sustainability*, vol. 11, no. 3, p. 772, 2019.
- [26] Natcom, *Democratic Socialist Republic of Sri Lanka, Initial National Communication under the United Nations Framework Convention on Climate Change*, State Printing Corporation, Padukka, Sri Lanka, 2000.
- [27] WWAP (United Nations World Water Assessment Programme), *The United Nations World Water Development Report 2015*, UNESCO, Water for a Sustainable World, Paris, France, 2015.
- [28] Asian Development Bank, *Strengthening Disaster Resilience*, Asian Development Bank, Mandaluyong, Philippines, 2019.
- [29] R. K. W. G. Nianthi and R. Shaw, "Climate change and its impact on coastal economy of Sri Lanka," in *The Global Challenge*, R. Krishnamurthy, Ed., Research Publishing, Colombo, Sri Lanka, 2015.
- [30] UNEP Green Infrastructure, *Guide for Water Management: Ecosystem-Based Management Approaches for Water-Related Infrastructure Projects*, UNEP Green Infrastructure, Nairobi, Kenya, 2014.
- [31] Nature 4 Climate. 2020, <https://nature4climate.org/>.
- [32] S. Lavorel, M. Colloff, S. McIntyre et al., "Ecological mechanisms underpinning climate adaptation services," *Global Change Biology*, vol. 21, no. 1, pp. 12–31, 2012.
- [33] M. Acreman and J. Holden, "How wetlands affect floods," *Wetlands*, vol. 33, no. 5, pp. 773–786, 2013.
- [34] J. Mercer, I. Kelman, B. Alftan, and T. Kurvits, "Ecosystem-based adaptation to climate change in Caribbean small island developing states: integrating local and external knowledge," *Sustainability*, vol. 4, no. 8, pp. 1908–1932, 2012.
- [35] M. J. Colloff, S. Lavorel, R. M. Wise, M. Dunlop, I. C. Overton, and K. J. Williams, "Adaptation services of floodplains and wetlands under transformational climate change," *Ecological Applications*, vol. 26, no. 4, pp. 1003–1017, 2016.
- [36] V. Acuña, J. R. Díez, L. Flores, M. Meleason, and A. Elozegi, "Does it make economic sense to restore rivers for their ecosystem services?" *Journal of Applied Ecology*, vol. 50, no. 4, pp. 988–997, 2013.
- [37] W. Lange, S. Sandholz, J. Viezzer, M. Becher, and U. Nehren, "Ecosystem-based approaches for disaster risk reduction and climate change adaptation in Rio de Janeiro state," in *Strategies and Tools for a Sustainable Rural Rio de Janeiro*, pp. 345–359, Springer, Cham, Switzerland, 2018.
- [38] Millennium Ecosystem Assessment, *Ecosystems and Human Well-Being: Synthesis*, Island Press, Washington, DC, USA, 2005.
- [39] S. Gabriëlsson and V. Ramasar, "Widows: agents of change in a climate of water uncertainty," *Journal of Cleaner Production*, vol. 60, pp. 34–42, 2013.
- [40] R. Munang, I. Thiaw, K. Alverson, M. Mumba, J. Liu, and M. Rivington, "Climate change and ecosystem-based adaptation: a new pragmatic approach to buffering climate change impacts," *Current Opinion in Environmental Sustainability*, vol. 5, no. 1, pp. 67–71, 2013.
- [41] T. Greiber, "Payment for ecosystem services," in *Legal and Institutional Frameworks*, p. 296, IUCN, Gland, Switzerland, 2009.
- [42] S. Liu, R. Costanza, S. Farber, and A. Troy, "Valuing ecosystem services," *Annals of the New York Academy of Sciences*, vol. 1185, no. 1, pp. 54–78, 2010.
- [43] R. Munroe, N. Doswald, D. Roe, H. Reid, A. Giuliani, and I. Castelli, *Does EBA Work? A Review of the Evidence on the Effectiveness of Ecosystem-Based Approaches to Adaptation*, BirdLife International, UNEP-WCMC, IIED and Cambridge University, Cambridge, UK, 2011.
- [44] L. Ruangpan, Z. Vojinovic, S. Di Sabatino et al., "Nature-Based Solutions for hydro-meteorological risk reduction: a state-of-the-art review of the research area," *Natural Hazards and Earth System Sciences*, vol. 20, no. 1, pp. 243–270, 2020.
- [45] M. Grasso, "The role of justice in the North-South conflict in climate change: the case of negotiations on the adaptation fund," *International Environmental Agreements: Politics, Law and Economics*, vol. 11, no. 4, pp. 361–377, 2011.
- [46] J. B. Smith, T. Dickinson, J. D. B. Donahue et al., "Development and climate change adaptation funding: coordination and integration," *Climate Policy*, vol. 11, no. 3, pp. 987–1000, 2011.
- [47] M. Grasso, *Justice in Funding Adaptation under the International Climate Change Regime*, Springer Netherlands, Dordrecht, Netherlands, 2010.
- [48] R. Vignola, B. Locatelli, C. Martinez, and P. Imbach, "Ecosystem-based adaptation to climate change: what role for policy-makers, society and scientists?" *Mitigation and Adaptation Strategies for Global Change*, vol. 14, no. 8, pp. 691–696, 2009.
- [49] K. Balooni, M. Inoue, T. K. Nath, and M. De Zoysa, *How Social Is Socially Oriented Forest Tenure and Land Use Change in Bangladesh and Sri Lanka? Asia Research Institute Working Paper Series*, Asia Research Institute, Singapore, 2001.
- [50] I. Landström, "Towards collaborative coastal management in Sri Lanka? a study of special area management planning in Sri Lanka's coastal region," *Geografiskaregionstudier*, vol. 70, p. 185, 2006.
- [51] CCCV, "Coping with climate change and variability: lessons from Sri Lankan communities," in *Proceedings of the National Workshop on Community Based Adaptation Colombo, Sri Lanka; UNDP Global Environment Facility/Small Grants Programme (UNDP, GEF/SGP)*, pp. 1–96, Colombo, Sri Lanka, July 2016.
- [52] UN-Habitat, Sri Lanka. 2020, Families at the centre <https://unhabitat.lk/photo-gallery/indian-housing-project-in-central-and-uva-provinces-gallery/families-at-the-centre/>.

- [53] C. Panabokke, *The Small Tank Cascade Systems of the Rajarata: Their Settings, Distribution Patterns and Hydrography*, Mahaweli Authority of Sri Lanka, Colombo, Sri Lanka, 2000.
- [54] F. G. Renaud, U. Nehren, K. Sudmeier-Rieux, and M. Estrella, "Developments and opportunities for ecosystem-based disaster risk reduction and climate change adaptation," *Ecosystem-Based Disaster Risk Reduction and Adaptation in Practice*, vol. 42, pp. 1–20, 2016.
- [55] N. Uy and R. Shaw, "The role of ecosystems in climate change adaptation and disaster risk reduction," *Ecosystem-Based Adaptation*, vol. 12, pp. 41–59, 2012.
- [56] Sri Lanka UN-REDD Programme, *Sri Lanka's Forest Reference Level Submission to the UNFCCC*, UN-REDD, Colombo, Sri Lanka, 2017.
- [57] J. Blockhus, A. Wickramasinghe, M. Nurse, and M. Pérez, "Non-timber forest products and local livelihoods in Ritigala, Sri Lanka," International Union for Conservation of Nature and Natural Resources Asia, Gland, Switzerland, 2002.
- [58] C. S. Reddy, G. Manaswini, C. S. Jha, P. G. Diwakar, and V. K. Dadhwal, "Development of national database on long-term deforestation in Sri Lanka," *Journal of Indian Society of Remote Sensing*, vol. 45, no. 5, pp. 825–836, 2017.
- [59] G. W. A. R. Dahdouh-Guebas, "Causes of forest dieback in montane forests in Sri Lanka," *Economic Review*, vol. 34, pp. 38–40, 2008.
- [60] Rainforest Protectors of Sri Lanka Projects, "Rainforest protectors of Sri Lanka," 2020, <http://www.rainforestprotectors.org/rainforest/Projects.aspx>.
- [61] Nature Uganda, *Ecosystem-based Approaches to Climate Change Adaptation, Local Guidance*, NatureUganda, Kampala, Uganda, 2015.
- [62] T. Ramilan, F. Scrimgoeur, and D. Marsh, "Modelling riparian buffers for water quality enhancement in the Karapiro catchment," in *Proceedings of the 54th Australian Agricultural and Resource Economics Society 2010 Conference*, Adelaide, Australia, February 2010.
- [63] K. D. M. S. S. Sarathchandra, N. D. K. Dayawansa, and M. I. M. Mowjood, "Situation analysis of socio environmental aspects of non point source water pollution in intensively cultivated areas of Nuwara Eliya," *Tropical Agricultural Research*, vol. 28, no. 4, pp. 425–434, 2017.
- [64] M. Soyza, M. Ranagalage, and L. Manawadu, "Model for river bank conservation and proper land use planning," in *Proceedings of the International Forestry and Environment Symposium 2013 of the Department of Forestry and Environmental Science*, University of Sri Jayewardenepura, Jayewardeneperu, Sri Lanka, July 2013.
- [65] H. P. Henegama, N. D. K. Dayawansa, and S. D. Silva, "An assessment of social and environmental implications of agricultural water pollution in Nuwara Eliya," *Tropical Agricultural Research*, vol. 24, no. 4, pp. 304–316, 2015.
- [66] D. C. Donato, J. B. Kauffman, D. Murdiyarso, S. Kurnianto, M. Stidham, and M. Kanninen, "Mangroves among the most carbon-rich forests in the tropics," *Nature Geoscience*, vol. 4, no. 5, pp. 293–297, 2011.
- [67] M. C. Acreman and G. E. Hollis, *Water Management and Wetlands in Sub-saharan Africa*, IUCN, Gland, Switzerland, 1996.
- [68] B. A. Middleton and N. Souter, "Functional integrity of wetlands, hydrologic alteration and freshwater availability," *Ecosystem Health and Sustainability*, vol. 2, no. 1, Article ID e01200, 2016.
- [69] Y. Liu, W. Yang, L. Leon et al., "Hydrologic modeling and evaluation of best management practice scenarios for the grand river watershed in southern Ontario," *Journal of Great Lakes Research*, vol. 42, no. 6, pp. 1289–1301, 2016.
- [70] W. R. Moomaw, G. L. Chmura, G. T. Davies et al., "Wetlands in a changing climate: science, policy and management," *Wetlands*, vol. 38, no. 2, pp. 183–205, 2018.
- [71] U. Sarkar, S. Nag, M. Das, G. Karnatak, and D. Sudheesan, *Conserving Wetlands—An Effective Climate Change Adaptation in India*, ICAR- Central Inland Fisheries Research Institute, Kolkata, India, 2016.
- [72] M. Hettiarachchi, K. Athukorale, S. Wijekoon, and A. de Alwis, "Urban wetlands and disaster resilience of Colombo, Sri Lanka," *International Journal of Disaster Resilience in the Built Environment*, vol. 5, no. 1, pp. 79–89, 2014.
- [73] J. D. S. Dela, *Fourth Country Report from Sri Lanka to the United Nations Convention on Biological Diversity*, Ministry of Education, Battaramulla, Sri Lanka, 2009.
- [74] CEA, *Wetland Site Report and Conservation Management Plan—Colombo Flood Detention Areas*, Central Environmental Authority of Sri Lanka, Colombo, Sri Lanka, 1994.
- [75] F. Dahdouh-Guebas and J. L. Pulkukkuttige, "A bibliometrical review on pre- and postsunami assumptions and facts about mangroves and other coastal vegetation as protective buffers," *Ruhuna Journal of Science*, vol. 4, pp. 28–50, 2009.
- [76] G. Bergkamp and B. Orlando, "Wetlands and climate change," in *Exploring Collaboration between the Convention on Wetlands and the United Nations Framework Convention on Climate Change* Background paper from the World Conservation Union (IUCN), Gland, Switzerland, 1999.
- [77] L. Emerton and E. Bos, *Counting Ecosystems as an Economic Part of Water Infrastructure*, IUCN, Cambridge, UK, 2004.
- [78] A. S. Ratnayake, Y. Sampei, N. P. Ratnayake, and B. P. Roser, "Middle to late Holocene environmental changes in the depositional system of the tropical brackish Bolgoda Lake, coastal southwest Sri Lanka," *Palaeogeography, Palaeoclimatology, Palaeoecology*, vol. 465, pp. 122–137, 2017.
- [79] M. E. Hanley, S. P. G. Hoggart, D. J. Simmonds et al., "Shifting sands? coastal protection by sand banks, beaches and dunes," *Coastal Engineering*, vol. 87, pp. 136–146, 2014.
- [80] B. Chatenoux and P. Peduzzi, "Impacts from the 2004 Indian Ocean Tsunami: analysing the potential protecting role of environmental features," *Natural Hazards*, vol. 40, no. 2, pp. 289–304, 2007.
- [81] A. Colls, N. Ash, and N. Ikkala, *Ecosystem-Based Adaptation: A Natural Response to Climate Change*, IUCN, Gland, Switzerland, 2009.
- [82] S. Sandilyan and K. Kathiresan, "Mangroves as bioshield: an undisputable fact," *Ocean & Coastal Management*, vol. 103, pp. 94–96, 2015.
- [83] H. Yanagisawa, S. Koshimura, K. Goto et al., "The reduction effects of mangrove forest on a Tsunami based on field surveys at Pakarang Cape, Thailand and numerical analysis," *Estuarine, Coastal and Shelf Science*, vol. 81, no. 1, pp. 27–37, 2009.
- [84] The World Bank and the United Nations, *Natural Hazards, Unnatural Disasters: The Economics of Effective Prevention*, The World Bank, Washington, DC, USA, 2010.
- [85] B. Satyanarayana, T. Van der Stocken, G. Rans et al., "Island-wide coastal vulnerability assessment of Sri Lanka reveals that sand dunes, planted trees and natural vegetation may play a role as potential barriers against ocean surges," *Global Ecology and Conservation*, vol. 12, pp. 144–157, 2017.

- [86] R. A. Feagin, N. Mukherjee, K. Shanker et al., “Shelter from the storm? use and misuse of coastal vegetation bioshields for managing natural disasters,” *Conservation Letters*, vol. 3, no. 1, pp. 1–11, 2010.
- [87] B. Satyanarayana, N. Koedam, K. De Smet et al., “Long-term mangrove forest development in Sri Lanka: early predictions evaluated against outcomes using VHR remote sensing and VHR ground-truth data,” *Marine Ecology Progress Series*, vol. 443, pp. 51–63, 2011.
- [88] A. R. Gunawardena, S. P. Nissanka, N. D. K. Dayawansa, and T. T. Fernando, “Above ground biomass estimation of mangroves located in Negombo-Muthurajawela wetland in Sri Lanka using ALOS PALSAR images,” *Tropical Agricultural Research*, vol. 27, no. 2, pp. 137–146, 2016.
- [89] D. Geneletti and L. Zardo, “Ecosystem-based adaptation in cities: an analysis of European urban climate adaptation plans,” *Land Use Policy*, vol. 50, pp. 38–47, 2016.

Research Article

A Study on Evaluating Water Resources System Vulnerability by Reinforced Ordered Weighted Averaging Operator

Meiqin Suo ¹, Jing Zhang,¹ Lixin He ¹, Qian Zhou,² and Tengpeng Kong¹

¹School of Water Conservancy and Hydroelectric Power, Hebei University of Engineering, Handan 056038, China

²Huazhong University of Science and Technology, Wuhan 430000, China

Correspondence should be addressed to Lixin He; helixin@hebeu.edu.cn

Received 20 August 2020; Revised 21 September 2020; Accepted 15 October 2020; Published 21 November 2020

Academic Editor: Huiyan Cheng

Copyright © 2020 Meiqin Suo et al. This is an open access article distributed under the Creative Commons Attribution License, which permits unrestricted use, distribution, and reproduction in any medium, provided the original work is properly cited.

Evaluating the vulnerability of a water resources system is a multicriteria decision analysis (MCDA) problem including multiple indicators and different weights. In this study, a reinforced ordered weighted averaging (ROWA) operator is proposed by incorporating extended ordered weighted average operator (EOWA) and principal component analysis (PCA) to handle the MCDA problem. In ROWA, the weights of indicators are calculated based on component score coefficient and percentage of variance, which makes ROWA avoid the subjective influence of weights provided by different experts. Concretely, the applicability of ROWA is verified by assessing the vulnerability of a water resources system in Handan, China. The obtained results can not only provide the vulnerable degrees of the studied districts but also denote the trend of water resources system vulnerability in Handan from 2009 to 2018. And the indicator that most influenced the outcome is per capita GDP. Compared with EOWA referred to various indicator weights, the represented ROWA shows good objectivity. Finally, this paper also provides the vulnerability of the water resource system in 2025 based on ROWA for water management in Handan City.

1. Introduction

With the rapid development of economy, the destruction of water environment, and the continuous change of global environment, the water resources system has suffered a series of water safety problems, such as water shortage, contradiction between supply and demand, and water pollution. The problems are constantly changing the function, structure, and characteristics of the water resources system directly or indirectly, thus affecting the vulnerability of the water resources system. Therefore, it is urgent for hydrologists and disaster scholars to study the vulnerability of water resources.

Vulnerability is widely used in various fields of academic research, such as drought vulnerability [1, 2] and ecological vulnerability [3, 4]. Vulnerability is a term commonly used to describe a weakness or flaw in a system, and it is vulnerable to specific threats and harmful events [5]. Although scholars have different understanding on vulnerability, there is no uniform definition about vulnerability in the water

resource system until now. Synthesizing the domestic and research results, the concept of water resources vulnerability was summarized by Zou et al. [6] as follows: the nature and state of the water resources system are affected and destroyed by the threats and damage from human activities and natural disasters, and it is difficult to restore to the original state and function after being damaged. The factors affecting the vulnerability of the water resources system contain the system itself and the stress exerted outside the system (such as climate change and human activities). The influencing factors of the water resources system itself involve its inherent structure, function, and complexity. It is generally believed that the more complex the system structure, the lower the soil and water loss rate, the stronger the groundwater regeneration capacity, the weaker the vulnerability of the system, and on the contrary, the stronger the vulnerability of the system. Considering the influencing factors mentioned above, it is necessary to apply multicriteria decision analysis (MCDA) technology to evaluate the vulnerability of the water resources system. Fortunately, the

EOWA method [7] as one effectively MCDA tool had been widely studied and applied. It considers not only the weight of the factors affecting the multicriteria decision system, but also the position of the factors in aggregation process and the weight of the experts. For example, Xiao et al. [8] discussed the problem of ordering qualitative data by using an EOWA operator and the processing of qualitative data in multi-attribute decision-making. Wei [9] put forward a group decision-making method of coal mine safety evaluation based on the EOWA operator, so as to improve the efficiency of safety management, raise the level of safety management, and reduce the cost of safety management.

The thought of EOWA is to transform fuzzy sets into specific values and multiply them by corresponding weight. And in the calculation process, order weight is considered because the important degrees of all experts are usually unequal. Due to the addition of ordered weight, the extreme value error is reduced. For example, Zarghami et al. applied the EOWA operator to group decision-making on water resources projects [10]. However, in the vulnerability assessment of the water resources system, many indicators should be considered objectively to reflect the characteristics from different aspects. However, the indicator weights of EOWA are determined artificially, which contains a large subjective arbitrariness. It is noted that the principal component analysis (PCA) can decompose the original multiple indicators into independent single indicator and carry out diversified statistics. It can not only make the independent single indicator unrelated, avoiding overlapping and cross between the indicators, but also retain the authenticity of the original indicator through dimensionality reduction thought. Thus, the multi-indicator problem can be integrated into a single-indicator form avoiding the subjective randomness of artificial decision-making by using PCA. For example, Pan and Xu [11] established a fuzzy comprehensive evaluation model based on PCA. In which, the evaluation factors were screened by PCA, and the characteristic value of the selected indicators was regarded as the weight, which reduced the influence of subjective factors and improved the accuracy of the model. Ren et al. [12] used the PCA to evaluate the integrated performance of different hydrogen energy systems and select the best scenario. Therefore, one potential methodology to handling MCDA problems and the subjectivity of weights is to incorporate the EOWA and PCA within a general framework, leading to an integrated assessment method.

Accordingly, the objective of this study is firstly to propose a reinforced ordered weighted averaging (ROWA) operator based on PCA and EOWA, to dispose the MCDA problems. The proposed operator would have the following advantages: (a) effectively reflecting the importance of different decision levels by order weight in the evaluation system, (b) avoiding overlap and cross among multiple indicators, and overcoming the subjective randomness of different weights by the cumulative contribution rate, and (c) determining the main factors affecting the evaluation system. And secondly, a case study of assessing the vulnerability of the water resources system in Handan City is offered for illustrating the applicability of the developed

ROWA operator. Afterwards, the results analysis is given specifically to provide the managers with objectively evaluated solution for the vulnerability of the water resources system in the past and the future. At last, comparisons between ROWA and EOWA are conducted to further illustrate the advantages of the proposed ROWA.

2. Methodology

2.1. EOWA. For MCDM problems, two key factors (the being evaluated indicators and the weights of indicators) should be ascertained and quantified. However, the second factor is generally provided by experts and denoted in verbal terms which make the evaluation process more subjective and complex. Therefore, this study will reinforce the EOWA operator by introducing APC to improve the second factors and enhance its applicability in handling MCDM problems. Definition and concept on EOWA will be presented as follows.

Xu [7] proposed EOWA based on the ordered weighted average (OWA) operator and extended glossary of terms. The method is to transform fuzzy sets into specific values and multiply them by corresponding weight, which can be defined as follows.

Definition 1. (see [13]). $\bar{S}^n \longrightarrow \bar{S}$, if $F = F = f(s_{\alpha_1}, s_{\alpha_2}, \dots, s_{\alpha_n}) = w_1 s_{\beta_1} \oplus w_2 s_{\beta_2} \oplus \dots \oplus w_n s_{\beta_n} = s_{\beta_n}$, where F is the total positive score of a scheme $\beta = \sum_{i=1}^n w_i \beta_i$, $w = (w_1, w_2, \dots, w_n)$ is a weighted vector associated with EOWA, $w_i \in [0, 1] (i \in N)$, $\sum_{i=1}^n w_i = 1$, and input s_{β_i} is the i th largest element in a set of language data $(s_{\alpha_1}, s_{\alpha_2}, \dots, s_{\alpha_n})$.

w_i is called ordered weight. s_{β_i} consists of two parts: indicator weight and indicator value. And indicator weights are not equal to each other in real problems [14]. Based on these, s_{β_n} of EOWA can be obtained as follows:

$$s_{\beta_n} = P_n d_n, \quad (1)$$

where P_n is the indicator weight and d_n is the indicator value.

The advantages of EOWA are as follows: (1) it can transform fuzzy sets into specific values; (2) using ordered weights to reduce extreme value error in the calculation because the important degrees for all inputs s_{β_n} are generally unequal. All of these make the calculation results more in line with the complexity, spatial, and temporal differences and fuzziness situation.

Ordered weight w_i in the EOWA operator [7] is obtained by the minimum variable method [15, 16], and the final expression [17] is as follows:

$$w_1 = \frac{2(2n-1) - 6(n-1)(1-\theta)}{n(n+1)}, \quad (2)$$

$$w_n = \frac{6(n-1)(1-\theta) - 2(n-2)}{n(n+1)}, \quad (3)$$

$$w_i = \frac{(n-j)}{(n-1)} \times w_1 + \frac{(j-1)}{(n-1)} \times w_n, \quad \text{if } i \in \{2, \dots, n-1\}, \quad (4)$$

where θ is an independent variable representing the optimism of the decision maker. In this study, the value of θ is 0.3 [14], representing that many criteria considered in this decision-making system are satisfied [17].

In multiobjective decision criteria, the model can be further expressed as follows [12]:

$$GS(A_j) = f(P_1S_1(A_j), P_2S_2(A_j), \dots, P_nS_n(A_j)), \quad (5)$$

where $GS(A_j)$ is the comprehensive score on district j vulnerability assessment, $S_i(A_j)$ is the value of vulnerability assessment indicator i for district j , f is the ROWA operator, P_i is the weight of vulnerability assessment indicator i , and n is the number of indicators for water resources vulnerability assessment.

Moreover, when the inputs $S_i(A_j)$ have different units, it is necessary to convert them into data on interval $[0, 1]$. A simple method of standardization is used [8] in this study, shown as follows:

$$S_i(A_j) = \begin{cases} \frac{S_i(A_j) - \min(S_i)}{\max(S_i) - \min(S_i)}, & \text{for positive inputs,} \\ \frac{\max(S_i) - S_i(A_j)}{\max(S_i) - \min(S_i)}, & \text{for negative inputs.} \end{cases} \quad (6)$$

Also, here the integral mean method [8] is used to assess the important degree of each district, normalized as follows:

$$CGS(A_j) = 1 - \frac{1}{n} \sum_{i=1}^n |S_i(A_j) - GS(A_j)|, \quad (7)$$

where $CGS(A_j)$ is the important degree of district j .

2.2. ROWA. It is noted that PCA can decompose original multiple indicators into independent single indicators and carry out diversified statistics. It can not only make the independent single indicator unrelated, avoiding overlapping and cross between the indicators, but also retain the authenticity of the original indicator through dimensionality reduction thought [18]. Therefore, the reinforced ordered weighted averaging (ROWA) operator is proposed based on EOWA and PCA in this study. ROWA would calculate the indicator weight (P_i) by component score coefficient and percentage of variance [19] based on PCA and then bring it into EOWA to calculate the vulnerability of each administrative district. Totally, the advantages of ROWA can be summarized as follows: (1) it can effectively reflect the importance of different decision levels by order weights in the evaluation system; (2) it can not only avoid overlapping and crossing of indicators but also retain the authenticity of the original indicator based on the cumulative contribution rate and thus avoid the subjective randomness; (3) it can determine the main factors affecting the evaluation system.

Specifically, the formulas for calculating the indicator weight (P_i) based on PCA are as follows:

$$P_i = \sum_{m=1}^n \frac{(F_{im} \times \alpha)}{\beta}, \quad (8)$$

$$F_{im} = SCC_{im} \times \sqrt{\gamma},$$

where SCC_{im} is the score coefficient of the indicator i to the component m ; F_{im} is the component score of the indicator i ; P_i is the weight for the vulnerability assessment indicator i ; α is the contribution rate of the principal component m ; β is the cumulative contribution rate of principal components; and γ is the eigenvalues of principal component m . SCC_{im} , α , β , and γ are calculated by SPSS.

And then, take P_i into formula (5) and get $CGS(A_j)$. At last, the final percentile score (F) of the vulnerability in the district j can be gained by the following formula:

$$F = CGS(A_j) \times 100. \quad (9)$$

According to calculation of EOWA and P_i , the specific solution process of ROWA can be summarized as shown in Figure 1.

Based on previous information and similar studies [20], the vulnerability of water resources systems can be classified into five classes: I, low vulnerability; II, medium vulnerability; III, medium-high vulnerability; IV, high vulnerability; and V, severe vulnerability.

2.3. Numerical Example. Here, an example is given below for clearly understanding the proposed ROWA method. Supposing that the vulnerability of the water resources system in four research areas (represented by A_1 , A_2 , A_3 , and A_4) should be evaluated, and the related indicators are 10, whose original data are shown in Table 1.

Accordingly, the calculation step of ROWA for this problem can be summarized as follows.

Step 1. Calculate indicator weight P_i .

After calculating with PCA method, the results show that under the criterion of cumulative contribution rate $\geq 85\%$, two principal components can be obtained, and the actual cumulative contribution rate is 93.73%. And when the values of SCC_{im} , α , β , and γ are obtained, P_i can be gained based on them, shown in Table 2.

Step 2. Solve order weight w_i .

w_i is calculated according to formulas (2), (3), and (4), and the results are shown in Table 3.

Step 3. Calculate comprehensive score $CGS(A_j)$.

After P_i is calculated, raw values are transformed according to formula (6). Then, values of $GS(A_j)$ and $CGS(A_j)$ can be calculated according to formulas (5) and (7), as shown in Table 4.

Step 4. Calculate percentile score F .

F is shown in Table 4.

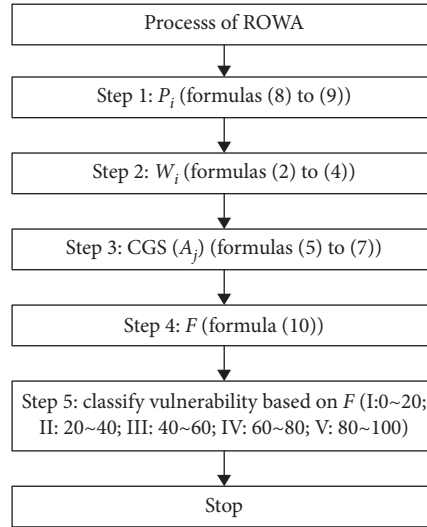


FIGURE 1: Process of ROWA.

TABLE 1: Original data.

	C1	C2	C3	C4	C5	C6	C7	C8	C9	C10
A1	537	6.3	1.7	0.3	6.8	15.8	1.3	0.8	4.6	130
A2	661	10.8	1.7	0.4	0.5	1.3	1.1	1	2.3	260
A3	801	2.5	1.5	0.5	88.5	36	0.8	0.9	3.2	600
A4	1058	5.9	1.3	0.6	39.6	26.5	0.9	1.2	2.5	580

TABLE 2: Weight for the vulnerability assessment indicator i .

Indicator	C1	C2	C3	C4	C5	C6	C7	C8	C9	C10
P_i	0.31	-0.02	-0.28	0.31	0.12	0.10	-0.25	0.31	-0.27	0.26

TABLE 3: Value of w_i .

w_1	w_2	w_3	w_4	w_5	w_6	w_7	w_8	w_9	w_{10}
0.002	0.024	0.045	0.067	0.089	0.111	0.133	0.155	0.176	0.198

TABLE 4: Value of $GS(A_j)$, $CGS(A_j)$, and F .

District	$GS(A_j)$	$CGS(A_j)$	F	VD
A1	0.07	0.60	60	IV
A2	0.08	0.53	53	III
A3	0.15	0.25	31	II
A4	0.14	0.31	25	II

Note. VD = vulnerable degree.

Step 5. Determine the degree of vulnerability based on score F .

Finally, according to allocation criteria, it is easy to judge the vulnerability of each region, as shown in Table 4.

It can be seen that A1 and A2 belong to high vulnerability and medium-high vulnerability, respectively, and A3 and A4 belong to medium vulnerability.

3. Case Study

3.1. The Profile of Research Area. Handan City is in the southern end of Hebei Province, southeast of North China. The geographical position is between $36^{\circ}04'N \sim 37^{\circ}01'N$ and $113^{\circ}28'E \sim 115^{\circ}28'E$. Because the city of Handan is surrounded by Taihang Mountains, North China Plain, Xingtai, and Anyang tightly, it is called the southern gate of Hebei Province. Its administrative area is shown in Figure 2.

In recent years, the total amount of water resources in Handan is about $16.7 \times 10^9 \cdot m^3$, and the per capita water resources is $191 \cdot m^3$ per year, which is only 9% of the per capita level of the whole country. And by the end of 2018, the total population of Handan was 10.51×10^6 with a population density of $871 \text{ person}/km^2$ and the population is increasing gradually. The proportion of surface water and groundwater to total water supply is 40.5% and 59.5%,



FIGURE 2: Administrative region of Handan.

respectively. In the water supply, the groundwater is regarded as the main water source, resulting in long-term serious overexploitation of local groundwater and continuous decrease of groundwater level. The water resources system of Handan City is being destroyed gradually, and its vulnerability is becoming more and more obvious. Therefore, for the sustainable development of water resources, it is meaningful to make a reasonable evaluation about the vulnerability of the water resources system in Handan.

3.2. Establishment of Indicator System

3.2.1. Principles for the Establishment of an Indicator System. When constructing an assessment system of water resources vulnerability, five principles should be followed: scientific principle, operational principle, comprehensive principle, leading principle, and regional principle [21]. They play a comprehensive role in building the evaluation indicator system of water resources system vulnerability and ensure the scientificity and rationality of the evaluation indicator system.

3.2.2. Selection of Indicators and Establishment of Indicator System. Water resources system is a huge and complex system, whose vulnerability is affected by many factors. It would be best to establish an indicator system including all the factors, but this is difficult and not realistic to achieve the data of all factors. Therefore, most of the studies selected some indicators to build the evaluation indicator system based on the actual situation of the study area and data acquisition [22]. Similarly, ten indicators are selected to study the vulnerability of the water resources system in Handan City in this study. The selected indicators are as follows: annual precipitation ($10^8 \cdot \text{m}^3$) (C1), water conservancy regulation capacity ($10^4 \cdot \text{m}^3$) (C2), groundwater exploitation rate (C3), groundwater regeneration capacity (C4), annual drought index (C5), soil and water loss rate (C6), population density (person/ km^2) (C7), per capita

GDP (yuan) (C8), per capita water consumption (m^3) (C9), and water resources utilization ratio (C10).

3.3. Administrative Divisions and Data Notes. In this study, the research area is divided into 17 districts according to the administrative division: the three districts of the city (SS), Fengfeng Kuang Qu (FK), Wu'an County (WA), Handan County (HD), Daming County (DM), Wei County (WX), Qiu Zhou County (QZ), Qiu County (QX), Jize County (JZ), Feixiang County (FX), Guangping County (GP), Cheng'an County (CA), Linzhang County (LZ), Cixian County (CX), Shexian (SX), Yongnian County (YN), and Guantao County (GT). It is noted that at the end of 2016, the city of Handan had been rezoned: Yongnian County and Feixiang County were renamed as Yongnian District and Feixiang District individually. Handan County was cancelled and divided into the city's three districts. In order to better reflect the vulnerability changes of the water resources system, the data of ten indicators in 17 districts from 2009 to 2016 and 16 districts from 2017 to 2018 are selected to analyze the successive annual trend of its vulnerability in Handan City. The related data are calculated according to Water Resources Bulletin and Statistical Yearbook of Handan City.

4. Result Analysis and Discussion

4.1. Analysis of the Water Resources System Vulnerability by ROWA. When the criterion of cumulative contribution rate is 75%, the indicator weights calculated by component score coefficient and percentage of variance were $P = P = (0.079, 0.022, 0.122, 0.116, 0.051, 0.121, 0.135, 0.068, 0.125, \text{ and } 0.161)$. And thus, the percentile score of the vulnerability of water resources systems from 2009 to 2018 can be acquired by the developed ROWA, which are shown in Figure 3. In all the studied districts, only DM appears a sustained decline from 81.50% to 60.03% during the decade and other districts show varying degrees of volatility. For example, the vulnerability of water resources systems in SS has three rising years: 2012, 2014, and 2016; in FK, there are

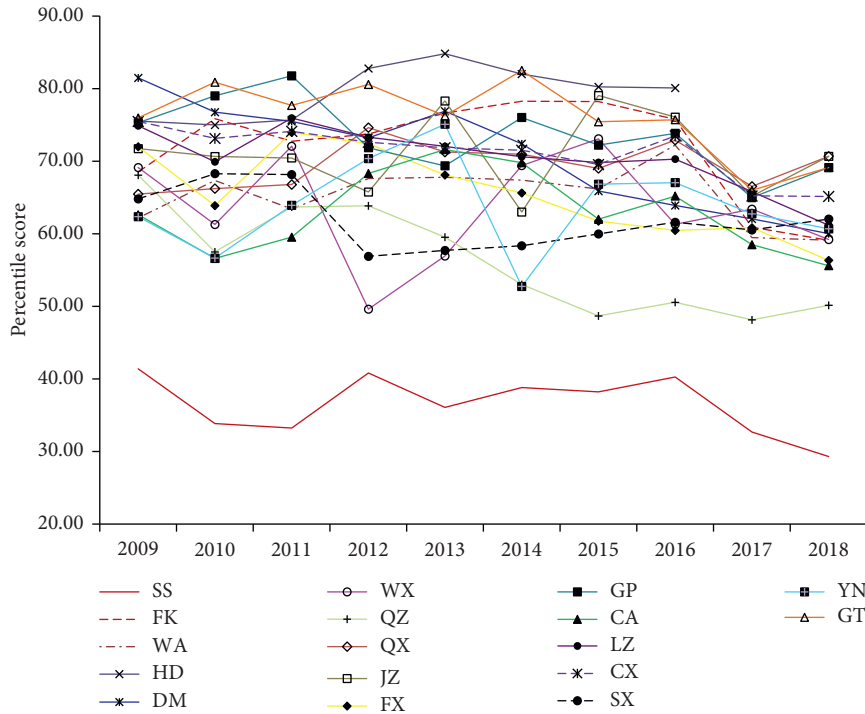


FIGURE 3: The percentile score of the water resources system vulnerability in Handan City.

two rising periods: from 2009 to 2010 and from 2011 to 2014; in WA, three increasing periods are from 2009 to 2012, from 2010 to 2012, and from 2015 to 2016; in HD, except for 2009, 2010, 2014, and 2016, the vulnerability of water resources systems in the other years is greater than the year before; in WX, there are also three rising periods: from 2010 to 2011, from 2012 to 2015, and from 2016 to 2017; in QZ, the two growing periods are from 2010 to 2012 and from 2015 to 2016; in QX, the three increasing periods are from 2010 to 2012, from 2015 to 2016, and from 2017 to 2018; in JZ, only the years of 2013, 2015, and 2018 are more vulnerable than the previous year; with the exception of 2011, the vulnerability has declined in all other years in FX; in GP, there are four ascending periods: from 2010 to 2011, from 2013 to 2014, from 2015 to 2016, and from 2017 to 2018; in CA, the vulnerability firstly increases from 2009 to 2013 and then decreases from 2014 to 2015, and grows again in 2016 and declines from 2017 to 2018 at last; in LZ and CX, there are the same ascending years: 2011 and 2016; in SX, three growing periods are from 2009 to 2010, from 2012 to 2016, and from 2017 to 2018; in YN, except for the years of 2010, 2014, and 2017, the vulnerability in all other years is greater than the previous year; in GT, there is an increasing trend in every two years from 2009 to 2018. In a word, although there are multiple rising periods in most districts, the percentage scores of their vulnerability decline significantly in 2018 compared to 2009 except for HD.

Correspondingly, the vulnerable degree of the studied districts in Handan City from 2009 to 2018 also can be obtained based on their percentile scores, which is denoted in Table 5. It can be known that only the average vulnerable degrees of the studied decade in SS and QZ are medium and

medium-high, while other districts are high. And the percentage of districts with high vulnerability in the decade is 88.24%, 76.47%, 82.5%, 76.47%, 70.59%, 64.71%, 76.47%, 82.35%, 75%, and 56.25%, respectively. Therefore, it can be concluded that although the proportion of districts with high vulnerability was large, it is gradually decreasing.

In addition, to clearly analyze the fluctuations of vulnerability, the main factors affecting the evaluation system in every district can also be acquired by the PCA method of ROWA, shown in Table 6. In detail, the districts mainly affected by C2 are FK and FX; the districts of HD and CX are principally influenced by C3; the districts mainly affected by C7 are QZ and QX; the indicator of C5 only has a major impact on GP; the indicator of C8 has major implications for many districts, including WA, DM, WX, JZ, LZ, SX, and GT; and the indicator of C10 mainly affects SS and CA. Overall, this result would provide a good guidance for managers in water resource rehabilitation and governance.

4.2. Comparison between ROWA and EOWA. To clearly explain the impact of indicator weight on the evaluation results, the comparison of results between ROWA and EOWA is conducted. Given space constraints, this paper takes the results in 2009 and 2018 as examples, shown in Tables 7 and 8 individually. In which, symbols of EOWA-1, EOWA-2, and EOWA-3 mean the vulnerability of the water resources system in Handan City calculated by EOWA with three different indicator weights: $P1 = (0.1, 0.1, 0.1, 0.1, 0.1, 0.1, 0.1, 0.1, 0.1, 0.1)$, $P2 = (0.05, 0.05, 0.05, 0.05, 0.05, 0.05, 0.3, 0.3, 0.05, 0.05)$, and $P3 = (0.05, 0.05, 0.05, 0.05, 0.05, 0.05, 0.05, 0.05, 0.3, 0.3)$. The percentile scores of all districts by the

TABLE 5: Vulnerable degree of the water resources systems in Handan City from 2009 to 2018.

District	Vulnerable degree									
	2009	2010	2011	2012	2013	2014	2015	2016	2017	2018
SS	III	II	II	III	II	II	II	III	II	II
FK	IV	IV	IV	IV	IV	IV	IV	IV	IV	III
WA	IV	IV	IV	IV	IV	IV	IV	IV	III	III
HD	IV	IV	IV	IV	V	V	V	V	—	—
DM	V	IV	IV	IV	IV	IV	IV	IV	IV	IV
WX	IV	IV	IV	III	III	IV	IV	IV	IV	III
QZ	IV	III	IV	IV	III	III	III	III	III	III
QX	IV	IV	IV	IV	IV	IV	IV	IV	IV	IV
JZ	IV	IV	IV	IV	IV	IV	IV	IV	IV	IV
FX	IV	IV	IV	IV	IV	IV	IV	IV	IV	III
GP	IV	IV	V	IV	IV	IV	IV	IV	IV	IV
CA	IV	III	III	IV	IV	IV	IV	IV	III	III
LZ	IV	IV	IV	IV	IV	IV	IV	IV	IV	IV
CX	IV	IV	IV	IV	IV	IV	IV	IV	IV	IV
SX	IV	IV	IV	III	III	III	III	IV	IV	IV
YN	IV	III	IV	IV	IV	III	IV	IV	IV	IV
GT	IV	V	IV	V	IV	V	IV	IV	IV	IV

Note. VD = vulnerable degree; I = low vulnerability (0 ~ 20); II = medium vulnerability (20 ~ 40); III = medium-high vulnerability (40 ~ 60); IV = high vulnerability (60 ~ 80); V = severe vulnerability (80 ~ 100).

TABLE 6: The main factors affecting the evaluation system.

D	IF	D	IF	D	IF	D	IF	D	IF	D	IF
SS	C10	HD	C3	QZ	C7	FX	C2	LZ	C8	YN	C4
FK	C2	DM	C8	QX	C7	GP	C5	CX	C3	GT	C8
WA	C8	WX	C8	JZ	C8	CA	C10	SX	C8		

Note. D = district; IF = influencing factor.

TABLE 7: Comparison of results between ROWA and EOWA in 2009.

District	ROWA		EOWA-1		EOWA-2		EOWA-3	
	F	Rank	F	Rank	F	Rank	F	Rank
SS	41.40	1	41.58	1	40.83	1	40.55	1
WA	62.20	2	62.38	2	62.17	3	62.18	3
YN	62.36	3	62.63	3	62.15	2	61.94	2
CA	62.64	4	62.94	4	62.52	4	62.44	4
SX	64.82	5	64.97	5	64.72	5	64.79	5
QX	65.48	6	65.44	6	65.15	6	65.02	6
QZ	68.09	7	68.51	8	67.97	8	67.69	7
FK	68.52	8	68.41	7	67.89	7	68.00	8
WX	69.14	9	69.15	9	68.95	9	69.06	9
JZ	71.75	10	71.80	10	71.48	10	71.41	10
FX	72.00	11	72.29	11	71.81	11	71.74	11
LZ	74.90	12	75.02	12	74.63	12	74.75	12
GP	75.31	13	75.21	13	75.03	14	74.92	13
CX	75.50	14	75.60	15	75.29	15	75.32	15
HD	75.55	15	75.48	14	74.92	13	75.00	14
GT	75.97	16	75.94	16	75.85	16	75.76	16
DM	81.50	17	81.54	17	81.45	17	81.45	17

three EOWA methods change with the different indicator weights in both 2009 and 2018, even the orders have changed in some districts. For example, in 2009, the percentile scores of WA, YN, QZ, FK, GP, CX, and HD are (62.38, 62.17, 62.18), (62.63, 62.15, 61.94), (68.51, 67.97, 67.69), (68.41, 67.89, 68.00), (75.21, 75.03, 74.92), (75.60, 75.29, 75.32), and

(75.48, 74.92, 75.00) by EOWA-1, EOWA-2, and EOWA-3, respectively, and their orders are (2, 3, 3), (3, 2, 2), (8, 8, 7), (7, 7, 8), (13, 14, 13), (15, 15, 15), and (14, 13, 14) by the three EOWA methods individually, bolded in Table 7; in 2018, the percentile scores of FK, WA, WX, JZ, and QX are (59.44, 58.58, 58.51), (59.40, 58.80, 58.66), (59.84, 58.69, 58.73),

TABLE 8: Comparison of results between ROWA and EOWA in 2018.

District	ROWA		EOWA-1		EOWA-2		EOWA-3	
	F	Rank	F	Rank	F	Rank	F	Rank
SS	29.31	1	30.26	1	28.37	1	28.34	1
QZ	50.15	2	50.67	2	49.60	2	49.51	2
CA	55.62	3	56.19	3	55.12	3	55.06	3
FX	56.34	4	56.83	4	55.87	4	55.78	4
FK	59.11	5	59.44	6	58.58	5	58.51	5
WA	59.12	6	59.40	5	58.80	7	58.66	6
WX	59.20	7	59.84	7	58.69	6	58.73	7
DM	60.03	8	60.53	8	59.63	8	59.60	8
YN	60.68	9	61.32	9	60.28	9	60.25	9
LZ	61.18	10	61.72	10	60.87	10	60.88	10
SX	62.03	11	62.29	11	61.93	11	61.70	11
CX	65.16	12	65.55	12	64.82	12	64.67	12
GP	69.14	13	69.39	13	68.70	13	68.70	13
GT	69.14	14	69.54	14	68.79	14	68.75	14
JZ	70.67	15	70.98	16	70.40	15	70.32	16
QX	70.69	16	70.89	15	70.42	16	70.29	15

TABLE 9: Vulnerability prediction of the water resources system in 2025 in Handan City.

District	F	VD	District	F	VD	District	F	VD	District	F	VD
SS	29.51	II	WX	65.44	IV	FX	63.56	IV	CX	72.87	IV
FK	72.83	IV	QZ	57.91	III	GP	76.20	IV	SX	60.92	IV
WA	67.70	IV	QX	68.00	IV	CA	64.11	IV	YN	66.92	IV
DM	75.28	IV	JZ	73.83	IV	LZ	73.69	IV	GT	78.44	IV

(70.98, 70.40, 70.32), and (70.89, 70.42, 70.29) with their orders being (6, 5, 5), (5, 7, 6), (7, 6, 7), (16, 15, 16), and (15, 16, 15) resulted from EOWA-1, EOWA-2, and EOWA-3, respectively, bolded in Table 8. By comparison, the percentile scores of WA, YN, QZ, FK, GP, CX, and HD are 62.20, 62.36, 68.09, 68.52, 75.31, 75.50, and 75.55 while their orders are 2, 3, 7, 8, 13, 14, and 15 by ROWA, respectively, in 2009; and the percentile scores of FK, WA, WX, JZ, and QX were 59.11, 59.12, 59.20, 70.67, and 70.69 with their orders being 5, 6, 7, 15, and 16 aroused from ROWA individually in 2018. It should be pointed that similar conditions have existed in other years.

In general, the results by ROWA are more effective than the ones by EOWA when the weights of indicators have changed. In practice, the weights of indicators for MCDM problems exactly change if they are determined by experts. Because the experts' numbers and/or subjectivity are constantly changing. Inversely, if the weights of indicators are calculated based on component score coefficient and percentage of variance in ROWA, the results for MCDM problems would not be affected by experts. Therefore, it can be obtained that ROWA is more objective and more fit for MCDM problems, and meanwhile provides the manager with an optimal and rational decision support system.

4.3. *Vulnerability Prediction of Water Resources System.* In order to provide better decision support for managers in future water resources management, the vulnerability of the water resources system in 2025 in Handan City is also assessed by the proposed ROWA based on the existing data,

shown in Table 9. It can be seen that except for SS and QZ are medium vulnerability and medium-high vulnerability, respectively, all other districts have the high vulnerability with the proportion reaching 87.5%. Therefore, even by 2025, the vulnerability of the water resources system in Handan City would remain high and will require great attention.

5. Conclusions

In this study, a new ROWA method based on EOWA and PCA has been proposed for dealing with multicriteria decision-making problems. In this method, under the criterion of cumulative contribution, the percentile score can be ranked by order weight, which can effectively reduce the extreme error. In addition, the indicator weight (P_i) is calculated based on the component score coefficient and percentage of variance by PCA. Therefore, the proposed ROWA can not only avoid overlapping and crossing of indicators but also retain the authenticity of the original indicator, thus avoiding the subjective randomness. Moreover, it also can determine the main factors affecting the vulnerability, which is convenient for decision makers to make decisions.

A case of water resources system vulnerability in Handan City has been studied for demonstrating applicability of the proposed methodology. The analyses show that except for the vulnerability of the water resources system in DM has a sustained decline, other districts display varying degrees of volatility during the decade. Although the proportion of districts with high vulnerability is large, it is gradually

decreasing from 2009 to 2018. And among the vulnerability assessment indicators, the one that most influenced the outcome is per capita GDP. Compared with EOWA referred to three different indicator weights, the vulnerability of the water resources system evaluated by ROWA has more rationality and objectivity. At last, the vulnerability of the water resources system in 2025 is also assessed by ROWA, which would be helpful for water management in Handan City.

Data Availability

The original data for the studied vulnerability were calculated according to Water Resources Bulletin and Statistical Yearbook of Handan City. The data can be gathered upon e-mail request to the corresponding author.

Conflicts of Interest

The authors declare that they have no conflicts of interest.

Acknowledgments

This research was funded by General Program of Natural Science Foundation of Hebei Province (no. D2019402235), Science and Technology Research and Development Project of Handan City (no. 1434201078-2), National Natural Science Foundation of China (no. 51879066), and Doctoral Foundation of Hebei University of Engineering (no. PP0250).

References

- [1] Y. Wang, J. Wang, Y. B. Yao, and J. S. Wang, "Evaluation of drought vulnerability in Southern China based on principal component analysis," *Ecology & Environmental Sciences*, vol. 23, pp. 1897–1904, 2014.
- [2] E. Johanna, J. Keighobad, and M. Hamid, "Drought vulnerability in the United States: An integrated assessment," *Water*, vol. 12, no. 7, p. 2033, 2020.
- [3] Z. Qiao, X. Yang, J. Liu, and X. L. Xu, "Ecological vulnerability assessment integrating the spatial analysis technology with algorithms: A case of the wood-grass ecotone of Northeast China," *Abstract and Applied Analysis*, vol. 2013, pp. 1–8, 2013.
- [4] X. Yu, Y. Li, M. Xi, F. L. Kong, M. Y. Pang, and Z. D. Yu, "Ecological vulnerability analysis of Beidagang National Park, China," *Frontiers of Earth Science*, vol. 13, no. 2, pp. 385–397, 2019.
- [5] M. Al-Kalbani, M. Price, A. Abahussain, M. Ahmed, and T. O'Higgins, "Vulnerability assessment of environmental and climate change impacts on water resources in Al Jabal Al Akhdar, Sultanate of Oman," *Water*, vol. 6, no. 10, pp. 3118–3135, 2014.
- [6] J. Zou, Y. R. Yang, and X. X. Li, "Concepts of vulnerability of surface water resources and its quantitative assessment," *Bulletin of Soil and Water Conservation*, vol. 27, no. 2, pp. 132–136, 2007.
- [7] Z. S. Xu, *Uncertain Multi-Attribute Decision Making Method and its Application*, Tsinghua University Press, Beijing, China, 2004.
- [8] G. C. Xiao, Y. Y. Shi, X. Xiao, and J. R. Zhang, "Based on the qualitative data EOWA operator multi-attribute decision-making method and its application," *Fuzzy Engineering and Operations Research*, Springer, Berlin, Germany, 2012.
- [9] C. F. Wei, "A group decision-making method based on EOWA and ILOWGA operators for coal mine safety evaluation," *International Journal of Engineering Innovations and Research*, vol. 6, pp. 245–248, 2017.
- [10] M. Zarghami, R. Ardakanian, A. Memariani, and F. Szidarovszky, "Extended OWA operator for group decision making on water resources projects," *Journal of Water Resources Planning and Management*, vol. 134, no. 3, pp. 266–275, 2008.
- [11] J. Pan and T. Xu, "Evaluation of water resources carrying capacity based on fuzzy comprehensive evaluation model based on PCA," *Jilin Water Conservancy*, vol. 8, pp. 44–46, 2017.
- [12] J.-Z. Ren, S.-y. Tan, and L.-c. Dong, "The assessment of hydrogen energy systems for fuel cell vehicles using principal component analysis and cluster analysis," *Mathematical Problems in Engineering*, vol. 2012, Article ID 191308, 2012.
- [13] X. F. Liu and W. H. Qiu, "Evaluation of venture group language for venture capital projects bas191308ed on EOWA," *Enterprise Economy*, vol. 5, pp. 41–43, 2007.
- [14] M. Q. Suo, Y. P. Li, and G. H. Huang, "Multicriteria decision making under uncertainty: An advanced ordered weighted averaging operator for planning electric power systems," *Engineering Applications of Artificial Intelligence*, vol. 25, no. 1, pp. 72–81, 2012.
- [15] R. Fullér and P. Majlender, "On obtaining minimal variability OWA operator weights," *Fuzzy Sets and Systems*, vol. 136, no. 2, 2003.
- [16] M. O'Hagan, "A fuzzy neuron based upon maximum entropy ordered weighted averaging," in *Proceedings of the International Conference on Uncertainty in Knowledge Bases*, Paris, France, 1990.
- [17] L. Liu, G. H. Huang, Y. Liu, G. A. Fuller, and G. M. Zeng, "A fuzzy-stochastic robust programming model for regional air quality management under uncertainty," *Engineering Optimization*, vol. 35, no. 2, pp. 177–199, 2003.
- [18] R. T. Liu, Q. Fu, W. Y. Li, Y. Feng, and G. L. Li, "Study and discussion on groundwater vulnerability," *Journal of Water Resources and Water Engineering*, vol. 17, no. 6, pp. 1–5, 2006.
- [19] H. W. Fang, S. Q. Sun, and Y. L. Zhu, "Application and analysis of principal component analysis in water quality assessment," *Environmental Science and Management*, vol. 3412, pp. 152–154, 2009.
- [20] L. Wan, J. Xia, S. Hong, H. Bu, L. Ning, and J. Chen, "Decadal climate variability and vulnerability of water resources in arid regions of Northwest China," *Environmental Earth Sciences*, vol. 73, no. 10, pp. 6539–6552, 2015.
- [21] M. M. Qiao, *Study on the Vulnerability of Water Resources in Suzhou City*, Suzhou University of Science and Technology, Suzhou, China, 2017.
- [22] Y. J. Zhu, *Study on Vulnerability Assessment of Water Resources in Wuhan City*, Central China Normal University, Wuhan, China, 2015.

Research Article

A Birandom Chance-Constrained Linear Programming Model for CCHP System Operation Management: A Case Study of Hotel in Shanghai, China

Zhe Bao,^{1,2} Ye Xu ,^{1,2} Wei Li,^{1,2} Xu Wang,¹ Meng R. Li,^{1,2} Ji H. Li,¹ and Han S. Yang¹

¹MOE Key Laboratory of Regional Energy and Environmental Systems Optimization,

College of Environmental Science and Engineering, North China Electric Power University, Beijing 102206, China

²Beijing Key Laboratory of Demand Side Multi-Energy Carriers Optimization and Interaction Technique, Beijing 100192, China

Correspondence should be addressed to Ye Xu; xuye@ncepu.edu.cn

Received 12 August 2020; Revised 2 October 2020; Accepted 30 October 2020; Published 19 November 2020

Academic Editor: Xander Wang

Copyright © 2020 Zhe Bao et al. This is an open access article distributed under the Creative Commons Attribution License, which permits unrestricted use, distribution, and reproduction in any medium, provided the original work is properly cited.

Due to its capability to reduce fuel consumption and increase energy efficiency, the combined cooling, heating, and power (CCHP) system has obtained great concern during the last decade. A large number of deterministic and stochastic optimization models were proposed for supporting the operation management of the CCHP system, but few studies noticed that users' demands in the real world may be subjected to twofold randomness with incomplete or uncertain information. In this study, a birandom chance-constrained linear programming (BCCLP) model is developed for identifying optimal operation strategies under random uncertainties. Compared with traditional stochastic programming models, the BCCLP model made the improvement through describing the energy demands as the birandom variables firstly, instead of traditional random variables. This way effectively avoided potential imbalance between energy supply and demand caused by oversimplified expression of uncertain parameters. A gas-fired CCHP system of a hotel in Shanghai, China, was used as a study case for demonstration. A variety of operation strategies are obtained under specific constraints-satisfaction conditions. It is concluded that the BCCLP model was capable of generating the cost-effective operation strategies and evaluating the tradeoffs between system economy and reliability. The influence imposed by some critical parameters on the system performance was examined through the sensitivity analysis, which provided the important guidance to the design and operational management of other similar CCHP systems in the future.

1. Introduction

Nowadays, with the rapid improvement of socioeconomic development, industrialization, and urbanization, the electricity and energy requirements were increased at a fast rate in China. The State Grid Energy Research Institute projected the increases in electricity and energy demands from 148 billion MWh and 126 billion MJ in 2018 to 226 billion MWh and 151 billion MJ in 2035 (growth at two rates of 52.7% and 19.8% approximately, resp.). As the main energy form for power generation, the utilization of fossil fuels was accompanied by a large number of pollutants (i.e., nitric oxides, carbon dioxide, and sulfur oxides), which led to global warming and brought serious pressure on ecosystem protection and human health [1, 2]. According to the 2016

BP Statistical Review of World Energy, China's energy structure has changed in recent years [3]. The proportion of coal consumption has slightly decreased from 69.8% (in 2012) to 61.47% (in 2016), while the proportion of nonfossil energy consumption, such as natural gas, has increased from 14.5% to 19.7%. From the above, it is foreseeable that, in order to reduce coal consumption and promote nonfossil energy development, a low-carbon diversified energy structure would be formed in the future, where the natural gas would play an important role.

Traditional energy-supply modes provided most of the electricity, heat, and cool quantity in large centralized facilities. However, the long-distance transmission network of these plants would cause electrical and thermal loss; meanwhile, the existence of direct discharged and unutilized

waste heat would reduce the energy-utilization efficiency [4]. With these premises, the distributed energy-supply modes with the cascade utilization of clean energy were favorable to realize the environment protection and sustainable development. Currently, the gas-fired CCHP (combined cooling, heating, and power) puts into use in electricity and energy supply extensively, particularly on a small-scale basis. Gas-fired CCHP system has the immense benefits; for example, (i) the operational pattern based on cascade utilization of clean energy has the ability to meet the electricity demand by the aid of GT (gas turbines) or ICE (internal-combustion engines) and simultaneously provide the cold and heat energy through recovering waste heat, while maintaining the high efficiency, keeping the high stability, and producing the minimal greenhouse gas and air pollutant emissions; (ii) as a typical distributed energy system, the properties including short-distance transmission, small physical size, and small-capacity modules were useful in reducing the electricity and energy loss in the transmission system, without the limitations in the government regulation, utility territory, and land availability; (iii) it had strong adaptability for various buildings, such as baseload generation, emergency backup, and peak/load shaving for industrial parks, university towns, airports, residential buildings, commercial buildings, and office buildings. Generally, a gas-fired CCHP system has strong advantages in protecting the atmospheric environment, improving energy efficiency, and realizing the cost savings. Therefore, its development prospect was expected [5, 6].

In recent years, the gas-fired CCHP system has obtained great concern in China [7]. In 2011, the National Development and Reform Commission, Ministry of Finance of the People's Republic of China, Ministry of Housing and Urban-Rural Development of the People's Republic of China and National Energy Administration issued the policy "guidance for NG distributed energy resources development" for promoting the utilization of natural gas resources and reducing the fuel consumption. Up to now, as a promising way, the practices of CCHP system for electricity and energy supply are presently spreading quickly in China, especially in the major cities such as Beijing, Shanghai, Tianjin, and Guangzhou, with a highly developed economy and strong dependence on the energy resources. For example, Shanghai Pudong International Airport had a projected CCHP system to generate combined cooling, heating, and electricity for meeting the airport's requirements. Beijing Olympics Energy Exhibition Center gas-fired CCHP system was established to provide all the air-conditioning, heating, domestic hot water, and part of power supply for the large-scale building, including National Stadium, National Aquatics Center, and the Information Building. As so far, the installed capacity of CCHP system has reached 50 million kW in China.

The practical applications demonstrated that the performances of CCHP systems were strongly influenced by the operational strategy. It is thus necessary to determine the optimal operational strategy of CCHP system for ensuring the high system efficiency and low pollutant emission. In general, there were usually two basic operation strategies for

CCHP systems: following the electric load (FEL) and following the thermal load (FTL), respectively. Some researchers have investigated the operation of CCHP systems under these two operation strategies [8–11]. For example, Mago et al. selected the CCHP and combined heat and power (CHP) systems as the studied targets and analyzed the economic and environmental benefits under various conditions following different operation strategies [8]. Results showed that the systems based on FTL performed better than those based on FEL. Mago and Hueffed presented the comprehensive benefits of a turbine-driven CCHP system with three different operation strategies, that is, FEL, FTL, and following seasonal strategy (FSS), respectively [10]. Comparison results demonstrated the advancements of the above three strategies, where average reductions of the system cost, primary energy consumption, and greenhouse gas emissions reached 2.6%, 12.1%, and 40.6%, respectively. Wang et al. analyzed the performance of CCHP system under two operational strategies [11]. It is concluded that greenhouse gas emissions and system cost under the FEL strategy were higher than FTL strategy; correspondingly, the advantage of the FTL strategy was reflected in the primary energy consumption index. From the above mentioned, each of the operational strategies has different strengths and weaknesses. FTL has the advantages in the reduction of energy consumption and the increase in energy-supply reliability. For gas-fired CCHP system, the energy-utilization efficiency and energy provision quality will directly affect the system's performance. It is necessary to develop an operational strategy of CCHP system which realized the high efficiency and sufficient reliability of energy supply and ensured that the users' demands were satisfied. Therefore, the gas-fired CCHP system under FTL strategy was expected.

The design and execution of the optimal operational strategy of CCHP systems were capable of realizing the maximization in total system revenues and thus have been the focus of many studies [12–20]. For instance, Abdollahi and Sayyaadi developed a multiobjective optimization model for realizing the energy-saving, economic, and environmental benefits of small-scale CCHP system [12]. Li et al. formulated an optimization model of the CCHP system aiming to improve the energy-utilization efficiency and economic benefit [14]. Yang and Zhai proposed the numerical model to generate optimal operation strategy of integration of CCHP system and solar thermal utilization [19]. As mentioned above, traditional deterministic optimization models have provided strong technical support for the system configuration and strategy generation, which were helpful in reducing the primary energy consumption, energy cost, emissions, and realizing the improvement in the system performance. However, some limitations in their extensive applications were unavoidable due to the existence of intrinsic and human-induced uncertainties (including the volatility in electric and thermal loads, the fluctuations in the price of electricity, and natural gas as well as the performance of the system equipment) in the CCHP system. Specifically, the electric and thermal loads are mostly presented as the random nature due to the disturbance of external meteorological factors and the deviation caused by

human' subjective judgments and understandings. The price of electricity and natural gas was influenced by the resources' availability and policy regulations and suitable to describe as the interval values, instead of fixed values. The performance of the system equipment mainly depended on their service time and the operational manner of staff and exhibited uncertain characteristics. Such uncertainties would bring significant difficulties to the formulation of CCHP management models and generation of effective operational strategies. It is thus desired that effective uncertain optimization models be advanced.

Currently, a number of inexact optimization methods have been widely applied in the energy system [21–31]. For instance, Ersoz and Colak developed four stochastic simulation methods for evaluating the investment feasibility of the CCHP system, including the parametric method, the Monte-Carlo method, the historical trend method, and the scenario-based method [22]. Ji et al. proposed a stochastic robust optimization method in CCHP system under random uncertainties [24]. Marino et al. proposed a two-stage stochastic collaborative decision model for supporting energy exchange for a CCHP system [25]. From the above, it can be seen that most researchers focused on dealing with the randomness in electric and thermal demands. That is because, compared with other uncertain variables, it will have a significant influence on energy provision pattern, which are the prominent goals of CCHP system. However, the above discussions about electric and thermal energy demands are mainly regarded as the random variables with a known distribution type as well as fixed distribution parameters. Few studies noticed that electric and thermal energy demands in the real world may be subjected to twofold randomness. In detail, it is widely accepted that electric and thermal energy demands are normally distributed random variable $N(\mu, \sigma^2)$ from the viewpoint of probability theory, where μ and σ represent the mean value and standard deviation, respectively. In fact, μ and σ are identified by various respondents with specific background and preference and may exhibit uncertain characteristics. Specifically, it is first assumed that the energy demands ξ are expressed as the random variables with the normal distributions (i.e., $\xi \sim N(\mu, \delta^2)$), where μ and δ denote the mean value and standard deviation, respectively. Based on various survey and estimation results from n group of respondents, n groups of random variables could be obtained (i.e., $(\mu_1, \delta_1^2), (\mu_2, \delta_2^2), \dots, (\mu_n, \delta_n^2)$), such that the μ and δ values are more suitable to be random variables (as based on the collected data above) rather than fixed values as are traditional random variables. Therefore, the term of μ and σ will become new random variables and electric and thermal energy demands will not be considered to be conventional random variables but the so-called birandom variables, a concept first proposed by Peng and Liu [32]. This concept has been integrated with some inexact multiobjective optimization models and successfully applied to the flow shop scheduling problem, the vendors' selection problem, and the hydropower station operation planning problem [33–35]. Therefore, as the first attempt in the related field, this study is to develop a birandom chance-constrained linear programming (BCCLP)

model for generating the operational strategies of gas-fired CCHP systems, where the electricity demands and thermal energy demands will be considered as the birandom variables. A gas-fired CCHP system of a five-star hotel in Shanghai Pudong New Area, China, was used as a study case for demonstration.

The rest of this paper is organized as follows: Section 2 provides an overview of the reference hotel and its energy source and the gas-fired CCHP system, including the load characteristics of the hotel and main components and operational framework of CCHP system. In Section 3, the BCCLP model for gas-fired CCHP systems is formulated and solved based on the primitive chance measure method. Section 4 analyzes the solutions generated from BCCLP model and discusses the sensitivity of critical system parameters. Some meaningful conclusions are summarized in Section 5.

2. Case Study

2.1. Load Characteristics of the Targeted Hotel. To demonstrate the advancement of the proposed optimization model in generating cost-effective and reliable operation strategies for the gas-fired CCHP system, a five-star hotel in Shanghai, China, was selected for this study. This hotel with a height of 90 m and a total area of $8 \times 10^4 \text{ m}^2$ approximately is located in Pudong district, one of the most prosperous areas in Shanghai with a total GDP of 1046 billion dollars in 2018. Therefore, the average occupancy rate of this hotel is always maintained at almost more than 80 percent all year. To ensure the high service quality and realize the maximization of economic benefits, the energy-supply security is critical for the long-term development of this hotel.

Figure 1 demonstrates the load characteristics of this hotel, where average monthly electric, cooling, and heating loads are shown in Figure 1(a). Obviously, the cooling and heating loads own remarkable variation trends, where the cooling loads from May to October are much larger than those of other months. The heating loads mainly focus on the months of December to February. It is noteworthy that although the monthly mean temperature in January is the lowest, being 1.9°C , nevertheless, the heating demands in January are limited. That is because Chinese New Year usually happens in January, leading to a reduction in the number of customers. Compared with the cooling and heating loads, the electricity demands are relatively consistent throughout the year. The average hourly electric, cooling, and heating loads for this building in a typical day are reflected in Figure 1(b). It is shown that the variation in average hourly electric loads in both summer and winter is synchronous with the design of local step tariff, which is divided into three periods, as peak period (8:00–11:00 and 18:00–21:00), flat period (6:00–8:00, 11:00–18:00, and 21:00–22:00), and valley period (22:00–6:00). Meanwhile, the shifts in outdoor temperature have an obvious influence on the heating and cooling loads. Specifically, the heating loads are very large in winter, being in a range of 4866.01 to 16474.03 kW, while being relatively lower in summer from 49.85 to 1052.53 kW; the cooling loads are higher in summer

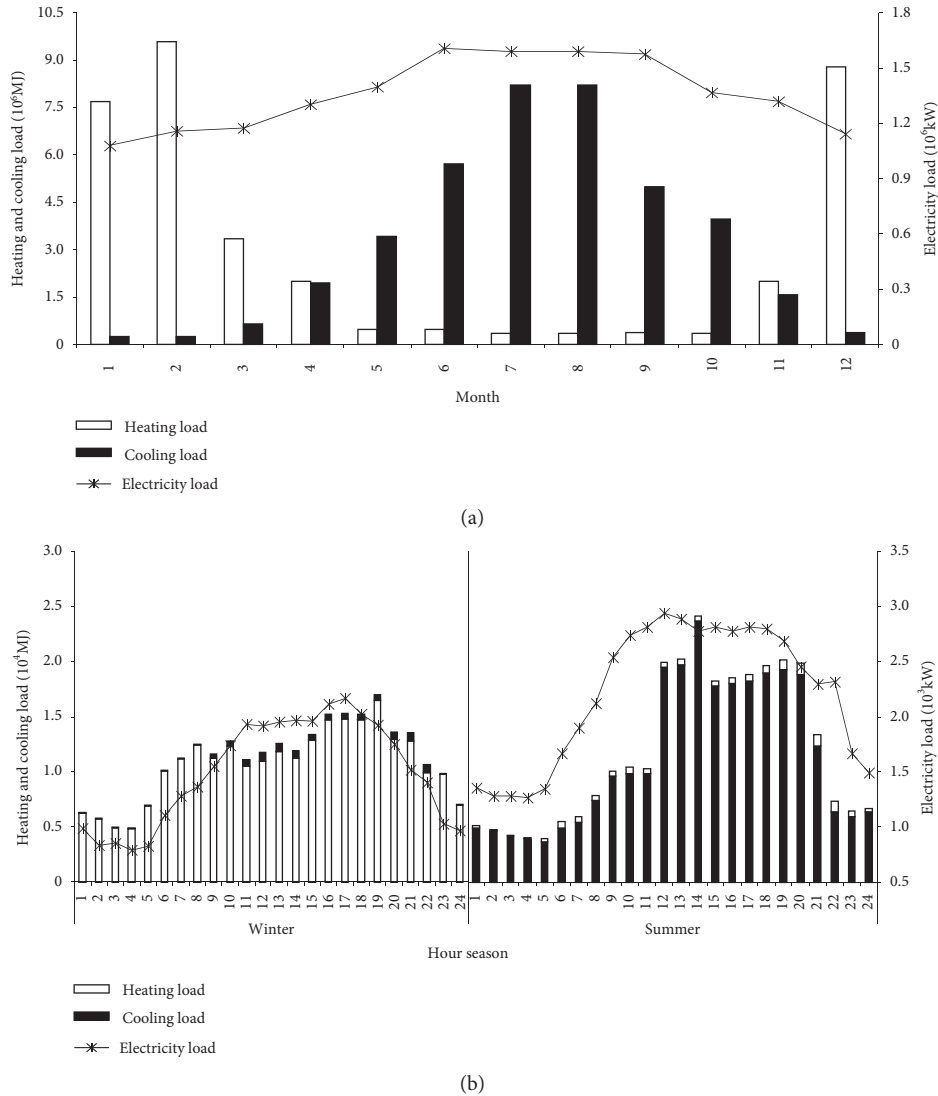


FIGURE 1: Electrical, cooling, and heating load of the hotel. (a) Average monthly load curves; (b) typical daily load curves over three seasons.

with 3712.71 to 23751.53 kW than that in winter from 12.94 to 818.71 kW. As mentioned above, the changes in outdoor temperature and electricity price have obvious influences on the heating, cooling, and electric loads, where the loads exhibited obvious variation trends. Therefore, it is essential for the CCHP system to identify accurate energy demands in order to generate a reasonable and feasible schedule strategy. In this study, the energy demands were described as the birandom variables (as depicted in Section 3) for reflecting their dynamic variation characteristics.

2.2. The Configuration and Operational Mechanism of the CCHP System. The schematic diagram of the gas-fired CCHP system is shown in Figure 2. The gas-fired CCHP system is composed of many modules, including a gas turbine (GT) with a total rated capacity of 6 MW, unfired dual pressure natural circulation heat recovery steam generators (HRSG), auxiliary boiler (AB), absorption chillers (AC), heat exchanger (HE), and electrical chillers (EC).

The operational framework of CCHP system is described as follows: firstly, the gas-fired turbine burns the natural gas and generates the electricity and high-temperature flue gas. Secondly, the high-temperature flue gas, produced as a byproduct and recovered by HRSG, is utilized by the AC or HE for meeting cooling and heating demands. It is regulated that if GT is incapable of supplying enough electricity or byproduct heat, additional electricity and fuel need to be purchased to compensate for meeting users' requirements. Next, it is designed that the insufficient cooling load is satisfied by EC based on the electricity generated by GT in priority or purchased from the grid. As for the unsatisfied heating load, it is provided by the AB through burning the natural gas. Finally, the gas-fired CCHP system is connected to the public supply network. It is regulated that the unsatisfactory electricity loads are purchased from the public power grid; nevertheless, the surplus electricity provided by the CCHP system is unavailable for the public power grid. This is because the transmission of excess electricity to the power grid will lead to the voltage flicker and short-circuit current, which affect the security and reliability of the power grid.

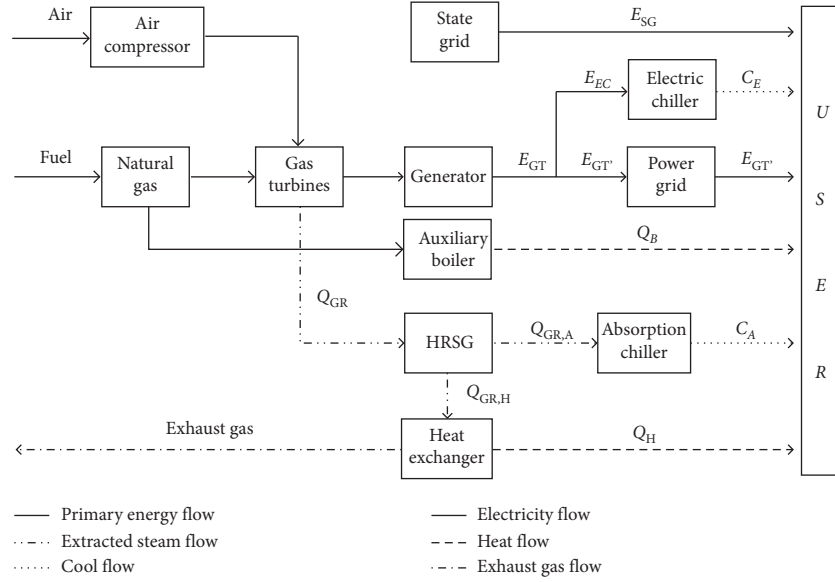


FIGURE 2: Structure and energy flow of the gas-fired CCHP system.

2.3. The Main Problems Associated with the CCHP System. As demonstrated [36], compared with traditional energy-supply pattern, CCHP system is capable of improving the overall efficiency, where less primary fuel is consumed to generate the same amount of electricity and thermal energy. However, there are still some problems which should be solved at this stage. (i) The mode at FTL operation strategy caused the surplus electricity, which accounted for 10% of the total electricity quantity among a year. It reached the highest value in winter, being 18%. (ii) The intrinsic uncertainties are associated with the gas-fired CCHP system, such as the volatility in electric and thermal loads, the fluctuations in the price of electricity and natural gas, and the unstable nature of equipment performance. The oversimplification in those uncertainties may affect the accuracy and rationality of the designed operational strategy. (iii) The site survey results indicated that the overall efficiency of the CCHP system is approximately 72%, which means that there still would be some improvement spaces in the system efficiency. It is thus expected to formulate an optimization model under random uncertainty, aiming to generate the cost-effective operational strategy of targeted gas-fired CCHP system.

3. The Operation Optimization Model of the Targeted CCHP System

3.1. Formulation of the BCCLP Model for the CCHP System. In this research, a BCCLP model was formulated for realizing the minimal system cost, improving the energy-utilization efficiency, and dealing with the uncertainties in the system. The model objective is to minimize operating cost and maintenance cost of the CCHP system; correspondingly, the constraints include the supply balance of electricity, heating, and cooling and operational limitations of system equipment, as well as nonnegative constraints.

Objective function:

$$\text{minimize } f = f_1 + f_2, \quad (1a)$$

$$f_1 = C_{ng} \sum_{t=1}^T \text{ngt}(t) + \text{ngb}(t) + C_{elec} \sum_{t=1}^T E_{sg}(t), \quad (1b)$$

$$f_2 = C_{GT} \sum_{t=1}^T E_{GT}(t) + C_B \sum_{t=1}^T Q_B(t) + C_{AC} \sum_{t=1}^T C_A(t) + C_{EC} \sum_{t=1}^T C_E(t), \quad (1c)$$

where f_1 is the total operational cost of the CCHP system in period t (RMB); f_2 is the total maintenance cost of the CCHP system in period t (RMB); t is the index of time period; $C_{ng}(t)$ is the natural gas price in period t (RMB/m³); $C_{elec}(t)$ is the electricity price in period t (RMB/kWh); $\text{ngt}(t)$ is the natural gas consumption of the gas turbine in period t (m³); $\text{ngb}(t)$ is the natural gas consumption of the auxiliary boiler in period t (m³); $E_{sg}(t)$ is the electricity purchased from the power grid in period t (kWh); C_{GT} is the maintenance cost of the gas turbine (RMB/kWh); C_B is the maintenance cost of the auxiliary boiler (RMB/MJ); C_{AC} is the maintenance cost of the absorption chiller (RMB/MJ); C_{EC} is the maintenance cost of the electricity chiller (RMB/MJ); $E_{sg}(t)$ is purchased electricity from local grid in period t (kWh); $E_{GT}(t)$ is the electricity generated from the gas turbine in period t (kW); $Q_B(t)$ is the quantity of heat sourced from the auxiliary boiler in period t (MJ); $C_A(t)$ is the quantity of cool provided by the absorption chiller in period t (MJ); $C_E(t)$ is the quantity of cool sourced from the electrical chiller in period t (MJ). As demonstrated in the objective function (1a)–(1c), equation (1b) was established for calculating the total operational costs of the CCHP system, where they are composed of two parts, that is, the purchasing costs of electricity and the combustion costs of natural gas, respectively. Equation (1c) was the function for describing the total

maintenance costs of the CCHP system, which include the maintenance costs of gas turbine, absorption chillers, electrical chillers, and auxiliary boiler, respectively. The decision variables mainly include $ngt(t)$, $ngb(t)$, $E_{sg}(t)$, $E_{GT}(t)$, $Q_B(t)$, $C_A(t)$, and $C_E(t)$, respectively.

Subject to the following,

(i) Electricity balance:

$$E_{SG}(t) + E_{GT'}(t) \geq E(t), \quad (1d)$$

$$E_{GT}(t) = ngt(t)H_{ng}\eta_{pe}\eta_{te}, \quad (1e)$$

$$E_{GT'}(t) = E_{GT}(t) - E_{EC}(t), \quad (1f)$$

$$E_{EC}(t) = \frac{C_E(t)}{COP_{EC}}, \quad (1g)$$

where $E_{GT'}(t)$ is the electricity output sourced from the gas turbine in period t (kWh); $\tilde{E}(t)$ is the electricity load demand of the building in period t (kWh); H_{ng} is the low calorific value of natural gas (MJ/m^3); η_{pe} is the electrical efficiency of the gas turbine; η_{te} is the thermal efficiency of the gas turbine; $E_{EC}(t)$ is the electricity consumption for the electrical chillers in period t (kWh); $C_E(t)$ is the quantity of cool generated from the electrical chillers in period t (MJ); COP_{EC} is the COP (coefficient of performance) value of the electrical chillers. Constraint (1d) regulated that the summation of generated and purchased electricity must be greater than or equal to practical demand in period t . Constraints (1e)–(1g) described how to calculate the electricity flow of the entire CCHP system in period t .

(ii) Heat balance:

$$Q_H(t) + Q_B(t) = H_Q(t), \quad (1h)$$

$$Q_H(t) = U_{ST}(t)\theta(t)\eta_{oh}, \quad (1i)$$

$$ST(t) = \frac{ET(t)(1 - \eta_{te})}{\eta_{pe}\eta_{te}}, \quad (1j)$$

$$Q_B(t) = ngb(t)\eta_{ceb}H_{ng}, \quad (1k)$$

$$0 \leq U_{ST}(t) \leq 1, \quad (1l)$$

where $Q_H(t)$ is the heat output sourced from the heat exchange in period t (MJ); $Q_B(t)$ is the heat output generated by the auxiliary boiler in period t (MJ); $H_Q(t)$ is the heating demand of the building in period t (MJ); $U_{ST}(t)$ is the recovery waste heat of the CCHP system in period t (MJ); $\theta(t)$ is the

proportion of the recovery waste heat allocated to the heat exchanger in period t ; η_{oh} is exhaust heat exchanger efficiency; η_{ceb} is the auxiliary boiler efficiency. Constraint (1f) required that the supplied heating amount must be equal to practical demand in period t . Constraints (1g)–(1i) define the heating power from heat exchanger and auxiliary boiler in period t , respectively. Constraint (1j) ensured that the value $U_{ST}(t)$ belongs the $[0, 1]$ range.

(iii) Cool balance:

$$C_A(t) + C_E(t) = C(t), \quad (1m)$$

$$C_A(t) = ST(t)(1 - U_{ST}(t))\eta_{hrer}COP_{AC}, \quad (1n)$$

where $C(t)$ is the cooling demand in period t (MJ); η_{hrer} is the heat efficiency of the absorption chillers; COP_{AC} is the COP (coefficient of performance) of the absorption chillers. Constraint (1k) was the function of the amount of total cooling supply that must be equal to the practical demand. Constraint (1l) restricted the cooling power from the absorption chillers in period t .

(iv) Other constraints:

$$0 \leq ET(t) \leq ET_{Max}, \quad (1o)$$

$$0 \leq Q_H(t) \leq Q_{HMax}, \quad (1p)$$

$$0 \leq Q_B(t) \leq Q_{BMax}, \quad (1q)$$

$$0 \leq C_A(t) \leq C_{AMax}, \quad (1r)$$

$$0 \leq C_E(t) \leq C_{EMax}, \quad (1s)$$

where ET_{Max} is the maximum generation power of the gas turbine (kW); Q_{HMax} is the maximum generation power of the heat exchanger (MJ); Q_{BMax} is the maximum generation power of the auxiliary boiler (MJ); C_{AMax} is the maximum generation power of the absorption chiller (MJ); C_{EMax} is the maximum generation power of the electrical chiller (MJ). Constraints (1m) to (1q) denoted that energy generated from relevant facilities must not exceed their generation capacity limits.

In this study, the BCCLP model was solved by the commercial software LINGO 12.0, which is a powerful tool to assist in formulating and solving the optimization models. The previous studies have demonstrated that LINGO is advantageous in tackling the energy and environmental management issues faster and simpler due to its easy-to-edit language and low computational burden [24, 37]. This is the reason why it was explored to support the operation management of CCHP system in this research. The hardware

setting for running LINGO in this study is listed as follows: (1) Operation System: Microsoft Windows 10; (2) CPU: Intel (R) Core (TM) i5-cc60U @ 3.20 GHz 3.20 GHz; (3) RAM: 4 GB.

3.2. Data Information. The parameters involved in the BCCLP model are divided into two types, including the parameters associated with the CCHP system and the parameters related to the users, respectively.

3.2.1. CCHP System Parameters. Based on on-site survey, the regulations released by the electricity authority, Shanghai Statistics Bureau, and Shanghai Statistics yearbook, the economic and technical parameters of CCHP system are identified and reflected in Table 1. The electricity price is divided into three levels, being 0.333 RMB/kWh at the valley time, 0.653 RMB/kWh at the flat time, and 1.104 RMB/kWh at the peak time, respectively. As for the natural gas price, it mainly depended on the market. Moreover, it is found that the maintenance costs and technical parameters of system facilities are stable relatively and thus are assumed to be deterministic values.

3.2.2. Energy-Demand Parameters. According to the on-site survey results, historical data record (from 2010 to 2018), the energy-demand parameters, including the electricity, heating, and cooling demands, are provided in Table 2. In this CCHP system, as described in the "Introduction" section, the energy requirements are affected by many factors, such as the population, production scale, and local meteorological condition, leading to the large variation range. Therefore, they are designed as the birandom variables with normal probability distribution.

3.3. The Solution Algorithm of the Formulated BCCLP Model. Based on the equilibrium chance-constrained measure proposed by (Peng and Liu, 2007), the constraints which included birandom parameters can be transformed to their equivalent deterministic forms as follows:

$$\begin{aligned} A(\omega)X \leq B(\omega) &\Leftrightarrow \text{Ch}^e\{A(\omega)X \leq B(\omega)\} \geq 1 - \alpha_r \\ &\Leftrightarrow \Pr\{\omega \in \Omega | \Pr\{A(\omega)X \leq B(\omega)\} \geq 1 - \alpha_r\} \geq 1 - \alpha_r \\ &\Leftrightarrow \mu_A X - \Phi^{-1}(\alpha_r) \sqrt{(X)^T \sigma_A X + (\sigma_B)^2} \\ &\quad - \Phi^{-1}(\alpha_r) \sqrt{(X)^T \sigma_{A'} X + (\sigma_{B'})^2} \leq \mu_B, \quad \forall r, \end{aligned} \quad (2a)$$

$$\begin{aligned} \tilde{D}(\omega)X \geq \tilde{E}(\omega) &\Leftrightarrow \text{Ch}^e\{D(\omega)X \geq E(\omega)\} \geq 1 - \alpha_r \\ &\Leftrightarrow \Pr\{\omega \in \Omega | \Pr\{D(\omega)X \geq E(\omega)\} \geq 1 - \alpha_r\} \\ &\quad \geq 1 - \alpha_r \\ &\Leftrightarrow \mu_D X + \Phi^{-1}(\alpha_r) \sqrt{(X)^T \sigma_D X + (\sigma_E)^2} \\ &\quad + \Phi^{-1}(\alpha_r) \sqrt{(X)^T \sigma_{D'} X + (\sigma_{E'})^2} \geq \mu_E, \quad \forall r, \end{aligned} \quad (2b)$$

where $\text{Ch}^e\{\cdot\}$ denotes the primitive chance of birandom event $\{\cdot\}$; α_r is a given level for birandom constraint (i.e., the significance level, which represents the admissible risk of constraint violation), which implies that the constraint should be satisfied with at least a probability level of $1 - \alpha_r$. α_r is a predetermined violation level for the birandom constraint (i.e., the admissible risk of constraint violation), which implies that the constraint should be satisfied with at least a probability level of $1 - \alpha_r$. The design principle of α_r value is that its range is wide as possible. The principle of designing the α_r value is ensuring its ranges are wide enough. In order to generate a variety of decision alternatives and provide more choosing opportunities to decision makers, a relatively wide range of designed parameter is necessary. Various α values are helpful for investigating the risks caused by demand-constraint violation, generating desired solutions of electricity and energy supply, and useful for managers in gaining insight into tradeoff between system cost and constraint-violation risk. φ is the standard normal distribution. According to inequations (2a) and (2b), model (1) can be converted into the corresponding deterministic model, where constraints (1c), (1i), and (1n) can be transformed as follows:

$$E_{SG}(t) + E_{GT'}(t) \geq E(t) \Leftrightarrow \text{Ch}^e\{E(t) | E_{SG}(t) + E_{GT'}(t) \geq E(t)\} \geq 1 - \alpha_r, \quad (3a)$$

$$Q_H(t) + Q_B(t) \geq H_Q(t) \Leftrightarrow \text{Ch}^e\{H_Q(t) | Q_H(t) + Q_B(t) \geq H_Q(t)\} \geq 1 - \alpha_r, \quad (3b)$$

$$C_A(t) + C_E(t) \geq C(t) \Leftrightarrow \text{Ch}^e\{C(t) | C_A(t) + C_E(t) \geq C(t)\} \geq 1 - \alpha_r. \quad (3c)$$

Finally, the solutions of the BCCLP model were obtained, that is, f_{opt} , $\text{ngt}(t)_{\text{opt}}$, $\text{ngb}(t)_{\text{opt}}$, $E_{SG}(t)_{\text{opt}}$, $E_{GT}(t)_{\text{opt}}$, $Q_B(t)_{\text{opt}}$, $C_A(t)_{\text{opt}}$, and $C_E(t)_{\text{opt}}$ respectively. The procedures of formulating and solving BCCLP model are summarized as follows:

Step 1. Collect system data and identify uncertain variables as the birandom variables.

Step 2. Determine the objective function and constraints in the proposed BCCLP model.

TABLE 1: Part of CCHP system parameters.

Parameters	Value
Major economic parameters	
Maintenance cost of gas turbine	0.03 RMB/kWh
Maintenance cost of absorption chiller	0.0002 RMB/MJ
Maintenance cost of auxiliary boiler	0.0006 RMB/MJ
Maintenance cost of electricity chiller	0.0005 RMB/MJ
Electricity price in peak period	1.104 RMB/kWh
Electricity price in flat period	0.653 RMB/kWh
Electricity price in valley period	0.333 RMB/kWh
Natural gas prices	2.32 RMB/m ³
Major technical parameters	
Efficiency of exhaust heat exchanger	0.776
Electrical efficiency of gas turbine	0.8
Thermal efficiency of gas turbine	0.18
Efficiency of auxiliary boiler	0.85
Recovery waste heat efficiency of the absorption chillers	0.695
Low calorific value of natural gas	35.175 MJ/m ³
Rated COP of absorption chiller	1.2
Rated COP of electric chiller	4.45

TABLE 2: Part of energy-demand parameters.

Parameter	Time (hour)	Probability distribution		
		Winter	Transition	Summer
Electricity demand	0	$N\sim(\mu, 17.47) \mu\sim(957.59, 12.32)$	$N\sim(\mu, 18.92) \mu\sim(1144.73, 13.28)$	$N\sim(\mu, 21.26) \mu\sim(1483.59, 14.84)$
	5	$N\sim(\mu, 16.30) \mu\sim(818.24, 11.53)$	$N\sim(\mu, 18.46) \mu\sim(1084.25, 12.98)$	$N\sim(\mu, 20.27) \mu\sim(1335.76, 14.18)$
	10	$N\sim(\mu, 22.79) \mu\sim(1729.39, 15.86)$	$N\sim(\mu, 25.19) \mu\sim(2151.23, 17.46)$	$N\sim(\mu, 28.12) \mu\sim(2729.59, 19.42)$
	15	$N\sim(\mu, 24.08) \mu\sim(1950.92, 16.72)$	$N\sim(\mu, 26.06) \mu\sim(2315.38, 18.04)$	$N\sim(\mu, 28.47) \mu\sim(2803.50, 19.65)$
	20	$N\sim(\mu, 22.86) \mu\sim(1740.10, 15.90)$	$N\sim(\mu, 25.10) \mu\sim(2133.95, 17.40)$	$N\sim(\mu, 26.72) \mu\sim(2444.49, 18.48)$
Cooling demand	0	$N\sim(\mu, 3.45) \mu\sim(8.36, 2.96)$	$N\sim(\mu, 12.17) \mu\sim(414.07, 8.78)$	$N\sim(\mu, 42.04) \mu\sim(6412.24, 28.69)$
	5	$N\sim(\mu, 3.45) \mu\sim(8.36, 2.96)$	$N\sim(\mu, 8.85) \mu\sim(187.62, 6.57)$	$N\sim(\mu, 32.41) \mu\sim(3699.37, 22.27)$
	10	$N\sim(\mu, 12.17) \mu\sim(413.80, 8.78)$	$N\sim(\mu, 29.22) \mu\sim(2963.16, 20.14)$	$N\sim(\mu, 51.73) \mu\sim(9892.39, 35.15)$
	15	$N\sim(\mu, 13.14) \mu\sim(496.56, 9.43)$	$N\sim(\mu, 34.99) \mu\sim(4354.16, 24.00)$	$N\sim(\mu, 68.68) \mu\sim(17784.38, 46.45)$
	20	$N\sim(\mu, 14.54) \mu\sim(629.47, 10.36)$	$N\sim(\mu, 34.65) \mu\sim(4263.59, 23.77)$	$N\sim(\mu, 70.70) \mu\sim(18880.49, 47.80)$
Heating demand	0	$N\sim(\mu, 43.78) \mu\sim(6982.48, 29.85)$	$N\sim(\mu, 27.36) \mu\sim(2572.12, 18.91)$	$N\sim(\mu, 10.32) \mu\sim(277.22, 7.55)$
	5	$N\sim(\mu, 43.63) \mu\sim(6931.14, 29.75)$	$N\sim(\mu, 22.42) \mu\sim(1668.22, 15.61)$	$N\sim(\mu, 10.27) \mu\sim(273.73, 7.51)$
	10	$N\sim(\mu, 57.68) \mu\sim(12399.04, 39.12)$	$N\sim(\mu, 29.44) \mu\sim(3010.78, 20.29)$	$N\sim(\mu, 13.46) \mu\sim(525.32, 9.64)$
	15	$N\sim(\mu, 58.82) \mu\sim(12912.45, 39.88)$	$N\sim(\mu, 30.59) \mu\sim(3269.98, 21.06)$	$N\sim(\mu, 12.72) \mu\sim(460.09, 9.15)$
	20	$N\sim(\mu, 58.93) \mu\sim(12963.79, 39.95)$	$N\sim(\mu, 31.72) \mu\sim(3462.72, 21.61)$	$N\sim(\mu, 17.80) \mu\sim(998.23, 12.53)$

Step 3. Formulate a BCCLP model based on steps 1 and 2.

Step 4. Establish the operation optimization model for the gas-fired CCHP system based on BCCLP model.

Step 5. Convert birandom constraints into their respective deterministic equivalents based on equilibrium chance-constrained measure.

Step 6. Solve BCCLP model and generate the final solutions of objective values and decision variables under various conditions.

4. Result Analysis and Discussion

4.1. Result Analysis. The BCCLP model was developed for determining the optimal operation strategies of the gas-fired CCHP system to manage the energy (including electricity,

heating, and cooling) flow reasonably and achieve the minimum cost. Therefore, this section is categorized into four groups: (i) cooling-supply system, (ii) heating-supply system, (iii) electricity-supply system, and (iv) system cost, respectively.

4.1.1. Cooling-Supply System. In order to minimize the operating and maintenance costs, the selection of operation strategies in the cooling-supply system (including absorption chillers and electrical chillers) is closely connected to operating efficiency and costs but also to the α value. Table 3 provides the operational strategies and resource consumption of the CCHP system under different α levels in the typical days of three seasons (i.e., winter, summer, and transition). As shown in Table 3, various α values will result in different operation strategies and schedule pattern. Firstly, the quantity of cooling sourced from both AC and EC

decreases with the increase in α value. For example, when α increases from 0.01 to 0.1, the cooling magnitude provided by AC at three seasons (i.e., winter, transition, and summer) was reduced, being from 8.53×10^3 , 63.13×10^3 , and 235.84×10^3 MJ to 8.43×10^3 , 62.96×10^3 , and 235.60×10^3 MJ, respectively; similarly, the quantity of cooling supplied by EC would decrease to 0.10×10^3 , 2.01×10^3 , and 38.83×10^3 MJ from 0.13×10^3 , 2.06×10^3 , and 38.93×10^3 MJ, respectively. This is due to the fact that the low α value corresponds to the high cooling requirement, leading to the high cooling output. Conversely, the high α value was associated with the low cooling demand, which was accompanied by the low cooling-generation amount.

In fact, other factors, including economic parameters and operational mechanism, also exert some influences on the operational strategies. Figure 3(a) shows the optimal operation strategy of the cooling-supply system during the typical days over three seasons. Figure 3(b) demonstrates the solutions of cooling-supply amounts of two facilities and their respective proportions during every month. According to Figure 3(a), the cooling demand is satisfied by the electric chiller at valley time (22:00–6:00); conversely, the absorption chiller is under full-load state during peak time (8:00–11:00; 18:00–22:00) and flat time (6:00–8:00; 11:00–18:00). This is because the change in the electricity price has an obvious influence on the operation strategies of the cooling-supply system, where the electricity price was divided into three levels. Such a change would lead to the various options of candidate equipment, where the electric chiller plays an important role at the valley time in order to realize the minimization of total system cost; correspondingly, the absorption chiller was used to provide the cooling output at other two periods. As shown in Figure 3(b), the cooling demand is covered mainly by the absorption chillers, where their annual average proportion will reach 97%. The main reason is that, compared with electric chiller, the absorption chiller utilized recovered waste heat sourced from the gas turbine, which results in the low average operational cost and high energy-utilization efficiency.

4.1.2. Heating-Supply System. The heat-supply system includes the heat exchanger and auxiliary boiler, where the generation of optimal operation strategies mainly considers the following three aspects: the reduction of energy-supply cost, the improvement in energy-conversion efficiency, and energy provision safety, respectively. Similar to the cool-supply system pattern, the violation level is associated with energy demands and thus affects the operation strategies of heat-supply system. As shown in Table 3, the total quantity of heating power decreases with the increase in α value. For instance, when α grows from 0.01 to 0.1, the total heat output has an obvious decrease during winter, transition, and summer, with the values changing from 257.45×10^3 , 67.00×10^3 , and 12.01×10^3 MJ to 257.17×10^3 , 66.76×10^3 , and 11.85×10^3 MJ, respectively. This is because, according to the BCCLP algorithm, the increase in α level is corresponding to the reduction of the heat demand, such that the

provision amounts would decrease. Apart from α level, the operating strategies are also influenced by the operational costs of the equipment. As shown in Figure 4, the heat demand is met totally by the heat exchanger. This is partly because the CCHP system executes the FTL strategy, which means that the heat exchanger will be adequate to cover all heat requirements, and there is no need to provide additional heat by the auxiliary boiler. Another reason is that the heat exchanger absorbed the recovered waste heat provided by the gas turbine, with a low cost compared to the auxiliary boiler.

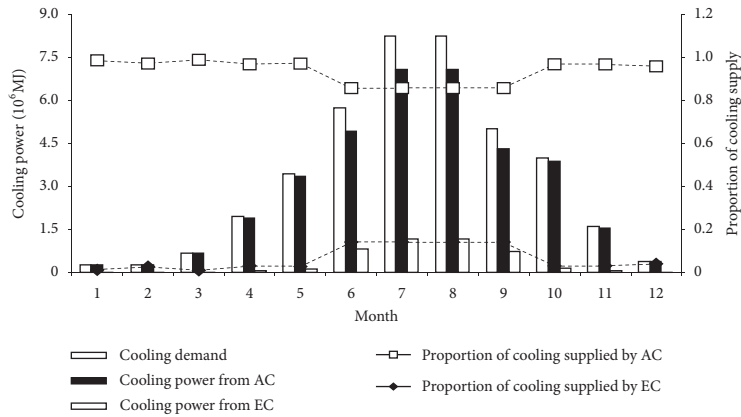
4.1.3. Electricity-Supply System. In the electric supply system, the electricity requirements are satisfied by both the gas turbine and purchased electricity from the grid, respectively. The electricity amounts provided by the above two means are reflected in Table 3 and Figure 5. As discussed in the previous section, the determination of α level also would affect electricity-provision strategy through changing the electricity demands. For example, as described in Table 3, the electric quantity supplied by the gas turbine and purchased from the grid over three seasons decreases with the increase in α level. Specifically, when α grows from 0.01 to 0.1, the electricity sourced from the gas turbine would be reduced from 23.11×10^3 , 10.95×10^3 , and 20.23×10^3 kW to 23.07×10^3 , 10.91×10^3 , and 20.12×10^3 kW in the winter, transition, and summer, respectively, while purchased electricity from grid would drop to 12.95×10^3 , 33.01×10^3 , and 41.69×10^3 kW from 13.11×10^3 , 33.20×10^3 , and 41.93×10^3 kW, respectively. Similarly, the operating strategy of this system also exhibited seasonal variation. Figure 5(a) demonstrated the electricity magnitude at a whole year. As shown in Figure 5(a), the electric demand from December to February is mainly satisfied by the gas turbine whose output would reach 32.59×10^3 , 23.07×10^3 , and 37.22×10^3 kW, respectively. Conversely, the electric demand from June to September is mainly provided by the purchased electricity, which was 44.96×10^3 , 41.69×10^3 , 41.66×10^3 , and 45.16×10^3 kW, respectively. The reason is that total electricity amounts generated from the gas turbine are the sum of the electricity supplied to the users and the electricity used to drive the electric chiller. In summer, the consumed electricity of electric chiller would increase with the increase in the cooling demand, which would lead to the reduction in generated electricity supplied to the users, leading to more purchased electricity. On the contrary, the electricity provided to the users would increase significantly when cooling demand becomes decreased in the winter. Meanwhile, the high heating demand needs more recovered heat to drive the heat exchanger in winter, which would result in an increase in the natural gas consumption, as shown in Figure 5(a).

Figure 5(b) described the average hourly electricity-provision quantity during the typical days over three seasons. As shown in Figure 5(b), in summer, the peak output of the gas turbine would be from 12:00 to 14:00 with the values of 1.62×10^3 , 1.64×10^3 , and 1.96×10^3 kW, respectively. As

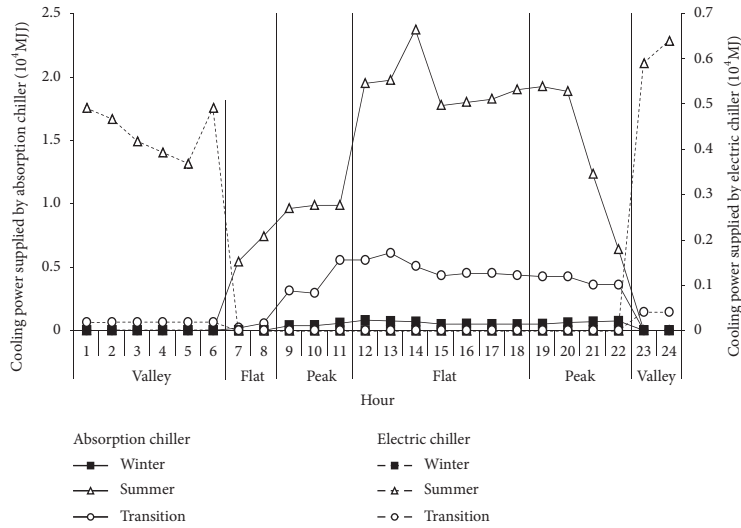
TABLE 3: CCHP's operation strategies under different α levers in typical day during winter, transition, and summer.

Item	$\alpha = 0.1$			$\alpha = 0.05$			$\alpha = 0.01$		
	Winter	Transition	Summer	Winter	Transition	Summer	Winter	Transition	Summer
Gas consumption (m^3)	16396.70	7756.32	14299.12	16406.02	7764.95	14307.37	16423.51	7781.13	14321.83
Supplied cooling by AC (MJ)	8425.95	62954.16	235598.58	8463.78	63013.72	235681.14	8534.62	63125.49	235836.02
Supplied cooling by EC (MJ)	103.56	2012.99	38833.40	113.96	2029.74	38865.52	133.46	2061.18	38925.79
Supplied heating by HE (MJ)	257116.17	66759.25	11847.16	257231.65	66843.22	11903.64	257448.28	67000.72	12009.58
Supplied electricity by GT (kW)	23070.16	10913.14	20118.87	23083.27	10925.28	20130.48	23107.88	10948.05	20226.90
Purchased electricity (kW)	12942.46	33006.19	41686.72	13004.89	33074.27	41762.36	13122.00	33201.97	41929.58
System cost (RMB)	1471820.00	1234922.00	1832058.00	1473759.00	1236843.00	1834206.00	1477396.00	1240445.00	1866149.00

Note. AC denotes absorption chillers; EC denotes electrical chillers; HE denotes heat exchanger; GT denotes gas turbine.



(a)



(b)

FIGURE 3: Operation strategies of cooling-supply system: (a) annual operation strategy; (b) typical daily operation strategy over three seasons.

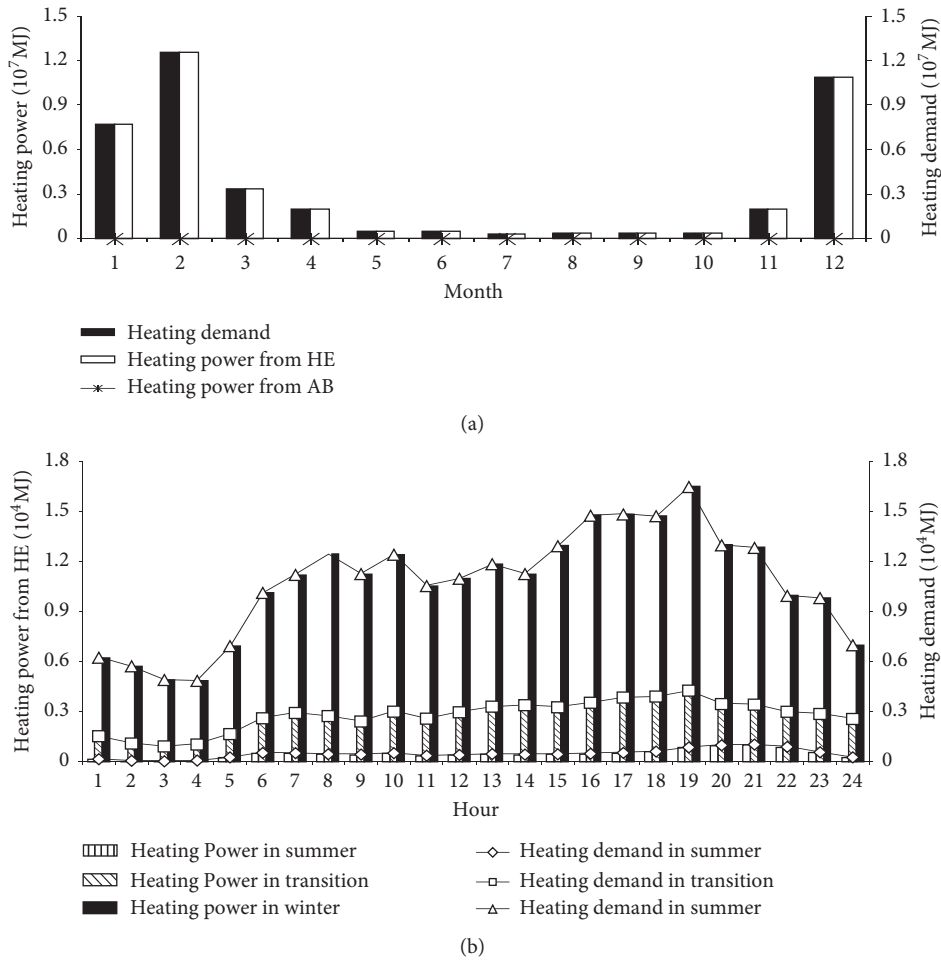


FIGURE 4: Operation strategies of heating-supply system: (a) annual operation strategy; (b) typical daily operation strategy over three seasons.

for other time periods, the output power of the gas turbine would be extremely low. Particularly at 3:00, it would be only 4.43 kW. In winter, the output of the gas turbine would be very large during the period of 16:00–19:00 and the peak hour would be at 19:00 with maximum output 1.68×10^3 kW. The minimum output would be 0.42×10^3 kW at 4:00. Such a change is mainly because the power curve of the gas turbine is consistent with the energy-demand curve. In detail, the recovered heat used for the heat exchanger would increase as the increase in heating demand level at winter, which means that the gas turbine would produce the electricity more compared to other periods.

4.1.4. System Cost. This section describes the objective value of the proposed model. As demonstrated in Table 3, there is a strong negative correlation between α level and total system cost. For example, when α grows from 0.01 to 0.1, the operating cost would be downward from 1.87×10^6 , 1.48×10^6 , and 1.24×10^6 RMB to 1.83×10^6 , 1.47×10^6 , and 1.23×10^6 RMB, respectively; correspondingly, the natural gas consumption would decrease to 16.40×10^3 , 7.76×10^3 , and 14.30×10^3 from 16.42×10^3 , 7.78×10^3 , and 14.32×10^3 , respectively. This was due to the fact that low α level (i.e., high

electricity and energy demand) corresponds to increased reliability in meeting the requirements, which led to the increases of system cost and natural gas consumption; conversely, high α level was related to a decreased security in satisfying the demands, thus resulting in the reductions of system cost and natural gas consumption. The above results disclose that there existed a tradeoff between the system cost and system-failure risk. There is a common problem associated with CCHP system that the energy supply may be insufficient to meet the peak demand; it thus recommends a more conservative solution with the high system cost as the operational strategy.

4.2. Discussion. From the above analysis, some factors, including the energy demand, electrical price, and natural gas price, exert the influence on the generated results of BCCLP model. Therefore, it is essential to perform the sensitivity analysis for evaluating the effect of those factors on the economy of the CCHP system in this section, where the energy demand, electrical price, and natural gas price are designed at the variation ranges +20% to +100%, -20% to +20%, and -20% to +20%, respectively. Table 4 reflects the influences of electrical price, natural gas price, and energy

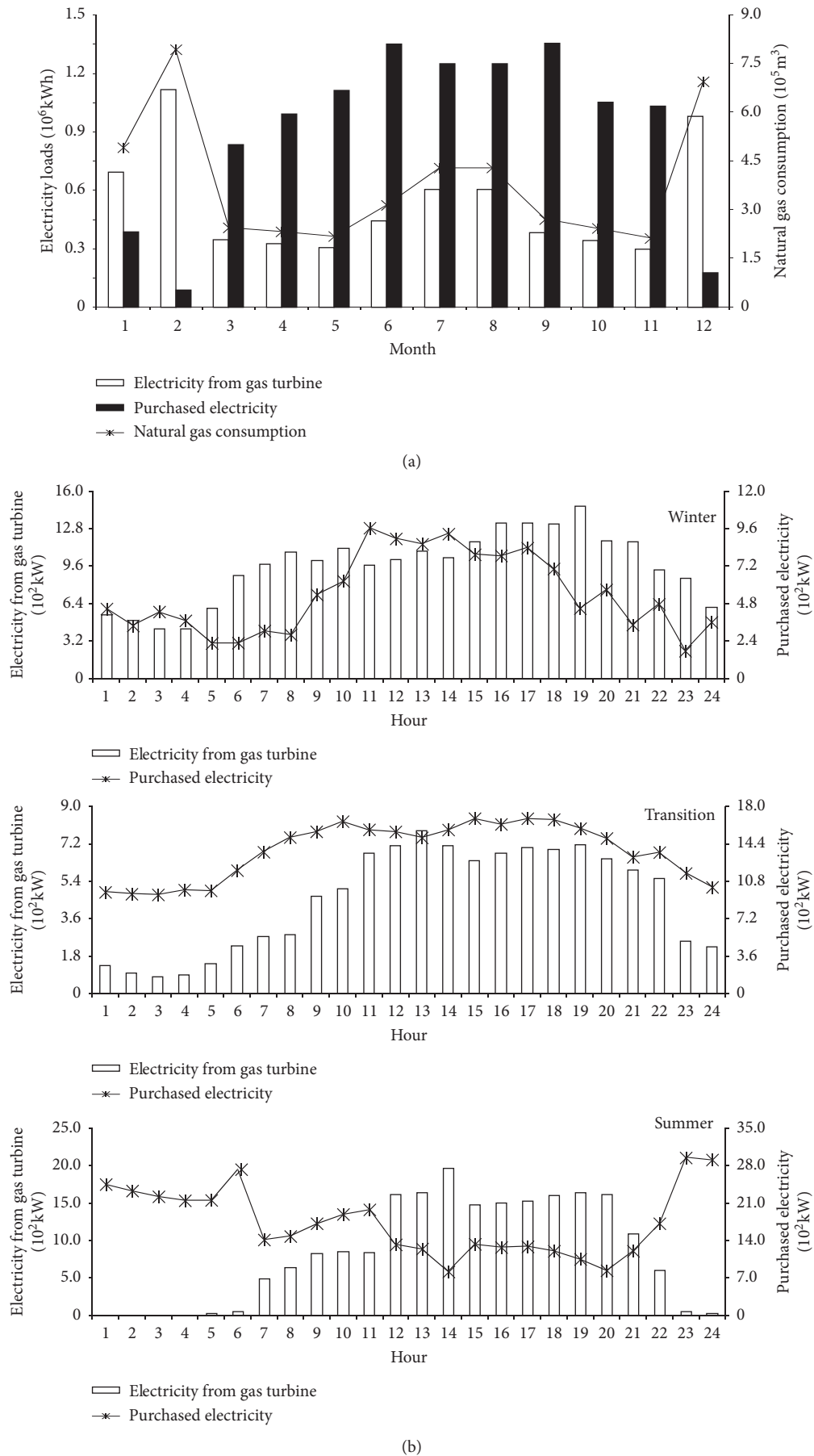


FIGURE 5: Operation strategies of electricity-supply system: (a) annual operation strategy; (b) typical daily operation strategy over three seasons.

TABLE 4: System cost variation based on change of sensitivity parameters.

Item	Parameter variation (%)	Winter		Transition		Summer	
		Cost (RMB)	Change rate (%)	Cost (RMB)	Change rate (%)	Cost (RMB)	Change rate (%)
Electricity price	-20	1414768	-3.88	1096544	-11.21	1672504	-8.71
	-10	1443294	-1.94	1165733	-5.60	1752281	-4.35
	+10	1500346	1.94	1304112	5.60	1911834	4.35
	+20	1528872	3.88	1373301	11.21	1991610	8.71
Natural gas price	-20	1235970	-16.02	1126954	-8.74	1626379	-11.23
	-10	1353895	-8.01	1180938	-4.37	1729218	-5.61
	+10	1589745	8.01	1288906	4.37	1934897	5.61
	+20	1707670	16.02	1342890	8.74	2037736	11.23
Heating demand	+25	1635522	11.12	1276131	3.34	1838961	0.38
	+50	1824295	23.95	1317339	6.67	1845865	0.75
	+100	2312825	57.14	1399756	13.35	1859673	6.03
Cooling demand	+25	1476254	0.30	1267951	2.67	1968859	7.47
	+50	1480688	0.60	1300980	5.35	2108684	15.10
	+100	1489555	1.20	1367038	10.70	2438152	33.08
Electricity demand	+25	1672031	13.61	1469416	18.99	2146366	17.16
	+50	1872241	27.21	1703909	37.98	2460675	34.31
	+100	2272663	54.41	2279530	84.59	3089293	68.62

demands on the system cost. Firstly, the total system cost is more sensitive to the change in electrical price in transition than that in summer and winter. For instance, as the electrical price increases from -20% to 20%, the fluctuations in system's cost in summer and winter are basically the same with no obvious increases, that is, only increase from -8.71 to 8.71% and from -3.88% to 3.88%, while a dramatic increase in the system cost from -11.23% to 11.23% could be observed in the transition period. The reason is that purchased electricity amounts in the transition are the highest among a year. Secondly, compared with the transition season, the natural gas price has a greater influence on the system cost in winter and summer. For example, the cost has a distinct variation in summer with an increase of 11.25% when the natural gas price increases by 20% and even rises up to 16.02% in winter. But in transition, a 20% increase of the natural gas price only causes a slight change of the system's cost by up to 8.74%. This is because the heating and cooling loads in winter and summer are much larger than those in transition, and thus there is more natural gas that needs to be purchased.

The energy demand is another key factor that influences the system cost. As shown in Table 4, the heating demand has a high sensitivity to the variation of the cost in winter and has a slight effect on the cost in summer. For example, the variation in the heating demand is assumed to be 100%, which would result in a 57.14% increase in the total cost in winter, but only an increase of 6.30% in summer. Compared with the heating demand, the cooling demand has the opposite sensitivity in the above seasons. For example, a 100% variation in cooling demand would lead to a 33.08% increase in the total cost in summer. The difference in energy demand among various seasons could explain this phenomenon. In winter, the heating demand is much larger than cooling demand, so it is the key factor. On the contrary, the cooling demand is very large in summer while the heating demand is relatively low, and thus the cost would be sensitive to cooling

demand. In transition, both heating and cooling demand would have a significant influence on the cost. In addition, electric demand would also have an important effect on the economy. For instance, a 100% increase in the electricity demand causes a change in the system's cost by up to 84.59%, 68.28%, and 57.41% at three seasons, respectively.

The sensitivity analysis result has revealed the influence rules of the above sensitive factors on the system economy, which could be classified into three categories: (i) in winter, the increase in natural gas price, heating, and electric demands would result in the large variation in total system costs; (ii) in summer, the cooling demand, electric demand, and the electrical price are key factors that affect the system economy; (iii) in transition, the system cost has moderate sensitivity to fluctuations of all parameters. It is beneficial to decision-makers for generating rational and reliable operational pattern through paying more attention to improve the accuracy of the key factors in the site survey and experts' consultation.

Moreover, the BCCLP model still needs to be improved, especially in the following three aspects. Firstly, the BCCLP model based on birandom chance-constrained linear programming is proposed for identifying the uncertainties associated with the CCHP system and generating a variety of cost-effective operation strategies reflecting the tradeoff between system economy and reliability; however, the energy generation, conversion, transition, and utilization processes in BCCLP model are formulated by some simplified mathematical equations. For example, there are only three equations to express the conversion of natural gas to electricity and heating quantity in this research. This simplified way is beneficial to formulate and solve the CCHP system operation optimization model but has difficulties in generating accurate and reliable solutions. This is because it is a complicated process in the actual production, which is related to a variety of operational conditions, including flue-gas temperature and turbine pressure. Therefore, it is necessary to enhance the

accuracy and applicability of optimization model through incorporating the output of the mechanism model or simulation software (i.e., Epsilon and Aspen) into the optimization model. Secondly, only the birandom variables are used to describe the energy demands of the CCHP system; in fact, some intrinsic and human-induced uncertainties might exist in the CCHP system. For instance, the electrical and natural price is influenced by the resources' availability and policy regulations and should be described as the interval values. Performance of the system equipment exhibits the uncertain characteristics caused by their service time and the subjective judgments of humans, which could be expressed as a fuzzy parameter. Hence, other uncertain optimization techniques, such as fuzzy and interval optimization methods, should be incorporated into the model in order to handle multiple uncertainties involved in the CCHP system. Thirdly, the minimization in the system cost is considered in the BCCLP model. In fact, the minimization in the system cost is considered as the objective function in the BCCLP model. In fact, the minimization of pollutant-emission amounts and the maximization of primary energy rate are also major concerns for the managers of CCHP system, in addition to the economic objective. To obtain a balance among various objectives in real-world decision makings, the multiobjective programming (MOP) technique is desired. Previously, MOP has been integrated with some optimization models and successfully applied in many CCHP system management problems [4, 10]. It has a strong potential to be incorporated with the proposed BCCLP model for handling more complicated cases in the future. Finally, the objective function in this study is assumed to be linear form; in fact, the relationship between maintenance cost and load rate may be nonlinear, rather than the linear form. This will lead to a nonlinear objective function. Because the focus of this research is to develop the BCCLP model for supporting the operation optimization of CCHP system, it is thus desired to examine the possibility of an integrated model of BCCLP and nonlinear programming in the future.

5. Conclusion

In this study, a BCCLP model was developed for determining the optimal operation strategies of the gas-fired CCHP system for a five-star hotel in Shanghai Pudong New Area, China. Because the system parameters, including electric demand, cooling demand, and heating demand, exhibit obvious dual-random characteristics in the parameters-identification process, such that the birandom variable was innovatively incorporated into the optimization model for describing their fluctuated characteristics them. A variety of optimal operation strategies for the gas-fired CCHP system were obtained through adjusting predetermined constraint-violation levels, which indicated that the BCCLP model was useful in helping local managers gain in-depth insights into the CCHP system, avoid the deviation caused by the oversimplified uncertain

expression, and analyze the tradeoffs between system economy and reliability, as well as establishing the cost-effective operation strategies. Several findings could be summarized as follows:

- (i) For the cooling-supply system, the cooling demand was satisfied mainly by the absorption chiller for one year. Meanwhile, due to the effect of step tariff on operational cost of electrical chiller, the cooling demand was provided totally by the electric chillers at valley time, and absorption chillers kept full-load operations during the rest periods.
- (ii) In terms of the heating-supply system, the heating demand was met totally by the heat exchanger due to its low running costs and high energy-utilization efficiency.
- (iii) For the electric supply system, the operating strategy exhibited the seasonal variation. The electric demand in winter was mainly by aid of the gas turbine; conversely, it was satisfied through buying electricity in summer.
- (iv) The sensitivity analysis reflected that five factors have the influences on system economy over three seasons, which suggested that comprehensive investigation and consultation are finished for improving the system performance. In the future, high-precision mechanism models or simulation software, multiobjective programming methods, and two types of uncertain optimization techniques should be incorporated into proposed model for tackling more complex issues.

Data Availability

The data used to support the findings of this study are included within the article.

Conflicts of Interest

The authors declare no conflicts of interest.

Authors' Contributions

Ye Xu, Zhe Bao, and Jiheng Li conceived and designed the research. Wei Li, Zhaoyi Huo, Hansheng Yang, and Zhe Bao collected the data. Zhaoyi Huo contributed to supervision. Ye Xu, Zhe Bao, Wei Li, and Hansheng Yang formulated the optimization model. Zhe Bao, Ye Xu, Jiheng Li, and Mengran Li performed the data analyses and manuscript preparation. Zhe Bao, Ye Xu, Wei Li, and Hansheng Yang wrote the paper. Wei Li, Ye Xu, and Jiheng Li gave the comments and helped to revise the paper.

Acknowledgments

The authors are very grateful to the Open Fund of Beijing Key Laboratory of Demand Side Multi-Energy Carriers Optimization and Interaction Technique (YDB 512001901516) for supporting this research.

References

- [1] Y. Liu, Y. Qian, H. Xiao, and S. Yang, "Techno-economic and environmental analysis of coal-based synthetic natural gas process in China," *Journal of Cleaner Production*, vol. 166, pp. 417–424, 2017.
- [2] X. Xie, H. Ai, and Z. Deng, "Impacts of the scattered coal consumption on PM_{2.5} pollution in China," *Journal of Cleaner Production*, vol. 245, 2019.
- [3] B. P. Global, *BP Statistical Review of World Energy June 2017*, 2017.
- [4] Z.-F. Tan, H.-J. Zhang, Q.-S. Shi, Y.-H. Song, and L.-W. Ju, "Multi-objective operation optimization and evaluation of large-scale NG distributed energy system driven by gas-steam combined cycle in China," *Energy and Buildings*, vol. 76, pp. 572–587, 2014.
- [5] G. Chicco and P. Mancarella, "Distributed multi-generation: a comprehensive view," *Renewable and Sustainable Energy Reviews*, vol. 13, no. 3, pp. 535–551, 2009.
- [6] R. Viral and D. K. Khatod, "Optimal planning of distributed generation systems in distribution system: a review," *Renewable and Sustainable Energy Reviews*, vol. 16, no. 7, pp. 5146–5165, 2012.
- [7] B. Yan, S. Xue, Y. Li, J. Duan, and M. Zeng, "Gas-fired combined cooling, heating and power (CCHP) in Beijing: a techno-economic analysis," *Renewable and Sustainable Energy Reviews*, vol. 63, pp. 118–131, 2016.
- [8] P. J. Mago, N. Fumo, and L. M. Chamra, "Performance analysis of CCHP and CHP systems operating following the thermal and electric load," *International Journal of Energy Research*, vol. 33, no. 9, pp. 852–864, 2009.
- [9] P. J. Mago and L. M. Chamra, "Analysis and optimization of CCHP systems based on energy, economical, and environmental considerations," *Energy and Buildings*, vol. 41, no. 10, pp. 1099–1106, 2009.
- [10] P. J. Mago and A. K. Hueffed, "Evaluation of a turbine driven CCHP system for large office buildings under different operating strategies," *Energy and Buildings*, vol. 42, no. 10, pp. 1628–1636, 2010.
- [11] Z. Wang, W. Han, N. Zhang, B. Su, M. Liu, and H. Jin, "Analysis of inlet air throttling operation method for gas turbine in performance of CCHP system under different operation strategies," *Energy Conversion and Management*, vol. 171, pp. 298–306, 2018.
- [12] G. Abdollahi and H. Sayyaadi, "Application of the multi-objective optimization and risk analysis for the sizing of a residential small-scale CCHP system," *Energy and Buildings*, vol. 60, pp. 330–344, 2013.
- [13] Z. Li, Q. An, J. Zhao, S. Deng, L. Kang, and Y. Wang, "Analysis of system optimization for CCHP system with different feed-in tariff policies," *Energy Procedia*, vol. 105, pp. 2484–2491, 2017.
- [14] F. Li, B. Sun, C. Zhang, and L. Zhang, "Operation optimization for combined cooling, heating, and power system with condensation heat recovery," *Applied Energy*, vol. 230, pp. 305–316, 2018.
- [15] S. Lu, Y. Li, and H. Xia, "Study on the configuration and operation optimization of CCHP coupling multiple energy system," *Energy Conversion and Management*, vol. 177, pp. 773–791, 2018.
- [16] C. Qin, J. Tang, and Y. Zhang, "An efficient algorithm for CCHP system sizing and an operational optimization model based on LP," *Journal of Natural Gas Science and Engineering*, vol. 25, pp. 189–196, 2015.
- [17] B. Su, W. Han, Y. Chen, Z. Wang, W. Qu, and H. Jin, "Performance optimization of a solar assisted CCHP based on biogas reforming," *Energy Conversion and Management*, vol. 171, pp. 604–617, 2018.
- [18] X. Wang, C. Yang, M. Huang, and X. Ma, "Multi-objective optimization of a gas turbine-based CCHP combined with solar and compressed air energy storage system," *Energy Conversion and Management*, vol. 164, pp. 93–101, 2018.
- [19] G. Yang and X. Zhai, "Optimization and performance analysis of solar hybrid CCHP systems under different operation strategies," *Applied Thermal Engineering*, vol. 133, pp. 327–340, 2018.
- [20] X. Zhu, X. Zhan, H. Liang et al., "The optimal design and operation strategy of renewable energy-CCHP coupled system applied in five building objects," *Renewable Energy*, vol. 146, pp. 2700–2715, 2020.
- [21] I. Ersoz and U. Colak, "Combined cooling, heat and power planning under uncertainty," *Energy*, vol. 109, pp. 1016–1025, 2016.
- [22] I. Ersoz and U. Colak, "A stochastic evaluation of investments in combined cooling, heat, and power systems," *Applied Thermal Engineering*, vol. 146, pp. 376–385, 2019.
- [23] C. He, Q. Zhang, J. Ren, and Z. Li, "Combined cooling heating and power systems: sustainability assessment under uncertainties," *Energy*, vol. 139, pp. 755–766, 2017.
- [24] L. Ji, D. X. Niu, and G. H. Huang, "An inexact two-stage stochastic robust programming for residential micro-grid management-based on random demand," *Energy*, vol. 67, pp. 186–199, 2014.
- [25] C. Marino, M. Marufuzzaman, M. Hu, and M. D. Sarder, "Developing a CCHP- microgrid operation decision model under uncertainty," *Computers & Industrial Engineering*, vol. 115, pp. 354–367, 2018.
- [26] X. Shen, Q. Guo, and H. Sun, "Regional integrated energy system planning considering energy price uncertainties: a two-stage stochastic programming approach," *Energy Procedia*, vol. 158, pp. 6564–6569, 2019.
- [27] C. Zhang, X. Xue, Q. Du, Y. Luo, and W. Gang, "Study on the performance of distributed energy systems based on historical loads considering parameter uncertainties for decision making," *Energy*, vol. 176, pp. 778–791, 2019.
- [28] C. Y. Zhou, G. H. Huang, J. P. Chen, and X. Y. Zhang, "Inexact fuzzy chance-constrained fractional programming for sustainable management of electric power systems," *Mathematical Problems in Engineering*, vol. 2018, Article ID 5749016, 13 pages, 2018.
- [29] C. Y. Zhou, G. H. Huang, and J. P. Chen, "Planning of electric power systems considering virtual power plants with dispatchable loads included: an inexact two-stage stochastic linear programming model," *Mathematical Problems in Engineering*, vol. 2018, Article ID 7049329, 12 pages, 2018.
- [30] L. Ji, D. X. Niu, G. H. Huang, W. Li, and Z. P. Liu, "Environmental and economic optimization model for electric system planning in ningxia, China: inexact stochastic risk-aversion programming approach," *Mathematical Problems in Engineering*, vol. 2015, Article ID 236958, 17 pages, 2015.
- [31] D. F. Teshomei, P. F. Correia, and K. L. Lian, "Stochastic optimization for network-constrained power system scheduling problem," *Mathematical Problems in Engineering*, vol. 2015, Article ID 694619, 17 pages, 2015.
- [32] J. Peng and B. Liu, "Birandom variables and birandom programming," *Computers & Industrial Engineering*, vol. 53, no. 3, pp. 433–453, 2007.

- [33] J. Xu and C. Ding, "A class of chance constrained multi-objective linear programming with birandom coefficients and its application to vendors selection," *International Journal of Production Economics*, vol. 131, no. 2, pp. 709–720, 2011.
- [34] J. Xu and Z. Tao, "A class of multi-objective equilibrium chance maximization model with twofold random phenomenon and its application to hydropower station operation," *Mathematics and Computers in Simulation*, vol. 85, pp. 11–33, 2012.
- [35] J. Xu and X. Zhou, "A class of multi-objective expected value decision-making model with birandom coefficients and its application to flow shop scheduling problem," *Information Sciences*, vol. 179, no. 17, pp. 2997–3017, 2009.
- [36] M. Liu, Y. Shi, and F. Fang, "Combined cooling, heating and power systems: a survey," *Renewable and Sustainable Energy Reviews*, vol. 35, pp. 1–22, 2014.
- [37] Y. Xu, G. H. Huang, X. S. Qin, and M. F. Cao, "SRCCP: a stochastic robust chance-constrained programming model for municipal solid waste management under uncertainty," *Resources, Conservation and Recycling*, vol. 53, no. 6, pp. 352–363, 2009.
- [38] L. Wang, G. Huang, X. Wang, and H. Zhu, "Risk-based electric power system planning for climate change mitigation through multi-stage joint-probabilistic left-hand-side chance-constrained fractional programming: a Canadian case study," *Renewable and Sustainable Energy Reviews*, vol. 82, pp. 1056–1067, 2018.

Research Article

Pricing Decisions in Closed-Loop Supply Chains with Competitive Fairness-Concerned Collectors

Yadong Shu ^{1,2}, Ying Dai ¹ and Zujun Ma ^{1,3}

¹Institute for Logistics and Emergency Management, School of Economics and Management, Southwest Jiaotong University, Chengdu 610031, China

²School of Mathematics and Statistics, Guizhou University of Finance and Economics, Guiyang 550025, China

³Logistics and E-commerce College, Zhejiang Wanli University, Ningbo 315100, China

Correspondence should be addressed to Ying Dai; ydai@swjtu.edu.cn

Received 10 May 2020; Revised 23 September 2020; Accepted 18 October 2020; Published 17 November 2020

Academic Editor: Xander Wang

Copyright © 2020 Yadong Shu et al. This is an open access article distributed under the Creative Commons Attribution License, which permits unrestricted use, distribution, and reproduction in any medium, provided the original work is properly cited.

Based on the Shapley value fairness concern framework, a fairness concern utility system is established for the closed-loop supply chain (CLSC) with one manufacturer, one retailer, and two competitive collectors. Under the five models (one centralized and four decentralized), the influence of competitive strength and fairness concern degree of collectors on the pricing decisions is analyzed. The following conclusions can be obtained: (1) When the manufacturer considers the fairness concern of the collectors, fairness concern is a way for the collectors to obtain more profit. Whether the manufacturer “proactively” considers the fairness concern of the collectors is an approach to benefiting the collectors but only in the case of “active” consideration, there is less self-loss to the manufacturer. (2) When the collectors’ fairness concern cannot be considered by the manufacturer, the equilibrium recycling price sets lower for the purpose of achieving more profit by the collectors. At this point, the profit of the collectors and the manufacturer is the lowest, and so is the return rate of the CLSC. (3) When the collectors do not care about whether they are being fairly treated but the manufacturer “actively” takes the fairness of the collectors into consideration, the collectors get “unexpected” attention from the manufacturer, which makes the performance of the collectors more positive than it is when their fairness concerns are taken into account. The profit increased by the collectors is more than that lost by the manufacturer, so the profit of the CLSC is the largest. Additionally, our findings provide some managerial insights on the pricing decision in the case where the collectors consider fairness concern.

1. Introduction

With the exhaustion of resources and the intensification of environmental pollution, increasing people are aware of the importance of the effective collecting and reuse of used products. On the one hand, the government has promulgated a series of environmental protection laws, requiring enterprises to collect and recycle at least a certain proportion of the collecting of used products [1–3]. On the other hand, many enterprises have been conscious of the important role played in collecting used products in sustainable development, which can not only reduce environmental pollution and enhance enterprises’ social reputation but also reduce production costs so that competitiveness is enhanced [4–6].

In order to make full play to their advantages, the manufacturer tends to outsource the recycling of waste products to the collectors who are specialized in recycling activities. The manufacturer focuses on the production of new products and the remanufacturing of waste products [7–9]. Both of the manufacturer and the collectors make a profit from reverse recycling activities. For example, in China, only the waste paper recycling business profit reached \$ 5.72 billion in 2017. Hence, there exists inevitable competition among multiple collectors in the process of collecting used products. How does the competition among the collectors affect the pricing decision in the CLSC? If the collection activity is profitable, such an appealing activity consequentially brings competitions. To whom is it

beneficial? Does it jeopardize the benefit of the members in the CLSC?

Additionally, the decision-makers are also interested in the fairness of the income distribution while pursuing the maximization of personal interests. For instance, Scheer et al. [10] also surveyed 417 car dealers in the United States and 289 auto dealers in Holland and found that they should pay more attention to the fairness of distribution when they trade with business partners. Subsequent research has also documented cases where both of the manufacturer and the retailers sacrifice their own margins for the benefit of their counterpart because of fairness concern [11–14].

It is worth noting that the existing research on fairness concern of CLSC considers the fairness concern of the manufacturer or the retailer but barely considers that of the collectors [15]. With the pressure of environmental regulations, increased consumers' awareness of environmental protection, and the profitability of collection activities, the collection of used products has become an indispensable link in CLSC management. More and more collectors engaging in the recycling of used products have stepped onto the stage of history and played an irreplaceable role.

To investigate the influence of fairness concern of collectors on CLSC decisions, this paper concentrates on a CLSC composed of one manufacturer, one retailer, and two collectors. Based on observations from current practice and the extant literature, five models are considered: (1) the centralized decision-making model C; (2) the model FY in which collectors are fairness-concerned and the manufacturer "passively" considers the fairness concern of collectors; (3) the model FN in which collectors are fairness-concerned but the manufacturer neglects the fairness concern of collectors; (4) the model NN in which collectors are not fairness-concerned and the manufacturer does not consider the fairness concern of collectors; (5) the model NY in which collectors are not fairness-concerned but the manufacturer "proactively" considers the fairness concern of collectors.

More specifically, this paper aims to analyze the following issues:

- (1) The equilibrium solution in the CLSC in the five models
- (2) The influence of fairness concern coefficient and competition intensity of the collectors on equilibrium solution in the CLSC
- (3) How to design incentive contracts to make the utility of decision-makers in the CLSC system realize Pareto improvement (see [16])

The main contributions of this paper are structured as follows. First, considering the impact of fairness concern of collectors on CLSC decision-making under multiple models, it is a supplement to existing research. Second, the decision-making is discussed when collectors are fairness-neutral but the manufacturer "actively" considers fairness concern of collectors. Third, in addition to considering the impact of fairness concern on decision-making in the CLSC, this paper also considers the impact of the competitive intensity of collectors on decision-making in the CLSC.

In a deeper sense, our work has enriched the research results that consider the factors of the decision-makers' behavior in the CLSC. The remaining parts of the paper are organized as follows: the next part introduces the relative literature review. The third part lists problem description and model hypotheses. The fourth part studies the optimal decision-making of the CLSC. The incentive contracts are given in the fifth part. And the last part provides the numerical analysis and the conclusions.

2. Literature Review

The paper discusses the change of equilibrium solution of the system considering the collectors' fairness concern under the five models. In general, the research work of the paper is based on a vast body of references.

The first part of the literature is related to pricing decision. Heydari et al. [17] addressed the problem of optimal decision-making for a three-tier dual-channel green supply chain. Esmaeili et al. [18] studied short-term and long-term pricing decisions of a closed-loop supply chain using Stackelberg game and evolutionary game theory, respectively. Ma et al. [19] showed the pricing decisions of closed-loop supply chain under four reverse channels when retailers consider marketing efforts. Diabat and Jebali [20] considered the network design of a closed-loop supply chain for consumer durables under recycling legislation and analyzed the influence of model parameters on pricing decisions. The study by Huang et al. [8] provided a reference for choosing single or dual recycling channels for recycling used products. Wen et al. [21] analyzed the impact of retailers' pricing strategies on the closed-loop supply chain under the consideration of consumer environmental responsibility; equal pricing is a win-win strategy when the acceptance of the remanufactured product reaches a certain threshold. Jalali et al. [22] believed that the presence of complementary products increases the difficulty in decision-making. Meng et al. [23] suggested that the government should not always provide consumption subsidies, because the consumption subsidies undermined the demand for new products while promoting the demand for remanufactured products. The research of Wang et al. [24] showed that the choice of recycling channels depends on the unit cost of self-recycling and the compensation of outsourcing recycling. However, the above research does not continue to discuss the influence of competitive factors on decision-making. Giri et al. [25] discussed the decision problem of retailer's competition under the same and the different wholesale prices. Savaskan and Wassenhove [26] discussed the design of the reverse channel under the competition of the retailer. Ferguson et al. [27] analyzed the impact of competition on recycling strategies. The research by Lee and Sana [28] showed that as price competition intensifies between collectors, the profitability of the supply chain decreases. Xing et al. [29] found that the degree of competition among recyclers changes in the opposite direction to the expected utility of manufacturers. The studies above show that the competitive factors play a pivotal role in the decision-making process of the supply chain.

The second part of the literature is related to fairness concern. Ho and Zhang [30] confirmed the existence of fairness concern in the supply chain through experiments. Zhang et al. [31] believed that the retailer's fairness concern would cause the loss of supply chain. Li et al. [32] found through theoretical research that the retailer's fairness concern is beneficial to supply chain decision-making. Huang [33] believed that different types of fairness concern of retailers have different effects on CLSC pricing decisions. Zhang et al. [34] believed that when the retailer's fairness concern is at a high level, it is not good for the manufacturer. Therefore, the manufacturer will not adopt green manufacturing strategy. The aforementioned studies were carried out from the perspective of retailers' fairness concern. Some researchers have expanded the scope of their research. For example, Li et al. [35] revealed that the impact of the manufacturer's fairness concern on supply chain decisions is related to the market share of retailers. Zhen et al. [36] believed that fairness concern from both of the manufacturer and the retailer may bring more profit to the supply chain when the retailer has multichannel. Huang et al. [9] believed that when the collector had fairness concern, the manufacturer should set higher transfer payments to encourage the collector to participate in recycling activities.

These studies present that fairness concern will affect supply chain decisions. However, these studies ignore the power and contribution of the players. Chen et al. [13] and Shu et al. [37] used the Nash bargaining solution as a fairness reference point to study the influence of fairness concern on supply chain decision-making. However, the Shapley fairness distribution principle is the best way when the alliance has more than two members, which emphasizes that the members of the alliance are allocated according to the size of their contributions [38]. Therefore, as a result of fairness reference, Shapley value naturally becomes a fairness reference point for building a fairness concern utility system. Unlike the studies above, this paper introduces the impact of fairness concern on decision-making while considering competition in the CLSC.

The third part of the literature is concerned with coordination. It is well known that in most cases the wholesale price contract cannot achieve a coordination of the supply chain. However, in reality, it is easy to perform and the supervision cost is low, so wholesale price contracts become favored by a large number of practitioners. Cui et al. [11] found that, in the linear demand condition when the fairness concern of the members was considered, only setting a higher wholesale price than the cost can achieve both the coordination of the supply chain and the Pareto improvement of the system. The same conclusion was acquired in the nonlinear demand condition by the authors in [39], who found that the supplier could offer wholesale price contracts to achieve the coordination of the supply chain only if one member of the supply chain had fairness concern. Du [40] proved that a fairness preference could change the equilibrium solutions, and in certain conditions, the wholesale price contracts could achieve the competitive coordination of the supply chain. When the fairness concern information

is asymmetrical, through a mass of experimental data by Katok et al., [41] showed that the fairness concern behaviors of the supply chain members had a great influence on the formation of contracts to achieve coordination. Other commonly used contracts also enable supply chain to achieve coordination. Karakostas et al. [42] suggested that a large majority of experimental subjects choose the revenue-sharing contract. This choice not only turns out to be the most efficient but at the same time is fair. Heydar et al. [43] realized the coordination of two-stage reverse supply chain through revenue-sharing contract. Monda and Giri [44] have shown that cost-sharing contracts could coordinate the two-cycle closed-loop green supply chain, and the performance of the supply chain can be improved through green innovation or marketing. The research of Li et al. [45] showed that the simple transfer payment contract coordination of the supply chain failed when the collectors had multiple fairness concerns. Zhang and Ren [46] achieved perfect coordination of CLSC by revenue-sharing and the two-part Tariff contract, and the influence of coordination parameters on optimal supply chain performance was also discussed. Wang et al. [47] also reached a similar conclusion in the CLSC with dual-collecting and the two-part Tariff contract works better. Based on the previous literature, the paper attempts to apply the two-part Tariff contract mechanism for achieving a Pareto improvement in a CLSC.

To sum up, the existing literature on the fairness concern of the supply chain has focused on whether the fairness concern is symmetrical or asymmetric and when one party hopes to be treated fairly, whether the other considers this fairness. There is no literature about the case where one party does not consider the fairness of profit distribution, while the other party "actively" considers that the other is fairness-concerned. To address this gap, the Stackelberg game is applied to analyze the competition between collectors under five models and study the impact of fairness concern in the CLSC on pricing decisions. The results suggest that as long as the manufacturer considers the fairness concern of the collectors, the profit of the collectors will increase, which is a profit-giving behavior. However, when the collectors' fairness concern cannot be considered by the manufacturer, the equilibrium recycling price is set lower for the purpose of achieving more profit by the collectors, and the efficiency of the CLSC is the lowest. We present some research results to highlight the contributions of this paper (see Table 1).

3. Problem Description and Model Assumptions

3.1. Problem Description. In order to discuss the impact of fairness concern of collectors on pricing decisions and coordination, this paper considers a CLSC system consisting of a manufacturer, a retailer, and two homogeneous collectors. The closed-loop supply chain system and the symbols involved are illustrated in Figure 1 and Table 2.

Throughout the entire CLSC, the manufacturer outsources the used product recycling business to dedicated collectors. The collectors collect the used products from the market at a certain price and transfer them to the

TABLE 1: The literature positioning of this paper.

Research	Considering the competition factors	Followers are fairness-concerned, and leaders consider the fairness concern of followers	Followers are unfairness-concerned, and leaders consider the fairness concern of followers
Heydari et al. [17]	×	×	×
Ma et al. [19]	×	√	×
Wen et al. [21]	×	×	×
Giri and Sharma [25]	√	×	×
Savaskan and Wassenhove [26]	√	×	×
Ho and Zhang [30]	×	√	×
Xiao et al. [32]	×	√	×
Shu et al. [37]	×	√	√
This paper	√	√	√

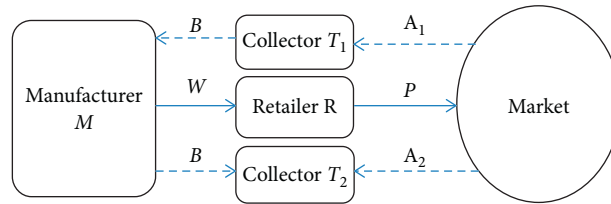


FIGURE 1: The closed-loop supply chain configuration.

TABLE 2: Symbol description.

Parameters	
M	Manufacturer
R	Retailer
T_i	Collector $i, i = 1, 2$
A	The potential capacity of the market
B	The sensitivity coefficient of the price
H	Quantity of used products that the collector pays no collecting cost
C	The cost of the new products produced by raw materials
C_r	The cost of remanufacture made by collecting used products
Δ	The per unit saving cost from collecting to remanufacturing, $\Delta = c - c_r$
δ	The substitution coefficient of the competition between the collectors, and $0 < \delta < 1$
$D(p)$	The retailer's market demand
G_i	Collection amount of the collector $i, G = G_1 + G_2$
r_{sc}	Collecting rate of the CLSC, and $r_{sc} = G/D$, and $0 < r_{sc} < 1$
C	The centralized decision-making model
TY	The collectors are fairness-concerned and the manufacturer considers (passive) fairness concern of the collectors
TN	The collectors are fairness-concerned but the manufacturer does not consider fairness concern of the collectors
NN	The collectors are not fairness-concerned and the manufacturer does not consider fairness concern of the collectors
NY	The collectors are not fairness-concerned but the manufacturer considers (active) fairness concern of the collectors
Subscript sc	The CLSC decision
Superscript “*”	The optimal solution of the CLSC
λ	Fairness concern coefficient of the collectors
φT_i	Fairness reference point of the collectors i
Decision variables	
P	Retail price set by the retailer
A_i	Recycling price set by the collector
B	Transfer price set by the manufacturer, $A_i < B < \Delta$
W	Wholesale price set by the manufacturer
Performance measures	
π_M^l	The profit of the manufacturer under the model $l, l \in \{FY, FN, NY, NN\}$
π_R^l	The profit of the retailer under the model $l, l \in \{FY, FN, NY, NN\}$
$\pi_{T_i}^l$	The profit of the collector T_i under the model $l, l \in \{FY, FN, NY, NN\}$
π_{sc}^l	The profit of the CLSC under the model $l, l \in \{FY, FN, NY, NN\}$
$u_{T_i}^l$	The utility of the collector T_i under the model $l, l \in \{FY, FN, NY, NN\}$

manufacturer at an appropriate price. The manufacturer processes the used products. After processing (such as repairs, remanufacturing, recycling materials, etc.), new products and remanufactured products are wholesaled to the retailer, who sells the new products and remanufactured products on the market. What needs to be pointed out is because this paper is a scientific research activity carried out in the context of improving recycling channels, increasing the return rate of used products, promoting sustainable development of society, and then improving people's quality of life, the focus is on reverse recycling channels. Since the retailer does not pay attention to the fairness of profit distribution but only his own income, the retailer is fairness-neutral.

3.2. Model Assumptions. On the premise of not affecting the main conclusions of this paper, the complex supply chain in reality is made a proper simplifying assumption.

Assumptions 1. The marketing demand $D(p)$. ($D(p) \geq 0$) is a deterministic decreasing function of p , expressed as

$$D(p) = a - bp. \quad (1)$$

Assumptions 2. Following Savaskan and Van Wassenhove [26] and Xing et al. [29], the collection amount is determined by the recycling price of the two collectors, and in the collection process, the two collectors form a competitive relationship, that is,

$$G_i = h + A_i - \delta A_j, \quad (i = 1, 2; j = 3 - i). \quad (2)$$

Here, δ denotes quantity of used products that is gained in the case that the collector pays no collecting cost, and $0 < \delta < 1$ indicates that the collection amount is more sensitive to its own recycling price.

Assumptions 3. No waste will occur in the process of recycling and remanufacturing the used products; that is, the conversion rate of the used products into new products is 1, and the new products and remanufactured products are homogeneous.

Assumptions 4. The new products and the remanufactured products are completely replaceable, and the retail price in the market is the same; that is, the products produced using the new materials and the remanufactured products are homogeneous ones and are sold in the market at the same price.

Assumptions 5. Members of the closed-loop supply chain play a Stackelberg master-slave game with the manufacturer as the leader and the retailer and the collector as followers. The manufacturer and the retailer are fairness-neutral and seek to maximize profits. When the collector is fairness-neutral, he seeks to maximize profit. When fairness attention is paid, he seeks to maximize utility.

Assumptions 6. The information among the manufacturer, the retailer, and the collectors is symmetrical; that is, they understand each other's costs, pricing strategies, and response functions.

From the assumptions and descriptions above, the objective functions of the manufacturer M , the retailer R , and the collector T_i are as follows:

$$\begin{cases} \max_{B,w} \pi_M = (w - c)D + \sum_{i=1}^2 (\Delta - B)G_i, \\ \max_p \pi_R = (p - w)D, \\ \max_{A_i} \pi_{T_i} = (B - A_i)G_i. \end{cases} \quad (3)$$

4. Problem Description and Model Assumptions

4.1. Construction of Shapley Reference Framework. The retailer, as a single decision-maker, ignores fairness of the alliance. With regard to an individual who has the tendency to fairness concern behavior, his utility is connected with actual profit and difference of fairness reference point. The background considered in paper is a convex game; as a result, Shapley value can be employed to describe equitable distribution. It emphasizes the distribution according to the ability and the contribution of the system members, and he pursues the relative fairness between the members instead of absolute fairness.

The system includes one manufacturer M and two collectors T_1 and T_2 , and the recycling prices of the two collectors are, respectively, A_1 and A_2 . The Shapley value distributions of all the members are $\{\varphi_M(v), \varphi_{T_1}(v), \varphi_{T_2}(v)\}$. It can be imagined that the Shapley value is a function of A_1 and A_2 . The system profit changes with the variation of A_1 and A_2 , and then the gross profit changes, accordingly, and so does the Shapley value. Next, we, respectively, calculate the system eigenvalue, namely, the profits of the system, all of which are zero in one-member system; namely, $v(M) = 0$, $v(T_1) = 0$, and $v(T_2) = 0$. Here, it only considers the remanufacturing profit created by the manufacturer. In the two-member system, when the two collectors coexist simultaneously, the profit is zero; that is, $v(T_1, T_2) = 0$. When there is only one manufacturer and one collector, the profit of the system can be presented as

$$v(M, T_i) = (\Delta - A_i)G'_i. \quad (4)$$

At this time, there is no competition between the collectors, so the collecting quantity is

$$G'_i = h + A_i. \quad (5)$$

When the system members are the collector and the manufacturer, the system profit is as follows:

$$v(M, T_i, T_j) = (\Delta - A_i)G_i + (\Delta - A_j)G_j. \quad (6)$$

It should be noted that the recycling price A_i differs in the cases of single and multiple collectors. Applying the

Shapley three principles of fairness (see [48, 49]), we calculate the fairness distribution of the manufacturer and the collectors as follows:

$$\begin{cases} \varphi_M(v) = (\Delta - A_i)\left(\frac{1}{2}h + \frac{1}{2}A_i - \frac{1}{3}\delta A_j\right) + (\Delta - A_j)\left(\frac{1}{2}h + \frac{1}{2}A_j - \frac{1}{3}\delta A_i\right), \\ \varphi_{T_i}(v) = \frac{1}{2}(\Delta - A_i)(h + A_i) - \frac{1}{3}\delta\Delta(A_i + A_j) + \frac{2}{3}\delta A_i A_j, \\ \varphi_{T_j}(v) = \frac{1}{2}(\Delta - A_j)(h + A_j) - \frac{1}{3}\delta\Delta(A_j + A_i) + \frac{2}{3}\delta A_i A_j, \end{cases} \quad (7)$$

according to

$$\begin{aligned} \frac{\partial^2 \varphi_M}{\partial A_i^2} &= -1 < 0, \\ \frac{\partial^2 \varphi_{T_i}}{\partial A_i^2} &= -1 < 0. \end{aligned} \quad (8)$$

The fairness distribution of the two collectors T_1 and T_2 is a concave function concerned with their own recycling price, so there exists the optimal recycling price which makes the Shapley maximum.

Thus, the utility function of collectors concerned with fairness concerns is

$$u_{T_i}^l = \pi_{T_i}^l + \lambda(\pi_{T_i}^l - \varphi_{T_i}). \quad (9)$$

Here, $l \in \{\text{FY, FN, NY, NN}\}$. φ_{T_i} expresses the relative fairness reference point of the collector. λ represents the fairness concern coefficient of collectors, and $\lambda \geq 0$. When λ becomes bigger, it means that the collectors pay more attention to revenue distributional fairness. When $l \in \{\text{FY, FN}\}$, there exists $\lambda > 0$, which means the collectors are concerned with both their own profit and the revenue distribution fairness. At this time, the aim of the collectors is to achieve utility maximization. When $l \in \{\text{NY, NN}\}$, there exists $\lambda = 0$; the collectors are to pursue profit maximization. Here, $u_{T_i}^l = \pi_{T_i}^l$. Based on assumptions, both the manufacturer and the retailer only pursue profit maximization.

4.2. The Model C. Supply chain is effective in the centralized model, where the utility always acts as a comparison benchmark of operational efficiency in different incentive contracts. In this model, all the members co-determine the optimal retailing price and recycling price to achieve the maximal profit. The wholesale price and the transfer price influence is not the variation of the gross profit but the distribution of it among the manufacturer, the retailer, and the collectors. The profit of supply chain π_{sc}^C is the following:

$$\max_{p, A_i} \pi_{sc}^C = (p - c)D + \sum_{i=1}^2 (\Delta - A_i)G_i. \quad (10)$$

Proposition 1. Under the model C, the optimal pricing decisions of the system are

$$\begin{aligned} p^{C*} &= \frac{a + bc}{2b}, \\ A_i^{C*} &= \frac{\Delta(1 - \delta) - h}{2(1 - \delta)}. \end{aligned} \quad (11)$$

By backward induction, we obtain Proposition 1. Proofs of all propositions and corollaries in the paper are provided in the Appendix.

4.3. The Model NN. In the model NN, the manufacturer, the retailer, and the collectors are all independent decision-makers, who are all fairness-neutral to achieve the maximal self-interest. The manufacturer is the leader, who first sets the wholesale price as well as the transfer price of used products. Then, the retailer sets the retail price. Meanwhile, the collectors set the recycling price. By the backward induction, the optimal pricing decision in the CLSC can be obtained.

Proposition 2. Under the model NN, the optimal pricing decisions of the system are

$$\begin{aligned} w^{\text{NN}*} &= \frac{a + bc}{2b}, \\ B^{\text{NN}*} &= \frac{(1 - \delta)\Delta - h}{2(1 - \delta)}, \\ p^{\text{NN}*} &= \frac{3a + bc}{4b}, \\ A_i^{\text{NN}*} &= \frac{(1 - \delta)\Delta + h(2\delta - 3)}{2(1 - \delta)(2 - \delta)}. \end{aligned} \quad (12)$$

Corollary 1. $A_i^{\text{NN}*} < A_i^{C*}$, $p^{C*} < p^{\text{NN}*}$, $r_{sc}^{C*} < r_{sc}^{\text{NN}*}$, $\pi_{sc}^{\text{NN}*} < \pi_{sc}^{C*}$.

Affected by double marginalization, the goal of all the members in CLSC is to maximize their profit, which usually lowers supply chain performance. When setting the transfer price, the manufacturer does not consider the profit of the collectors. The influence of double marginalization causes the collectors to cut down the recycling price, thus decreasing the collection quantity, which leads to the loss of CLSC efficiency. However, because the declining rate of the collecting quantity is not as fast as the demanding quantity, the return rate has increased.

4.4. The Model FY. In the model FY, when the collectors are fairness-concerned, they seek the maximization of the utility. In the meantime, the manufacturer also takes the collectors' fairness concern into account.

Proposition 3. *Under the model FY, the optimal pricing decisions of the system are*

$$\begin{aligned} B^{FY*} &= \frac{\Delta(1-\delta)(6+9\lambda-2\lambda\delta)-h(6+3\lambda+\lambda\delta)}{12(1-\delta)(1+\lambda)}, \\ A_i^{FY*} &= \frac{\Delta(1-\delta)(6+3\lambda+2\lambda\delta)+h[6(2\delta-3)+\lambda(5\delta-9)]}{4(1-\delta)[3(2-\delta)+\lambda(3-\delta)]}. \end{aligned} \quad (13)$$

Particularly, when $\lambda = 0$, the model FY goes back to the model NN.

Corollary 2

- (1) $\partial A_i^{FY*} / \partial \lambda > 0$, $\partial B^{FY*} / \partial \lambda > 0$;
- (2) $B^{FY*} > B^{NN*}$, $A_i^{FY*} > A_i^{NN*}$.

Corollary 2 indicates that (1) when the collectors are fairness-concerned, "reciprocity" is developed between the collector and the manufacturer; namely, the manufacturer who knows the collectors' fairness concern raises the transfer price, and at the same time, the collectors also raise the recycling price to indirectly "reward" the manufacturer. Corollary 2 also suggests that, in the model FY, the more fairness-concerned the collectors are, the more efforts the two parties are willing to pay. (2) Compared with the model NN, in the model FY, due to considering the fairness concern of the collectors, the manufacturer will raise the transfer price to deliver part of the profit to the collectors. After knowing the strategy, the collectors will also put up the recycling price to indirectly "reward" the manufacturer, which is beneficial to increase the collection quantity of the used products so as to achieve the goal of saving resources and protecting the environment.

4.5. The Model FN. In the model FN, when the collectors are fairness-concerned, which is not considered by the manufacturer, the manufacturer makes his own decision based on the reaction function when the collectors are fairness-concerned.

Proposition 4. *Under the model FN, the optimal pricing decisions of the system are*

$$\begin{aligned} B^{FN*} &= \frac{(1-\delta)\Delta-h}{2(1-\delta)}, \\ A_i^{FN*} &= \frac{\Delta(1-\delta)(3+2\lambda\delta)-3h[(3-2\delta)+\lambda(2-\delta)]}{2(1-\delta)[3(2-\delta)+\lambda(3-\delta)]}. \end{aligned} \quad (14)$$

Particularly, when $\lambda = 0$, the model FN goes back to the model NN.

Corollary 3. $A_i^{FN*} < A_i^{FY*}$, $B^{FN*} < B^{FY*}$, $r_{sc}^{FN*} < r_{sc}^{FY*}$.

Corollary 3 shows, compared with the case where the collectors' fairness concern is recognized by the manufacturer, in the model FN, when this kind of fairness concern is not recognized, the collectors will passively take action to indirectly "revenge" the manufacturer by lowering recycling price, which is harmful to the development of the CLSC; therefore, the goal of resource saving and environmental protection cannot be achieved.

4.6. The Model NY. In reality, the party in a leadership position who gets most of the profit will do something to care about subordinates; for example, the manufacturer will raise the transfer price to promote the loyalty of the collectors and simultaneously make the collectors pay more collecting efforts, thus improving return rate. It not only meets relevant laws and regulation but also acquires more benefit by reproduction. However, when the collectors are satisfied with current status or have already acknowledged their own efforts and what they get, the collectors will not care about distribution fairness of the manufacturer's profit, which is simplified as the model NY.

When the manufacturer "actively" considers fairness concern of the collectors, the manufacturer will make the decision according to the reaction function when the collectors are fairness-concerned. That is, the manufacturer will make decisions based on the model FY, while the collectors, based on the model NN.

Proposition 5. *Under the model NY, the optimal pricing decisions of the system are*

$$\begin{aligned} B^{NY*} &= \frac{(1-\delta)\Delta(6+9\lambda-2\lambda\delta)-(6+\lambda\delta+3\lambda)h}{12(1+\lambda)(1-\delta)}, \\ A_i^{NY*} &= \frac{\Delta(1-\delta)(6+9\lambda-2\lambda\delta)-h(18+15\lambda-12\delta-11\lambda\delta)}{12(1-\delta)(2-\delta)(1+\lambda)}. \end{aligned} \quad (15)$$

Particularly, when $\lambda = 0$, the model NY goes back to the model NN. Because of the complexity of expressions, the parameter analyses are placed in numerous analysis section.

5. Incentive Contract in the Model FY

The goal of introducing contracts is to improve the profits of participants. Under the model NN, a large number of studies have shown that a variety of contracts can make supply chain coordination. Under the model FN and the model NY, it is difficult for the manufacturer to know the utility function of the collectors. Therefore, it is difficult for the supply chain leader (manufacturer) to understand the payment function of the contract receiver (collectors), and it is unrealistic to achieve perfect coordination of the supply chain.

This section only discusses the model FY; that is, the collectors are fairness-concerned, and the manufacturer who considers the collectors' fairness concern designs incentive contracts. Here, the Pareto improvement of the CLSC is realized by two-part Tariff contract mechanism. The paper regards the retailer as an independent decision-maker, so his decisions under incentive contracts will not change.

Assume the contract to the collector T_i offered by the manufacturer is (F_i, B^t) . F_i presents the manufacturer's franchise fees offered by the collector, which helps the manufacturer gain the service by the collector. B^t shows transfer price under incentive contracts and the superscript "t" symbolizes the decisions under the contracts, so the decision models of the manufacturer and the collector go as follows:

$$\begin{aligned} \max \pi_M^t &= (w^t - c)D^t + \sum_{i=1}^2 (\Delta - B^t)G_i^t + F_1 + F_2, \\ \text{s.t.} \quad &\begin{cases} \pi_{T_i}^t = (B^t - A_i^t)G_i^t - F_i, \\ u_{T_i}^t = \pi_{T_i}^t + \lambda(\pi_{T_i}^t - \varphi_{T_i}^t) \geq u_{T_i}^{\text{FY}*} \quad (\text{IV}), \\ \frac{\partial u_{T_i}^t}{\partial A_{T_i}^t} = 0 \quad (\text{IC}), \\ i = 1, 2. \end{cases} \end{aligned} \quad (16)$$

Proposition 6. *Based on the incentive contract proposed by the manufacturer, there exists the only system equilibrium solution in the CLSC, and the manufacturer's optimal transfer price B^{t*} and the collector's optimal collection price A_i^{t*} are, respectively, as follows:*

$$\begin{aligned} B^{t*} &= \frac{\Delta B^{t1} - 3\delta B^{t2} + \delta^2 B^{t3} + hB^{t4}}{12(1 + \lambda)B^{t5}}, \\ A_{T_i}^{t*} &= \frac{\Delta A_{T_i}^{t1} - hA_{T_i}^{t2}}{4B^{t5}}. \end{aligned} \quad (17)$$

Among them,

$$\begin{aligned} B^{t1} &= 9(8 + 24\lambda + 24\lambda^2 + 7\lambda^3) - 2\delta^3\lambda^2(3 + \lambda), \\ B^{t2} &= 36 + 104\lambda + 103\lambda^2 + 28\lambda^3, \\ B^{t3} &= 36 + 102\lambda + 111\lambda^2 + 29\lambda^3, \\ B^{t4} &= \delta^2\lambda^2(3 + \lambda) - 9\lambda(2 + \lambda)^2 - 3\delta(12 + 16\lambda + 9\lambda^2 + 2\lambda^3), \\ B^{t5} &= 6 + 15\lambda + 6\lambda^2 + \delta^2\lambda(3 + \lambda) - \delta(6 + 17\lambda + 6\lambda^2), \\ A_{T_i}^{t2} &= 12 + 12\lambda(3 - \delta) + 5\lambda^2(3 - \delta), \\ A_{T_i}^{t1} &= 3(4 + 8\lambda + 3\lambda^2) - 2\delta^2\lambda^2 - \delta(12 + 22\lambda + 5\lambda^2). \end{aligned} \quad (18)$$

6. Numerical Analysis

In the previous part, the two-part Tariff contract mechanism is established to improve the efficiency of the CLSC. In this section, numerous analyses are applied to verify its efficiency and the influence of fairness concern and competitive intensity between collectors on decisions of the CLSC is studied. Denote the model parameters $a = 1000$, $b = 1$, $h = 20$, $c = 120$, $cr = 40$, and $\Delta = 80$. By replacing these parameters into the above models, the paper discusses the influence of fairness concern and competitive intensity between the collectors on decisions of the CLSC.

6.1. Impact of Distributional Fairness Concern λ on the CLSC. In order to analyze the impact of distributional fairness concern on decisions of the CLSC, it is assumed that the collectors' competitive intensity remains unchanged (let $\delta = 0.2$). The influence of the collectors' fairness concern on pricing decisions of the CLSC is shown in Figure 1. Figure 2(a) manifests that, under coordination, the collectors' transfer price offered by the manufacturer is higher. Moreover, when the manufacturer does not consider the fairness concern of the collectors, this transfer price is unchanged with the collectors' fairness concern whether in the model NN or FN. But in the model FY or NY, whether the concern of the manufacturer about the collectors is "active" or "passive," the transfer price of the manufacturer will amplify with coefficient of the collector's fairness concern.

Figure 2(b) indicates under the coordination, after getting a higher transfer price, the collectors will also raise recycling price to "repay" the manufacturer. When the collectors' fairness concern does not receive the manufacturer's response, the collectors will rapidly reduce recycling price, which is the lowest this time. Conversely, when the collectors are not fairness-concerned but the manufacturer "proactively" considers the collectors are fairness-concerned, the collectors become more active, willingly accepting a higher recycling price than that obtained in the case where their fairness concern is responded to by the manufacturer, and this price is just lower than that in coordination state.

Figure 2(c) suggests in coordination state, due to the highest recycling price of the collectors and the largest

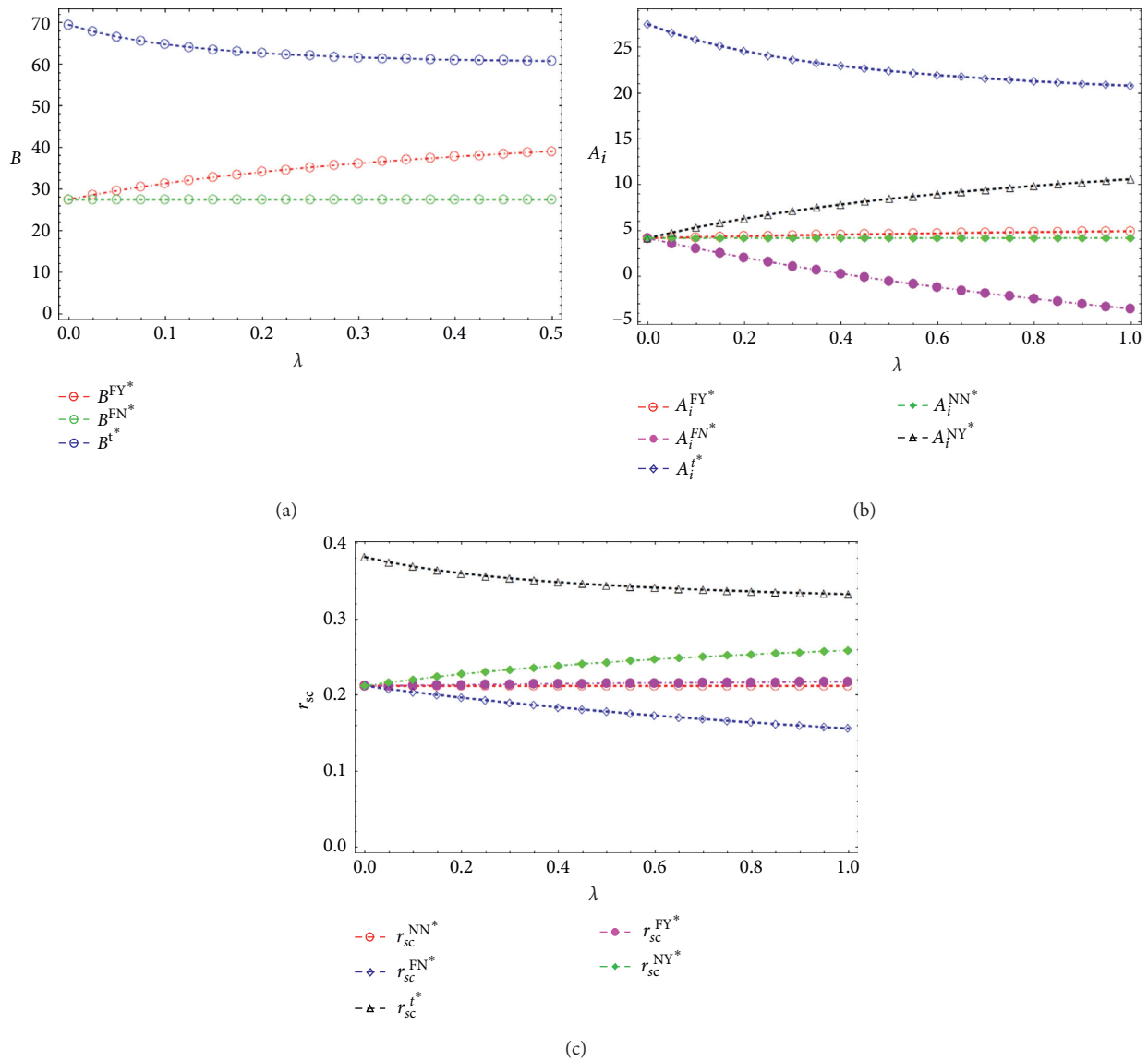


FIGURE 2: The impact of fairness concern on decisions of the CLSC. (a) The influence of fairness concern on transfer price. (b) The influence of fairness concern on recycling price. (c) The influence of fairness concern on return rate of the CLSC.

collection quantity and the unchanged retail price of the retailer in all models, the return rate is the most efficient when sales volume is invariant. However, the return rate will decrease as fairness concern increases. In the model FN, the collectors' substantially reducing the recycling price to indirectly "punish" the manufacturer leads to the lowest return rate, which "hurts" the CLSC as well as sustainable development of enterprises and society. This figure also shows, whether the concern of the manufacturer about the collectors is "active" or "passive," the return rate is higher than that when the manufacturer does not concern the collectors' fairness. Clearly, considering the long-term development, whether the collectors are fairness-concerned or not, the fairness concern of the manufacturer about the collectors is the most beneficial to the CLSC members and the environment.

From Figure 3(a), it is known that, in coordinated state, the profit of the manufacturer is the maximum. Because the fairness concern of the collectors will always sacrifice the manufacturer's profit, in the models FY, NY, and FN, only if there is one party who considers the collectors' fairness concern, the loss of the manufacturer's profit is minimal. When the collectors are fairness-concerned but the manufacturer neglects it, the loss is the maximum. From Figure 3(b), it suggests that only when the manufacturer considers the collectors' fairness concern, whether it is "active" or "passive," will the collectors' profit get massively promoted. In particular, the concern is "active"; the profit gets faster growth. In Figure 3(c), when the collectors' fairness concern is not responded to by the manufacturer, the CLSC efficiency is the lowest and decreases faster. When the collectors get "active" attention by the manufacturer, the

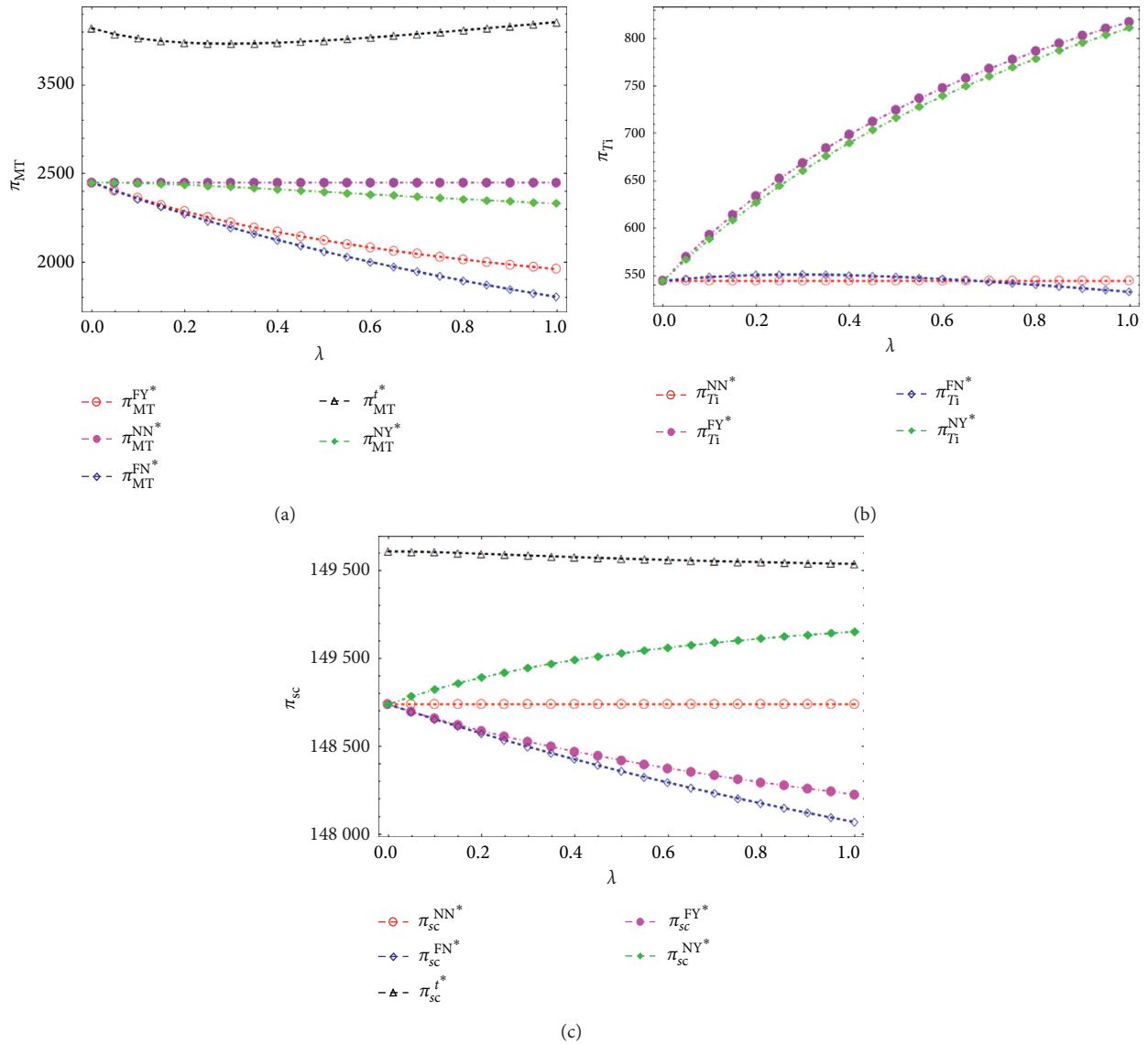


FIGURE 3: The influence of fairness concern on profit of the CLSC members. (a) The influence of fairness concern on profit of the manufacturer. (b) The influence of fairness concern on profit of the collectors. (c) The influence of fairness concern on profit of the CLSC.

growth speed of the collectors' profit is faster than decreasing speed of the manufacturer's profit, which increases the profit and performance of the CLSC.

6.2. Impact of Competitive Intensity δ on the CLSC. To analyze the influence of competitive intensity between collectors on decisions of CLSC, assume the fairness concern coefficient of the collectors remains unchanged ($\lambda = 0.4$). In order to satisfy different parameter conditions, δ denotes competitive intensity between the collectors which varies from 0 to 0.5, the range of which changes with the parameter.

From Figure 4, it is known that, no matter what the model is, the manufacturer's transfer price decreases with increase of the competitive intensity. This is because the manufacturer knows the substitution relation between the collectors; he will not worry about the recycling of used

products. While the collectors receive the information of the manufacturer's decreased transfer price, out of fairness consideration, the collectors will cut down the recycling price, which leads to the loss of return rate and efficiency of the CLSC. Therefore, as a channel leader, it is indispensable for the manufacturer to take some measures to control the competitive intensity of the collection channel.

6.3. Impact of per Unit of Saving Cost Δ on the CLSC. As is shown in Figure 5, in various models, the more saving cost in recycling used products the manufacturer has, the more willing he is to pay a higher price for reproduction. Because of the symmetry information, when getting a higher transfer price, the collectors will be more willing to pay a higher recycling price to conduct recycling activities.

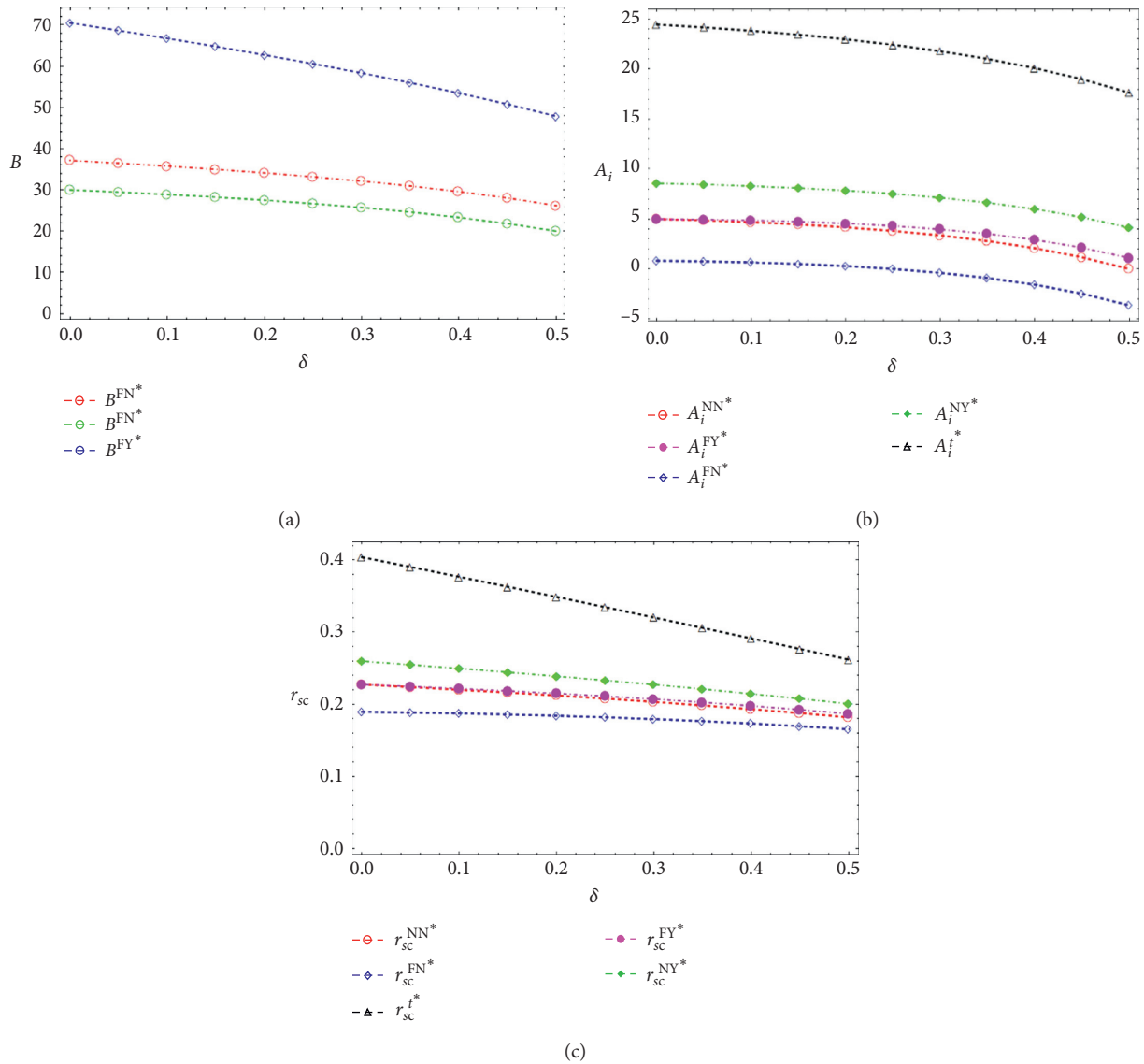


FIGURE 4: The influence of competitive intensity on decisions of the CLSC (a) The influence of fairness concern on profit of the manufacturer. (b) The influence of competitive intensity on transfer price. (c) The influence of competitive intensity on return rate of the CLSC.

7. Management Insights, Limitation, and Future Research

The paper mainly studies the influence of the collectors' fairness concern on the CLSC in the case where the collectors are competitive. The manufacturer, as a leader of the CLSC, who has the advantage of priority decisions, first sets the wholesale price and the transfer price and then the retailer and the collectors decide on the retail price and recycling price recycling price. Through the backward induction method, the equilibrium solutions of the system are generated under five models.

7.1. Management Insights. From the analysis results, some managerial insights can be derived on the pricing decision in the case where the collectors consider fairness concern, as follows.

- (1) In the model NN, collectors are unfairness-concerned, and the manufacturer does not consider the collectors' fairness concern. At this point, the manufacturer realizes the maximum profit. It is obvious that, as the leader of the closed-loop supply chain, he gets most of the profits. Naturally, he hopes that the followers not pay too much attention to the distribution of income but also diligently serve him.
- (2) In the model NY, the manufacturer "passively active" considers the fairness concern of the collectors and raises transfer price to surrender part of the profit so that the collectors also raise the recycling price to "reward" the manufacturer indirectly. A virtuous circle is formed between the two parties with their mutually beneficial behavior, which has a positive effect on sustainable development of the CLSC.

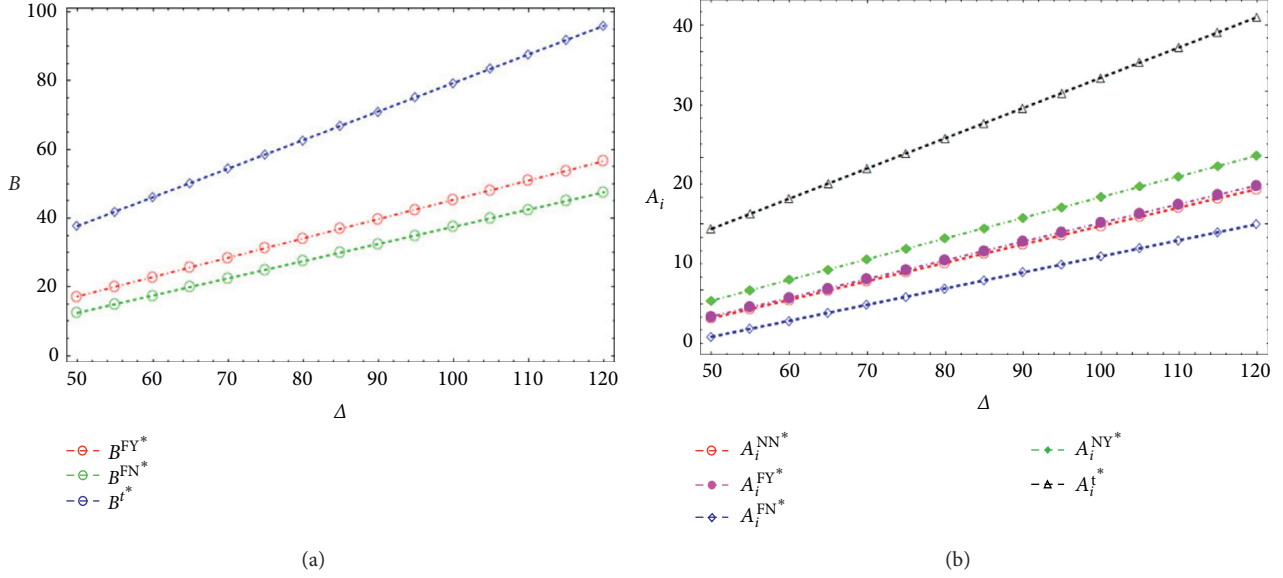


FIGURE 5: The influence of per saving cost on decisions of the CLSC. (a) The influence of per saving cost on transfer price. (b) The influence of per unit of saving cost on recycling price.

- (3) In the model FN, when the collectors are fairness-concerned and the manufacturer ignores the collectors' fairness concern, the equilibrium recycling price sets lower for the purpose of achieving more profits by the collector, thus "hurting" both and "harming" the long-term development of the CLSC.
- (4) In the model FY, when the collectors are fairness-concerned and that is considered by the manufacturer, this fairness concern improves the collectors' benefit but "hurts" the manufacturer's. Therefore, the manufacturer is more eager to establish an effective and practical contract to increase the interest. Considering that the collectors are fairness-concerned and the manufacturer takes it into account, a two-part Tariff contract is proposed in this paper. All the theoretical and numerous analyses suggest both of the profits of the manufacturer and the collectors achieve Pareto improvement with the proposed contract.
- (5) Fourthly, fierce competition will result in a lower efficiency of the CLSC. As a channel leader, it is necessary for the manufacturer to establish corresponding mechanism to control the competition and maintain a long-term healthy development of the CLSC.

7.2. Limitation and Future Research. Among these four decentralized cases, whether the collectors are fairness-concerned or the manufacturer pays the collectors' fairness concern will not change the pricing decision of the retailer, which is based on the model assumptions that the fairness concern of the collectors only impacts reverse channel. Therefore, considering the influence of the collectors' efforts and the manufacturer's social responsibility on the decisions

of the CLSC, which will affect not only the reverse channel, but also the forward channel, merits further research.

The other limitations of this paper are that we did not consider the retailer's Shapley fair distribution. How about it? In addition, we did not consider the evolutionary stable strategies of the manufacturers and the collectors.

Appendix

Proof of Proposition 1. The Hessian matrix of π_{sc}^C about p and A_i goes as follows:

$$H = \begin{pmatrix} -2b & 0 \\ 0 & -2 \end{pmatrix}. \quad (A.1)$$

From the above formula, it can be inferred that Hessian matrix is negative definite; that is, π_{sc}^C about p and A_i is a strictly concave function. Hence, there exists the only optimum solution maximizing profits of the CLSC. With the first-order condition, the optimal price decision in the model C can be obtained. \square

Proof of Proposition 2

- (1) According to

$$\frac{\partial^2 \pi_R^{NN}}{\partial p^2} = -2b < 0, \quad (A.2)$$

it can be inferred that the profit function of the retailer is strictly a concave function, and there exists the only optimal solution p which makes the profit of the retailer maximum. With the first-order condition, we get

$$p^{NN*} = \frac{a + bw^{NN*}}{2b}. \quad (A.3)$$

(2) According to

$$\frac{\partial^2 \pi_{T_i}}{\partial A_i^2} = -2 < 0, \quad (A.4)$$

it can be inferred that the profit of the collector is strictly a concave function, so there exists the only optimal solution which makes maximum profit of the collector. With the first-order condition, we get

$$A_i^{NN*} = \frac{B^{NN*} - h + \delta A_j}{2}. \quad (A.5)$$

According to the symmetry of the collectors,

$$A_i^{NN*} = \frac{B^{NN*} - h}{2 - \delta}. \quad (A.6)$$

(3) Replacing p^{NN*} and A_i^{NN*} into the objective function of the manufacturer, we get

$$\pi_M^{NN} = \frac{1}{2}(w - c)(a - bw) + \frac{2}{2 - \delta}(\Delta - B)(h + B - B\delta). \quad (A.7)$$

Therefore, the Hessian matrix of the profit function of the manufacturer π_M^{NN} about wholesale price w and transfer price B is

$$H = \begin{pmatrix} -b & 0 \\ 0 & \frac{-4(1 - \delta)}{2 - \delta} \end{pmatrix}. \quad (A.8)$$

From the above expression, Hessian matrix is negative definite. π_M^{NN} is a strictly concave function about B and w . So there exists the only optimal solution which makes maximum profit of the manufacturer. With the first-order condition, the optimal pricing decision in model NN is

$$\begin{aligned} w^{NN*} &= \frac{a + bc}{2b}, \\ B^{NN*} &= \frac{(1 - \delta)\Delta - h}{2(1 - \delta)}. \end{aligned} \quad (A.9)$$

Furthermore, the retailer's optimal sailing price and collector's optimal collection price are, respectively, as follows:

$$\begin{aligned} p^{NN*} &= \frac{3a + bc}{4b}, \\ A_i^{NN*} &= \frac{(1 - \delta)\Delta + h(2\delta - 3)}{2(1 - \delta)(2 - \delta)}. \end{aligned} \quad (A.10)$$

□

Proof of Corollary 1

$$A_i^{C*} - A_i^{NN*} = \frac{\Delta(1 - \delta) + h}{2(2 - \delta)} > 0,$$

$$p^{C*} - p^{NN*} = \frac{-a + bc}{4b} < 0,$$

$$r_{sc}^{C*} - r_{sc}^{NN*} = \frac{-2\delta[\Delta(1 - \delta) + h]}{(2 - \delta)(a - bc)} < 0,$$

$$\pi_{sc}^{C*} - \pi_{sc}^{NN*} = \frac{(a - bc)^2}{16b} + \frac{[\Delta(1 - \delta) + h]^2(1 - \delta)}{2(2 - \delta)^2} > 0. \quad (A.11)$$

□

Proof of Proposition 3 From,

$$\frac{\partial^2 u_{T_i}^{FY}}{\partial (A_i^{FY})^2} = -(2 + \lambda) < 0, \quad (A.12)$$

it can be known that the utility function of the collectors is a strictly concave function about collection price and there exists the only optimal solution A_i^{FY*} , making the maximum $u_{T_i}^{FY}$. With the first-order condition, we get

$$A_i^{FY*} = \frac{2\delta(3 + \lambda)A_j^{FY} + 6(1 + \lambda)B^{FY*} + (6 + 9\lambda)h + \lambda\Delta(3 - 2\delta)}{6(2 + \lambda)}. \quad (A.13)$$

By symmetry, the expression of A_i^{FY*} can be acquired. Substituting A_i^{FY*} into the manufacturer's profit function, B_i^{FY*} can be acquired. □

Proof of Corollary 2

$$(1) \frac{\partial A_i^{FY*}}{\partial \lambda} / \partial \lambda = 3\delta[\Delta(3 - 2\delta) + h]/4 [3(2 - \delta) + \lambda(3 - \delta)]^2 > 0, \frac{\partial B_i^{FY*}}{\partial \lambda} / \partial \lambda = h(3 - \delta) + (3 - 5\delta + 2\delta^2)\Delta / 4(1 - \delta)(1 + \lambda)^2 > 0.$$

$$(2) B^{FY*} - B^{NN*} = \lambda[\Delta(1 - \delta)(3 - 2\delta) + h(3 - \delta)] / 12(1 - \delta)(1 + \lambda) > 0, A_i^{FY*} - A_i^{NN*} = \lambda\delta [\Delta(3 - 2\delta) + h] / 4(2 - \delta)[3(2 - \delta) + \lambda(3 - \delta)] > 0. \quad \square$$

Proof of Proposition 4. In the model FN, when the collectors are fairness-concerned, which is ignored by the manufacturer, that is, the manufacturer's optimal decision is the same as that in the model NN, we get

$$B^{FN*} = \frac{(1 - \delta)\Delta - h}{2(1 - \delta)}. \quad (A.14)$$

Meanwhile, the collectors will make decisions according to self-utility maximization under fairness concern. We get

$$A_i^{FN*} = \frac{6(1 + \lambda)(B^{FN*} - h) + 3\lambda(h - \Delta) + 2\lambda\delta\Delta}{2[3(2 - \delta) + \lambda(3 - \delta)]}. \quad (A.15)$$

By replacing B^{FN^*} into the equation above, the theorem gets proven. \square

Proof of Corollary 3

$$\begin{aligned} A_i^{\text{FN}^*} - A_i^{\text{FY}^*} &= \frac{\lambda[\Delta(1-\delta)(2\delta-3) + h(\delta-3)]}{4(1-\delta)[3(2-\delta) + \lambda(3-\delta)]} < 0, \\ B_i^{\text{FY}^*} - B_i^{\text{FN}^*} &= \frac{\lambda[\Delta(1-\delta)(3\delta-2) + h(3-\delta)]}{12(1-\delta)(1+\lambda)} > 0, \\ r_i^{\text{FY}^*} - r_i^{\text{FN}^*} &= \frac{2\lambda[\Delta(1-\delta)(3\delta-2) + h(3-\delta)]}{(a-bc)[3(2+\lambda) + \delta(3+\lambda)]} > 0. \end{aligned} \quad (\text{A.16})$$

Proof of Proposition 5. Because the collectors are fairness-neutral, according to the profit maximization in the model NN, we get

$$A_i^{\text{NY}^*} = \frac{B^{\text{NY}^*} - h}{2 - \delta}. \quad (\text{A.17})$$

While considering that the collectors are fairness-concerned, the manufacturer thinks the collector's decision is made according to the model FY, that is,

$$A_i^{\text{NY}^*} = \frac{6(1+\lambda)(B^{\text{NY}^*} - h) + 3\lambda(h - \Delta) + 2\lambda\delta\Delta}{2[3(2-\delta) + \lambda(3-\delta)]}. \quad (\text{A.18})$$

The collectors make decisions of profit maximization according to the above equation. By replacing the above equation into the objective function of the manufacturer, with the first-order condition, there is

$$B^{\text{NY}^*} = \frac{\Delta(1-\delta)(6+9\lambda-2\lambda\delta) - h(6+3\lambda+\lambda\delta)}{12(1-\delta)(1+\lambda)}. \quad (\text{A.19})$$

By replacing B^{NY^*} into $A_i^{\text{NY}^*}$, the theorem gets proven. \square

Proof of Proposition 6. By backward induction, according to the collector's individual rationality constraint (IR) and incentive constraint (IC), we get A_i^i and F_i . By replacing them into the objective function of the manufacturer, the optimal transfer price and the collection price can be obtained. \square

Data Availability

The data used to support the findings of this study are included within the article. Since the data used in this study are all used to verify the conclusions obtained in the paper under certain system conditions and are set for complex expressions that cannot obtain analytical solutions, different data can be set in different research environments. The implementation scripts in the form of some mathematics files are available from the authors upon request.

Conflicts of Interest

The authors declare no conflicts of interest.

Authors' Contributions

Y.S. and Y.D. contributed to writing; Y.S. and Z.M. provided the case and idea; Y.D. and Z.M. provided revised advice.

Acknowledgments

The authors gratefully acknowledge the support of National Natural Science Foundation of China (Nos. 71103149, 61472093, and 71761005); Humanities and Social Sciences Foundation of Ministry of Education of China (No. 16YJA630005); Major Project of Philosophy and Social Science Research of Sichuan Province (No. SC17A030); Soft Science Research Project of Chengdu City (No. 2016-RK00-00266-ZF); and Academic Project of Guizhou University of Finance and Economics (No. [2017]573 6-024).

References

- [1] "European Policy instruments," 2016, <https://www.eea.europa.eu/themes/policy/intro>.
- [2] "Japanese environmental laws," 2007, <http://www.env.go.jp/en/laws>.
- [3] "Updated informative digest," 2018, <http://www.arb.ca.gov/regact/levii01/uid.pdf>.
- [4] V. Smith and G. Keoleian, "The value of remanufactured engines: life-cycle environmental and economic perspectives," *Journal of Industrial Ecology*, vol. 8, no. 1, pp. 193–221, 2004.
- [5] A. Atasu, L. N. Van Wassenhove, and M. Sarvary, "Efficient take-back legislation," *Production and Operations Management*, vol. 18, no. 3, p. 243, 2009.
- [6] H. S. Heese, K. Cattani, G. Ferrer, W. Gilland, and A. V. Roth, "Competitive advantage through take-back of used products," *European Journal of Operational Research*, vol. 164, no. 1, p. 143, 2005.
- [7] R. C. Savaskan, S. Bhattacharya, and L. N. Van Wassenhove, "Closed-loop supply chain models with product remanufacturing," *Management Science*, vol. 50, no. 2, p. 239, 2004.
- [8] M. Huang, M. Song, L. H. Lee, and W. K. Ching, "Analysis for strategy of closed-loop supply chain with dual recycling channel," *International Journal of Production Economics*, vol. 144, no. 2, p. 510, 2013.
- [9] J. Xiao and Z. Huang, "A stochastic differential game in the closed-loop supply chain with third-party collecting and fairness concerns," *Sustainability*, vol. 11, no. 8, p. 2241, 2019.
- [10] L. K. Scheer, N. Kumar, and J.-B. E. M. Steenkamp, "Reactions to perceived inequity in U.S. and Dutch interorganizational relationships," *Academy of Management Journal*, vol. 46, no. 3, p. 303, 2003.
- [11] T. Cui, J. Raju, and Z. Zhang, "Fairness and channel coordination," *Management Science*, vol. 53, no. 8, pp. 1303–1314, 2007.
- [12] X. Pu, L. Gong, and G. Han, "A feasible incentive contract between a manufacturer and his fairness-sensitive retailer engaged in strategic marketing efforts," *Journal of Intelligent Manufacturing*, vol. 30, pp. 193–206, 2019.
- [13] J. Chen, Y.-W. Zhou, and Y. Zhong, "A pricing/ordering model for a dyadic supply chain with buyback guarantee financing and fairness concerns," *International Journal of Production Research*, vol. 55, no. 18, p. 5287, 2017.
- [14] B. Du, Q. Liu, and G. Li, "Coordinating leader-follower supply chain with sustainable green technology innovation on their fairness concerns," *International Journal of Environmental Research and Public Health*, vol. 14, no. 11, p. 1357, 2017.

- [15] Y. Shu, Y. Dai, and Z. Ma, "Pricing decisions in closed-loop supply chains with peer-induced fairness concerns," *Sustainability*, vol. 11, no. 18, p. 5071, 2019.
- [16] J. Heydari, T.-M. Choi, and S. Radkhah, "Pareto improving supply chain coordination under a money-back guarantee service program," *Service Science*, vol. 9, no. 2, p. 91, 2017.
- [17] J. Heydari, K. Govindan, and A. Aslani, "Pricing and greening decisions in a three-tier dual channel supply chain," *International Journal of Production Economics*, vol. 217, p. 185, 2019.
- [18] M. Esmaili, G. Allameh, and T. Tajvidi, "Using game theory for analysing pricing models in closed-loop supply chain from short- and long-term perspectives," *International Journal of Production Research*, vol. 54, no. 7, pp. 2152–2169, 2016.
- [19] P. Ma, K. W. Li, and Z.-J. Wang, "Pricing decisions in closed-loop supply chains with marketing effort and fairness concerns," *International Journal of Production Research*, vol. 55, no. 22, p. 6710, 2017.
- [20] A. Diabat and A. Jebali, "Multi-product and multi-period closed loop supply chain network design under take-back legislation," *International Journal of Production Economics*, vol. 231, p. 107879, 2021.
- [21] D. Wen, T. Xiao, and M. Dastani, "Pricing and collection rate decisions in a closed-loop supply chain considering consumers' environmental responsibility," *Journal of Cleaner Production*, vol. 262, p. 121272, 2020.
- [22] H. Jalali, A. H. Ansariipoor, and P. De Giovanni, "Closed-loop supply chains with complementary products," *International Journal of Production Economics*, vol. 229, p. 107757, 2020.
- [23] L. Meng, Q. Qiang, Z. Huang, B. Zhang, and Y. Yang, "Optimal pricing strategy and government consumption subsidy policy in closed-loop supply chain with third-party remanufacturer," *Sustainability*, vol. 12, no. 6, p. 2411, 2020.
- [24] N. Wang, Q. He, and B. Jiang, "Hybrid closed-loop supply chains with competition in recycling and product markets," *International Journal of Production Economics*, vol. 217, pp. 246–258, 2019.
- [25] B. C. Giri and S. Sharma, "Manufacturer's pricing strategy in a two-level supply chain with competing retailers and advertising cost dependent demand," *Economic Modelling*, vol. 38, no. 1, p. 102, 2014.
- [26] R. C. Savaskan and L. N. Van Wassenhove, "Reverse channel design: the case of competing retailers," *Management Science*, vol. 52, no. 1, p. 1, 2006.
- [27] M. Ferguson and L. Toktay, "The effect of competition on recovery strategies," *Production and Operations Management*, vol. 15, no. 3, pp. 351–368, 2006.
- [28] D. Lee and S. Sana, "Pricing decisions in a competitive closed-loop supply chain with duopolistic recyclers," *Mathematical Problems in Engineering*, vol. 2020, Article ID 5750370, 22 pages, 2020.
- [29] E. Xing, C. Shi, J. Zhang, S. Cheng, J. Lin, and S. Ni, "Double third-party recycling closed-loop supply chain decision under the perspective of carbon trading," *Journal of Cleaner Production*, vol. 259, p. 120651, 2020.
- [30] T.-H. Ho and J. Zhang, "Designing pricing contracts for boundedly rational customers: does the framing of the fixed fee matter?" *Management Science*, vol. 54, no. 4, pp. 686–700, 2008.
- [31] L. Zhang, B. Xue, and X. Liu, "Carbon emission reduction with regard to retailer's fairness concern and subsidies," *Sustainability*, vol. 10, no. 4, p. 1209, 2018.
- [32] Q. Li, T. Xiao, and Y. Qiu, "Price and carbon emission reduction decisions and revenue-sharing contract considering fairness concerns," *Journal of Cleaner Production*, vol. 190, pp. 303–314, 2018.
- [33] Z. Huang, "Stochastic differential game in the closed-loop supply chain with fairness concern retailer," *Sustainability*, vol. 12, no. 8, p. 3289, 2020.
- [34] H. Zhang, Z. Zhang, X. Pu, and Y. Li, "Green manufacturing strategy considering retailers' fairness concerns," *Sustainability*, vol. 11, no. 17, p. 4646, 2019.
- [35] B. Li, P. Hou, and Q. Li, "Cooperative advertising in a dual-channel supply chain with a fairness concern of the manufacturer," *IMA Journal of Management Mathematics*, vol. 28, no. 2, pp. 259–277, 2017.
- [36] X. Zhen, D. Shi, S. Tsai, and W. Wang, "Pricing decisions of a supply chain with multichannel retailer under fairness concerns," *Mathematical Problems in Engineering*, vol. 2019, Article ID 9547302, 22 pages, 2019.
- [37] Y. Shu, Y. Dai, and Z. Ma, "Pricing decisions in closed-loop supply chains with multiple fairness-concerned collectors," *IEEE Access*, vol. 8, pp. 151335–151349, 2019.
- [38] L. Petrosjan and G. Zaccour, "Time-consistent Shapley value allocation of pollution cost reduction," *Journal of Economic Dynamics and Control*, vol. 27, no. 3, pp. 381–398, 2003.
- [39] C. Ozgun, Y. Chen, and J. Li, "Channel coordination under fairness concerns and nonlinear demand," *European Journal of Operational Research*, vol. 207, no. 3, pp. 1321–1326, 2010.
- [40] S. Du, T. Nie, C. Chu, and Y. Yu, "Reciprocal supply chain with intention," *European Journal of Operational Research*, vol. 239, no. 2, pp. 389–402, 2014.
- [41] E. Katok and V. Pavlov, "Fairness in supply chain contracts: a laboratory study," *Journal of Operations Management*, vol. 31, no. 3, pp. 129–137, 2013.
- [42] A. Karakostas, A. Sonntag, and D. J. Zizzo, "Contract choice: efficiency and fairness in revenue-sharing contracts," *The Scandinavian Journal of Economics*, vol. 119, no. 4, pp. 962–986, 2017.
- [43] J. Heydari, K. Govindan, and R. Sadeghi, "Reverse supply chain coordination under stochastic remanufacturing capacity," *International Journal of Production Economics*, vol. 202, pp. 1–11, 2018.
- [44] C. Mondal and B. C. Giri, "Pricing and used product collection strategies in a two-period closed-loop supply chain under greening level and effort dependent demand," *Journal of Cleaner Production*, vol. 265, p. 121335, 2020.
- [45] X. Li, X. Cui, Y. Li, D. Xu, and F. Xu, "Optimisation of reverse supply chain with used-product collection effort under collector's fairness concerns," *International Journal of Production Research*, 2019.
- [46] Z. Zhang and M. Ren, "Closed-loop supply chain coordination strategy for the remanufacture of patented products under competitive demand," *Applied Mathematical Modelling*, vol. 40, no. 13–14, pp. 6243–6255, 2016.
- [47] N. Wang, Y. Song, Q. He, and T. Jia, "Competitive dual-collecting regarding consumer behavior and coordination in closed-loop supply chain," *Computers & Industrial Engineering*, vol. 144, p. 106481, 2020.
- [48] X.-X. Zheng, Z. Liu, K. W. Li, J. Huang, and J. Chen, "Cooperative game approaches to coordinating a three-echelon closed-loop supply chain with fairness concerns," *International Journal of Production Economics*, vol. 212, p. 92, 2019.
- [49] X.-X. Zheng, D.-F. Li, Z. Liu, F. Jia, and J.-B. Sheu, "Coordinating a closed-loop supply chain with fairness concerns through variable-weighted Shapley values," *Transportation Research Part E: Logistics and Transportation Review*, vol. 126, pp. 227–253, 2019.

Research Article

An Inexact Inventory Theory-Based Water Resources Distribution Model for Yuecheng Reservoir, China

Meiqin Suo ¹, Fuhui Du,¹ Yongping Li,² Tengpeng Kong,¹ and Jing Zhang¹

¹School of Water Conservancy and Hydroelectric Power, Hebei University of Engineering, Handan 056038, China

²School of Environment, Beijing Normal University, Beijing 100875, China

Correspondence should be addressed to Meiqin Suo; suomeiqin@hebeu.edu.cn

Received 11 August 2020; Revised 11 September 2020; Accepted 11 October 2020; Published 31 October 2020

Academic Editor: Huiyan Cheng

Copyright © 2020 Meiqin Suo et al. This is an open access article distributed under the Creative Commons Attribution License, which permits unrestricted use, distribution, and reproduction in any medium, provided the original work is properly cited.

In this study, an inexact inventory theory-based water resources distribution (IIWRD) method is advanced and applied for solving the problem of water resources distribution from Yuecheng Reservoir to agricultural activities, in the Zhanghe River Basin, China. In the IIWRD model, the techniques of inventory model, inexact two-stage stochastic programming, and interval-fuzzy mathematics programming are integrated. The water diversion problem of Yuecheng Reservoir is handled under multiple uncertainties. Decision alternatives for water resources allocation under different inflow levels with a maximized system benefit and satisfaction degree are provided for water resources management in Yuecheng Reservoir. The results show that the IIWRD model can afford an effective scheme for solving water distribution problems and facilitate specific water diversion of a reservoir for managers under multiple uncertainties and a series of policy scenarios.

1. Introduction

The economic development of a region depends heavily on the water distribution of its large reservoirs. However, reservoir water resource management is complex that involves many factors and processes. For example, it is related with the local natural conditions, the adjustable water diversion from upstream in case of drought, the storage capacity and maintaining condition under different inflow levels, the laying of channels/pipes and the loss in the process of water diversion and supply, and different demands of various water users. Each factor/process has many uncertainties, which become more complex depending on the quality of the obtained data [1]. In addition, with the different levels of economic development, water demand will change dynamically with various temporal and spatial scales. Therefore, effectively optimizing the water distribution of a reservoir under uncertainty would be helpful to realize the sustainable development of the region, especially reducing the risk of water shortage under severe drought.

Over the past decades, a number of simulation and optimization methods were developed for reservoir water

resources management under uncertainty [2–19]. Among them, inexact two-stage stochastic programming (ITSP) is effective for analyzing policy scenarios, and taking corrective actions after a random event has taken place in order to minimize “penalties” that may appear due to incorrect policy [11]. Meanwhile, ITSP can reflect the random uncertainty quantified as probability density functions (PDFs) and handle uncertain parameters or variables with variable ranges in programming problems by interval numbers. Interval-fuzzy mathematics programming is useful for decision problems of fuzzy goals and constraints with fuzziness by establishing fuzzy sets and fuzzy functions under interval uncertainty [20].

However, many parameters in actual problem have no information of probability distribution and change with the different temporal and spatial scales and may be presented as intervals. In addition, these intervals have no determined boundaries at sometimes, such as the system cost, and its boundary is difficult to ascertain associated with the volatility of the market and the change in supply and demand and thus shown with fuzziness. It is noted that when the range of interval parameter is so wide that the final result of

the model has a wide interval solution, the manager would feel difficult to make decision by ITSP. According to the past studies [21–24], it is known that the interval-fuzzy mathematics programming (IFMP) could well indicate the fuzzy uncertainty by fuzzy number and membership degree and provides interval solution with a certain satisfaction degree under flexible constraints, to avoid the trouble of making decision resulting from the wide interval solution. Accordingly, multiple uncertainties would be handled by incorporating ITSP and IFMP within a general framework.

On the contrary, in reservoir water resource management system, there is a series of process that needs to be considered besides the above described uncertainties. In particular, when the drought is severe and the reservoir is insufficient, the water diversion would be necessary to satisfy the local water demand. In this case, a scheme of water diversion needs to be established according to the adjustable water diversion from upstream, the local water demand, and the reservoir storage limit, including total diversion quantity, diversion batch size, and period per time. The past models for water diversion of reservoirs mainly focused on the total quantity of water diversion, but few studied the specific diversion batch and period [25–29]. As an economic model, the inventory model can effectively tackle the problem of supply and demand and provide the most economical material purchase batch and period. But the past inventory models rarely studied the planning problems for water resources [30–35]. Since water as a resource has been gradually marketized, the combination of inventory model and other uncertain optimization technologies would undoubtedly make the research studies on the planning of water resources system more rich and perfect and has better applicability.

Therefore, the objective of this study is to develop an inexact inventory theory-based water resources distribution (IIWRD) method through incorporating inventory theory, ITSP, and IFMP within a general framework. The IIWRD method will be helpful for quantitatively analyzing a series of policy scenarios under multiple uncertainties; more importantly, it can afford the specific scheme for water diversion associated with different policy scenarios, including the total water diversion, diversion batch, and period per time. Then, IIWRD is applied to planning water resources distribution of Yuecheng Reservoir that is located in Zhanghe River Basin, China. The results will help to identify desired schemes of water diversion and water allocation under different inflow levels with maximized system benefit and satisfaction degree. Furthermore, the system benefit and total water diversion under different scenarios of inflow levels and unit diversion costs are analyzed to help managers make decision. Comprehensively, three special characteristics of IIWRD make it unique after comparing with the existing methods: (i) it can effectively handle multiple forms of uncertainties, (ii) it is helpful to quantitatively analyzing a series of policy scenarios that are related with various levels of economic penalties, and (iii) it can facilitate specific water diversion of a reservoir under multiple uncertainties.

2. Water Resources Distribution in Yuecheng Reservoir

The Yuecheng Reservoir is a superlarge reservoir directly under the administration of the state, located in Ci County of Handan City, Hebei Province, controlling a river basin area of $18.1 \times 10^3 \text{ km}^2$. Its main task is flood control, irrigation, urban water supply, and electricity generation. Its total capacity is $1.3 \times 10^9 \text{ m}^3$ and can partially solve the industrial and living water of Handan City and Anyang City. According to historical statistics, the accumulated water supply of the reservoir was $17.17 \times 10^9 \text{ m}^3$ from 1962 to 2005, and the total water supply to Hebei Province and Henan Province was $11.73 \times 10^9 \text{ m}^3$ and $5.44 \times 10^9 \text{ m}^3$ [36], respectively. In addition, it can irrigate a farmland of $1.47 \times 10^5 \text{ ha}$ through Minyou Canal in Hebei Province and Zhangnan Canal in Henan Province. The irrigated areas of Minyou and Zhangnan refer to 15 counties, with many kinds of crops, but mainly wheat, corn, and cotton.

Recently, due to the rainfall decrease and the building of water diversion channels in the upstream river basin, the incoming runoff of Yuecheng Reservoir is reducing year by year, resulting in serious irrigation water shortage and critical water supply problems, especially in the Zhangnan irrigation area. For example, the average annual water supply of Zhangnan irrigation area from the reservoir was $51.7 \times 10^6 \text{ m}^3$ from 1981 to 1986, and from 1991 to 1996, it was $30.5 \times 10^6 \text{ m}^3$, but from 2001 to 2006, it was only $7.0 \times 10^6 \text{ m}^3$ [37]. Moreover, in order to ensure the safe flood of the reservoir, the water of the reservoir on the level of 132 m would be leaked before the main flood period, about $85 \times 10^6 \text{ m}^3$. After entering the flood period, because the rainfall in the Zhangwei River Basin is small, the river flow and runoff are few, and the water storage of the reservoir would be not enough. As the important water sources of industry and agriculture for Handan City and Anyang City, Yuecheng Reservoir plays a significant role in the economic life in the two cities and bear a huge pressure of water supply [38].

There are three large reservoirs in the upstream that can divert water to Yuecheng Reservoir, namely, Guanhe, Back bay, and Zhangze. According to the data, from 1960 to 2004, the average annual abandoned water of Zhangze Reservoir was $112 \times 10^6 \text{ m}^3$, the average annual leaked water from Guanhe and Back bay was $23 \times 10^6 \text{ m}^3$ and $37 \times 10^6 \text{ m}^3$. Under this condition, if continuous rainfall occurs in the Zhanghe River Basin and the upstream reservoirs store water fully, it could be considered transferring water from them to Yuecheng Reservoir to relieve the local drought [38]. Since the water allocation of Yuecheng Reservoir to Handan City and Anyang City is generally preferred to meet municipal and industrial use, the agricultural water often appears insufficient, having to take the high cost of groundwater to solve water shortage problems. By calculating, the diversion cost from the upstream reservoirs is much less than the cost of groundwater extraction. Therefore, in order to promote the agricultural development and increase its income in the two cities and make full use of the abandoned water from the

upstream reservoirs, the problem of water distribution from Yuecheng Reservoir to three main crops (wheat, corn, and cotton) of 15 counties in the two irrigation areas would be studied in this paper (shown in Figure 1). It is noted that the water allocation of Yuecheng Reservoir to municipality and industry in two cities is excluded.

3. Statement of Problems

The system of water distribution from Yuecheng Reservoir to agriculture involves many processes and components, and there is a lot of uncertainty between them and each other. For example, the water demand for irrigation of three kinds of crops is related to their crop coefficients, evapotranspiration, and growth periods; thus, it is difficult to get definite values. However, they can be obtained with a range by calculating, which are $[3.12, 3.46] \times 10^3 \text{ m}^3/\text{ha}$, $[2.08, 2.31] \times 10^3 \text{ m}^3/\text{ha}$, and $[2.08, 2.31] \times 10^3 \text{ m}^3/\text{ha}$ [39] for wheat, corn, and cotton, individually. In addition, although some uncertainty can be expressed as interval numbers, their boundaries still show uncertainties, such as the unit cost of water diversion has a relationship with total diversion quantity, draw cost of the upstream reservoirs, and the water loss in the diversion way, all of them are difficult to be estimated. Therefore, the unit cost of water diversion would be expressed as a fuzzy-interval number, being [24, 28, 32, 36] RMB/ 10^3 m^3 in this study, convenient for analyzing the influence of different diversion costs to total diversion quantity. Moreover, because of the significant changes in the annual precipitation and great differences among the seasonal rainfall in the reservoir, as well as the uncertainty of water supply to municipality and industry in the two cities, the water distribution from the reservoir to agriculture is difficult to determine. At this time, the expected objectives for three crops in each subarea need to be set according to their actual planting quantities and then be corrected on the basis of various possible irrigation levels happened. Thus, an effective comprehensive multiple uncertainties method for water distribution from Yuecheng Reservoir to agriculture is expected.

However, in the system of water distribution of Yuecheng Reservoir, when the drought is so serious that the local water demand cannot be met, it would be necessary to consider water diversion from the upstream. At the moment, the manager needs to consider all the problems happened in the process of water diversion, such as reservoir capacity limits, adjustable water from upstream basin, the water supply cost of the upstream basin, the setup cost for water diversion per time, and the storage cost of the reservoir. In addition, under certain amount of water diversion, if it is too much per time, it will not only bring pressure to the reservoir but also cause the stagnation pressure; if it is too little per time, it will increase the diversion frequency and the setup cost. Therefore, the problems of water diversion from the

upstream and water allocation of agriculture under minimized system cost should be handled.

4. Modelling Formulation

Before constructing the inexact inventory theory-based water resources distribution (IIWRD) model for Yuecheng Reservoir, methods of inexact two-stage stochastic programming (ITSP), interval-fuzzy mathematics programming (IFMP), and inventory theory need to be introduced. ITSP is effective for analyzing policy scenarios, and taking corrective actions after a random event has taken place in order to minimize “penalties” that may appear due to incorrect policy. In addition, it can deal with uncertainties expressed as discrete intervals and PDFs. A typical ITSP model can be rewritten as follows [11]:

$$f^\pm = \max C_{T_1}^\pm X^\pm - \sum_{h=1}^v p_h D_{T_2}^\pm Y^\pm, \quad (1a)$$

subject to

$$A_{r_1}^\pm X^\pm - A_{r_2}^\pm Y^\pm \leq w_h^\pm, \quad r_1, r_2 \in M; M = 1, 2, \dots, m_1; \\ h = 1, 2, \dots, v, \quad (1b)$$

$$A_{r_3}^\pm X^\pm + A_{r_4}^\pm Y^\pm \leq B^\pm, \quad r_3, r_4 \in M; M = 1, 2, \dots, m_2, \quad (1c)$$

$$x_j^\pm \geq 0, x_j^\pm \in X^\pm, \quad j = 1, 2, \dots, n_1, \quad (1d)$$

$$y_{jh}^\pm \geq 0, y_{jh}^\pm \in Y^\pm, \quad j = 1, 2, \dots, n_2; h = 1, 2, \dots, v, \quad (1e)$$

where w_h^\pm is the discrete value of an interval random variable with probability level p_h , $h = 1, 2, \dots, v$ and $\sum_{h=1}^v p_h = 1$ and superscripts – and + are lower and upper bounds of interval parameters, respectively. In addition, X^\pm and Y^\pm are first- and second-stage decision variables, individually; the right-hand side coefficients in equation (1b) are presented as probability distributions. An interval x^\pm is defined as a range with known upper and lower bounds but unknown distribution: $x^\pm = [x^-, x^+] = \{t \in x | x^- \leq t \leq x^+\}$, where x^- and x^+ are the lower and upper bounds of x^\pm , individually [11].

However, in real-world problems, the quality of uncertain information obtained mostly cannot be sufficiently satisfactory to be expressed as probabilities or simply presented as interval values. For example, the lower and upper bounds of interval parameters may be fuzzy in nature, resulting in dual uncertainties. Such complexities in uncertainties cannot be handled by the above ITSP model. It is noted the method of IFMP with mixed fuzzy-interval number (FIN) has advantages in tackling such complexities. In detail, the IFMP can be formulated as follows [20]:

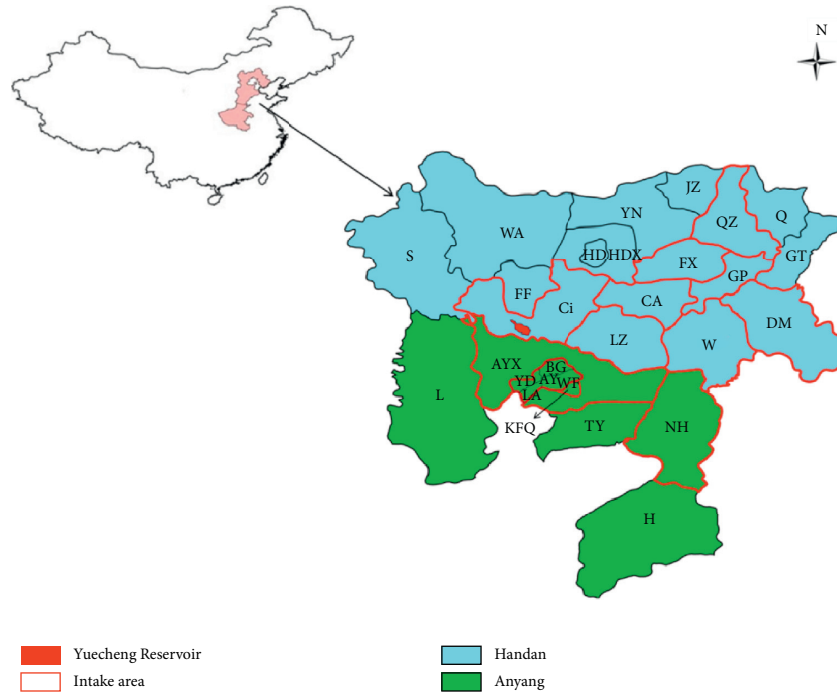


FIGURE 1: Study area (JZ, Jize County; Q, Qiu County; YN, Yongnian County; GT, Guantao County; WA, Wu’an County; HDX, Handan County; HD, Handan District; S, Shexian; FF, Fengfeng Kuangqu; QZ, Quzhou County; FX, Feixiang County; GP, Guangping County; CA, Chengan County; W, Wei County; Ci, Ci County; LZ, Linzhang County; DM, Daming County; WF, Wenfeng District; BG, Beiguan District; YD, Yindu District; LA, Long’an District; AYX, Anyang County; NH, Neihuang County; KFY, Kaifaqu; L, Linzhou District; H, Hua County; TY, Tangyin County. QZ, FX, GP, CA, W, Ci, LZ, and DM are irrigated by Minyou Channel and belongs to Handan Municipality, while WF, BG, YD, LA, AY, NH, and KFY are irrigated by Zhangnan Channel and belongs to Anyang Municipality).

$$\text{Max } \lambda^\pm, \tag{2a}$$

subject to

$$C^\pm X^\pm \geq f^- + \lambda^\pm (f^+ - f^-), \tag{2b}$$

$$A^\pm X^\pm \leq \underline{B}^+ - \lambda^\pm \Delta \underline{B}^\pm, \tag{2c}$$

$$X^\pm \geq 0, \tag{2d}$$

$$0 \leq \lambda^\pm \leq 1, \tag{2e}$$

where B^\pm is a mixed fuzzy-interval number (FIN); let $\Delta \underline{B}^\pm = \underline{B}^+ - \underline{B}^- = [\underline{B}^+, \overline{B}^+] - [\underline{B}^-, \overline{B}^-] = [\underline{B}^+ - \overline{B}^-, \overline{B}^+ - \underline{B}^-]$, where \underline{B}^- and \overline{B}^- are the lower and upper boundaries of the lower interval number, respectively; \underline{B}^+ and \overline{B}^+ are the lower and upper boundaries of the upper interval number, individually. In models (2a)–(2e), λ^\pm is a control variable. The variable λ^\pm represents the degree of satisfaction for the fuzzy objective and/or constraints. When λ^\pm equals to 1, it would be related to a solution with the highest possibility of satisfying the constraints/objective under advantageous conditions; inversely, when λ^\pm equals to zero, it would correspond to a solution that has the lowest possibility of meeting the constraints/objective under demanding conditions.

In the system of water distribution of a reservoir, water diversion would be a prior option when the drought is serious that the local water demand cannot be met. In this case, a series of problems related with water diversion needs to be considered, such as the reservoir capacity, the quantity of water diversion, the diversion period, the cost of water supply, the setup cost for water diversion per time, and the storage cost of the reservoir. Actually, all the problems can be treated as an inventory problem and solved by the economic order quantity (EOQ) model. Based on the assumption of shortages without allowing, a typical EOQ model can be formulated as follows.

Assuming that a material is needed to be produced or purchased, and there is no lead time. The demand is D units per unit time, and the relative costs include K (setup cost for ordering one batch (\$)), C (unit cost for producing or purchasing each unit (\$/unit)), and $C1$ (holding cost per unit per unit of time held in inventory (\$/month)). The objective is to determine when and how much to replenish inventory in order to minimize the sum of the produce or purchase costs per unit time [40].

Let the batch be Q and the period be t , then $t = Q/D$. Since the period is variable, it is needed to calculate how much the total cost is in a given time (e.g., one month). Under this condition, the sum of the two costs (holding cost

and ordering cost) described above can be converted into the cost for per month and formulated as follows:

$$f(Q) = \frac{C_1 Q}{2} + \frac{KD}{Q} + CD. \quad (3a)$$

By calculating the extreme of $f(Q)$, namely, it can be obtained:

$$\frac{C_1}{2} - \frac{KD}{Q^2} = 0, \quad (3b)$$

$$Q^2 = \frac{2KD}{C_1}, \quad (3c)$$

$$Q^* = \sqrt{\frac{2KD}{C_1}}. \quad (3d)$$

Then, it has $f''(Q) = 2KD/Q^3$ and $f''(Q) > 0$ (when $Q > 0$). According to the extremum theorem, $\min f(Q) = f(Q^*)$ when $Q^* = \sqrt{2KD/C_1}$. It is the batch formula under the given conditions, usually regarded as the economic order quantity (EOQ) model.

In summary, the models of ITSP, IFMP, and EOQ will be incorporated in this study, which leads to an inexact inventory theory-based water resources distribution (IIWRD) method. Therefore, the IIWRD model can tackle multiple uncertainties within an optimization programming framework by expressing uncertain parameters as discrete intervals, membership functions, probabilistic distributions, and their combinations. Moreover, it can provide corrective measures for the expected objectives against different random events happened. Meanwhile, the inventory scheme also can be gained for handling water diversion problems in water resources management of reservoirs.

To reflect the dynamic variation in water distribution of Yuecheng Reservoir, the water diversion from upstream to

Yuecheng Reservoir and the water allocation from Yuecheng Reservoir to irrigated areas are considered. Because of the limitation of adjustable water diversion from upstream reservoirs, the total amount cannot completely solve the water shortage of the study area, only in the premise of guaranteeing the minimum water supply as much as possible to avoid the water shortage risk. Hence, there may be un-irrigated fields under low irrigation level because the use of groundwater is too expensive. In addition, there are some assumptions for the system of water distribution including: (1) water sources for irrigation mainly include surface water and groundwater in this study area. However, since the groundwater is difficult to be used in different places, it would be used in the local area without distributing, while only distributes the surface water; (2) the proportion between surface water and groundwater for irrigation is constant, and the irrigation from groundwater can be satisfied; (3) the external water use of Yuecheng Reservoir to other areas would be ignored in special years, and only the water distribution to irrigation areas of Minyou and Zhangnan in Handan City and Anyang City individually are considered; (4) since most of the water distribution of Yuecheng Reservoir is used to irrigate the three crops (wheat, corn, and cotton) of the two irrigation areas, other uses of the surface water in the irrigation areas would be ignored in this study. The objective of this study is to maximize the system benefit, which equals the net irrigation benefit minus the diversion cost and shortage penalty. Accordingly, the IIWRD model for this study system can be formulated as follows:

$$\text{Max } \lambda^\pm, \quad (4a)$$

subject to the following:

Constraint of system benefit:

$$\begin{aligned} & \sum_{i=1}^{15} \sum_{j=1}^3 IT_{ij}^\pm NB_{ij}^\pm - \sum_{h=1}^7 p_h \left(\frac{1}{2HC^\pm \sqrt{2SC^\pm D_h^\pm / HC^\pm + C^\pm D_h^\pm} + \sqrt{SC^\pm D_h^\pm HC^\pm / 2}} \right) \\ & - \sum_{i=1}^{15} \sum_{j=1}^3 \sum_{h=1}^7 p_h IS_{ijh}^\pm PC_{ij}^\pm \geq f^- + \lambda^\pm (f^+ - f^-). \end{aligned} \quad (4b)$$

Constraint of water balance:

$$+AQ_h^+ - \lambda^\pm (AQ_h^+ - AQ_h^-), \quad \forall h. \quad (4c)$$

$$\sum_{i=1}^{15} \sum_{j=1}^3 (IT_{ij}^\pm - IS_{ijh}^\pm) ZZXS_{ij}^\pm \leq D_h^\pm$$

Constraint of minimum irrigation:

$$IT_{ij}^\pm - IS_{ijh}^\pm \geq IT_{ij \min}^- + \lambda^\pm \Delta IT_{ij \min}, \quad \forall i, j, h. \quad (4d)$$

Constraint of reservoir capacity:

$$D_h^\pm + AQ_h^\pm - \lambda^\pm (AQ_h^+ - AQ_h^-) - \sum_{i=1}^{15} \sum_{j=1}^3 (IT_{ij}^\pm - IS_{ijh}^\pm) ZXS_{ij}^\pm \leq RC^\pm, \quad \forall h. \quad (4e)$$

Constraint of adjustable water diversion:

$$D_h^\pm \leq AD^\pm, \quad D_h^\pm \geq 0, \quad \forall h. \quad (4f)$$

Constraint of diversion batch:

$$Q_h^\pm = \sqrt{\frac{2SC^\pm D_h^\pm}{HC^\pm}}, \quad \forall h. \quad (4g)$$

Constraint of satisfaction degree:

$$0 \leq \lambda^\pm \leq 1. \quad (4h)$$

The notation in models (4a)–(4h) is as follows:

i : the irrigation subarea, $i = 1, 2, \dots, 15$.

j : the kind of crops, $j = 1$ (wheat), 2 (corn), 3 (cotton).

h : the inflow of Yuecheng Reservoir, $h = 1, 2, \dots, 7$.

p_h : the probability of inflow h , $p_h > 0$ and $\sum_{h=1}^7 p_h = 1$.

f^\pm : net benefit of the study system (10^6 RMB).

AD^\pm : adjustable water diversion from upstream reservoir (10^6 m³).

AQ_h^\pm : the water available for irrigation in Yuecheng Reservoir under inflow h (10^6 m³).

CC^\pm : unit cost for water diversion (RMB/ 10^3 m³).

D_h^\pm : amount by which total water-allocation target is not met when the inflow is h (10^6 m³).

HC^\pm : holding cost of water per unit in the reservoir (RMB/ 10^3 m³).

IA_{ijh}^\pm : the actual irrigation quantity of crop j in subarea i when the inflow is h (ha).

IT_{ij}^\pm : the irrigation quota for crop j in subarea i (ha).

$IT_{ij\min}^\pm$: the minimum planting quantity of crop j in subarea i (ha).

IS_{ijh}^\pm : the unirrigation quantity of crop j in subarea i when the inflow is h (ha).

NB_{ij}^\pm : the net irrigation benefit for crop j in subarea i per unit of surface water allocated (10^3 RMB/ha).

Q_h^\pm : the diversion batch under the inflow h (m³).

PC_{ij}^\pm : the reduction of net benefit for crop j in subarea i when per unit of surface water not delivered (10^3 RMB/ha).

RC^\pm : storage capacity of the reservoir (10^6 m³).

SC^\pm : setup cost for water diversion one batch (RMB).

T_h^\pm : the diversion period under the inflow h (hour).

ZXS_{ij}^\pm : the water demand of crop j per unit in subarea i (10^6 m³/ha).

In models (4a)–(4h), D_h^\pm and IS_{ijh}^\pm are decision variables, which are influenced by the inflow of Yuecheng Reservoir. The detailed solution process for solving models (4a)–(4h) can be summarized as follows:

Step 1. Transform models (4a)–(4h) into two submodels, where submodel (A) with λ^+ corresponding to f^+ should be formulated first.

Step 2. Solve submodel (A) and obtain the solutions of λ_{opt}^+ , D_{hopt}^+ , Q_{hopt}^+ , and IS_{ijh}^- .

Step 3. Calculate $IA_{ijh\text{opt}}^+$ according to $IA_{ijh}^+ = IT_{ijh}^+ - IS_{ijh}^-$ and obtain T_{hopt}^+ and f_{opt}^+ by $f_{\text{opt}}^+ = \sum_{j=1}^{k_1} c_j^+ x_j^+ + \sum_{j=k_1+1}^{n_1} c_j^+ x_j^- - \sum_{h=1}^v (1/2HC^- \sqrt{2SC^- Y_h^- / HC^-} + C^- Y_h^- + \sqrt{SC^- Y_h^- HC^-} / 2)$.

Step 4. Formulate submodel (B) with λ^- corresponding to f^- .

Step 5. Solve submodel (B) and obtain the solutions of λ_{opt}^- , D_{hopt}^- , Q_{hopt}^- , and IS_{ijh}^+ .

Step 6. Calculate $IA_{ijh\text{opt}}^-$ according to $IA_{ijh}^- = IT_{ijh}^- - IS_{ijh}^+$ and obtain T_{hopt}^- and f_{opt}^- by $f_{\text{opt}}^- = \sum_{j=1}^{k_1} c_j^- x_j^- + \sum_{j=k_1+1}^{n_1} c_j^- x_j^+ - \sum_{h=1}^v P_h (1/2HC^+ \sqrt{2SC^+ Y_h^+ / HC^+} + C^+ Y_h^+ + \sqrt{SC^+ Y_h^+ HC^+} / 2)$.

Step 7. Integrate the two submodel solutions to obtain the optimal solutions for the IFTSIP model, which can be expressed as $D_{\text{topt}}^\pm = [D_{\text{topt}}^-, D_{\text{topt}}^+]$, $Q_{\text{topt}}^\pm = [Q_{\text{topt}}^-, Q_{\text{topt}}^+]$, $T_{\text{hopt}}^\pm = [T_{\text{hopt}}^-, T_{\text{hopt}}^+]$, $IS_{ijh\text{opt}}^\pm = [IS_{ijh\text{opt}}^-, IS_{ijh\text{opt}}^+]$, $IA_{ijh\text{opt}}^\pm = [IA_{ijh\text{opt}}^-, IA_{ijh\text{opt}}^+]$, $\lambda_{\text{opt}}^\pm = [\lambda_{\text{opt}}^-, \lambda_{\text{opt}}^+]$, and $f_{\text{opt}}^\pm = [f_{\text{opt}}^-, f_{\text{opt}}^+]$.

Step 8. Stop.

5. Data Acquisition and Analysis

In this study, the surface water irrigation target of three kinds of crops in each subarea is shown in Table 1 [41]. Table 2 presents the net irrigation benefit and penalty of each crop in every subarea, which are expressed as different intervals based on the various times and spaces. For example, the net irrigation benefit of corn in Ci County is $[2.78, 3.30] \times 10^3$ RMB/ha, which is obtained by the following calculation: (a) the unit yield of corn in Ci County is from 6.10 t/ha to 6.25 t/ha, in which 6.10 t/ha and 6.25 t/ha present the minimum and maximum values of the unit yield, respectively; (b) the net benefit of corn is from 570 RMB/t to 660 RMB/t; and (c) the ratio of corn by irrigation is about 0.8. Therefore, the minimum value of net irrigation benefit of unit yield of corn in Ci County is 2.78 RMB/ha $[6.10 \text{ t/ha} \times 0.8 \times 570 \text{ RMB/t}]$, which would be the lower bound of the interval, while the maximum value is 3.30 RMB/ha $[6.25 \text{ t/ha} \times 0.8 \times 660 \text{ RMB/t}]$, which

TABLE 1: Surface water irrigation targets.

Subarea	Irrigation target, IT_{ij}^+ (ha)		
	Wheat	Corn	Cotton
QZ	[1730, 1830]	[1770, 1870]	[870, 1000]
FX	[2570, 2680]	[2000, 2200]	[1050, 1150]
GP	[1430, 1570]	[1050, 1200]	[550, 650]
CA	[2730, 2925]	[1716, 1820]	[1820, 2080]
WX	[2550, 2670]	[2280, 2490]	[144, 174]
CX	[1145, 1207.5]	[1145, 1250]	[95, 117.5]
LZ	[4860, 5140]	[4400, 4740]	[600, 734]
DM	[2070, 2175]	[990, 1072.5]	[55.5, 64.5]
WF	[1980, 2025]	[2010, 2160]	[130, 150]
BG	[420, 450]	[420, 450]	[7, 10]
YD	[645, 675]	[630, 675]	[4.5, 6.5]
LA	[1950, 2070]	[1590, 1680]	[225, 255]
AY	[8000, 8667.5]	[9167.5, 10000]	[450, 492.5]
NH	[1354.7, 1430.6]	[437, 483]	[89.7, 128.8]
KFQ	[255, 270]	[240, 270]	0

TABLE 2: Net irrigation benefits and penalties.

	Wheat	Corn	Cotton
Net irrigation benefit when water demand is met, NB_{ij}^+ (10^3 RMB/ha)			
QZ	[2.18, 2.67]	[2.75, 3.25]	[1.91, 3.43]
FX	[2.38, 2.90]	[3.44, 4.09]	[2.54, 4.41]
GP	[2.34, 2.85]	[3.35, 3.96]	[1.91, 3.31]
CA	[2.54, 3.14]	[3.50, 4.17]	[2.01, 3.43]
WX	[2.24, 2.74]	[2.73, 3.25]	[1.84, 3.19]
CX	[2.20, 2.69]	[2.78, 3.30]	[1.88, 3.38]
LZ	[2.55, 3.11]	[3.53, 4.20]	[1.98, 3.43]
DM	[2.32, 2.83]	[3.00, 3.54]	[1.40, 2.57]
WF	[2.34, 2.90]	[2.73, 3.22]	[0.96, 1.96]
BG	[2.44, 3.04]	[3.10, 3.75]	[1.98, 3.68]
YD	[2.34, 2.90]	[3.25, 3.91]	[2.35, 4.41]
LA	[1.33, 1.73]	[2.28, 2.80]	[1.18, 2.45]
AY	[2.42, 3.00]	[2.91, 3.46]	[1.10, 2.33]
NH	[2.28, 2.81]	[3.05, 3.62]	[1.91, 3.68]
KFQ	[2.55, 3.18]	[3.00, 3.59]	
Penalty when water is not delivered, PC_{ij}^- (10^3 RMB/ha)			
QZ	[3.27, 3.42]	[3.65, 3.75]	[3.83, 3.93]
FX	[3.50, 3.65]	[4.49, 4.59]	[4.81, 4.91]
GP	[3.45, 3.60]	[4.36, 4.46]	[3.71, 3.81]
CA	[3.74, 3.89]	[4.57, 4.67]	[3.83, 3.93]
WX	[3.34, 3.49]	[3.65, 3.75]	[3.59, 3.69]
CX	[3.29, 3.44]	[3.70, 3.80]	[3.78, 3.88]
LZ	[3.71, 3.86]	[4.60, 4.70]	[3.83, 3.93]
DM	[3.43, 3.58]	[3.94, 4.04]	[2.97, 3.07]
WF	[3.50, 3.65]	[3.62, 3.72]	[2.36, 2.46]
BG	[3.64, 3.79]	[4.15, 4.25]	[4.08, 4.18]
YD	[3.50, 3.65]	[4.31, 4.41]	[4.81, 4.91]
LA	[2.33, 2.48]	[3.20, 3.30]	[2.85, 2.95]
AY	[3.60, 3.75]	[3.86, 3.96]	[2.73, 2.83]
NH	[3.41, 3.56]	[4.02, 4.12]	[4.08, 4.18]
KFQ	[3.78, 3.93]	[3.99, 4.09]	0

would be the upper bound of the interval. The net irrigation benefits of other crops in each subarea also can be obtained by the same method. The amount of adjustable water diversion from upstream reservoirs is $[112 + 23, 112 + 37] \times 10^6 \text{ m}^3$, which is estimated based on the sum of annual abandoned water from Zhangze Reservoir and Guanghe and Back bay Reservoir from 1960 to 2004

[38]. Since the irrigation areas of Minyou and Zhangnan are the important grain production base in Handan City and Anyang City individually, the minimum planting quantity of each crop in every subarea is the lowest irrigation area in order to ensure the local ecology and grain yield, whose value accounts for 40%–50% percent of its total planting area [42]. The setup cost for water diversion in this paper mainly considers the travelling expenses for diversion agreement per time, whose value is [260, 370] RMB by calculating the costs of tickets, meals, and accommodation. According to “Notice on the trial implementation of financial benchmark yield and annual operating standard rates” [43], the holding cost of Yuecheng Reservoir is [30, 40] RMB/ 10^3 m^3 by calculating the ratio between the sum of three costs: maintenance fee (41.5×10^6 RMB), salary and welfare funds for managers (12.13×10^9 RMB), the reservoir management fee (1.82×10^6 RMB), and the annual runoff of the reservoir [44, 45]. In addition, due to the lack of related information, the distribution of water supply of Yuecheng Reservoir for irrigation is difficult to obtain. Based on data statistics, the range of $[0, 302.71106] \text{ m}^3$ is selected as the available water for irrigation, and the water supply level for irrigation can be divided into seven discrete intervals, which are very low (VL, 17%), low (L, 9%), low to medium (L-M, 14%), medium (M, 25%), medium to high (M-H, 20%), high (H, 10%), and very high (VH, 5%), and the corresponding water quantities are 0, $[29.58, 46.39] \times 10^6 \text{ m}^3$, $[83.39, 108.05] \times 10^6 \text{ m}^3$, $[108.05, 127.25] \times 10^6 \text{ m}^3$, $[127.25, 148.16] \times 10^6 \text{ m}^3$, $[198.26, 222.76] \times 10^6 \text{ m}^3$, and $[233.06, 302.71] \times 10^6 \text{ m}^3$ [39].

6. Result Analysis and Discussion

6.1. Water Diversion Analysis. When the random event of water supply happened and makes the local water demand not to meet, the corrective action of water diversion of Yuecheng Reservoir from upstream would be taken to reduce the water shortage. The total diversion quantity is related to various inflows, irrigation quota (expected irrigation objectives), and the minimum planting quantity. If the manager is optimistic about the inflow level (upper bound), adjustable diversion (upper bound), and diversion cost (lower bound) and promises to farmers with the upper bound of the irrigation quota, the water diversion from upstream reservoirs will be more; accordingly, the crop areas of water shortage will be less, and vice versa. The diversion batch is mainly affected by the total amount of water diversion, setup cost, and holding cost, meaning the quantity per time. The diversion period is the ratio of diversion batch and the total amount of water diversion, indicating the time interval between two water diversions.

Table 3 shows the optimal scheme of water diversion of Yuecheng Reservoir from upstream reservoir under different inflows, including total diversion quantity, diversion batch, and period. It can be seen that the total amount of water diversion in the reservoir gradually decreases with the increase in inflow level, which results in the same tendency to diversion batch. This indicates that when the reservoir inflow is high, the agricultural water demand in each subarea can be

TABLE 3: Results of water diversion.

Inflow levels	Diversion quantity (10^6 m^3)	Diversion batch (10^3 m^3)	Diversion period (h)
VL	[135.00, 149.00]	[49.30, 51.79]	[3.04, 3.20]
L	[135.00, 149.00]	[49.30, 51.79]	[3.04, 3.20]
L-M	[92.31, 109.48]	[40.76, 44.39]	[3.55, 3.87]
M	[72.94, 84.97]	[36.23, 39.11]	[4.03, 4.35]
M-H	[52.08, 65.72]	[30.62, 34.39]	[4.58, 5.15]
H	—	—	—
VH	—	—	—

Note: symbols of “VL,” “L,” “L-M,” “M,” “M-H,” “H,” and “VH” mean “very low,” “low,” “low to medium,” “medium,” “medium to high,” “high,” and “very high,” respectively.

satisfied without water diversion. Conversely, when the inflow level is low, the reservoir needs a lot of water diversion to ensure the minimum irrigation. For example, when the inflow level is very low and low, the total amount of water diversion is $[135, 149] \times 10^6 \text{ m}^3$ and $[135, 149] \times 10^6 \text{ m}^3$, individually, in which $135 \times 10^6 \text{ m}^3$ and $149 \times 10^6 \text{ m}^3$ are the lower and upper bounds of adjustable water diversion, respectively, while the related diversion batch is $[49.30, 51.79] \times 10^3 \text{ m}^3$. Under this condition, although the diversion batch is oppositely larger, the diversion period is relatively short because the total water diversion is the largest of all inflow levels. This indicates that the continued water shortage in the study area can be solved only by many times of water diversion. Similar characteristics can be found under other inflow levels. Totally, it can be seen that when the total water diversion decreases gradually, the diversion period will become relatively long. The symbol of “/” in Table 3 indicates the diversion period does not exist at levels of high and very high.

6.2. Water-Allocation Analysis. After taking water diversion, the optimized water allocations to irrigated crops under different inflow levels also can be obtained by the proposed IIWRD model. It is noted that the optimized irrigation quantity is influenced by not only the different inflow levels and water diversion quantity but also the net irrigation benefits and water shortage penalties of crops. Figure 2 shows the optimal irrigation quantity of wheat in each subarea under various inflow levels. It can be seen that when the inflow level is very low, there is still a big difference between the total water diversion and expected water quota even though the total amount of water diversion takes the maximum value within the allowable range of adjustable water diversion. Therefore, the actual irrigation quantity of wheat in most of subareas only can get the minimum irrigation quantity, which is [692, 915] ha, [1028, 1340] ha, [572, 785] ha, [1020, 1335] ha, [458, 603.75] ha, [828, 1087.5] ha, [792, 1012.5], [168, 225] ha, [258, 337.5] ha, [780, 1035] ha, [3200, 4333.75] ha, and [541.6, 715.3] ha in subareas of Quzhou, Feixiang, Guangping, Weixian, Cixian, Daming, Wenfeng, Beiguan, Yindu, Long’an, Anyang, and Neihuang, respectively. When the inflow level is low to medium, medium, and medium to high, the actual irrigation quantity of wheat in all subareas can reach the upper bound of expected water quota, which is 1830 ha, 2680 ha, 1570 ha, 2925 ha, 2670 ha, 1207.5 ha, 5140 ha, 2175 ha, 2025 ha,

450 ha, 675 ha, 2070 ha, 8667.5 ha, 1430.5 ha, and 270 ha in subareas of Quzhou, Feixiang, Guangping, Cheng’an, Weixian, Cixian, Linzhang, Daming, Wenfeng, Beiguan, Yindu, Long’an, Anyang, Neihuang, and Kaifaqu, respectively. Meanwhile, the lower bound of expected water quota for wheat can be acquired in more and more subareas with the total increasing water supply. When the inflow level is high and very, both of the upper and lower bounds of expected water quota for wheat in all subareas can be reached simultaneously.

Figure 3 illustrates the optimal irrigation quantity of corn in each subarea under various inflow levels. For the crop of corn, the actual irrigation quantity has acquired both upper and lower bounds of the expected water quota in all subareas when the inflow level is from very low to very high. Their specific values are [1770, 1870] ha, [2000, 2200] ha, [1050, 1200] ha, [1716, 1820] ha, [2280, 2490] ha, [1145, 1250] ha, [4400, 4740] ha, [990, 1072.5] ha, [2010, 2160] ha, [420, 450] ha, [630, 675] ha, [1590, 1680] ha, [9167.5, 10000] ha, [437, 483] ha, and [240, 270] ha in subareas of Quzhou, Feixiang, Guangping, Cheng’an, Weixian, Cixian, Linzhang, Daming, Wenfeng, Beiguan, Yindu, Long’an, Anyang, Neihuang, and Kaifaqu, individually. Because of its higher net irrigation benefit and higher water shortage penalty, corn has priority to be irrigated over wheat and cotton in the same subarea under every inflow level. Therefore, with the addition of water diversion, the upper and lower bounds of the expected water quota for corn would be firstly reached even when the inflow level is very low.

Figure 4 depicts the optimal irrigation quantity of cotton in each subarea under various inflow levels. After comparing, although cotton and wheat have similar average net irrigation benefits, the water shortage penalty of cotton is higher than that of wheat in subareas of Quzhou, Feixiang, Guangping, Cheng’an, Weixian, Cixian, Linzhang, Beiguan, Yindu, and Neihuang. Accordingly, in these subareas, the expected quota for cotton can be met prior to that of wheat when the inflow level is from very low to very high, which are [870, 1000] ha, [1050, 1150] ha, [550, 650] ha, [1820, 2080] ha, [144, 174] ha, [95, 117.5] ha, [600, 734] ha, [7, 10] ha, [4.5, 6.5] ha, [225, 255] ha, and [89.7, 128.8] ha, respectively. For the cotton in subareas of Daming, Wenfeng, Long’an, and Anyang, due to their lower net irrigation benefits and lower water shortage penalties than that of the other subareas, their expected quota would be considered later when

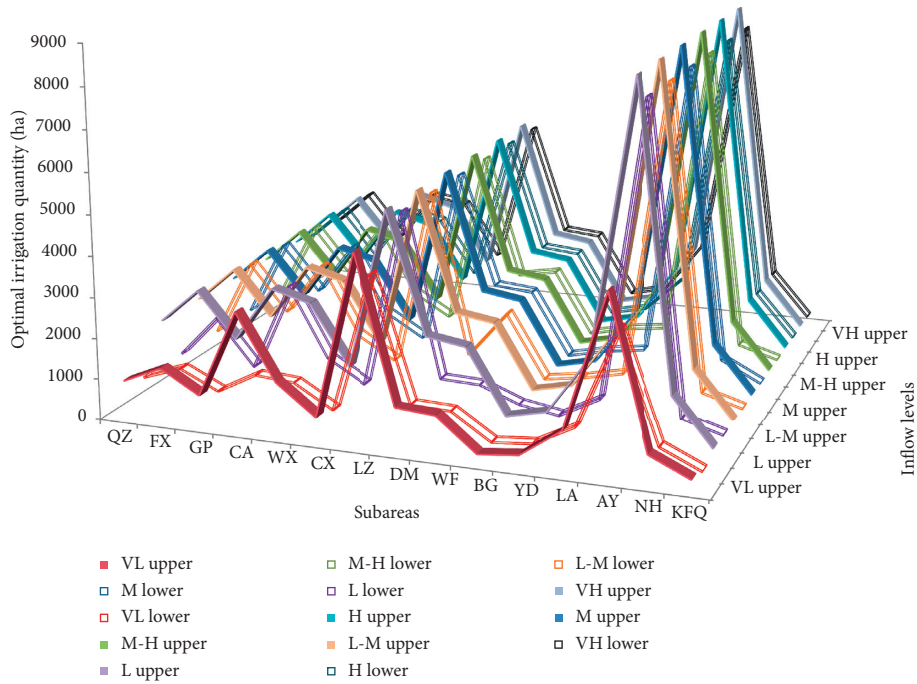


FIGURE 2: Optimal irrigation quantity of wheat in each subarea under different inflow levels.

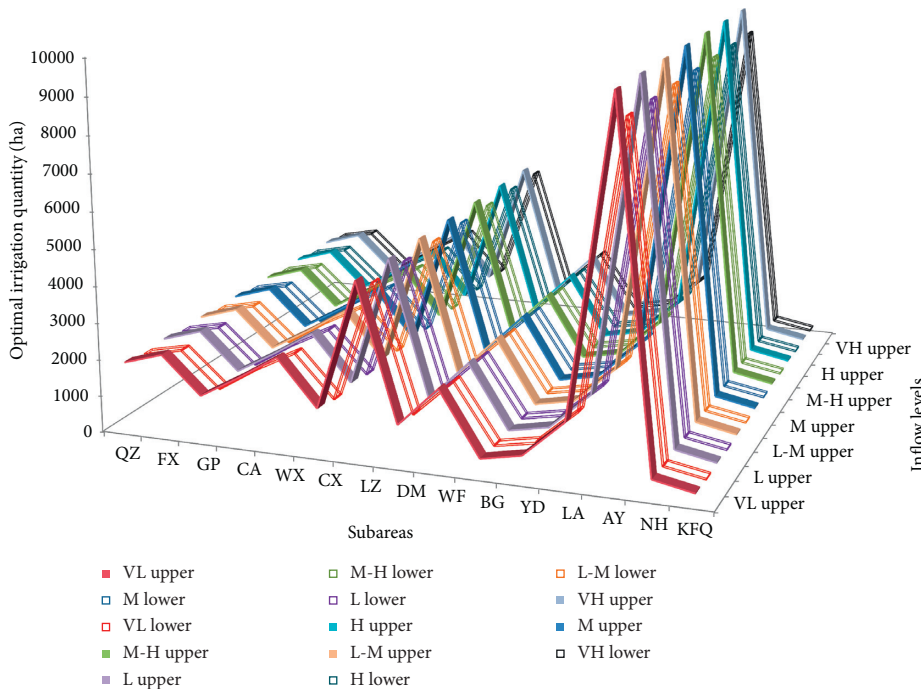


FIGURE 3: Optimal irrigation quantity of corn in each subarea under different inflow levels.

the inflow level is very low, whose optimal irrigation quantities are [22.2, 64.5]ha, [52, 75]ha, [90, 255]ha, and [180, 492.5]ha individually; When the inflow level is from low to medium to high, their optimal irrigation quantities are [22.2, 64.5]ha, [52, 150]ha, [90, 255]ha, and [180, 492.5]ha individually; until when the inflow level is high and very high, both the upper and lower bounds of their expected quotas can be met simultaneously, which are

[55.5, 64.5]ha, [130, 150]ha, [225, 255]ha, and [450, 492.5]ha, respectively.

6.3. System Benefit and Uncertainty Analysis. The expected maximum benefit of this study is [165.12, 231.3] × 10⁶ RMB by solving the IIWRD model, while the corresponding satisfaction degree (λ_{opt}^{\pm}) is [0.032, 0.972]. This interval result

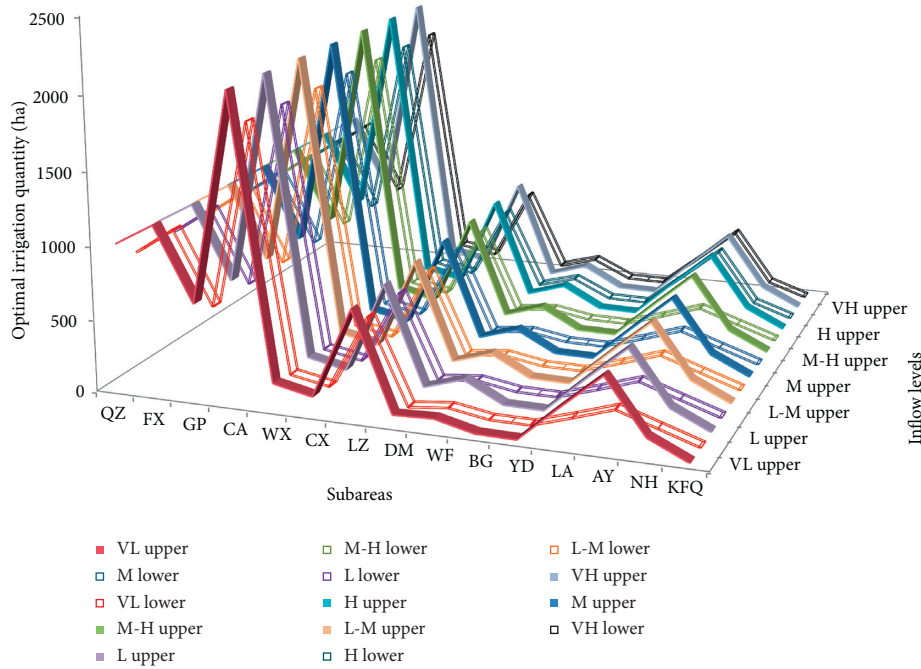


FIGURE 4: Optimal irrigation quantity of cotton in each subarea under different inflow levels.

indicates that when the actual value of each variable fluctuates in its interval, the system benefit would correspondingly change between f_{opt}^+ and f_{opt}^- under different satisfaction degrees. When the inflow level, potential probability distribution, and benefit and punishment and other economic data are given different values, the related decision would change accordingly between the upper and lower bounds of the solution interval. λ^\pm means the satisfaction degree of decision-makers in balancing the environment and economic benefit. In detail, $\lambda_{\text{opt}}^- = 0.032$ is consistent with the lower system benefit ($f_{\text{opt}}^- = 165.12 \times 10^6$ RMB), indicating the maximum satisfaction degree under inferior situation. In contrast, $\lambda_{\text{opt}}^+ = 0.972$ is consistent with the higher system benefit ($f_{\text{opt}}^+ = 231.3 \times 10^6$ RMB), indicating the maximum satisfaction degree of the superior situation. Therefore, the solution of λ_{opt}^\pm represents the degree of meeting the system objectives and constraints under uncertainty.

In addition, the uncertain unit diversion cost expressed as FIN (fuzzy-interval number) directly influences the system benefit and its related satisfaction degree. To clearly understand their relationship, the results under various unit diversion costs are obtained by solving the IIWRD model (as shown in Table 4). It is noted that "S1," "S2," "S3," "S4," and "S5" indicate different scenarios in consistent with five-unit diversion cost, respectively. In detail, the scenario of "S1" represents the lower and upper bounds of the unit diversion cost are fuzzy ($\underline{C}^\pm = [\underline{C}^-, \underline{C}^+]$), and the corresponding system benefit and satisfaction degree of this fuzzy decision are $f_{\text{opt}}^\pm = [165.12, 231.30] \times 10^6$ RMB and $\lambda_{\text{opt}}^\pm = [0.032, 0.972]$ individually. The scenario of "S2" indicates the lower and upper bounds of the unit diversion cost are determinate ($\underline{C}^\pm = [\underline{C}^-, \overline{C}^+]$), meaning the fuzzy boundary is simplified as

certain information); accordingly, the system benefit and satisfaction degree are $f_{\text{opt}}^\pm = [164.85, 231.63] \times 10^6$ RMB and $\lambda_{\text{opt}}^\pm = [0.028, 0.977]$, respectively. When the lower bound of unit diversion cost is determinate but the upper bound is fuzzy (the scenario of "S3," $\underline{C}^\pm = [\underline{C}^-, \underline{C}^+]$), the system benefit and satisfaction degree are $f_{\text{opt}}^\pm = [165.12, 233.23] \times 10^6$ RMB and $\lambda_{\text{opt}}^\pm = [0.032, 0.999]$, individually. When the unit diversion cost has fuzzy lower bound and certain upper bound (the scenario of "S4," $\underline{C}^\pm = [\underline{C}^-, \underline{C}^+]$), the system benefit and satisfaction degree are $f_{\text{opt}}^\pm = [165.15, 231.30] \times 10^6$ RMB and $\lambda_{\text{opt}}^\pm = [0.032, 0.972]$, respectively. When the upper bound of unit diversion cost is fuzzy but the lower bound is certain and close to the lower boundary of lower interval (the scenario of "S5," $\underline{C}^\pm = [\underline{C}^-, \underline{C}^+]$), the system benefit and satisfaction degree are $f_{\text{opt}}^\pm = [165.42, 231.63] \times 10^6$ RMB and $\lambda_{\text{opt}}^\pm = [0.036, 0.977]$, individually. In scenarios of "S3," "S4," and "S5," both of the lower bound of system benefit and the satisfaction degree are higher than or equal to the result of "S1" scenario ($f_{\text{opt}}^- = 165.15 \times 10^6$ RMB and $\lambda_{\text{opt}}^- = 0.032$). This is because of the lower bound of uncertain unit diversion cost and/or the relaxation of allowable default in the inferior situation. The relaxation of system constraints represents an increase in the risk of constraints default. Under the lower risk of constraints default, the decision can be obtained with lower system benefit but higher system credibility. Higher system benefit will result in a larger risk of system constraints default.

Table 5 shows the total amount of water diversion under scenarios of different inflow levels and various unit diversion costs. It can be known that when the inflow level is very low and low, due to the serious water shortage, although the unit diversion cost changes (S1: [27.89, 32.38] RMB/ 10^3 m³, S2:

TABLE 4: System benefit and satisfaction degree under different scenarios of unit diversion cost.

	Scenarios of unit diversion cost				
	S1	S2	S3	S4	S5
System benefit (10 ⁶ RMB)	[165.12, 231.30]	[164.85, 231.63]	[165.12, 233.23]	[165.15, 231.30]	[165.42, 231.63]
Satisfaction degree	[0.032, 0.972]	[0.028, 0.977]	[0.032, 0.999]	[0.032, 0.972]	[0.036, 0.977]

TABLE 5: Diversion quantity under different scenarios of inflow levels and unit diversion cost (10⁶ m³).

Inflow levels	Scenarios of unit diversion cost				
	S1	S2	S3	S4	S5
VL	[135.00, 149.00]	[135.00, 149.00]	[135.00, 149.00]	[135.00, 149.00]	[135.00, 149.00]
L	[135.00, 149.00]	[135.00, 149.00]	[135.00, 149.00]	[135.00, 149.00]	[135.00, 149.00]
L-M	[92.31, 109.48]	[92.22, 109.60]	[92.31, 110.16]	[92.32, 109.48]	[92.42, 109.60]
M	[72.94, 84.97]	[72.87, 85.06]	[72.87, 85.50]	[72.95, 84.97]	[73.02, 85.06]
M-H	[52.08, 65.72]	[52.00, 65.82]	[52.08, 66.30]	[52.09, 65.72]	[52.17, 65.82]
H	0	0	0	0	0
VH	0	0	0	0	0

[24, 36] RMB/10³ m³, S3: [28, 32.38] RMB/10³ m³, S4: [27.89, 32] RMB/10³ m³, and S5: [24, 28.43] RMB/10³ m³, the total amount of water diversion has not changed, and all are [135, 149] × 10⁶ m³. This indicates that, in the case of severe water shortage, the influence of unit diversion cost can be neglected in order to ensure the minimum irrigation quantity of each crop in every subarea. When the inflow level is low-medium, medium, and medium-high, the total amount of water diversion is fluctuated as the unit diversion cost changes. For example, when the inflow level is low-medium, the total water diversion of five scenarios is [72.94, 84.97] × 10⁶ m³, [72.872, 85.06] × 10⁶ m³, [72.94, 85.50] × 10⁶ m³, [72.95, 84.97] × 10⁶ m³, and [73.02, 85.06] × 10⁶ m³, respectively; similar characteristics exist in the solutions of total water diversion under the inflow level of medium and medium-high. When the inflow level is high and very high, the total water diversion is zero. It can be seen that when the inflow level is extreme, the small fluctuation of the unit diversion cost has no effect on the total water diversion. When the inflow level is normal in scenarios of “S3”–“S5,” the lower bound of total water diversion increases with the decrease in the unit diversion cost, corresponding to the gradual increase in the satisfaction degree; the upper bound of total water diversion firstly decreases and then increases, in accordance with the satisfaction degree change. According to the results, it can be obtained that the influence of unit diversion cost changes on the system benefit and total water diversion needs to be considered when the inflow level is normal situation.

7. Conclusions

In this study, an inexact inventory theory-based water resources distribution (IIWRD) model has been proposed for the system of water distribution of a reservoir. This method is developed based on three techniques of ITSP, IFMP, and inventory theory. Therefore, the IIWRD model can not only indicate various uncertainties expressed as discrete intervals, probabilistic distributions, membership functions, and their

combinations but also provide recourse measures for the expected objectives against different random events happened and the corresponding specific water diversion, including total diversion quantity, diversion batch size, and period. Meanwhile, it also can offer the manager the optimal schemes under different scenarios in realizing the maximum system benefit and help decision-makers to avoid the risk of water shortage. In addition, this method can also provide the system benefit under different satisfaction degrees and related schemes of water diversion and agricultural water allocation and a narrow solution range, which is convenient for decision-makers to make decisions.

A case of Yuecheng Reservoir in the Zhanghe River Basin diverting water from upstream and allocating water to agriculture in Handan City and Anyang City has been studied for demonstrating applicability of the proposed methodology. Through using the inventory theory, not only the optimal schemes of water diversion (the total diversion quantity, diversion batch size, and period) under different inflow levels are obtained but also the actual irrigation quantity of each crop is gained. They will help generate desired policies for managers with maximized system benefit and satisfaction degree. Moreover, a variety of uncertainties in the system is well addressed by the advanced IIWRD model. Therefore, the obtained results can effectively help the reservoir managers to solve the problems of water diversion and allocation and set up the optimal management schemes under different inflow levels and satisfaction degrees. In addition, the uncertainty analysis of system benefit and water diversion under different unit diversion costs and various inflow levels indicates that the developed IIWRD model is applicable for reflecting uncertainties and solving problems of water distribution of a reservoir in water resources management system.

Data Availability

The original data used to support the findings of this study are included within the article.

Conflicts of Interest

The authors declare that they have no known conflicts of interest or personal relationships that could have appeared to affect the work represented in this paper.

Acknowledgments

This research was supported by the National Natural Science Foundation of China (no. 51409077), General Program of Natural Science Foundation of Hebei Province (no. D2019402235), Science and Technology Research and Development project of Handan City (no. 1434201078-2), and Scientific Research Project of Hebei University of Engineering (no. 201901400356).

References

- [1] F. Kuria and R. Vogel, "Uncertainty analysis for water supply reservoir yields," *Journal of Hydrology*, vol. 529, pp. 257–264, 2015.
- [2] Q. M. Liang and J. J. Pan, "Analysis of the water supply scheduling in Yuecheng reservoir," *Water Conservancy Science and Technology and Economy*, vol. 16, no. 11, pp. 1206–1207, 2010.
- [3] L. Divakar, M. S. Babel, S. R. Perret, and A. Das Gupta, "Optimal allocation of bulk water supplies to competing use sectors based on economic criterion—an application to the Chao Phraya river basin," *Journal of Hydrology*, vol. 401, no. 1–2, pp. 22–35, 2011.
- [4] Y. Han, Y. F. Huang, S. F. Jia, and J. H. Liu, "An interval-parameter fuzzy linear programming with stochastic vertices model for water resources management under uncertainty," *Mathematical Problems in Engineering*, vol. 2013, Article ID 942343, 12 pages, 2013.
- [5] Y. Zhou, Y. P. Li, G. H. Huang, and Y. Huang, "Development of optimal water-resources management strategies for kaidukongque watershed under multiple uncertainties," *Mathematical Problems in Engineering*, vol. 2013, Article ID 892321, 14 pages, 2013.
- [6] M. Kang and S. Park, "Modeling water flows in a serial irrigation reservoir system considering irrigation return flows and reservoir operations," *Agricultural Water Management*, vol. 143, pp. 131–141, 2014.
- [7] T. Fowe, H. Karambiri, J.-E. Paturel, J.-C. Poussin, and P. Cecchi, "Water balance of small reservoirs in the Volta basin: a case study of Boura reservoir in Burkina Faso," *Agricultural Water Management*, vol. 152, pp. 99–109, 2015.
- [8] Y. Xu and G. H. Huang, "A risk-based interval two-stage programming model for agricultural system management under uncertainty," *Mathematical Problems in Engineering*, vol. 2016, Article ID 7438913, 13 pages, 2016.
- [9] H. Zhang, M. H. Ha, H. Y. Zhao, and J. W. Song, "Inexact multistage stochastic chance constrained programming model for water resources management under uncertainties," *Mathematical Problems in Engineering*, vol. 2017, Article ID 1680813, 14 pages, 2017.
- [10] A. Seifi and K. W. Hipel, "Interior-point method for reservoir operation with stochastic inflows," *Journal of Water Resources Planning and Management*, vol. 127, no. 1, pp. 48–57, 2001.
- [11] Y. P. Li and G. H. Huang, "Interval-parameter two-stage stochastic nonlinear programming for water resources management under uncertainty," *Water Resources Management*, vol. 22, no. 6, pp. 681–698, 2008.
- [12] X. S. Qin and Y. Xu, "Analyzing urban water supply through an acceptability-index-based interval approach," *Advances in Water Resources*, vol. 34, no. 7, pp. 873–886, 2011.
- [13] X. Guo, T. Hu, T. Zhang, and Y. Lv, "Bilevel model for multi-reservoir operating policy in inter-basin water transfer-supply project," *Journal of Hydrology*, vol. 424–425, pp. 252–263, 2012.
- [14] Y. Wu and J. Chen, "Estimating irrigation water demand using an improved method and optimizing reservoir operation for water supply and hydropower generation: a case study of the Xinfengjiang reservoir in southern China," *Agricultural Water Management*, vol. 116, pp. 110–121, 2013.
- [15] E. S. Matrosov, I. Huskova, J. R. Kasprzyk, J. J. Harou, C. Lambert, and P. M. Reed, "Many-objective optimization and visual analytics reveal key trade-offs for London's water supply," *Journal of Hydrology*, vol. 531, pp. 1040–1053, 2015.
- [16] M. Q. Suo, P. F. Wu, and B. Zhou, "An integrated method for interval multi-objective planning of a water resource system in the eastern part of Handan," *Water*, vol. 9, no. 7, pp. 1–17, 2017.
- [17] F.-J. Chang and K.-W. Wang, "A systematical water allocation scheme for drought mitigation," *Journal of Hydrology*, vol. 507, pp. 124–133, 2013.
- [18] H. Y. Guo, H. H. Shi, and X. S. Wang, "Dependent-chance goal programming for water resources management under uncertainty," *Scientific Programming*, vol. 2016, Article ID 1747425, 7 pages, 2016.
- [19] J. Z. Salazar, P. M. Reed, J. D. Quinn, M. Giuliani, and A. Castelletti, "Balancing exploration, uncertainty and computational demands in many objective reservoir optimization," *Advances in Water Resources*, vol. 109, pp. 196–210, 2017.
- [20] Y. P. Li, G. H. Huang, and S. L. Nie, "Mixed interval-fuzzy two-stage integer programming and its application to flood-diversion planning," *Engineering Optimization*, vol. 39, no. 2, pp. 163–183, 2007.
- [21] Y. P. Li, G. H. Huang, Y. F. Huang, and H. D. Zhou, "A multistage fuzzy-stochastic programming model for supporting sustainable water-resources allocation and management," *Environmental Modelling & Software*, vol. 24, no. 7, pp. 786–797, 2009.
- [22] S. Wang and G. H. Huang, "Interactive two-stage stochastic fuzzy programming for water resources management," *Journal of Environmental Management*, vol. 92, no. 8, pp. 1986–1995, 2011.
- [23] Y. Xu, G. H. Huang, and T. Y. Xu, "Inexact management modeling for urban water supply systems," *Journal of Environmental Informatics*, vol. 20, no. 1, pp. 34–43, 2012.
- [24] Y. Lv, G. Huang, and W. Sun, "A solution to the water resources crisis in wetlands: development of a scenario-based modeling approach with uncertain features," *Science of The Total Environment*, vol. 442, pp. 515–526, 2013.
- [25] P. Guo, G. H. Huang, and Y. P. Li, "An inexact fuzzy-chance-constrained two-stage mixed-integer linear programming approach for flood diversion planning under multiple uncertainties," *Advances in Water Resources*, vol. 33, no. 1, pp. 81–91, 2010.
- [26] S. Wang and G. H. Huang, "A two-stage mixed-integer fuzzy programming with interval-valued membership functions approach for flood-diversion planning," *Journal of Environmental Management*, vol. 117, pp. 208–218, 2013.
- [27] Y. Wang, W. Zhang, Y. Zhao, H. Peng, and Y. Shi, "Modelling water quality and quantity with the influence of inter-basin

- water diversion projects and cascade reservoirs in the middle-lower Hanjiang river,” *Journal of Hydrology*, vol. 541, pp. 1348–1362, 2016.
- [28] Y. Li, Q. Cui, C. Li et al., “An improved multi-objective optimization model for supporting reservoir operation of China’s south-to-north water diversion project,” *Science of The Total Environment*, vol. 575, pp. 970–981, 2017.
- [29] M. Yu, C. Wang, Y. Liu, G. Olsson, and C. Wang, “Sustainability of mega water diversion projects: experience and lessons from China,” *Science of The Total Environment*, vol. 619–620, pp. 721–731, 2018.
- [30] S. S. Sana, “A production-inventory model of imperfect quality products in a three-layer supply chain,” *Decision Support Systems*, vol. 50, no. 2, pp. 539–547, 2011.
- [31] J.-R. Lin, T.-H. Yang, and Y.-C. Chang, “A hub location inventory model for bicycle sharing system design: formulation and solution,” *Computers & Industrial Engineering*, vol. 65, no. 1, pp. 77–86, 2013.
- [32] W. Zhu and Z. Wu, “The stochastic ordering of mean-preserving transformations and its applications,” *European Journal of Operational Research*, vol. 239, no. 3, pp. 802–809, 2014.
- [33] M. Schneider, K. Biel, S. Pfaller, H. Schaede, S. Rinderknecht, and C. H. Glock, “Using inventory models for sizing energy storage systems: an interdisciplinary approach,” *Journal of Energy Storage*, vol. 8, pp. 339–348, 2016.
- [34] D. C. Wilson and A. R. Ek, “Imputing plant community classifications for forest inventory plots,” *Ecological Indicators*, vol. 80, pp. 327–336, 2017.
- [35] J. M. Maestr, M. I. Fernández, and I. Jurado, “An application of economic model predictive control to inventory management in hospitals,” *Control Engineering Practice*, vol. 71, pp. 120–128, 2018.
- [36] J. X. Liu and Z. A. Yang, “Discussion on the water allocation plan of Yuecheng reservoir,” *Haihe Water Resources*, vol. 2, pp. 16–18, 2008, in Chinese.
- [37] P. Du, *Research on Water Quantity and Quality Management Model of River Basin under Uncertainty*, North China Electric Power University, Beijing, China, 2013.
- [38] F. Yi and J. Li, “Analysis of increasing water storage in Yuecheng reservoir after reinforcement,” *Haihe Water Resources*, vol. 5, pp. 69–70, 2011, in Chinese.
- [39] W. Li, Y. P. Li, C. H. Li, and G. H. Huang, “An inexact two-stage water management model for planning agricultural irrigation under uncertainty,” *Agricultural Water Management*, vol. 97, no. 11, pp. 1905–1914, 2010.
- [40] M. Q. Suo, Y. P. Li, G. H. Huang, Y. R. Fan, and Z. Li, “An inventory-theory-based inexact multi-stage stochastic programming model for water resources management,” *Mathematical Problems in Engineering*, vol. 2013, Article ID 482095, 15 pages, 2013.
- [41] J. Laherrere, “Estimates of oil reserves,” in *Proceedings of the EMF/IEA/IEW meeting IIASA*, Laxenburg, Austria, June 2001.
- [42] M. M. Li, *Study on the Optimizing Allocation of Anyang City Water Resources*, Gansu Agricultural University, Lanzhou, China, 2008.
- [43] T. F. Wang, “Construction and accounting for the project of water diversion cost,” *Guide of Sci-Tech Magazine*, vol. 18, p. 304, 2012, in Chinese.
- [44] W. K. Ma, “Analysis of the flood dispatching of “96.8” in Yuecheng reservoir,” *Haihe Water Resources*, vol. 1, pp. 33–35, 2006, in Chinese.
- [45] T. F. Wang, “The construction and accounting of the cost of water diversion project,” *Guide of Science and Technology*, vol. 18, p. 304, 2012, in Chinese.